Louisiana State University
LSU Digital Commons

LSU Historical Dissertations and Theses | Graduate School

1987

The Effect of Micromorphological Development on the Elastic Moduli of Fly Ash-Lime Stabilized Bentonite.

Gokhan I. Baykal
Louisiana State University and Agricultural & Mechanical College

Follow this and additional works at: https://digitalcommons.lsu.edu/gradschool_disstheses

Recommended Citation

Baykal, Gokhan I., "The Effect of Micromorphological Development on the Elastic Moduli of Fly Ash-Lime Stabilized Bentonite." (1987). *LSU Historical Dissertations and Theses*. 4435.
https://digitalcommons.lsu.edu/gradschool_disstheses/4435

This Dissertation is brought to you for free and open access by the Graduate School at LSU Digital Commons. It has been accepted for inclusion in LSU Historical Dissertations and Theses by an authorized administrator of LSU Digital Commons. For more information, please contact gradetd@lsu.edu.

Order Number 8811393

The effect of micromorphological development on the elastic moduli of fly ash-lime stabilized bentonite

Baykal, Gökhan I., Ph.D.

The Louisiana State University and Agricultural and Mechanical Col., 1987

Copyright ©1988 by Baykal, Gökhan I. All rights reserved.

U·M·I
300 N. Zeeb Rd.
Ann Arbor, MI 48106

PLEASE NOTE:

In all cases this material has been filmed in the best possible way from the available copy. Problems encountered with this document have been identified here with a check mark __✓__.

1. Glossy photographs or pages __✓__
2. Colored illustrations, paper or print _____
3. Photographs with dark background __✓__
4. Illustrations are poor copy _____
5. Pages with black marks, not original copy _____
6. Print shows through as there is text on both sides of page _____
7. Indistinct, broken or small print on several pages __✓__
8. Print exceeds margin requirements _____
9. Tightly bound copy with print lost in spine _____
10. Computer printout pages with indistinct print _____
11. Page(s) _____ lacking when material received, and not available from school or author.
12. Page(s) _____ seem to be missing in numbering only as text follows.
13. Two pages numbered _____. Text follows.
14. Curling and wrinkled pages _____
15. Dissertation contains pages with print at a slant, filmed as received _____
16. Other _____

_____

_____

U·M·I

THE EFFECT OF MICROMORPHOLOGICAL DEVELOPMENT ON THE ELASTIC MODULI OF FLY ASH-LIME STABILIZED BENTONITE

A Dissertation

Submitted to the Graduate Faculty of the
Louisiana State University and
Agricultural and Mechanical College
in partial fulfillment of the
requirements for the degree of
Doctor of Philosophy

in

The Department of Civil Engineering

by
Gökhan I. Baykal
B.S., Istanbul Technical University, 1980
M.S., Bogazici University, 1982
December 1987

©1988

GOKHAN I. BAYKAL

All Rights Reserved

ACKNOWLEDGEMENTS

I would like to express my deep appreciation to Prof. Ara Arman for his encouraging guidance, advice and invaluable supervision throughout the course of my study. Without his assistance and equally important constructive criticism, this study might never have been undertaken and completed.

I would like to express my sincere gratitude to Prof. Ray Ferrell Jr. for his understanding, encouraging guidance and supervision throughout the study. I also wish to thank to Prof. Roger Seals, Prof. Mehmet Tumay and Prof. Yalcin Acar, committee members, for their invaluable suggestions.

The author expresses his deep appreciation to his parents for their unfailing financial and spiritual support and never failing confidence in him, and to his sister, Feza for her continous support, help and encouragment.

The financial support of Louisiana Transportation Research Center is acknowledged which made this study possible. I would like to thank to the chairman of the department of civil engineering, Prof. Roger Seals for providing financial support.

TABLE OF CONTENTS

LIST OF TABLES

LIST OF FIGURES

LIST OF SYMBOLS

A	: Anhydrite, Ca_2SO_4
C	: CSH (Calcium Silicate Hydrate)
CAH	: Calcium Aluminate Hydrate
EDS	: Energy Dispersive Spectral Analysis
E	: Ettringite, $3CaO.Al_2O_3.3CaSO_4.32H_2O$
F	: Feldspar
G	: C_4AH_{13}
H	: Hematite, Alpha-Fe_2O_3
I	: Alite, C_3S, major constituent of cement
J	: C_3AH_6
K	: Calcite, $CaCO_3$
L	: Lime, CaO
M	: Montmorillonite
N	: Magnetite
P	: Periclase, MgO
Q	: Quartz
R	: Portlandite, $Ca(OH)_2$
SEM	: Scanning Electron Microscope
UCS	: Unconfined Compressive Strength
W	: Afwillite, hydration product of C_3S. $3CaO.2SiO_2.3H_2O$
WDS	: Wave Dispersive Spectral Analysis
XRD	: X-Ray Diffraction

ABSTRACT

The mineralogical and micromorphological changes occuring in fly ash-lime stabilized bentonite were observed and related to changes in elastic moduli of the stabilized mixture. Compacted fly ash, fly ash-lime, bentonite-lime, bentonite-fly ash, and bentonite-fly ash-lime mixtures were prepared and cured at 23°C and 50°C, for 1, 28, 90 and 180 days. The development of microstructure and cementitous crystals were observed by a scanning electron microscope, an energy dispersive spectrum analyzer and a X-Ray diffractometer. The elastic moduli and strengths were obtained from unconsolidated undrained triaxial and unconfined compressive strength tests. The physical test results were compared with changes observed by scanning electron microscopy and X-Ray diffraction.

CSH gel Type I, II and III, ettringite, afwillite and tetracalcium aluminate thirteen hydrate crystals were identified in the cured specimens. The elastic modulus of the fly ash-lime stabilized bentonite was higher than the untreated bentonite and the increase in elastic modulus corresponded to the curing times when new cementitious crystals were observed. Acicular crystals (CSH Type I and II) and ettringite crystals spanned the pores and increased

the contact points where blocky aggregates of equant crystals (CSH III) engulfed the fly ash grains providing support. The compressive strength increased, and the strain at failure decreased resulting in an increase in the elastic modulus. Some fly ash grains providing support for montmorillonite aggregates dissolved and created weak spots in the matrix, causing a decrease in elastic modulus at longer curing periods. At 50°C curing temperature the same cementitious crystals were observed as at 23°C. However, the rate of the reactions increased considerably.

CHAPTER I

INTRODUCTION

Fly ash-lime, fly ash or lime are used for the stabilization of soils in the construction of bases and subbases for pavements. In Louisiana highly plastic fine grained soils are dominant and good quality aggregates are becoming scarce resulting in the need to utilize in situ soils modified by stabilizing agents such as lime. Partial or complete substitution of lime by self-cementitious fly ash has been considered for stabilization of fine grained soils. Pavement structure analysis and design require a thorough understanding of changes taking place in the moduli of the stabilized soils. This in turn requires that soil-additive mixes be designed such that their properties (including elastic moduli) meet design provisions. The elastic modulus is a mechanical property and can be determined from physical tests. However an understanding of the micromorphological development causing changes in the elastic modulus is important to explain and project the effect of fly ash-lime stabilization to longer curing times and to other soils. This study was initiated to determine the micromorphological and mineralogical changes in a fly ash-lime stabilized bentonite and their relation to changes in the elastic moduli of the stabilized mixture.

The main objective of this study is to determine the

changes occuring in a fly ash-lime stabilized pure clay (a bentonite composed primarily of montmorillonite) with increased curing time and to relate this to changes in the elastic moduli of the stabilized mixture. A laboratory study was undertaken using bentonite to simulate the montmorillonite-rich soils of Louisiana. Locally produced lime and self-cementitious fly ash were used with the bentonite to answer the following questions:

1- How does adding fly ash and lime to bentonite affect the elastic modulus and compressive strength?

2- How does fly ash-lime stabilization of bentonite compare with only fly ash or only lime stabilization in terms of observed reaction products and changes in elastic moduli?

3- What type of cementitious minerals are forming? Where do they form and how do they relate to increases in strength and elastic modulus?

4- What is the effect of increased curing temperature (50°C) on the morphological development of cementitious minerals, compressive strength and elastic modulus of fly ash-lime stabilized bentonite? Do the same cementitous minerals form at 23°C and 50°C?

5- How can the information obtained from this study be applied to natural soils and to pavement design?

The literature contains many references related to mineralogical or physical changes of the stabilized soils. Most of the work are limited to either only mineralogical or physical changes in stabilized soils. This study provides an

integrated investigation of the three major aspects of stabilization: mineralogical, micromorphological and physical. The information obtained from mineralogical, micromorphological and physical investigations were used to explain the changes in elastic modulus. An improved understanding of the changes in elastic modulus will help in developing improved pavement design criteria.

Mixtures of fly ash, fly ash-lime, bentonite-fly ash, bentonite-lime, bentonite-fly ash-lime were prepared and cured at 23°C and 50°C. The elastic moduli and strengths were obtained from unconsolidated undrained triaxial and unconfined compressive strength tests. Changes in soil fabric and growth of cementitious crystals were evaluated by studying fractured surfaces of the cured samples with a scanning electron microscope. X-Ray diffraction methods were used to track the formation of cement compounds. The physical test results were compared with changes observed by X-Ray diffraction and scanning electron microscopy.

CHAPTER II

LITERATURE REVIEW

Introduction

" Soil stabilization is the collective term for any physical, chemical or biological method or any combination of such methods employed to improve certain properties of a natural soil to make it serve adequately an intended engineering purpose (108)". The most common application of soil stabilization is the strengthening of the soil components of highway and airfield pavements. Its chief advantages are (71), it:

1- Allows the in-situ soil to be used in construction.
2- Affects the pavement thickness by improving subgrade conditions.
3- Allows use of low cost materials, instead of more expensive material in the pavement cross section.
4- Allows waste materials to be used in highway construc tion.

In general, fine-grained soils rarely have adequate strength and durability for use as base or subbase courses in the pavement cross-section. In order to improve the durability and strength of soils, various chemical additives such as, portland cement, lime and lime-fly ash are used in addition to mechanical stabilization. These additives improve the engineering behavior of the soils through two

mechanisms:

1- Modification of soil by decreasing plasticity index, decreasing volumetric shrinkage and improving drainage characteristics (71).

2- Improvement of strength and durability most probably due to resulting cementitous products.

Lime-fly ash-soil mixtures incorporating fine grained soils, which occur naturally at the site may lack initial mechanical stability due to the absence of aggregate skeleton so chemical considerations come into play. Stabilization of some base courses (and stabilized ·ades) may rest on lime-fly ash-soil chemical reactions (71). It is important to understand what type of reaction products form in the stabilized soils that cause the physical changes.

Cement Hydration

Although only fly ash and lime are used in this study a summary of the hydration of portland cement will be imperative. The reported reaction products for soil-lime and fly ash-lime are similar to the reaction products which occur in cements.

Portland cement is a mixture of four principal compounds; tricalcium silicate (C_3S, 50 to 70 %); beta dicalcium silicate (C_2S, 20 to 30 %); tricalcium aluminate (C_3A, 5 to 12 %) and tetracalcium aluminoferrite (C_4AF, 5

to 12 %). Upon hydration C_3S develops a high strength relatively quickly. Beta-C_2S develops a similar strength more slowly. The other two phases develop little strength (95).

The microstructural changes that occur during hydration of cement were reviewed by Taylor (95) . He stated, "The relatively large grains of unhydrated cement are replaced by the smaller particles of hydration products, which are formed partly in space originally occupied by water. The products form initially as coatings on the surfaces of the cement grains, from which they both grow outwards and eat inwards. Within a few hours, the coatings begin to join up, and the paste stiffens or sets. On further reaction, the gel becomes denser, and the paste hardens. This happens on a time scale of weeks and longer; if the paste is continously kept wet, the strength continues to increase over a period of years."

The most prominent phase detected by X-Ray powder diffraction techniques from a fully hydrated alite (C_3S) paste is calcium hydroxide. The other constituent is calcium silicate hydrate, which is almost amorphous and gives only two very weak and diffuse peaks, at about 3.1A and 1.8A (95). In cement pastes, CSH and calcium hydroxide are again the major products (95).

The Al^{3+}, Fe^{3+} and SO_4^{2-} ions provided by the cement are incorporated partly in crystalline phases containing Al^{3+} or Fe^{3+}. Three main types are (95):

1- AFt (Al-Fe-tri) phases typfied by ettringite, $C_6AS_3H_{12}$. These form prismatic or acicular crystals of hexagonal cross section. Primary ettringite occurs as relatively long (4 to 5 micrometers) narrow rods with parallel sides and no branching. Secondary ettringite, produced by sulphate attack from exterior sources of sulfate, tends to be shorter, thicker, and have hexagonal cross-sections. Ettringite formation is accompanied by large volume increases which may be the cause of sulfate induced failures and which are the basis of expansive cements. Apparently high expansion occurs only when there is a plentiful supply of calcium hydroxide. When there is a deficiency of calcium hydroxide, ettringite formation is accompanied by much less expansion and a strong matrix can develop.

2- AFm (Al-Fe-mono) phases, typfied by monosulphate or mono-sulphoaluminate C_4ASH_{12} . These form platy hexagonal crystals.

3- Hydrogarnet phases, belonging to the solid solution series of C_3AH_6, C_3FH_6, C_3AS_3, C_3FS_3 ; these form roughly equidimensional crystals of cubic symmetry (95).

During the first few hours of hydration ettringite is formed and then is completely replaced by an AFm phase. Hydrogarnet phases form only after much longer curing times, and possibly only with some cements (95).

CSH tend to grow as foils, and as space becomes more restricted, these begin to crumple, and the morphology of the cement paste becomes increasingly less clearly defined.

In the densest regions, the foil morphology is no longer detectable (95).

CSH is present in cement pastes in a variety of morphologies. "The most prominent type of particle of C-S-H gel, especially at early ages, is the elongated material usually found radiating outward from cement grains. These particles have been called "spines", " acicular particles" " aciculae ", " prismatic or rod shaped crystals", "fibrous crystals", " tubular crystals ", "rolled sheet or acicular projections" and various other names (22)". They are prominent in C_3S and beta-C_2S pastes (106). These are refered to as "Type I" particles (7).

Fibrous CSH Type I particles may be from 0.5 to 2 micrometers long , and usually less than 0.2 micrometers across. They have pointed ends and they often branch into two or more portions at the outer tip. Lathlike and rolled sheet type crystals are also reported (85).

CSH Type II (22) is composed of small cement grains enmeshed in a network. Fibrous crystals (same size as CSH Type I) with branches every half micrometer form and these branches intersect with each other and intergrow at the point of intersection forming a reticular network (22). It has been called "reticular network", " interlocking structure " , "honeycomb morphology ", etc. (22). "Barnes (7) reported a variant to this structure in which the 3-D character of the interconnecting network is preserved, but in which individual "rods" are replaced by much more nearly

equant grains typically about 0.5 micrometers in length and almost the same in transverse directions . This habit is designated as a "Type IIA" structure."

Type III CSH gel consists of small, irregularly equant or flattened particles, less than 0.3 micrometers on each side (22).

"Type IV C-S-H gel has a dimpled appearance, with either regular pores or close packed equant grains . The grain size is typically only about 0.1 micrometer (22) ".

Calcium hydrate monosulphate hydrate, and C_4AH_{13} have hexagonal platy microstructures. The plates are several micrometers across but are only about 0.1 micrometers in thickness, and tend to show a characteristic edge-to-face contact at fracture surfaces (22).

Calcium hydroxide forms relatively massive crystals. The crystals grow within water filled pores surrounding and in some cases completely engulfing partially hydrated grains. The crystals may grow up to 0.1 mm in size in the paste (6).

The properties of the hydration products are summarized in Table 1 from Barnes (6). C-S-H morphology is variable with typical dimensions averaging 0.1 micrometers. Calcium hydroxide forms relatively large (0.01 up to 0.1 mm) equant crystals. AFt phases are seen as prismatic needles with 10 by 1 micrometer dimensions. Thin hexagonal platelets or irregular rosettes are typical for AFm phase (1 by 0.1 micrometers). All of these morphologies are

TABLE 11
PROPERTIES OF HYDRATION PRODUCTS

Compound	*Specific gravity*	*Typical morphology*	*Typical dimensions*	*Resolved by*[a]
C–S–H	2·1–2·6	Variable	~0·1 μm	SEM, TEM
CH	2·24	Equant crystals	0·01–0·1 mm	OM, SEM
AFt	~1·75	Prismatic needles	10 × 1 μm	OM, SEM
AFm	1·95	Thin hexagonal platelets or irregular 'rosettes'	1 × 0·1 μm	SEM

[a] SEM = scanning electron microscopy, TEM = transmission electron microscopy, OM = optical microscopy.

Table 1. Properties of Portland Cement Hydration Pro (After Barnes (6)).

observed by scanning electron microscopy.

Substitution of sulphur, aluminum, potassium, iron and other minerals in these cementitious minerals may change their dimensions and morphology. The descriptions of the cementitious minerals are general and deviations due to the variability of the chemical compositions of the minerals studied are possible.

Soil-Lime Reaction

Several reactions occur when lime is added to fine grained soils. The addition of lime modifies the response of the soil system to water. "Current theories about lime stabilization involve mechanisms based on base exchange, flocculation, carbonation and cementation. These processes all play some role; the first three however can probably be regarded as side effects rather than the actual case" (16). Base exchange and flocculation, or agglomeration are short term reactions and they produce immediate changes in soil plasticty , workability and strength and load deformation properties. A soil and lime pozzolanic reaction may occur depending on the type of the soil being stabilized. This is a slow, long-term reaction in which calcium reacts with dissolved silica and alumina. The source of the silica and alumina may be clay minerals, feldspars, micas or amorphous silicate or aluminum silicate minerals (87). The solubility of silica and alumina increases as the pH of the clay-lime

mixture rises toward its limiting value of 12.4 . The pozzolanic reactions result in the formation of various cementing agents which increase mixture strength and durability (16).

There are two mechanisms reported for the formation of cementitious crystals in soil stabilization: a) through solution, b) hydration-crystallization. In through solution mechanism it is believed that the edges of the clay particles are dissolved to form cementitious crystals. Eades and Grim (92) reported that the edges of the clay particles are attacked first and the whole clay mineral structure deteriorated without the formation of any substantial new crystalline phase. Stocker (92) indicated that lime attacked to the edges of 2:1 clay minerals and reaction products formed at the edges, however contrary to Eades and Grim's belief, Stocker found that only a small portion of the clay was involved in the cementitious reactions . He showed that even strongly cemented clay preserved its original crystalline structure. Ormsby and Boltz (78) suggested the possibility of formation of cementitious crystals directly on the surface of the clay. In summary a complete deterioration of clay structure is not likely, however an alteration of the clay structure is possible in lime stabilized soils.

The reaction products in lime stabilized soils are generally either calcium silicate hydrates (CSH) or calcium aluminate hydrates (CAH) because silica, alumina and

calcium are the most abundantly available ions in the soil-lime system (C= CaO, S=SiO_2, A= Al_2O_3 and H= H_2O in short hand notation) .

Montmorillonite-Lime reaction Products

To understand the effects of lime on the engineering behavior of stabilized fine grained soil, the chemical reaction between soil and lime must be examined. Several researchers have studied the reactions between different types of soil and lime. In this section montmorillonite-lime reaction products will be reviewed because the major constituent of bentonite used in this study is montmorillonite.

Goldberg and Klein (35) stabilized bentonite with up to 8 percent hydrated lime but they could not detect any new X-ray diffraction peaks after curing. The only difference was that the lime peaks dissappeared.

Eades and Grim (28) used slurries and compacted samples of bentonite and hydrated lime to determine the reaction products of stabilization. Slurries were prepared with 20 percent lime by dry weight of soil and were cured 3 to 60 days at 60°C. The compacted samples were prepared using 2 to 12 percent lime by dry weight of bentonite and were cured at 60°C for 60 days. A non-crystalline product was evident, but its identification was not conclusive. They have reported that most probably the non-crystalline mineral was CSH gel.

Hilt and Davidson (44) used montmorillonite and lime mixtures cured at 23°C for 30 days and found new X-Ray diffraction peaks at d-spacings of 8.11A, 10.0A, 7.1A. They reported the isolation of a reaction product and their X-Ray study suggested that this product was isostructural with tetracalcium aluminate hydrate. Their analytical chemical results showed that it contained considerably more silica than alumina.

Glenn and Handy (33) prepared slurries of pure bentonite and hydrated lime and cured them at 22°C for two years. X-Ray powder diffraction and single crystal data indicated that the reaction products were calcium silicate hydrate, 10A tobermorite, alpha-C_4AH_{13}, beta-C_4AH_{13} and new diffraction peaks of 7.6A, 3.79A and 2.54A. A 7.95A hexagonal platey product was isolated from this mixture.

Diamond, White and Dolch (25) conducted X-Ray diffraction studies on slurries and compacted bentonite-lime mixtures which were cured for 55 days at 60°C. Compacted samples were prepared by adding 29 percent lime by dry weight of bentonite. They reported broad X-Ray peaks at 3.06A and 2.74 A . Either CSH gel or CSH(I) was present depending on the conditions of reaction . No calcium aluminate hydrate was detected. A slurry which was prepared with 80 percent lime and 20 percent montmorillonite, and cured for 60 days at 45°C gave similar reaction products and a broad X-Ray diffraction peak at 9A.

Croft (16) studied the crystalline reaction products of

montmorillonite-lime pastes cured at 40°C. The reaction products formed were polymorphic varieties of C_4AH_{13} and CSH(I). At elevated curing temperatures (50°C) similar mineral phases formed, however their degree of crystallinity was higher. For compacted samples, weak new reflections appeared at approximate d-spacings of 8.2A, 3.9A, 3.4A, 3.0A, 2.78A and 1.8A . The low angle spacing was indicative of the presence of C_4AH_{13} as a hydrated polymorph, with the spacings at 3.9A and 3.4A substantiating this identification. The spacings at 3.0A, 2.78A and 1.8A were attributed to poorly crystallized CSH(I).

Kronert and Wetzel (56) studied a slurry of lime and montmorillonite cured at 60°C up to 56 days. After five days of curing, tetracalcium aluminate hydrate was present which dissappeared after 28 days with an increase in the production of hydrogranite.

Stocker (92) studied the diffusion of lime into unpulverized clay lumps in the lime stabilized mixtures of a heavy montmorillonitic clay soil. By using chemical analysis techniques he found that all lime clay reaction products had the composition , $C_{11}S_{4.5}A_1H_x$. Montmorillonite reacted with diffused lime giving a reaction product with Si/Al molar ratio of 4.5/1 .

Sabry (87) conducted X-Ray diffraction and scanning electron microscope studies of compacted natural montmorillonitic clays stabilized with up to eight percent lime by dry weight which had been cured for 90 days at 40°C . He

reported that calcium silicate hydrates were the predominant cementing materials.

Joshi, Natt and Wright (48) studied lime injected bentonite after curing for periods of time up to 18 months . Scanning electron microscope (SEM) and energy dispersive spectrum analysis (EDS) and X-Ray diffraction (XRD) studies were conducted. The XRD studies showed alteration of bentonite. New peaks emerged at 3.26A, 3.13A and 2.46A but they were not attributed to any cementing compounds. SEM studies indicated the formation of needle and rod-shaped morphologies which were reported to be calcium silicate hydrate. EDS studies indicated that the calcium to silicon ratio decreased with increasing distance from the lime injected seam. Also the Ca/Si ratio for needle and rod-shaped compounds in the hardened layer was generally 0.8, suggesting the compound is CSH(I). The Ca/Si ratio in the samples obtained at the end of 1, 7, 21, and 28 days varied from 0.3 to 0.7 . The trend was erratic, suggesting diffusion and translocation of calcium at different rates through areas of high moisture content within the clay slurry.

The reported montmorillonite-lime reaction products varied from one study to the other considerably without a trend, depending on the mixture proportions, sources and types of materials used, curing temperature and time, and to whether slurries, pastes or compacted samples were used. It may be concluded that in most cases cementitious minerals

formed. CSH(I) is the most widely reported reaction product. In one case CASH mineral formation was reported. In some cases the cementitious minerals may have formed but may have not been detected by the author. Determination of the cementitious minerals using X-Ray diffraction techniques is very difficult due to poorly crystalline nature of the cementitious minerals forming which further complicates the problem. From the above information it can be deduced that in the study of cementitious crystals different techniques should be used conjunctively. Scanning electron microscopy, energy dispersive spectral analyzer and X-Ray diffraction techniques compliment each other when used together. The observations made with one technique can be verified by using the other technique. Elevated curing temperatures can be used but at 60°C different minerals were observed. The reported cementitious minerals at 50°C curing were the same as the 21°C cured samples so 50°C curing should be used as the upper limit for elavated curing.

Fly Ash

Fly ash is the dust of inorganic residues produced from the combustion of pulverized coal in electrical generating plants and is collected from the flue gases by either mechanical or electrostatic devices. Commonly the fly ash particles are spheres with diameters ranging from one to 100 micrometers, averaging 7 micrometers (42,71). Fly ash is

composed of solid spheres and two types of hollow spheres. Cenospheres are completely hollow thin walled particles while pleospheres are hollow spheres filled with smaller spheres (21). Some fly ash grains are not spherical. The size of these particles range from ten to 300 micrometers (42,71). Insufficient burning of the coal or the mineralogical composition of the original coal particle may be the reason for the irregular shapes of these particles (21).

ASTM C618 specification categorizes fly ash by two classes: Class F, and Class C. Class F fly ash is required to have the total weight of alumina, silica and iron oxide to be at least 70 percent of the total weight. The required minimum value for Class C fly ash is 50 percent (88). The typical chemical compositions of fly ash produced from bituminous coals (low calcium), subbituminous coals (high calcium), and lignite coals (high calcium) are presented in Table 2. The silica content of high calcium fly ash is variable and may be as high as those of some low calcium fly ashes (19). Alumina content may not be as variable. The iron oxide content of high calcium fly ash is usually lower than the low calcium fly ash. The magnesium oxide content of high calcium fly ash is usually higher than low calcium fly ashes. High calcium fly ash has typically high SO_3 content and this may reflect either readily soluble alkali sulfates (primarily sodium) , or calcium sulfate (anhydride), or both. Loss on ignition reflects the efficiency of the

TYPICAL CHEMICAL ANALYSIS OF FLY ASH

	Bituminous Ash	Subbituminous Ash	Lignite Ash
Silica (SiO_2)	49.2	38.4	44.4
Alumina (Al_2O_3)	23.6	19.0	18.4
Iron Oxide (Fe_2O_3)	14.7	4.5	5.4
Sum of SiO_2,Al_2O_3,Fe_2O_3	87.5	61.9	68.2
Magnesia (MgO)	0.8	4.0	4.2
Sulfur Trioxide (SO_3)	1.0	1.6	1.6
Moisture Content	0.2	0.1	0.0
Loss of Ignition	2.7	0.4	0.5
Calcium Oxide (CaO)	1.0	24.1	18.2

Table 2. The Chemical Compositions of Bituminous calcium) Ash, Subbituminous Ash (high calcium Lignite (high calcium) Ash (After Smith and Raba (89)).

combustion process rather than an intrinsic characteristic of fly ash that can be traced to coal chemistry. Fly ash produced in modern efficient plants may have lower carbon contents than fly ash produced in older inefficient plants (19). The major distinction between "Class C" and "Class F" fly ash is the CaO content. "Class C " fly ash have higher CaO contents than "Class F " fly ash. The CaO found in "Class C" fly ash is not in free state or in other words it is not available for reactions (69). Almost all of the CaO present in the fly ash is combined with the silicates and aluminates due to the high temperatures in the furnace. The free lime (CaO) is only a small percentage of the CaO content obtained from chemical analyses.

The chemical composition and physical properties of fly ash are affected by several factors (83):

1- The origin and the rank of coal.

2- The degree of pulverization.

3- The design of the boiler unit.

4- The charging and the firing techniques.

5- The collection, handling and storage techniques.

The mineral composition of fly ash originates from the rock detritus which collects in the fissures and layers of coal seams and constitutes 8 to 14 weight percent of the coal (36,42,71). The common mineral constituents of coal ashes are presented in Table 3 (21). The minerals at the top of the list in Table 2 such as clays, micas , feldspars, quartz and iron oxides are commonly found in soils. The minerals on

Mineral	Type	Composition
Kaolinite	clay	$Al_2O_3.2SiO_2.H_2O$
Illite	clay	$K_2O.3Al_2O_3.6SiO_2.3H_2O$
Muscovite	mica	$K_2O.3Al_2O_3.6SiO_2.3H_2O$
Biotite	mica	$K_2O.MgO.Al_2O_3.3SiO_2.H_2O$
Orthoclase	feldspar	$K_2O.Al_2O_3.6SiO_2$
Albite	feldspar	$Na_2O.Al_2O_3.6SiO_2$
Quartz	silica	SiO_2
Hematite	iron oxide	Fe_2O_3
Magnetite	iron oxide	Fe_3O_4
Calcite	carbonate	$CaCO_3$
Dolomite	carbonate	$CaCO_3.MgCO_3$
Siderite	carbonate	$FeCO_3$
Gypsum	sulfate	$CaSO_4.2H_2O$
Halite	chloride	NaCl
Sylvite	chloride	KCl
Pyrites	sulfide	FeS_2
Rutile	oxide	TiO_2

Table 3. Common Mineral Constituents of Coal Ashes (Laguros (58)).

the lower portion of the list are also found in soils , but as they tend to be more soluble, they are generally found in soils from areas that receive less rainfall (21). All of these minerals or their high temperature polymorphs or glasses may be found in fly ash.

Lime-Fly Ash Reaction Products

Fly ash chemically react with calcium hydroxide at ordinary temperatures to form compounds possesing cementitious properties. The reactions that occur in the lime-fly ash-water system to form cementitious materials were studied by several researchers. Leonard and Davidson (60) investigated the pozzolanic reaction products of a slurry of hydrated lime and fly ash cured at 23°C for one year. They reported new X-Ray diffraction peaks at 17.3A, 12.6A, 3.08A . For other mixtures which were cured at elevated temperatures of 40°, 50°, 60° C , they reported no new peaks. The initial product was non-crystalline, after which there was slow crystallization to CSH(I), similar to the mineral tobermorite.

Minninck (74) studied hydrated lime and fly ash samples cured at 140°C, or autoclaved, and reported new X-Ray diffraction peaks at 3.31A, 3.05A, 2.97A and 2.77A. In another study Minnick (73) indicated that the major cementing compounds formed in lime fly ash mixtures were probably calcium silicate hydrates and possibly ettringite.

Low sulphate sulfoaluminate might also be formed.

Croft studied the reaction products of lime-fly ash mixtures by using X-Ray diffraction, differential thermal analysis, and electron microscopy techniques and reported the formation of calcium silicate hydrate I and hydrated calcium aluminate in the form of C_4AH_{13} (17). The first indications of crystalline reaction products began to appear after 28 days at a curing temperature of 50°C. Combination of montmorillonite clay with lime and fly ash produced no reaction products other than those present in the lime-fly ash mixtures alone.

It may be concluded that CSH(I) is the cementitious reaction product which is consistently reported by different researchers. Ettringite and C_4AH_{13} were also reported.

Particle Hydration

The chemical compositions of the individual fly ash grains vary considerably as presented earlier in this section. It is important to study the participation of fly ash grains in the reactions at the individual particle level. There have been many studies on the effects of hydration of fly ash on an individual particle to particle basis. Idorn (47) lists three mechanisms of particle hydrations :

1- The particle reacting with calcium hydroxide is surrounded by an integrated layer of C-S-H gel (54).

2- The fly ash particles are completely inert fillers within the surrounding cement paste (22).

3- The fly ash particle dissolves and resulting (C-S-H and calcium aluminate hydrates) products precipitate leaving a space between the remaining portion of the fly ash particle and cement paste (92).

A combination of all the above mentioned mechanisms can be found together, because of the chemical variability of the fly ash from particle to particle (21).

Grutzeck, Roy and Sheetz suggested a hydrating hollow cenosphere model and explained the morphology at various stages of hydration (40). At early stages "Pull out " features, in which the fly ash particle has been cleanly removed or " pulled out " when the sample was broken for observation, were observed. An equal number of smooth surfaced voids and spheres were visible at this stage. At later stages a crust of radiating C-S-H fibers surrounded the dissolving fly ash sphere and fewer pull out features with rough surfaces were observed. Once a sphere was completely consumed, the mottled interior surface remained as a remnant of the original sphere.

Barnes and Dolch (5) studied the morphology of the contact zone developed between portland cement paste on a glass slide and reported a duplex film of 1 micrometer total thickness on the glass surface which modeled the aggregate paste interaction zone. Fresh cement paste developed two part (duplex film) films on the glass surface. The upper

portion was C-S-H gel and the lower part which was in direct contact with glass slide was $Ca(OH)_2$. Rod shaped projections normal to the interface were observed which were identified as C-S-H gel (Type I). After a few days some part of the gel rods was transfered into shortened , nearly equiaxed shapes. In other areas after about three days of hydration , transformation to the reticulated network morphology occured (Type II C-S-H gel). As hydration proceeded these duplex films might become tied to bulk cement paste by deposition of additional calcium hydroxide, ettringite or other hydration products.

Diamond, Ravina and Lovell (20) reported the same type of duplex films on fly ash grains. The cementitious reactions should occur through this film by diffusion. " A similarity between early hydration shells which form around hydrating portland cement grains, and the duplex film coating was reported. In the past it was interpreted that the enclosed grain was actively hydrating to develop a C-S-H bearing shell around a grain of portland cement. However Diamond et al. (20) suggested that, some of the shells may represent the effects of deposition from solution onto surfaces of grains that are chemically inactive." Ghose et al. (32) observed similar double films covering fly ash spheres. Some of the fly ash spheres did not react at all. Diamond (21) stated that depending on the chemical compositions, many fly ash spheres might not react and inert fly ash spheres might not be detrimental to strength .

Vivian (102) studied portland cement pastes which contained up to one third of their weight as inert quartz particles and he reported approximately the same compressive strengths as those consisting of cement particles.

Unconfined Compressive Strength

"The service conditions for lime-treated soils vary substantially depending on use. For subgrade and subbase application, high strength is not required but for base course use the mixture must develop good strength to assure stability and integrity of the stabilized layer (100)". Unconfined compressive strength is widely used to evaluate the properties of the stabilized soils. Several correlations have been reported to find many significant engineering properties e.g. shear strength, modulus of elasticity, and flexular strength can be approximately calculated. Unconfined compressive strength is also indicative of mixture durability.

Changes in Elastic Moduli

The addition of fly ash and lime to stabilize a base course, changes the stress strain properties of stabilized soil . The marked effect of addition of lime, to the compressive stress strain properties of fine grained soils

is shown in Figure 1. The failure stress is increased, and the ultimate strain of the stabilized soil is decreased relative to the natural soil. Improvement in stress strain characteristics occur immediately and improvement continues with increase in curing time (99).

"As a result of studies conducted with representative Illinois soils stabilized with lime (99) it has been possible to develop a generalized compressive stress strain relation for cured soil lime mixtures. These mixtures appeared to be strain susceptible , and the ultimate strain at maximum compressive stress was approximately one percent, regardless of soil type and curing period. The comporessive modulus of elasticity at a confining pressure of 105 kPa could be estimated (99) from the unconfined compressive strength of the lime soil mixture according to the following relation.

$$E = 70 + 0.124\ q \qquad \ldots\ldots(1)$$

In which E is the compressive modulus of elasticity in MPa and q is the unconfined compressive strength in kPa. The elastic modulus obtained from triaxial compression tests can be used to determine the thickness of pavements.

In summary, several reaction products form in soil-lime and soil-fly ash-lime mixtures after curing. The reported reaction products vary, however CSH(I) is consistently reported by most of the researchers. The alteration of clay

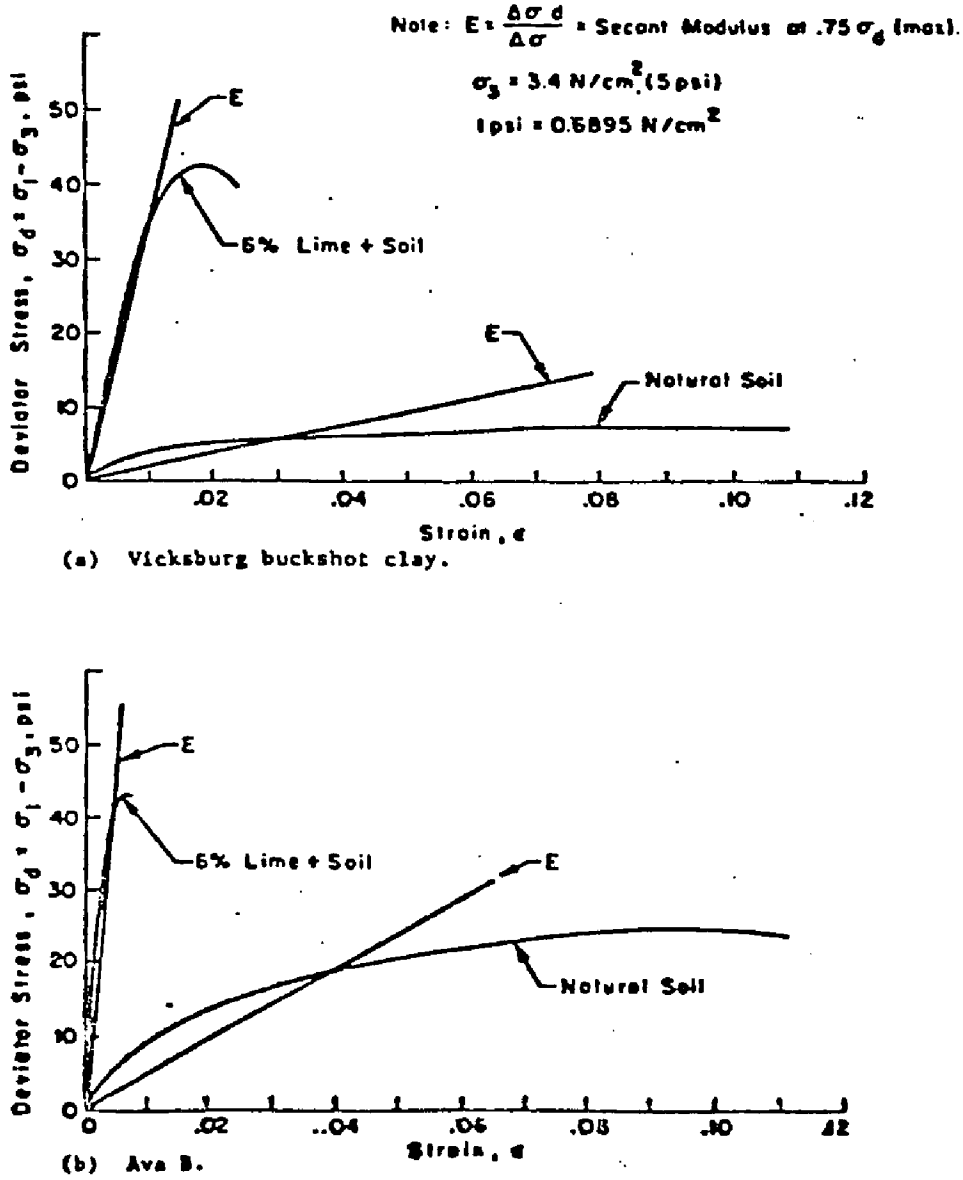

Figure 1. Typical Stress-Strain Curve Illustrating Immediate Effects of Lime Treatment (after Thompson (99)).

particles through dissolution of the edges of the clay particles is possible but complete deterioration of the clay structure is unlikely. The long-term increase in strength is due to cementation. The chemical compositions of the fly ash particles are variable, so their participation in the reactions should be studied at the particle to particle level. Elevated curing temperatures can be used and 50°C curing appears to be the upper limit at which same minerals will form as in case of 23°C curing. X-Ray diffraction technique, when used alone may not be satisfactory to track the newly forming cementitious minerals due to their poor crystallinity and small quantities. A combination of techniques should be used to determine the mineralogical changes in stabilized soil. The morphologies of the cement hydration products are similar to the cementitious crystals that form in stabilized soils.

CHAPTER III

METHODOLOGY

Various studies on lime, fly ash, and portland cement stabilization have been conducted since last three decades. Many studies have been performed on their engineering properties while some studies have emphasized special importance of the chemical reactions between stabilizing agents and soil. Mostly X-Ray diffraction, differential thermal analysis, and electron microscope studies of the isolated reaction products have been used. However very few mineralogical studies are reported using compacted samples (in this study compacted samples were used).

The scanning electron microscope is an excellent tool to observe the microfabric of the fractured surfaces in three-dimensions. Ease of sample preparation and the large depth of focus of this equipment makes it very suitable for applied soils research. A scanning electron microscope was used throughout this study to observe the fractured surfaces of compacted stabilized mixtures. An energy dispersive spectral analyzer provided rapid qualitative microchemical analyses of the cementitious minerals. The use of X-Ray diffraction equipment was essential to observe any changes in the mineral composition of the stabilized mixture with increased curing time. Compressive strengths were obtained mainly from unconsolidated undrained triaxial tests and

unconfined compressive strength tests which are widely used to evaluate the quality of the stabilized mixture. Many correlations between unconfined compressive strength and significant engineering parameters are reported in the literature (99). Triaxial compression tests were conducted on the samples to simulate the stress-strain behavior under field conditons.

At the inception of this study, the optimum proportion for bentonite-fly ash-lime mixture was determined. To understand the relative effect of each component of the mixture, bentonite-lime, bentonite-fly ash, fly ash-lime and fly ash mixtures were prepared. The compaction moisture contents were determined. The samples were compacted and cured for one day, 28, 90 and 180 days at 23°C and 50°C. Triaxial and/or unconfined compression tests were conducted on the cured samples, stress-strain curves and the elastic moduli were obtained. Broken samples were prepared for X-ray diffraction and scanning electron microscope analyses. Scanning electron micrographs and X-Ray diffractograms were used to identify newly forming minerals. Ca/Si and Al/Si ratios were obtained by an energy dispersive spectral analyzer at selected points. The flow chart for the study is presented in Figure 2.

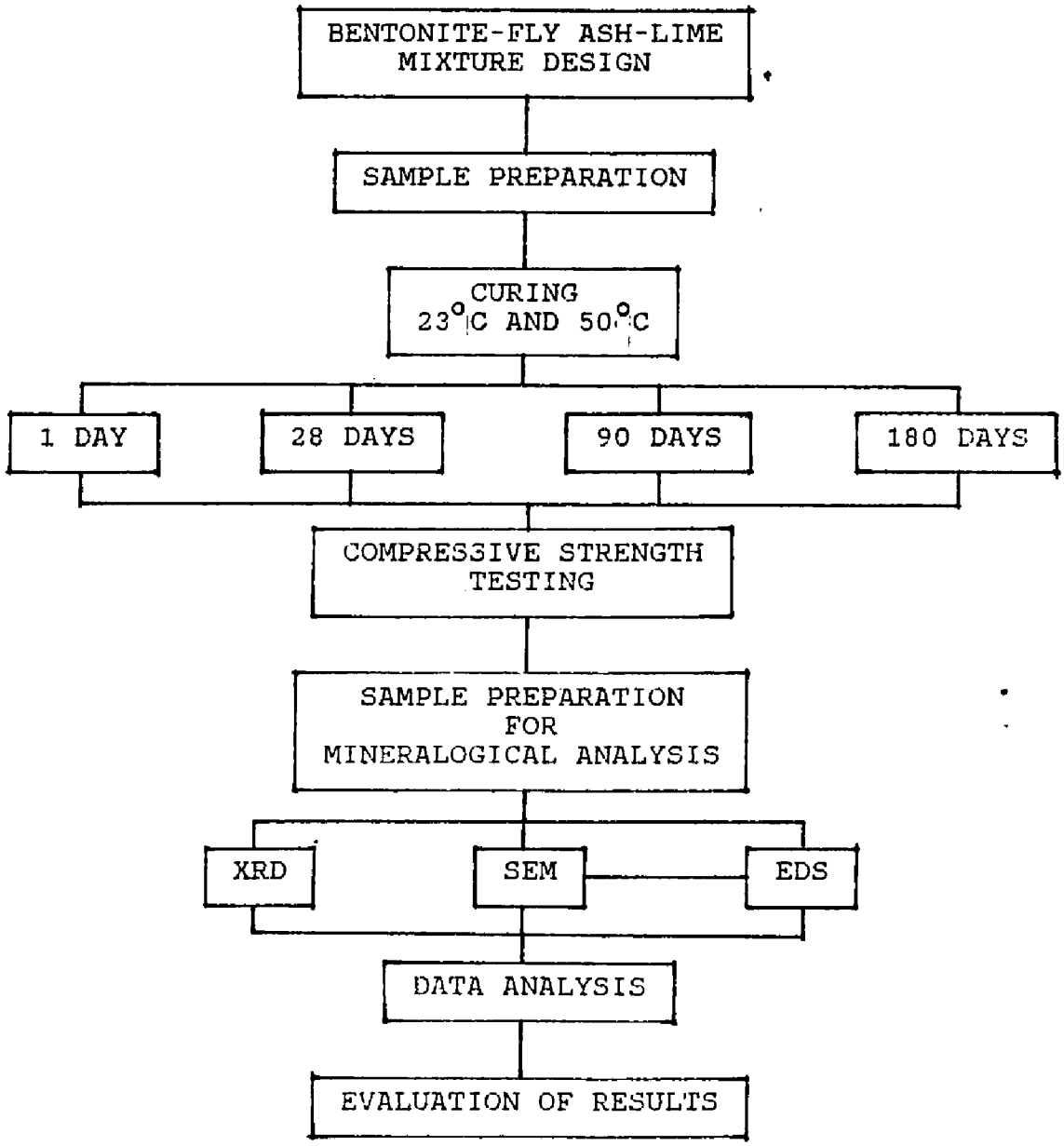

Figure 2. Flow Chart of the Study.

Mixture Design

In this study the amount of lime to stabilize bentonite has been determined by Eades and Grim's pH method (27) and Hilt and Davidson's plastic limit method (45). According to Eades and Grim the percentage of lime which increases the pH of the mixture to 12.4 (the pH of lime saturated solution at 25°C is 12.4) is the optimum lime modification point. Bentonite-lime slurries with one to eight percent lime by dry weight were prepared and the pH values were obtained after one hour. The increase in pH with increasing lime percentage is presented in Figure 3. The pH of bentonite is 9.5 and increases to 12.4 with the addition of four percent lime by dry weight and no further increase in pH is observed. The optimum lime addition for bentonite is four percent by dry weight.

Hilt and Davidson's (45) method uses the plastic limit to determine the optimum lime content. The plastic limit of the mixture increases as the lime percentage increases and then it levels off. The lime percentage at which the increase in plastic limit stops is the quantity required for stabilization. The results of plastic limit tests of bentonite with different lime percentages are presented in Figure 3. The plastic limit corresponding to three percent lime by dry weight is 45 and it increases to 56 with the addition of 5.5 percent lime. The plastic limit slightly increases to 57 with 6.5 percent lime by dry weight and then levels off.

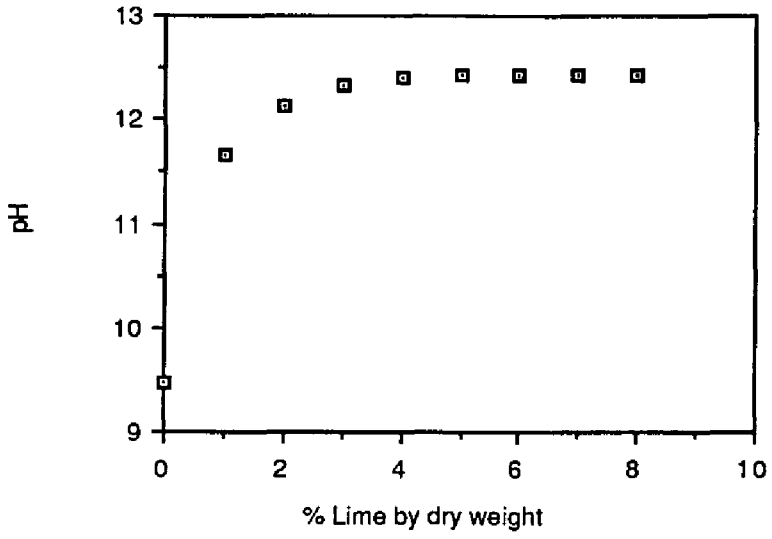

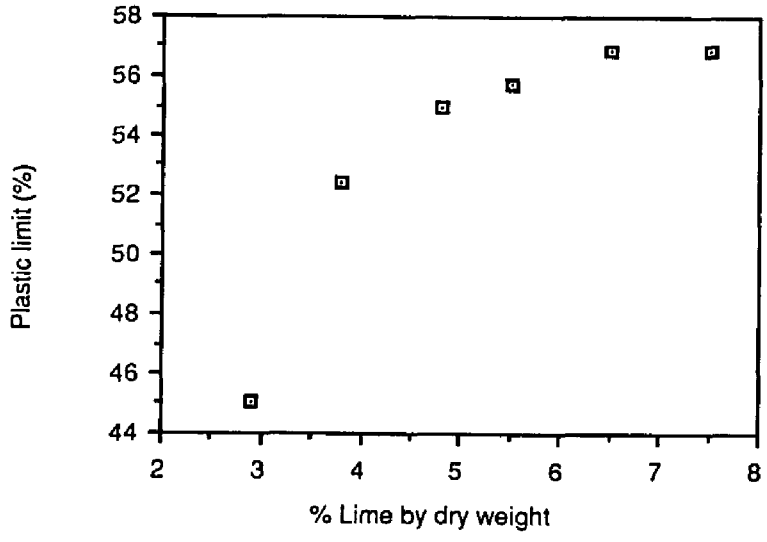

Figure 3. pH and Plastic Limit of Bentonite-Lime Versus % Lime.

Based on these data the optimum lime content for stabilization of bentonite appears to be 6 percent by dry weight. Five percent lime by dry weight of bentonite, the average of the two estimates, was used in this study.

To determine the amount of fly ash to be added to the bentonite-lime mixture, different percentages of fly ash were added (8.5 to 30 percent by dry weight of the total mixture) and samples were compacted at 33 percent water content and cured for one day at 23°C after which unconfined compressive strengths were determined. The results are presented in Figure 4. The unconfined compressive strength of the bentonite-lime mixture with the addition of 8.5 percent fly ash developed 716 kPa (103.7 psi) and remained the same as the fly ash percentage was increased to 12.3 . A sharp increase in unconfined compressive strength to 1147 kPa (166.1 psi) was observed when the amount of fly ash was increased from 12.3 to 21.9 percent. With 30 percent fly ash addition, the unconfined compressive strength increased to 1245 kPa (180.3 psi). The dry densities increased from 1.19 to 1.32 Mg/m^3 (74.3 to 82.4 pcf). Based on the above results, 20 percent fly ash by dry weight was selected as the mixture to be studied throughout this study. With 20 percent fly ash addition a considerable strength increase was observed. It is obvious that the strength increase will continue with more fly ash addition but using very high percentages of fly ash (above 25, 30 percent) is not typical in soil stabilization.

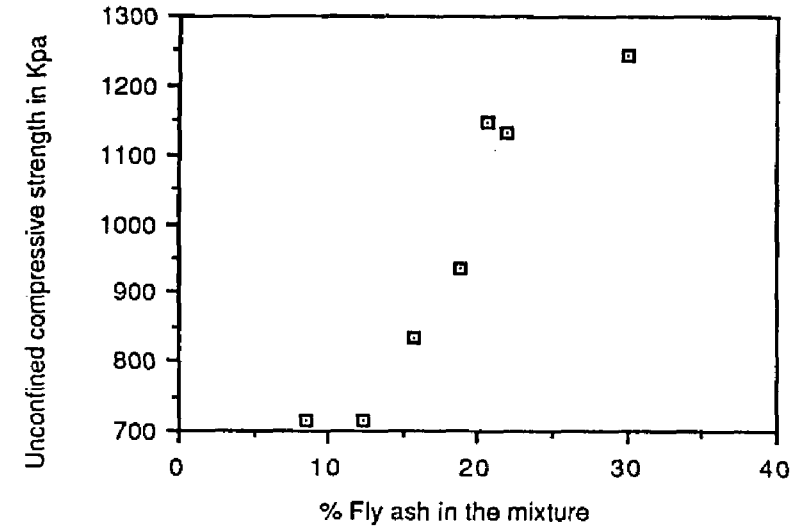

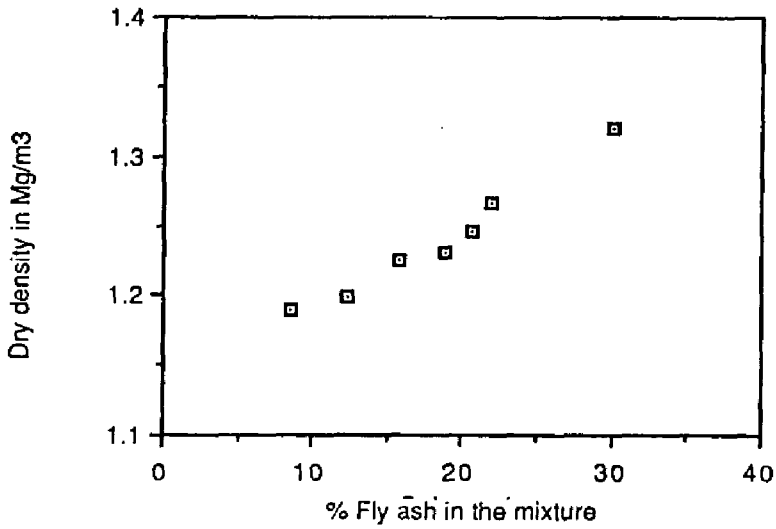

Figure 4. The Effect of Fly Ash Percentage on Unconfined Compressive Strength and Dry Density of Bentonite-Fly Ash-Lime Mixture, Compacted at 33% Water Content, Cured for One Day at 21°C.

The unconfined compressive strength and dry density versus water content curves for different percentages of fly ash for bentonite-fly ash-lime mixtures are presented in Appendix A. Generally for all fly ash percentages, the unconfined compressive strength increased with increased water content up to a certain water content, and at higher water contents a decrease was observed. Generally, dry densities decreased with increase in water content to around 30 to 35 percent. The water contents corresponding to maximum unconfined compressive strengths were selected to compact the samples. The mixture proportion for this study is selected to be: 75 % bentonite , 20 % fly ash , 5 % lime by dry weight.

The effects of only lime or fly ash additives on microstructure development and strength were assessed by removing one additive from the principal mixture at a time. The dry weight ratios of the remaining materials were the same as the dry weight ratios in the principal bentonite-fly ash-lime mixture. Pure fly ash samples and fly ash-lime mixtures were prepared to observe the cementitious minerals forming in the mix during hydration. The percentages by weight and codes used to identify each mixture are summarized in Table 4.

TABLE 4

THE MIXTURE PROPORTIONS AND CODES

Mixture	Code	% Bentonite	% Fly ash	% Lime
Bentonite-Fly Ash-Lime	S	75	20	5
Bentonite-Fly ash	F	79	21	0
Bentonite-Lime	L	94	0	6
Fly ash-Lime	FL	0	80	20
Fly Ash	FA	0	100	0

A Harvard miniature compaction device was used to mold the samples. This apparatus consists of a compaction mold, specimen mold holder, tamper, collar remover and specimen ejector. The mold has an inside diameter of 3.334 cm (1.313 in) and a height of 7.153 cm (2.816 in). The compaction tamper consists of a rod and spring mechanism. Two springs are available with the compaction tamper which can be adjusted to 89 N (20 lb) and 178 N (40 lb) loadings. In this study the 89 N (20 lb) spring is used. The compaction is done by inserting the tamper into the mold until it is in contact with the surface of the soil and then pressing down firmly until the spring starts to compress. This compaction method is assumed to duplicate the kneading action of sheepsfoot rollers. The suggested ASTM method for Harvard compaction apparatus states that a minimum of 5 layers and 10 tamps, at a rate of 10 tamps per 15 seconds, per layer are needed to obtain reproducible results. The comparison of the densities achieved by standard proctor and Harvard miniature compaction tests

for bentonite is presented in Figure 5. The Harvard test with 10 tamps per layer for 5 layers produces slightly higher densities than the densities obtained by the standard proctor test for bentonite. The optimum water content increased from 20 percent for standard proctor test to 34 percent for Harvard compaction test and the maximum dry densities obtained are 1.23 Mg/m^3 (76.8 pcf) and 1.33 Mg/m^3 (82.99 pcf), respectively. Because the compaction effort used for standard proctor test is of impact type as opposed to kneading action of Harvard miniature compaction test the optimum water contents are different.

Constituents for one sample at a time were weighed, mixed and compacted to minimize the possibility of reactions occuring before the test samples were made. For compaction the mass of each lift was controlled. The compacted samples were wrapped in cellophane film and placed in plastic bags which in turn were placed in the humidity room for 23°C curing or in an oven for 50°C curing.

Determination of Compaction Water Contents

During the determination of the percentage of fly ash in the bentonite-lime-fly ash mixture it was observed that the unconfined compressive strength increased with increasing water content eventhough the dry density decreased. It is very difficult to decide on an optimum water content in the classical sense. Supposedly, the higher the dry density the higher

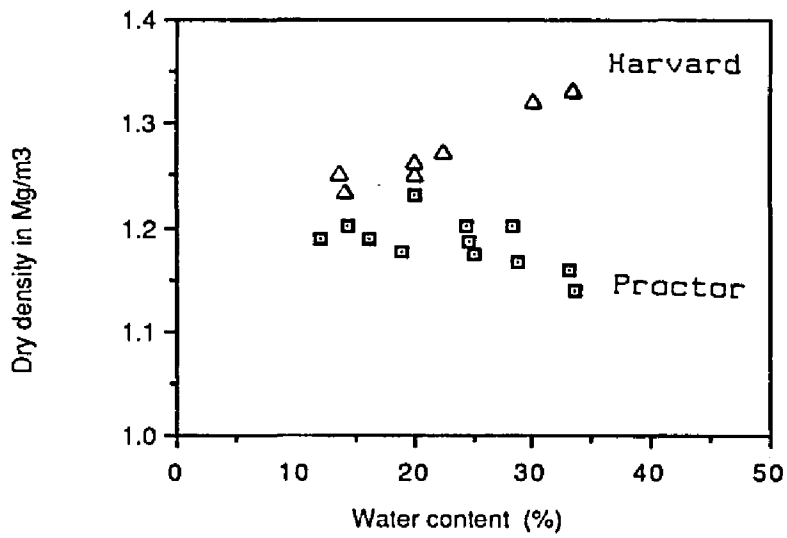

Figure 5. The Water Content-Density Relationship for Bentonite from Standard Proctor and Harvard Miniature Compaction Tests.

will be the compressive strength. The water content corresponding to the maximum compressive strength would be used instead of water content corresponding to the maximum dry density because this water content (corresponding to maximum UCS) is thought to promote the optimum development of cementitous products.

Bentonite-fly ash-lime; bentonite-fly ash; bentonite-lime; fly ash-lime; and fly ash were compacted at different water contents, cured for one and seven days , and their unconfined compressive strengths were determined. All samples were compacted immediately after mixing and they were cured at 23°C. A Soiltest Model U600 unconfined compressive strength testing machine was used. The strain rate was maintained at 0.25 mm/min (0.01 in/min). The unconfined compressive strength and dry density versus water content curves for one and seven day-cured samples are presented in Appendix A. The water contents that will be used in the mixtures are shown in Table 5.

TABLE 5

THE COMPACTION WATER CONTENTS OF MIXTURES

Mixture	Code	Water Content (%)	Dry Density (Mg/m^3)
Bentonite-Fly ash-Lime	S	34	1.25
Bentonite-Fly Ash	F	24	1.40
Bentonite-Lime	L	40	1.15
Fly ash-Lime	FL	20	1.65
Fly ash	FA	11	1.90

Triaxial and Unconfined Compression Tests

The samples were tested by using an ELE loading frame, ELE triaxial cell, ELE constant pressure cell, 7 kN load cell , Transtek model 3132 LVDT and Hewlett Packard data acqusition system. The strain rate used was 0.25 mm/min. Samples with and without confining pressure were tested with a thin membrane wrapped around them. Water was used as the confining media. Obtaining the unconfined compressive strengths and the elastic moduli were the objectives of these tests. Because low confining pressures are involved with stabilized base and subbase material, a confining pressure of 100 kPa (14.5 psi) was used.

Three tests with zero kPa and three tests with 100 kPa confining pressure were conducted for each curing period and

temperature for the bentonite-fly ash-lime mixture. A total of three samples were tested for each curing time and for each temperature for bentonite-fly ash, and bentonite-lime mixtures , two with no confining pressure and one with 100 kpa confining pressure.

Fly ash-lime and fly ash samples were tested by compression testing device (Cox and Sons, Inc.) with a 223 kN (50000 lb) Strainsert brand load cell, at a strain rate of 0.25 mm/min (0.01 in/min). A total of 24 samples for fly ash-lime and 16 samples for fly ash were tested with no confining pressure.

The 50°C cured samples were removed from the oven prior to testing and tests were conducted after they were cooled to room temperature (about 23°C) . Each sample was weighed and three diameter and three height measurements were taken prior to testing. After the tests were completed the samples were measured again and they were prepared for scanning electron microscopy, X-Ray diffraction and water content determinations.

Sample Preparation for SEM and XRD

The surface to be studied by SEM may be prepared by fracturing or cutting. Cutting is a shearing action which induces damage. Fracture surfaces are likely to correspond more closely with the original undisturbed state because there are fewer steps in their preparation relative to techniques such as embedding in resin, sectioning, polishing

and etching (33). However, fracture surfaces are not random sections, they are biased to areas with lower tensile strengths.

The sample from the compression test was placed on a plexiglass plate and ten, 0.5 to 1.0 cm subsamples were obtained by bending and fracturing. Large chunks were first broken with the help of a knife and they were further crumbled into smaller pieces by hand. Representative pieces were put into 15 ml vials and sealed for freezing and vacuum drying. Care was taken not to pick up any portion of the sample disturbed by the knife. The remaining portion of the sample was placed into an oven at 105°C for water content determinations. After drying, the samples were placed in plastic bags , sealed and stored for further evaluation by X-Ray diffraction and plastic limit tests.

The fabric observed by the scanning electron microscope (SEM) is affected by the sample preparation technique. Since the electron microscope operates under high vacuum, the specimen must be dry (33). Otherwise gas evolution and evaporation may cause enough pressure in the instrument to create electrical discharge from the high voltage terminal or the image quality may deteriorate due to charge build up on the specimen. The molecules of gas and vapor coming off the sample may also scatter the electrons causing a loss in resolution . The best drying technique should ensure that the morphology of the minerals and their spatial dispositon in the sample examined are the same as in the natural state of the material (68).

There are three commonly used techniques to dry samples for observation with scanning electron microscope: air drying, freeze drying and critical point freeze drying.

Air drying may be suitable for stiff soils, partly saturated soils, and other soils that do not undergo significant shrinkage. In more plastic soils as water is removed surface tension forces further increase the compressive forces on the soil fabric and may seriously modify the arrangement of the particles (33).

The principal idea behind freeze drying is to quickly freeze the sample and remove the glassy ice by sublimation under vacuum. While the ice is being removed no meniscus should form in the pores and capillary spaces between the particles so surface tension forces and fabric disruption are absent. The sample is quench frozen by immersion in liquid nitrogen, liquid freon, liquid propane, or a variety of other liquids.

The third method of drying is the critical point method. At a temperature and pressure above a certain critical point, the physical properties of a liquid and its vapor become undistinguishable . The two phases are no longer seperated by a boundary layer and surface tension forces vanish . By this technique the water may either be removed directly or first be replaced by a water-miscible liquid such as alcohol and the new liquid phase is subsequently removed at a temperature and pressure above its critical point.

In this study freeze drying, with liquid nitrogen as the freezing agent, was used and vacuum drying was performed at

room temperature without a refrigerant. The use of liquid nitrogen for freezing also served to stop the reactions after compression tests. Small pieces of each sample were dipped into liquid nitrogen for 2 minutes. Frozen samples were immediately transfered to a desiccator and 30 miliTorr vacuum was applied to dry the specimens. After 24 hours the samples were put into 15 ml vials, sealed and stored for coating.

Coating of SEM Samples

All nonconductive materials must be coated with a thin layer of conductive material in order to be observed by SEM. Most of the samples were gold coated by using a sputter coater. Selected samples were carbon coated by the evaporation technique. Although gold coating gives very low X-Ray count rate and gold peaks coincide with the sulphur peak, most EDS analyses were conducted on gold coated samples. The gold coated samples produced the highest resolution images.

Methodology for SEM Study

One problem with the SEM is establishing the representative nature of photos because the operator often photographs the most unusual features. To avoid this, the whole sample was surveyed at a magnification of 350* and a portion of the sample with minimal topographical change was selected, and

photographed. The magnification was increased to 2000* and a minimum of 20 frames were studied and representative pictures taken. Energy dispersive spectral X-Ray analyses were conducted on special interest areas and elemental compositions were plotted. When needed, pictures at higher magnifications such as 5000 and 10000* were taken. Notes describing special features and operating conditions were recorded in a log book. Representative scanning electron micrographs are presented in the results section. Low magnification refers to 350* magnification photomicrographs and intermediate magnification refers to ones taken at magnifications from 2000 to 3500* . Over 5000* magnification photos are discussed as high magnification ones in the text. Bar scales on all photomicrographs permit the direct comparision of crystal sizes.

X-Ray Spectrum Analysis

There are two types of equipment commonly used for X-Ray chemical determinations: Wavelength dispersive spectrometers (WDS) and energy dispersive spectrometers (EDS) . The wavelength dispersive spectrometers identify the characteristic X-Rays by diffraction from crystals. The energy dispersive spectrometers segregate X-Rays according to their energy.

EDS is useful in obtaining rapid qualitative analysis of a sample while WDS is prefered for quantitative information and analysis of light or trace elements. In this study, the energy dispersive spectrometer was used. Ca/Si and Al/Si

ratios were obtained from EDS analyses and the data are presented in the results section. The wavelength dispersive spectrometer was used to obtain the chemical compositions of individual fly ash grains. The results are presented in the materials section.

Some Limitations of X-Ray Analysis

To conduct an X-Ray analysis, considerations must be given to count rate, geometry, take off angle, specimen topography and specimen preparation. In a typical EDS analysis, a total of thousands to hundreds of thousands of X-Ray counts are accumulated . If the count rate is too low, a long period of analysis is required and the extended interaction of the primary electron beam damages the specimen. It was established that 60 seconds was adequate for most samples and it minimized damage to the specimen.
If the take off angle is low, the X-Rays generated within the specimen must travel a greater distance through the specimen to reach the detector, resulting in the increased absorbtion of X-Rays and a lower count rate. During all SEM analyses, lowest possible specimen height settings were used to maximize the take-off angle. For rough specimens, each point on the specimen may have a different effective take off angle. In addition, the specimen topography may bias an analysis through the greater absorbtion of X-Rays from one area than from another. Increased working distance, tilting and observation

of the specimen from several different orientations may partially alleviate this problem but will not eliminate it entirely (78). In this study the Ca/Si and Al/Si ratios varied widely in the same specimen. The fractured surfaces were rough and protrusions and depression areas may have caused serious problems in X-Ray analyses.

X-Ray Diffraction Methodology

A Philips APD-3720 X-Ray diffractometer with Cu K-alpha radiation and a diffracted beam monochromator was used. The peak heights and d-spacings were analyzed with a Digital Research Corperation mini computer with the Philips APD software.

The ovendried sample which was stored in a sealed plastic bag, was placed on a plexiglass plate and ten, one cm chunks were broken from the sample and ground with a hand tamper. Then the powder was placed into a mechanical grinder for 15 minutes. The powder was loaded in a specimen holder by using a side loading technique to obtain random orientation. The X-Ray diffractograms were obtained from two degrees to 70 degrees two-theta. The d-spacings of various cementing compounds which were obtained from the literature were input into the computer and an APD peak search program was run. Peak overlap, poor crystallinity of the newly formed cementitious minerals, and the weight percentages of reaction products prevented the successfull application of the automated

identification routines. Manual identification procedures were followed after stripping the montmorillonite peaks from the sample diffractograms. The powder X-ray diffractograms are presented in the results section and complete listings of peaks are tabulated in Appendix B.

CHAPTER IV

MATERIALS

Bentonite

The bentonite, Aquagel, was supplied by NL Industries Company, Houston, Texas in powder form. A representative X-Ray powder diffractogram of bentonite with the major peaks labeled, is shown in Figure 6. The major mineral constituents are montmorillonite (M) and quartz (Q). Calcite (K), feldspar (F), biotite (B) and hematite (H) are also present. Small unidentified peaks are present with d-spacings of 2.33A (1), 1.87A (2), 1.79A (3), 1.78A (4), and 1.62A (5). As seen from the high background in the 20 to 30° two-theta region, amorphous material is also present. A complete listing of the observed d-spacings is presented in Appendix B.

Fly Ash

The fly ash used in this study was obtained from Cajun Electric Company Power Plant, near New Roads, Louisiana. Three five gallon containers were filled with fly ash and sealed. In the laboratory these three containers were mixed and placed into one gallon air-tight tin cans lined with air-tight plastic bags to prevent the further reaction of the fly ash with atmospheric moisture.

The physical and chemical properties of fly ash are

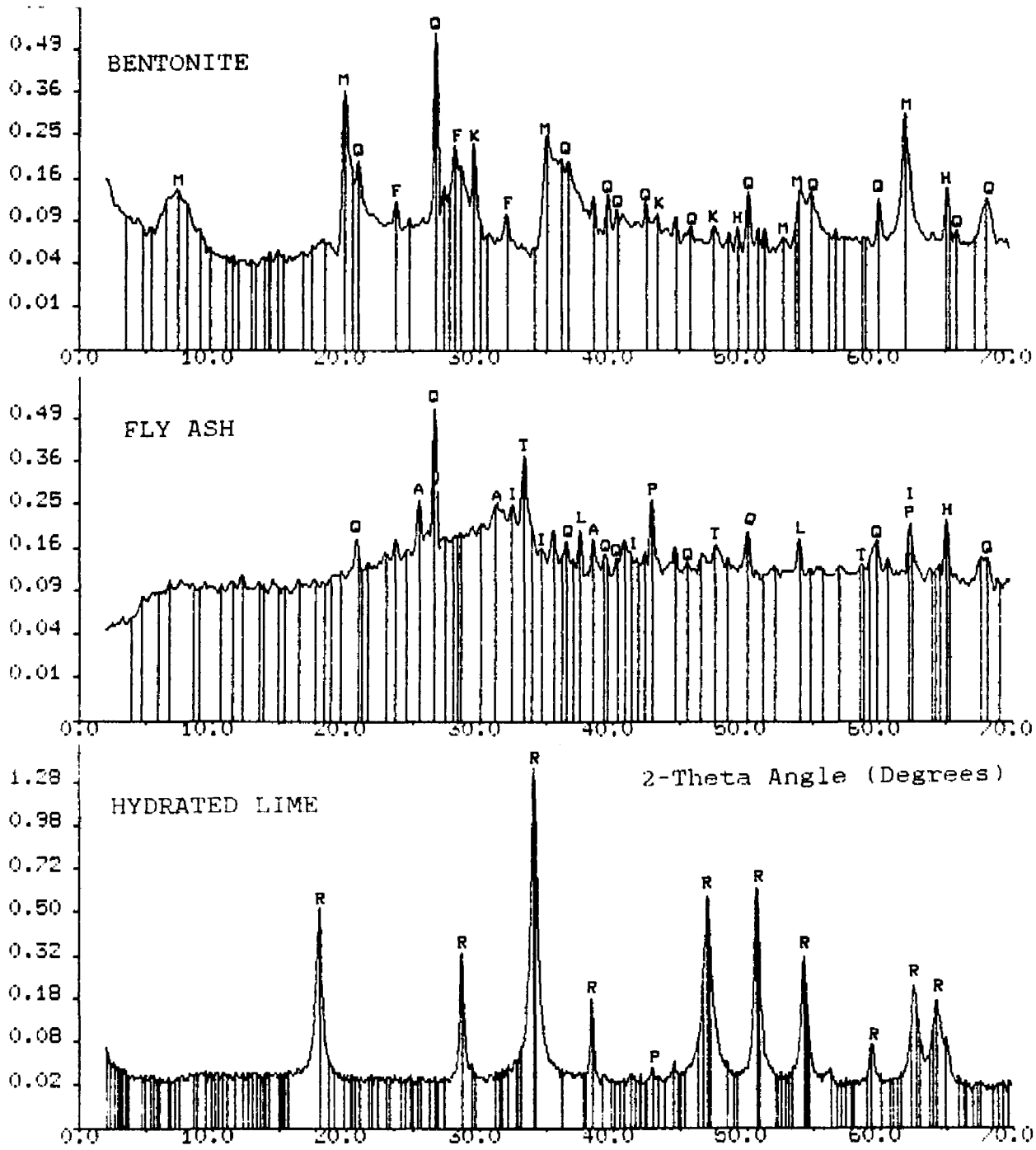

Figure 6. Powder X-Ray Diffraction Patterns of Bentonite, Fly Ash, and Hydrated Lime. Q=quartz, M=montmorillonite, F=feldspar, K=calcite, H=hematite, A=anhydrite, L=lime, T=tricalcium aluminate, R=portlandite, I=alite, P=periclase. For d-spacings presented by numbers refer to the text.

presented in Table 6. This fly ash is an ASTM Type C fly ash. It was found to have a 22.3 % lime (CaO) content.

The fly ash is composed of varying diameter spheres and finely crystalline powdered material. The smallest crystals are most probably anhydrite and other soluble phases. The chemical compositions of the spheres vary. Microprobe analysis of 40 fly ash grains revealed that these spheres may be grouped in four categories according to their chemical compositions. Bar diagrams illustrating their chemical compositions are presented in Figures 7 and 8. The first category has a $SiO_2 + Al_2O_3$ content of more than 75 percent. The second category has a $SiO_2 + Al_2O_3$ content between 50 and 75 percent. The third category has $SiO_2 + Al_2O_3$ content between 50 and 30 percent. The second and third categories of fly ash spheres have considerable quantities of CaO. The fourth category has less than five percent $SiO_2 + Al_2O_3$ and it is mostly composed of FeO. A representative X-Ray powder diffractogram of the fly ash is presented in Figure 6. The identified mineral constituents are quartz (Q), tricalcium aluminate (T), periclase (P), anhydrite (A), lime (CaO) (L), alite (I), hematite (H) and magnetite (MA). Amorphous material is evident by the high background between 20 to 30 ^{o} two-theta.

The presence of tricalcium aluminate, anhydrite and lime is the major reason for the self-cementitious behavior of this fly ash. Periclase is generally considered to be

TEST PROPERTY	VALUE
TYPE	BAYOU
TESTED FOR CLASS	C
PHYSICAL PROPERTIES:	
FINENESS, % RET. #325	17.2
PAI WITH CEMENT,28 DAYS,% OF CONTROL	106.2
WATER REQUIREMENT, % OF CONTROL	90.2
AUTOCLAVE EXPANSION, %	+0.05
SPECIFIC GRAVITY	2.66
SP.GR.UNIFORMITY,%VAR.FROM AVG.	1.1
FINENESS UNIFORMITY,PCT.PTS.FROM AVG	2.1
CHEMICAL PROPERTIES:	
LOSS ON IGNITION, %	.85
SULFUR TRIOXIDE, %	1.6
TOTAL OXIDES, %	69.5
CALCIUM OXIDE, %	22.3
MAGNESIUM OXIDE, %	4.2
ALKALIES, %	.72

Table 6. The Chemical and Physical Properties of the Fly Ash Used in the Study.

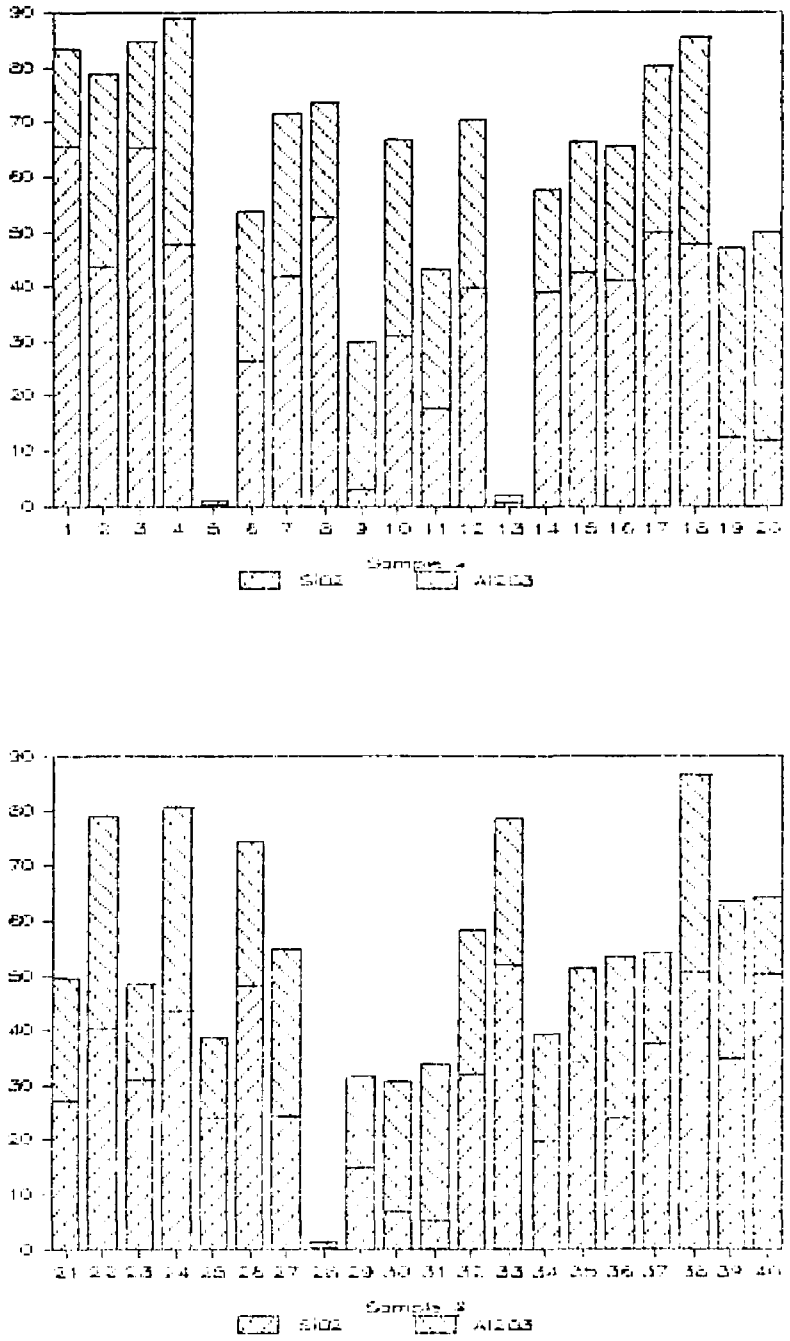

Figure 7. Bar Diagrams Representing the Weight Percent of SiO_2 and Al_2O_3 in 40 Fly Ash Spheres. Individual Spheres were Analyzed with the Electron Microprobe.

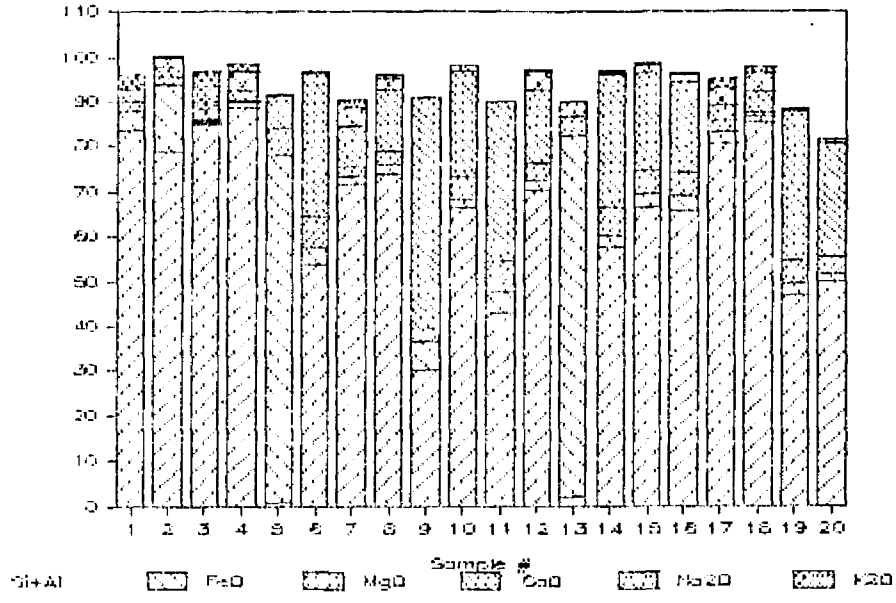

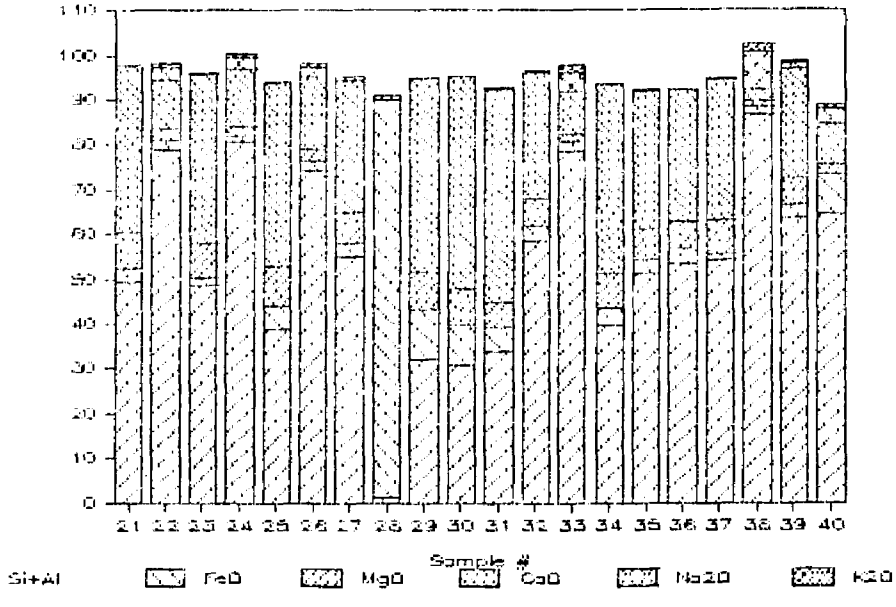

Figure 8. Bar Diagrams Representing the Weight Percent of FeO, MgO, CaO, Na_2O, K_2O and Combined SiO_2 and AlO_2 in 40 Fly Ash Spheres. Individual Spheres were Analyzed with the Electron Microprobe.

unreactive under normal temperature and pressure. The unidentified peaks are 3.75A (1), 2.64A (2), and 2.02A (3).

Hydrated Lime

The hydrated lime was supplied by the Pelican Company, Baton Rouge, Louisiana. A chemical analysis of the hydrated lime yielded 99.5 percent CaO and MgO (calcitic lime). A representative X-Ray powder diffractogram of lime is presented in Figure 6. The major component is portlandite (R). A trace of periclase (P) and calcite (K) are also present.

CHAPTER V

RESULTS

In this chapter the results of physical and mineralogical tests will be presented for in the order: fly ash, fly ash-lime, bentonite-fly ash, bentonite-lime, bentonite-fly ash-lime. Results for samples cured at 23°C will be discussed first in each section. For each mixture, the stress-strain curves will be discussed then the micromorphology of the mixture at different curing periods will be presented with a set of micrographs. Finally the X-Ray powder diffraction patterns will be presented.

Fly Ash (Cured at 23°C)

The changes in the unconfined compressive strength (UCS) of hydrated fly ash are illustrated in Figure 9. After 28 days of curing the UCS increases from 10237 kPa (1482.3 psi) to 18367 kPa (2659.5 psi). A minor increase to 19745 kPa (2859.1 psi) is observed between 28 and 90 days. The 180 day-cured sample has an unconfined compressive strength of 26030 kPa (3769.1 psi). These values are one order of magnitude greater than the highest unconfined compressive strength values obtained for bentonite-fly ash, bentonite-lime, and bentonite-lime-fly ash mixtures. The increased compressive strength can be attributed to the formation of

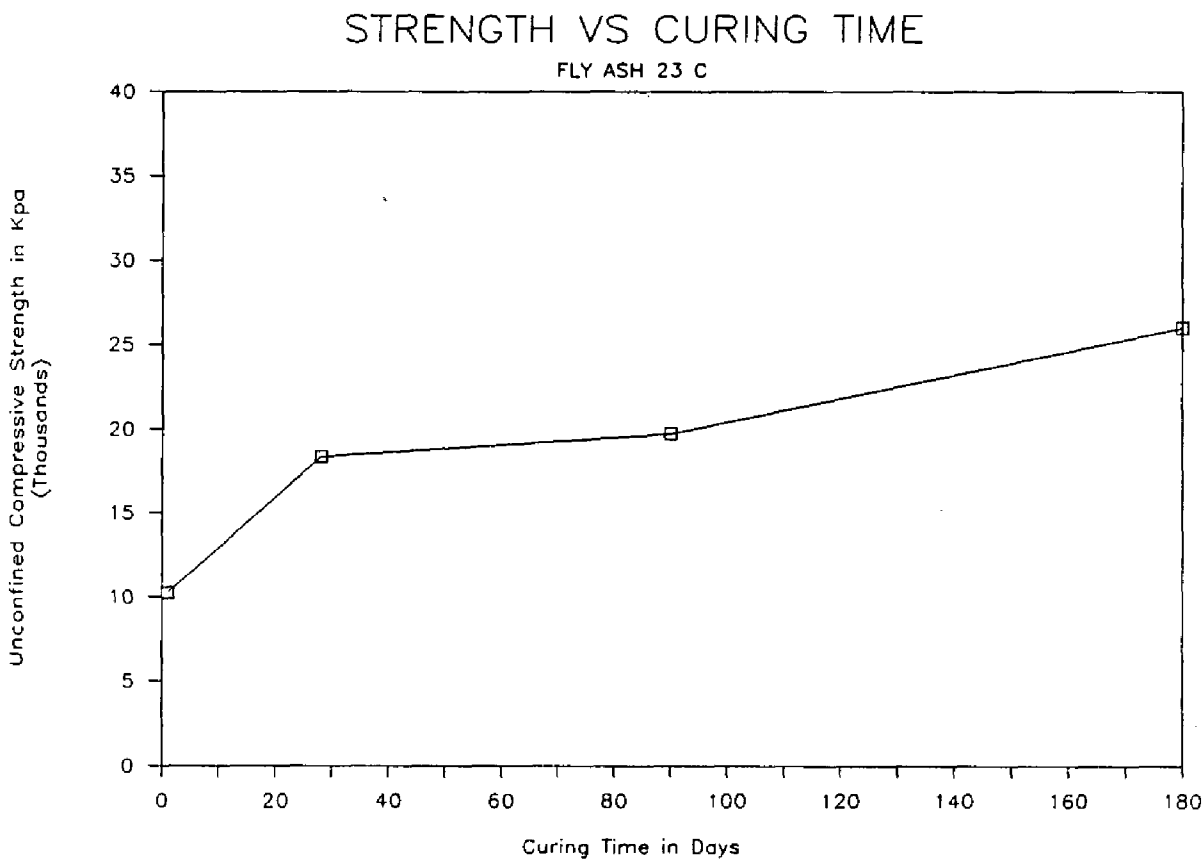

Figure 9. Unconfined Compressive Strength Versus Curing Time for Fly Ash Cured at 23°C.

cementitious compounds between fly ash spheres during curing.

Figure 10A shows the unreacted fly ash in powder form. Fly ash is mostly composed of spheres with diameters ranging from 0.5 to 20 micrometers. Larger spheres up to 100 micrometers in diameter may also be present. Note that the spheres are very distinct and there are no fine cementing crystals between the fly ash spheres. With the addition of water and curing for varying lengths of time some materials are dissolved and reprecipitated to form cementitious compounds in the voids. At low magnifications the fly ash particles appear to be embedded in a continous cement matrix (Figure 10B, one day cured). The matrix after 90 days of curing (Figure 10C) appears more densely packed than the matrix in the one day cured sample (Figure 10B). At intermediate magnifications (Figure 10D) CSH Type I needles (N) protrude into the pore walls in some areas as a result of crystallization from the amorphous appearing cementitious matrix (M).

The detailed morphology of the cementing crystals is illustrated in Figures 11A, 11B, 11C and 11D . The dominant features are CSH Type I and Type II needles. The CSH Type I needles, protruding into the pores are approximately three micrometers long. The faces of these crystals are roughly parallel but they narrow toward their outer ends. Type II CSH crystals (N) are similar to those of type I but they form a three dimensional interlocking network composed of

Figure 10. Scanning electron micrographs of original and cured fly ash samples. A) Loose spheres and fine crystals characterize the unreacted fly ash. B) Fly ash spheres (S) are encased in a matrix (M) in samples cured at 23°C for one day. C) The development of the matrix presented in B, is seen after 90 days of curing at 23°C. Plates (P) are bridging the pores. D) The fracture surface presented at B at intermediate magnification. The matrix (M) engulfs the fly ash grains (S) and needles (N) protrude into the pores.

A
10μm
C
100μm
B
100μm
D
10μm

Figure 11. Scanning electron micrographs of the cementitious crystals in fly ash cured at 23°C. A) Fine crystals of original fly ash disolved and formed a matrix of three-dimensional network of needles (N) supporting fly ash grains (S) after one day of curing. B) Hexagonal plates (P) are bridging the pores after 28 days of curing. C) Engulfing matrix (M) and supporting randomly oriented hexagonal plates (P) after 90 days of curing. Note the plates are getting larger. D) Randomly oriented hexagonal plates after 180 days of curing.


A
10µm
B
10µm
C
10µm
D
10µm

0.5 to 1.5 micrometer long needles (Figure 11A, one day cured). The fly ash spheres are less distinct because some have begun to react and others are covered with cementitious products.

After 28 days of curing, hexagonal plates (P1, P2) are seen in the pores (Figure 11B). They are very thin and less than five micrometers across. They may form roughly parallel or randomly oriented aggregates which fill the pores between the particles and act as braces in the pores. Their development and orientation seems to depend on the availability of open pore space. The aggregate in the larger circular pore space (P1) is randomly oriented and composed of smaller crystals than at (P2) where the roughly parallel plates are found along the walls of an elongated pore. The plates are five to seven micrometers across and less than 0.2 micrometers thick and XRD methods suggest they are tetracalcium aluminate thirteen hydrate (C_4AH_{13}). Needles morphologically similar to CSH Type I and CSH Type II co-exist with these plates.

Figure 11C shows the C_4AH_{13} plates (P) after 90 days of curing. These plates are six to ten micrometers across and less than 0.2 micrometers thick. They are randomly oriented. EDS anlyses of these plates yield a Ca/Si ratio of 1.25 and an Al/Si ratio of 1.47 . After 180 days of curing the plates are ten to twenty micrometers across and less than 0.3 micrometers thick (Figure 11D). EDS analyses of these plates produced a Ca/Si ratio of 2.76 and an Al/Si ratio of 1.47 .

Increased curing time results in thicker plates with a higher Ca/Si ratio.

Figure 12A shows a fractured surface of the 180 day-cured sample at low magnification. A comparision of this fracture surface (Figure 12A) to the fracture surface of the one day-cured sample (Figure 10B) reveals that the pore-filling matrix between the fly ash spheres has become more densely populated with fine crystals and more reaction products are observed. Figures 12B and 12C illustrate representative portions of the cementitious matrix at intermediate magnification. In Figure 12B the imprint of a 55 micrometer diameter fly ash sphere is seen after 28 days of curing. The sharpness of the depression suggests that the fly ash sphere was not altered. A mat of one to three micrometer roughly spherical crystals (SC) connected with fibrous crystals (FC) lines the cavity. The crystals formed a coating on the sphere. The interparticle pores are approximately 0.5 micrometers in diameter . Other fly ash spheres below the mat have radiating needles (N) similar to CSH Type I material on them. EDS analyses of the mat give a Ca/Si ratio of 1.6. Figure 12C illustrates the same features after 90 days of curing. The sizes of the roughly spherical crystals (SC) are similar but there are more fibrous crystals (FC) connecting them. The hexagonal plates are supporting this mat. EDS analyses of the mat yield a Ca/Si ratio of 1.08 and Al/Si ratio of 1.38 . The chemical composition is very similar to the composition of the early-

Figure 12. Scanning electron micrographs of fly ash samples cured at 23°C. A) After 180 days of curing, the matrix has become more densely populated with fine crystals. Hexagonal crystals (P) are seen at low magnification. B) A represantative portion of the cementitious matrix after 28 days of curing at intermediate magnification. The sharpness of the depression from the imprint of a 55 micrometer fly ash grain suggests that the fly ash sphere was not altered. A mat of roughly spherical crystals (SC) connected with fibrous crystals (FC), hexagonal plates (P) and needles (N) are present. C) Same features presented at B after 90 days of curing. The size of the roughly spherical crystals are the same but there are more fibrous crystals connecting them. D) The morphology of the mat at high magnification after 180 days of curing. Roughly spherical crystals (SC) are connected with a three-dimensional network of fibrous crystals (FC).

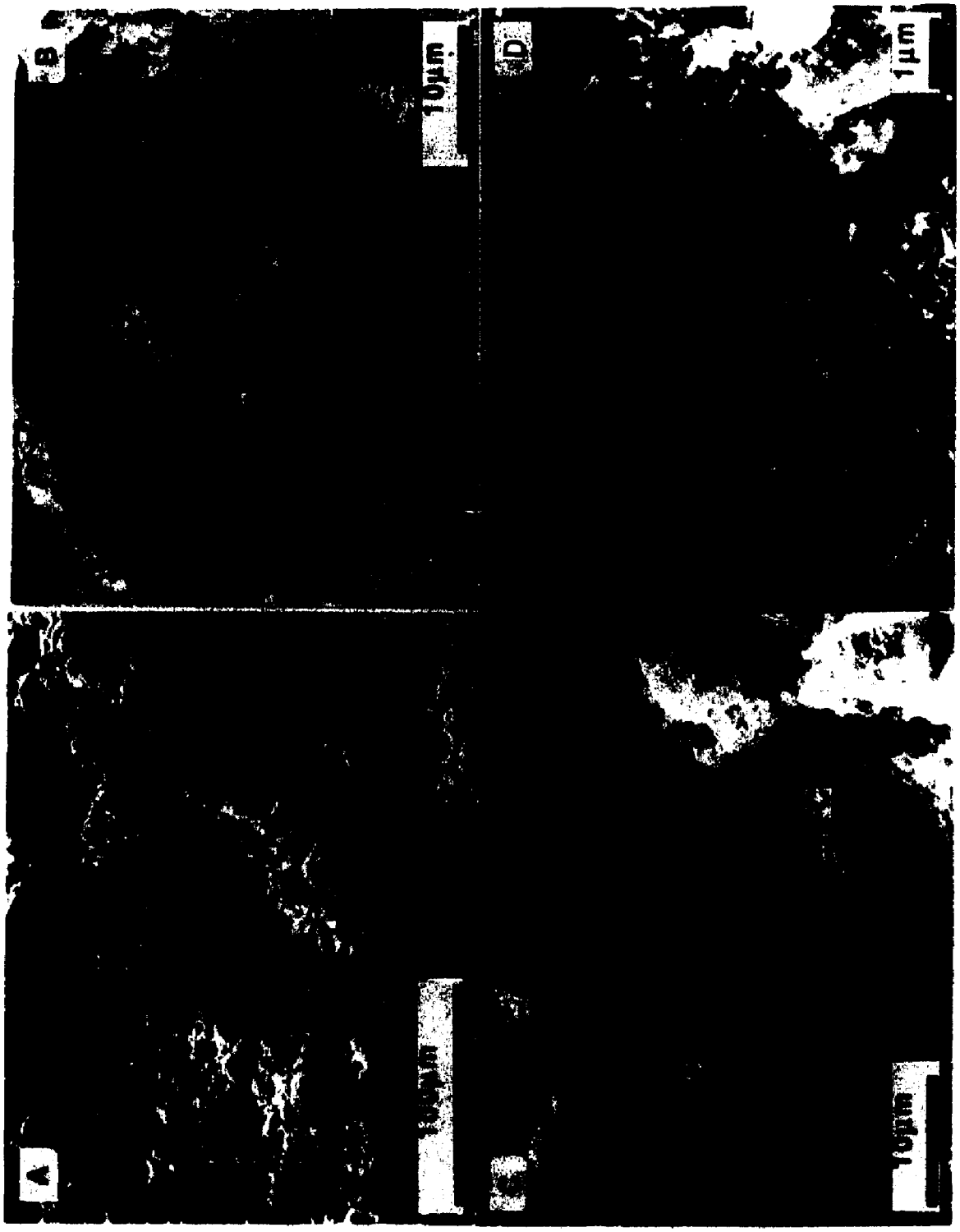
A
10µm
B
10µm
C
10µm
D
1µm

formed (Figure 11B) plates. The mat morphology is better illustrated (Figure 12D) at a higher magnification for the 180 day-cured sample. The diameters of these roughly spherical crystals (SC) range between 0.5 to 1.5 micrometers and they are connected to each other with a three dimensional network of fibrous crystals (FC).

The rigid behavior of the fly ash may be related to the development of this network of roughly spherical crystals supported by plates as illustrated in Figure 11C. In this specimen, a grain was pulled out during fracture exposing how it was supported. The grain was surrounded by plates at the bottom and by the roughly spherical crystal mat at the sides. There was no place for this grain to move so the failure occured at very low strains and because of the supporting mat the strength was improved considerably.

In summary, the pores between the fly ash spheres are spanned by a three dimensional network of fibers . After 28 days of curing, roughly spherical crystals form at the intersection points of these fibers. With increased curing time the fibrous crystals become more numerous. After 90 days of curing hexagonal plates are formed which co-exist with the roughly spherical crystals. These plates span the pores, and with increased curing time the sizes of the plates increase and their Ca/Si ratio is increased. The increase in the number of the fibrous crystals which connect the roughly spherical crystals and the enlargement of the plates result in an improved compressive strength.

X-Ray Diffractograms

XRD patterns for the cured samples are presented in Figure 13. A complete list of all the peaks may be found in Appendix B. The major mineral is quartz (Q) and the peaks produced by it are labeled on the pattern for the one day cured sample. Comparision with the original fly ash (Figure 6B) reveals no change in the relative intensities of these peaks in the samples. Tri-calcium aluminate (T) is the second most abundant mineral. The minor mineral constituents of the original powder , anhydrite, lime, and alite are not as easily recognized in the cured samples. The anhydrite (A) peak is present with a very low peak intensity after one day of curing and it dissappears after 28 days of curing. The intensity of the lime (CaO) peak (L) is very low relative to the intensity in the powder form after just one day of curing. There is no further change in its intensity with longer curing time. The intensity of the tri-calcium aluminate (T) peak decreases with increasing curing time.

The new cementitous minerals that are recognized are CSH Type I and tetracalcium aluminate thirteen hydrate (C_4AH_{13}). In the scanning electron micrographs the CSH Type I minerals are seen as needles and the C_4AH_{13} mineral are seen as thin hexagonal plates. The 8.2A, 2.88A and 2.45A d-spacings are assigned to C_4AH_{13} (G). These peaks are not found in the unreacted fly ash, they appear after one day and the intensity of the 2.45A peak increases up to 90 days of

Figure 13. Powder X-Ray Diffraction Patterns of 1, 28, 90 and 180 Day Cured Fly Ash (Cured at 23°C). Q=quartz, T=tricalcium aluminate, A=anhydrite, G=C_4AH_{13}, C= CSH I, P=periclase, H=hematite, L=lime, I=alite. For d-spacings represented by numbers refer to the text.

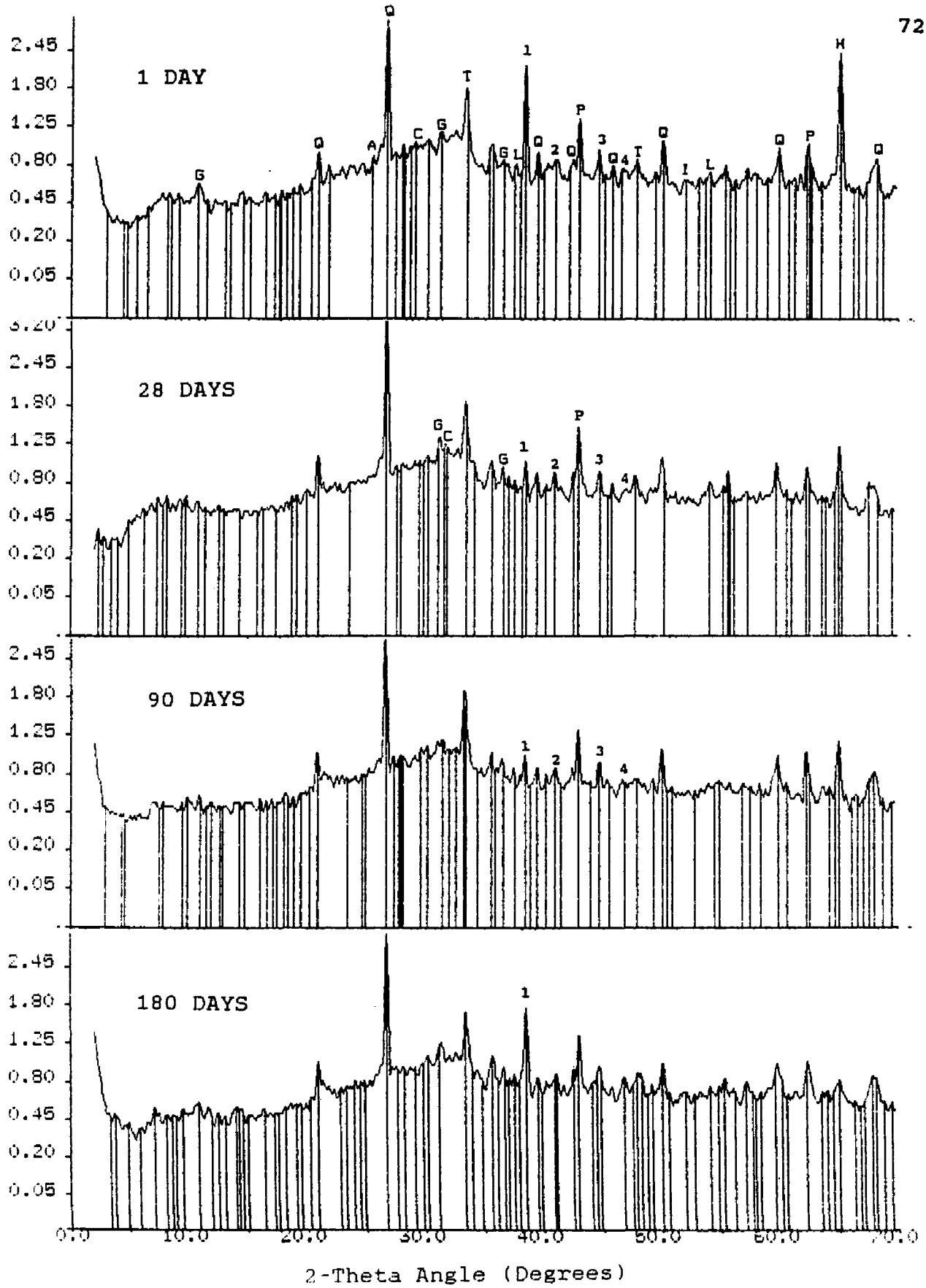
1 DAY
28 DAYS
90 DAYS
180 DAYS
2.45
1.80
1.25
0.80
0.45
0.20
0.05
0.0
10.0
20.0
30.0
40.0
50.0
60.0
70.0
2-Theta Angle (Degrees)

peak which appears after one day of curing and its intensity increases up to 90 days and decreases between 90 and 180 days. A low intensity 3.02A calcite (K) peak is observed after 28 and 90 days of curing and is not seen after 180 days. The intensity of the 1.43A hematite (H) peak fluctuates without a recognizable trend. A decrease in the intensity of the 1.49A alite peak (I) is observed up to 28 days of curing. The intensity of the 2.10A periclase (P) peak does not change. There are other unidentified peaks which are tabulated below. They represent minerals that could not be readily identified because of the absence of additional peaks, low peak intensities, or severe overlap by other minerals.

TABLE 7

UNIDENTIFIED PEAKS IN FLY ASH CURED AT 23°C.

D-Spacing	Remarks
2.33 (1)	Is present in unreacted fly ash, its relative intensity increases at one day,decreases at 28 days and shows a sharp increase at 180 days of curing.
2.21 (2)	Its intensity decreased relative to the unreacted fly ash and then stayed constant.
2.02 (3)	Unchanged.
1.95 (4)	Its intensity is enhanced after 180 days.

The X-Ray diffractograms showed that the major reactive components of the fly ash are tricalcium aluminate, anhydrite and lime. The anhydrite and lime peaks dissappear and the relative intensity of the tricalcium aluminate peak decreases. Tetracalcium aluminate thirteen hydrate and calcium silicate hydrate I are two new minerals that are detected in the X-Ray diffractograms. The low intensities of the peaks assigned to these minerals reveal that the new minerals are present in very small quantities and they are poorly crystalline. Other cementitious minerals may be present but their identities can not be determined by XRD techniques. The data obtained from the scanning electron microscopy complements the identification of the new cementitious minerals. For example the CSH Type I needles seen in the micrographs confirms the assignment of the 3.07A peak to CSH I. The plates are typical of C_4AH_{13} .

Fly Ash (Cured at 50°C)

The changes in the unconfined compressive strength of the 50°C cured fly ash sample with time are presented in Figure 14. The unconfined compressive strength of the one day-cured sample is 10923 kPa (1582 psi) and it increases to 18877 kPa (2733 psi) after 28 days. After 90 days, the unconfined compressive strength is 26948 kPa (3902 psi) and it decreases to 22630 kPa (3276 psi) after 180 days. The 180 day UCS is slightly lower than that recorded for the 23°C cured sample.

At the elevated temperature, the CSH I needles (N) are more numerous than the needles found in the 23°C cured samples (Figure 15A). Roughly spherical crystals are connected with fibrous crystals in the one day cured sample (not shown). After 28 days of curing, the fibrous crystals become more numerous and hexagonal plates are seen in the pore spaces. After 90 days the mat becomes more densely populated with roughly spherical crystals. Figure 15B shows an imprint of a 22 micrometer diameter sphere. During fracturing the outer shell of the sphere broke and half of the impression is covered by the reacted shell (R). The other half is a typical mat . At higher temperatures, the fly ash spheres are more directly in the cementitious reactions. EDS analyses of the shell yield (R) a Ca/Si ratio of 1.53, and an Al/Si ratio of 0.86. The Ca/Si ratio of the

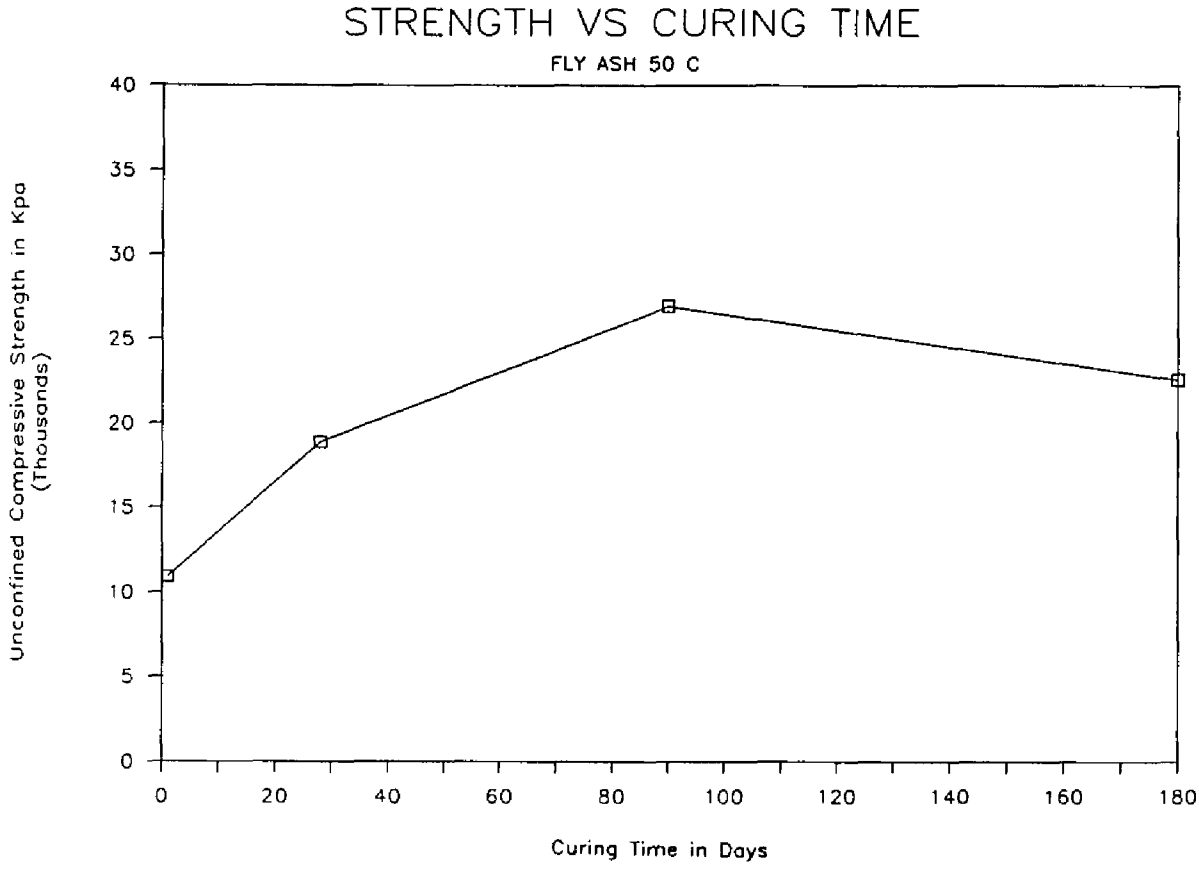

Figure 14. Unconfined Compressive Strength Versus Curing Time of Fly Ash Cured at 50°C.

Figure 15. Scanning electron micrographs of fly ash samples cured at 50°C. A) Needles (N) and the initial stages of plates (P) after one day of curing. Needles radiate on fly ash grains and they protrude into the pores. B) At higher temperatures the fly ash grains are more directly involved in the cementitious reactions. The reacted shell (R) of a fly ash grain is seen after 90 days of curing. C) A representative fracture surface of 180 day cured sample. The mat (M) engulfs the fly ash spheres and the hexagonal plates (P) span the pores. D) Reacted crust (R) on a fly ash grain is seen after 180 days of curing.

A
10μm
B
10μm
C
10μm
D
10μm

The dominant features in the 180 day-cured sample are similar to the ones seen at other curing periods. These features are roughly spherical crystal mats, needles and plates (Figure 15C, intermediate magnification). The mat (M) engulfs the fly ash spheres while the hexagonal plates (P) span the pores. The plates at (P) have a Ca/Si ratio of 2.4 and an Al/Si ratio of 0.69 . The compositions of the plates are different from the ones observed at the lower curing temperature. In Figure 15D there is an eleven micrometer fly ash sphere . Half of it is covered with cementitous material (R) and the other half is not. EDS analyses on both parts showed a very low Ca intensity: for the covered part the Ca/Si ratio is 0.17, the Al/Si ratio is 0.43 and for the uncovered part the Ca/Si ratio is 0.18 and the Al/Si ratio is 0.35 .

In summary roughly spherical crystals are seen as early as after one day and the CSH I needles are more numerous than at the lower curing temperature. Hexagonal plates are present at both curing temperatures.

X-Ray Diffractograms

The powder X-Ray diffractograms of the 50°C cured fly ash samples are presented in Figure 16. A complete list of all the peaks may be found in Appendix B. The X-Ray diffractograms are mostly similar to the 23°C cured fly ash samples. The low intensity anhydrite peak that was present

Figure 16. Powder X-Ray Diffraction Patterns for 50°C Cured Fly Ash. Q=quartz, T=tricalcium aluminate, P=periclase, G= C_4AH_{13}, L=lime, H=hematite, C= CSH I.

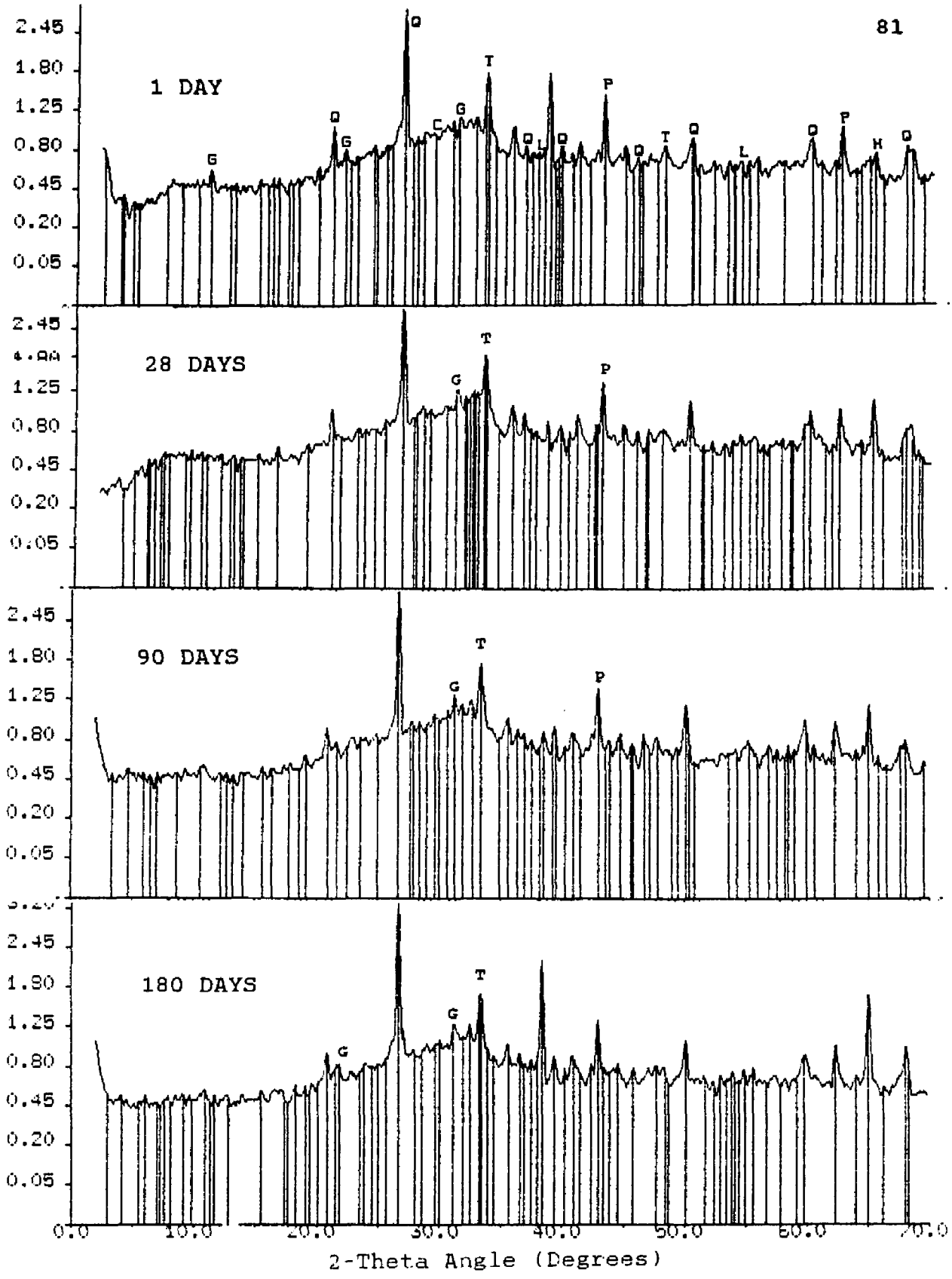
1 DAY
28 DAYS
90 DAYS
180 DAYS
2.45
1.80
1.25
0.80
0.45
0.20
0.05
Q
T
P
G
C
L
H
0.0
10.0
20.0
30.0
40.0
50.0
60.0
70.0
2-Theta Angle (Degrees)

in the 23°C one day-cured sample is not seen in the 50°C one day-cured sample. CSH Type I (C) and C_4AH_{13} (G) are the new cementitious minerals. The intensity of the 1.43A hematite peak (H) increases with increasing curing time.

Fly Ash-Lime (Cured at 23°C)

The changes in the unconfined compressive strength with time of the fly ash-lime mixture are shown in Figure 17. A major increase in the unconfined compressive strength (UCS) from 7188 kPa (1041 psi) to 18265 kPa (2645 psi) is observed between one and 28 days. The UCS of the one day-cured fly ash-lime is lower than the UCS of the one day-cured fly ash. This is due to the dilution of the fly ash by the addition of 20 percent hydrated lime and due to the lower dry unit weight of the fly ash-lime mixture relative to the dry unit weight of the fly ash. The UCS for the fly ash-lime mixture reaches 26492 kPa (3836 psi) at 90 days and further increases to 32236 kPa (4668 psi) at 180 days. After 28 days the unconfined compressive strengths (UCS) of the fly ash-lime and fly ash mixtures are similar, but at 90 and 180 days the fly ash-lime mixture has higher unconfined compressive strength. This is due to the increased availability of hydrated lime for the formation of calcium silicate hydrates and calcium aluminate hydrates.

Figure 18A illustrates a fractured surface of the one day-cured sample. The matrix material (M) fills the pores between the fly ash grains. At this curing time the outlines of the fly ash spheres (S) are visible and the matrix has micropores. Figure 18B shows a fractured surface of the 90 day-cured sample, when a major strength increase was observed. The outlines of the fly ash grains are less

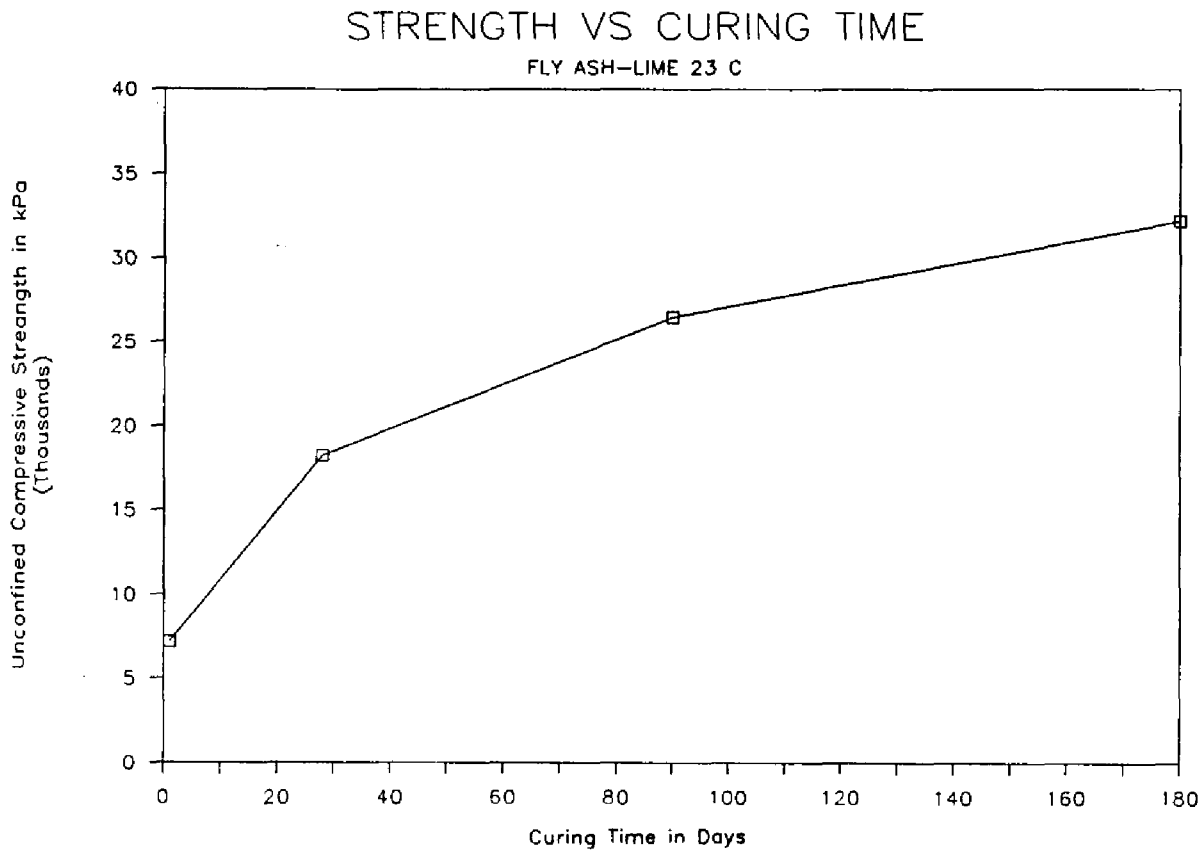

Figure 17. Unconfined Compressive Strength Versus Curing Time of Fly Ash-Lime Cured at 23°C.

Figure 18. Scanning electron micrographs of fly ash-lime samples cured at 23°C. A) A matrix of fine crystals (M) fills the pores between the fly ash grains after one day of curing. The outlines of the fly ash grains (S) are visible. B) A representative fracture surface of the 90 day cured sample at low magnification. The outlines of the fly ash grains are less distinct indicating more extensive cementation of the spheres. C) Matrix material (M) engulfing the fly ash grains and hexagonal plates (P) bridging the pores after 28 days of curing at intermediate magnification. D) A fly ash sphere (S) covered with reaction products after 28 days of curing.

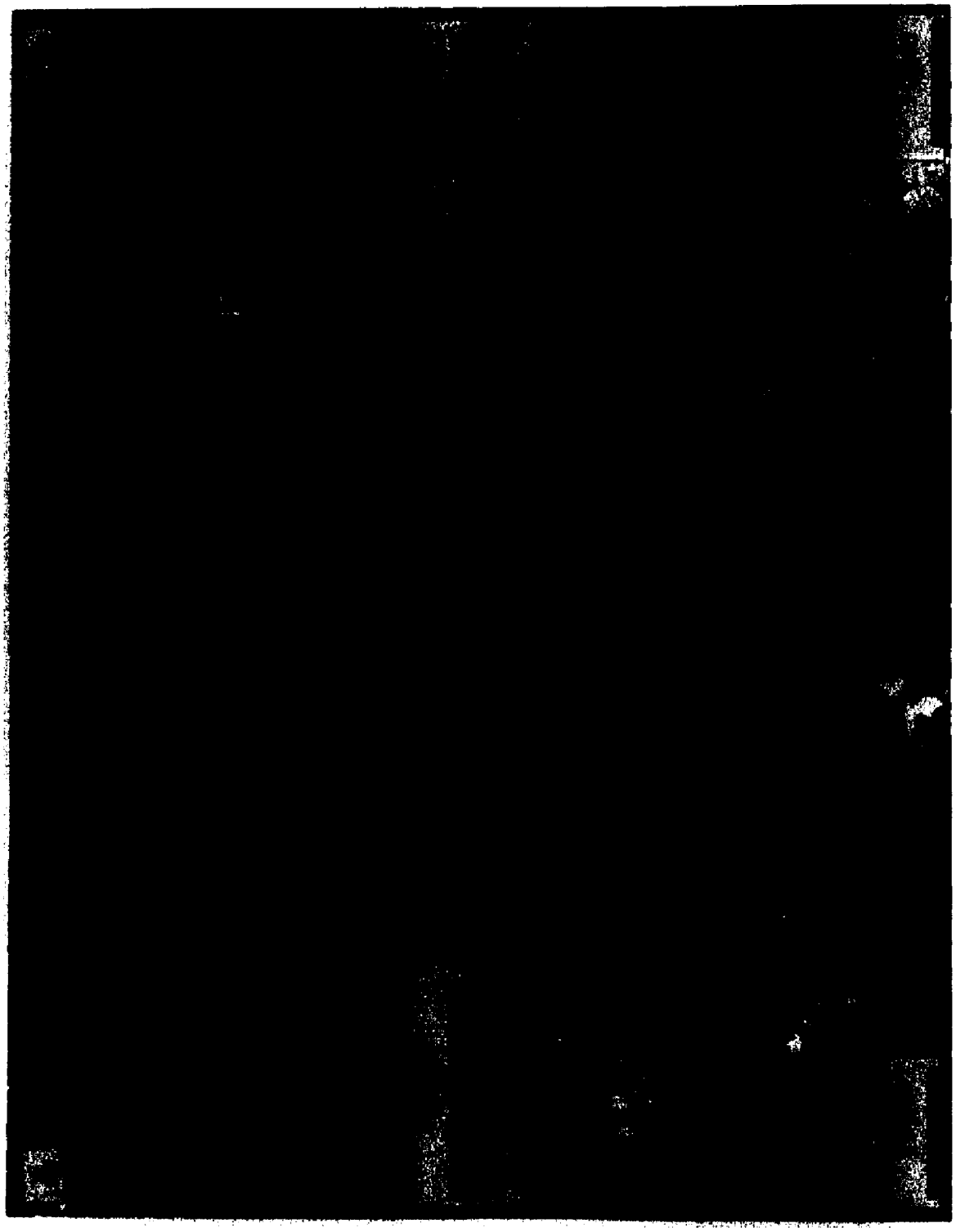

distinct indicating more extensive cementation of the spheres. There are more fine crystals in the matrix with increased curing time. A 100 micrometer diameter broken fly ash sphere is seen which is filled with smaller spheres and cementitious material. Pull out features are present. The matrix material (M) is seen at an intermediate magnification in Figure 18C for the 28 day-cured sample and it fills the pore space between the fly ash grains. All of the pores are spanned with plates (P). A 17.5 micrometer diameter fly ash sphere (S) covered with a reaction product is seen in Figure 18D. The tiny blades are one micrometer long, edge to face oriented relative to each other and their long axes are tangent to the surface of the fly ash sphere.

The detailed morphologies of the cementitious products are presented at intermediate magnification in figures 19A, 19B, 19C and 19D. Figure 19A illustrates a fracture surface of the one day-cured sample. Edge-to-face oriented, two to three micrometer diameter plates (P) are present . EDS analyses on these plates yield a Ca/Si ratio of 4.09 and an Al/Si ratio of one . The matrix material (M) consists of roughly spherical crystals, needles and small blades. At this intermediate magnification it is better illustrated that the fine crystals are more numerous in the matrix after 28 days of curing (Figure 19B) than after one day of curing (Figure 19A). The platy crystals look like calcite. Note how the fly ash spheres are embedded in the matrix (M). There is no space for these grains to move. The pore

Figure 19. Scanning electron micrographs of the cementitious reaction products in fly ash-lime samples cured at 23°C at intermediate magnification. A) The initial stages of plates (P) after one day of curing. B) The matrix material (M) engulfs the fly ash grains after 28 days of curing. C) A representative fracture surface of the 90 day cured sample. Edge to face oriented hexagonal plates (P) are bridging the pores. D) After 180 days of curing some of the plates appear to be etched longitudinally (1).

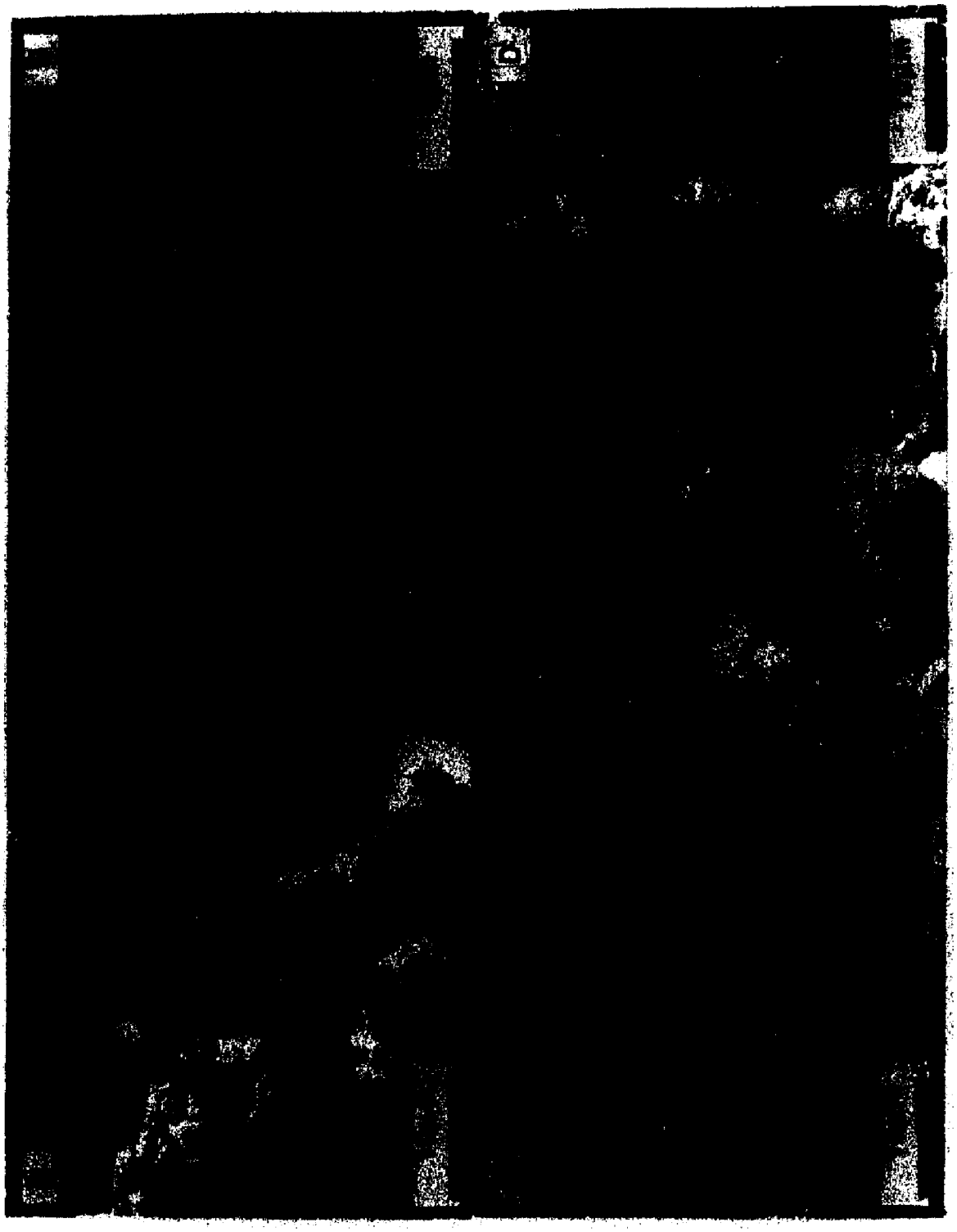

bridging edge-to-face oriented plates completely surround the fly ash spheres.

Figure 19C illustrates a fractured surface of the 90 day-cured sample. Edge-to-face oriented five micrometer diameter plates (P) are present. They appear to be better developed than the plates observed in the one and the twentyeight day-cured samples. Their outlines are sharp. EDS analyses of the area (P) yield a Ca/Si ratio of 3.98 and an Al/Si ratio of 1.18 . EDS analyses of the crystals forming the imprint of a five micrometer diameter fly ash sphere at (P) yield a Ca/Si ratio of 3.39 and an Al/Si ratio of 0.89 .

Figure 19D shows a fractured surface of the 180 day-cured sample. The plates (1) appear to be etched longitudinally. EDS analyses on one of the etched plates yield a Ca/Si ratio of 3.99 and an Al/Si ratio of 1.22 which is the same as the plates in Figure 19C. EDS analyses of the matrix (M) formed by one to three micrometer diameter roughly spherical crystals connected to each other by fibers, yield a Ca/Si ratio of 1.91 and an Al/Si ratio of 0.68 . EDS analyses of the plate (P) , yield a Ca/Si ratio of 3.03 and an Al/Si ratio of 1.42 . There is an imprint of a 35 micrometer diameter fly ash particle. The matrix material which is composed of roughly spherical crystals and rods, fills the pores between fly ash grains and plates are present between them. This figure illustrates the interaction between the fly ash spheres and cementitious

matrix and helps to explain qualitatively why this material behaves as a rigid material. The displacement of the fly ash spheres is restricted by the matrix and the plates which fill the pores between the fly ash grains.

Figure 20A shows the imprint of a 22 micrometer diameter fly ash sphere at high magnification in the one day-cured sample. A network of roughly spherical crystals (SC), blades (B) and needles (N) is present. The needles and blades are edge-to-face oriented with roughly spherical crystals and rods lying between them. The diameters of the spheres enmeshed in this mat are between 0.4 to three micrometers. EDS analyses at the center yield a Ca/Si ratio of 2.72 and an Al/Si ratio of 0.73 . The roughly spherical crystal morphology of the 90 day-cured sample is presented in Figure 20B at high magnification. These aggregates are composed of one to three micrometer diameter roughly spherical crystals (SC) and one to 1.5 micrometers long, 0.2 micrometer diameter fibrous crystals (FC). The fibrous crystals are different from the fibrous crystals found in the mat structure of the fly ash . They are better developed and fewer in number than in the fly ash. Figure 20C presents a fractured surface of the 90 day-cured sample at intermediate magnification. All the pores are filled with plates. An aggregate of fine equant crystals (E) less than 0.5 micrometers in diameter is seen. This appears to be CSH Type III. Figure 20D illustrates a 40 micrometer long, 30 micrometer wide pull out feature in the 180 day-cured

Figure 20. Scanning electron micrographs of the details of the cementitious products of fly ash-lime samples at 23°C. A) An imprint of a fly ash sphere (S) at high magnification after one day of curing. A network of roughly spherical crystals (S), blades (B) and needles (N) are present. B) The roughly spherical crystal morphology of the 90 day cured sample is seen at high magnification. Fibrous crystals (FC) connect the roughly spherical crystals (SC) forming a mat. C) A representative fracture surface after 90 days of curing at intermediate magnification. An aggregation of fine equant crystals (E) is present engulfing the fly ash grains. D) A pull-out feature is seen after 180 days of curing. The grain was surrounded by hexagonal plates (P) at the bottom and was surrounded by a dense mat (M) of roughly spherical crystals on the sides.

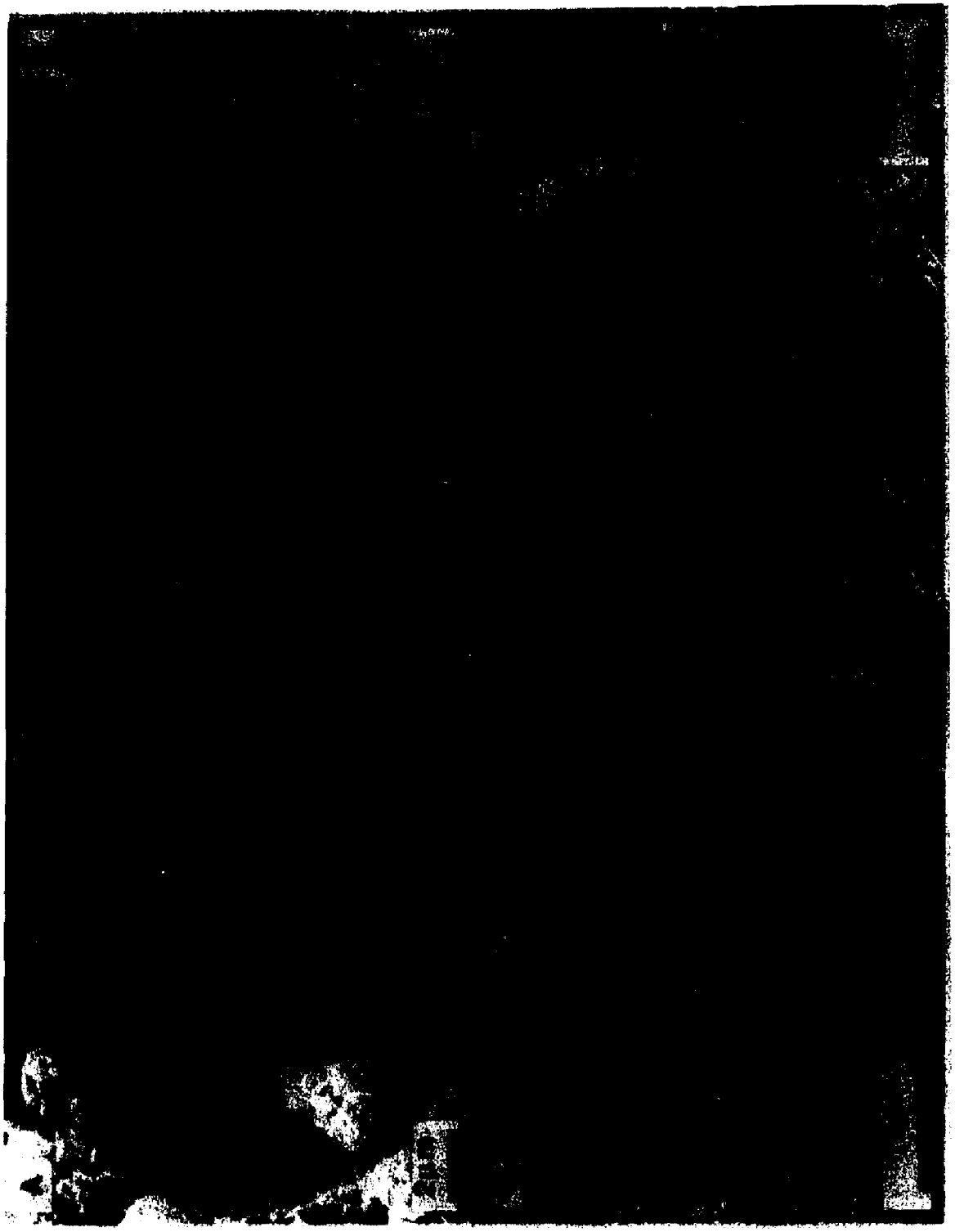

sample. The grain was surrounded by hexagonal plates (P) at the bottom and was surrounded by a dense mat of roughly spherical crystals (M) on the sides.

In summary, the increase in the number of fine crystals in the matrix and the spanning of the pores by the hexagonal plates seem to be the reasons for strength improvement. Unidentified roughly spherical crystals, CSH Type III and tetracalcium aluminate thirteen hydrate are the new minerals.

X-Ray Diffractograms

The X-Ray diffractograms for the fly ash-lime mixtures (80% fly ash and 20% lime) at different curing periods are presented in Figure 21. The major mineral is portlandite (R). The intensities of portlandite peaks decrease after 28 days of curing but show an increase after 90 days. A decrease in peak intensities is observed after 180 days. This fluctuation may be due to varying orientation of the powder sample or other sample heterogenities. The second major mineral is quartz (Q) and its peaks remain unchanged. One of the major constituents of fly ash powder, anhydrite is not seen even after one day of curing which suggests that it is totally consumed. The tricalcium aluminate peak (T) is present at all times and appears to be unchanged. Periclase peaks (P) are present at all times.

The identified new cementitious minerals are

Figure 21. Powder X-Ray Diffraction Patterns of the 23°C Cured Fly Ash-Lime Mixture. R=portlandite, Q=quartz, T=tricalcium aluminate, G= C_4AH_{13}, A=anhydrite, H=hematite, J=C_3AH_6. For d-spacings represented by numbers, refer to the text.

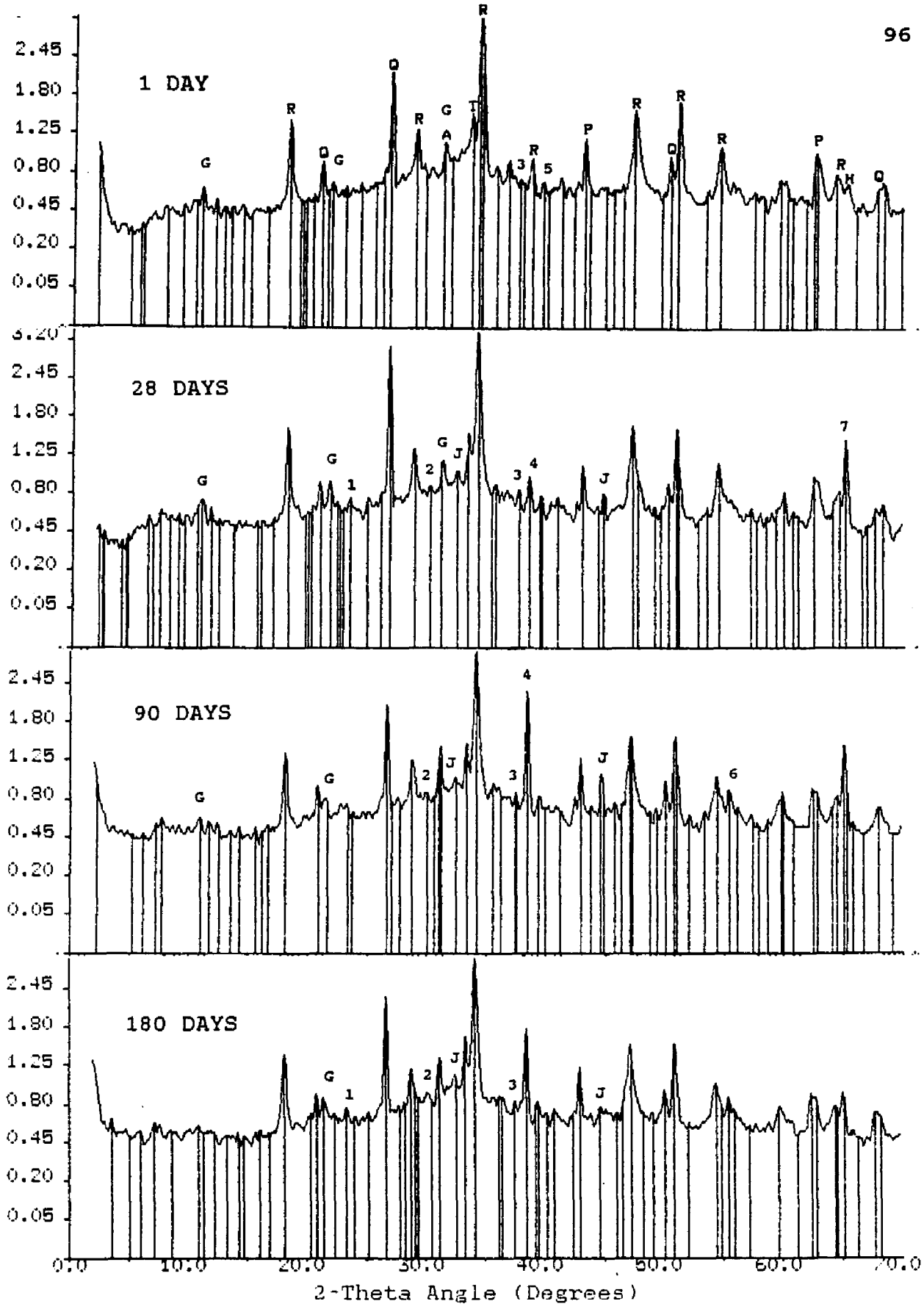
1 DAY
28 DAYS
90 DAYS
180 DAYS
2.45
1.80
1.25
0.80
0.45
0.20
0.05
0.0
10.0
20.0
30.0
40.0
50.0
60.0
70.0
2-Theta Angle (Degrees)

tetracalcium aluminate thirteen hydrate (C_4AH_{13}) and tricalcium aluminate six hydrate (C_3AH_6). The hexagonal plates that are seen in the scanning electron micrographs and d-spacings of 8.14A, 4.08A, and 2.87A confirm the presence of this mineral. The intensities of the 4.08A and 2.87A peaks increase after 28 days of curing. The 2.76A and 2.02A peaks are tentatively identified as C_3AH_6. These are cubic crystals. The unidentified peaks are listed below.

TABLE 8

UNIDENTIFIED PEAKS IN FLY ASH-LIME CURED AT 23°C.

D-spacing	Remarks
3.80 (1)	Appears after 28 days and its intensity increases slightly.
2.96 (2)	Appears after 28 days.
2.39 (3)	Intensity increases after 28 days.
2.33 (4)	Is present after one day and its intensity increases sharply after 90 days and decreases after 180 days.
2.28 (5)	Unchanged.
1.66 (6)	Appears after 90 days.
1.43 (7)	Appears after 28 days with high intensity, its intensity decreases after 180 days.

A significant observation is the presence of the portlandite peaks even after 180 days of curing. Apparently the sample was not completely hydrated even at the end of

the 180 day curing period. The increase in the intensities of C_4AH_{13} (G) and C_3AH_6 (J) after 28 days corresponds to a major strength increase which suggests that these new cementitious minerals are responsible for the strength increase. The 2.33A (4) and 1.43A (7) peaks seem to be important because of their high intensities at certain curing periods but no specific cementitious minerals having these d-spacings could be identified.

Fly Ash - Lime (Cured at 50°C)

The changes in the unconfined compressive strength of the 50°C cured fly ash-lime mixture are illustrated in Figure 22. The unconfined compressive strength of the one day-cured sample is 7372 kPa (1067 psi) which is approximately the same as the strength of the 23°C cured sample. Major strength increase occured between one and twenty-eight days when an unconfined compressive strength of 32398 kPa (4691 psi) is obtained. The strength increase continues at 90 days to 39472 kPa (5716 psi) and levels off at this curing period with no further increase.

The cementitious compounds in the higher temperature samples are morphologically similar to the 23°C cured samples so only some highlights will be presented in this section. The one day-cured sample has two dominant features. The matrix (M) which is composed of roughly spherical grains, and edge-to-face oriented hexagonal plates (P) (Figure 23A). EDS analyses of the plates yield a Ca/Si ratio of 5.31 and an Al/Si ratio of 1.41 . The matrix is more abundant after 90 days of curing (Figure 23B) . The outlines of the fly ash particles are not distinct. The morphology of the roughly spherical crystals is better defined at this curing period. The crystals (M) are 0.5 to one micrometer long and they are found in aggregations. EDS analyses on these roughly spherical crystals gave a Ca/Si

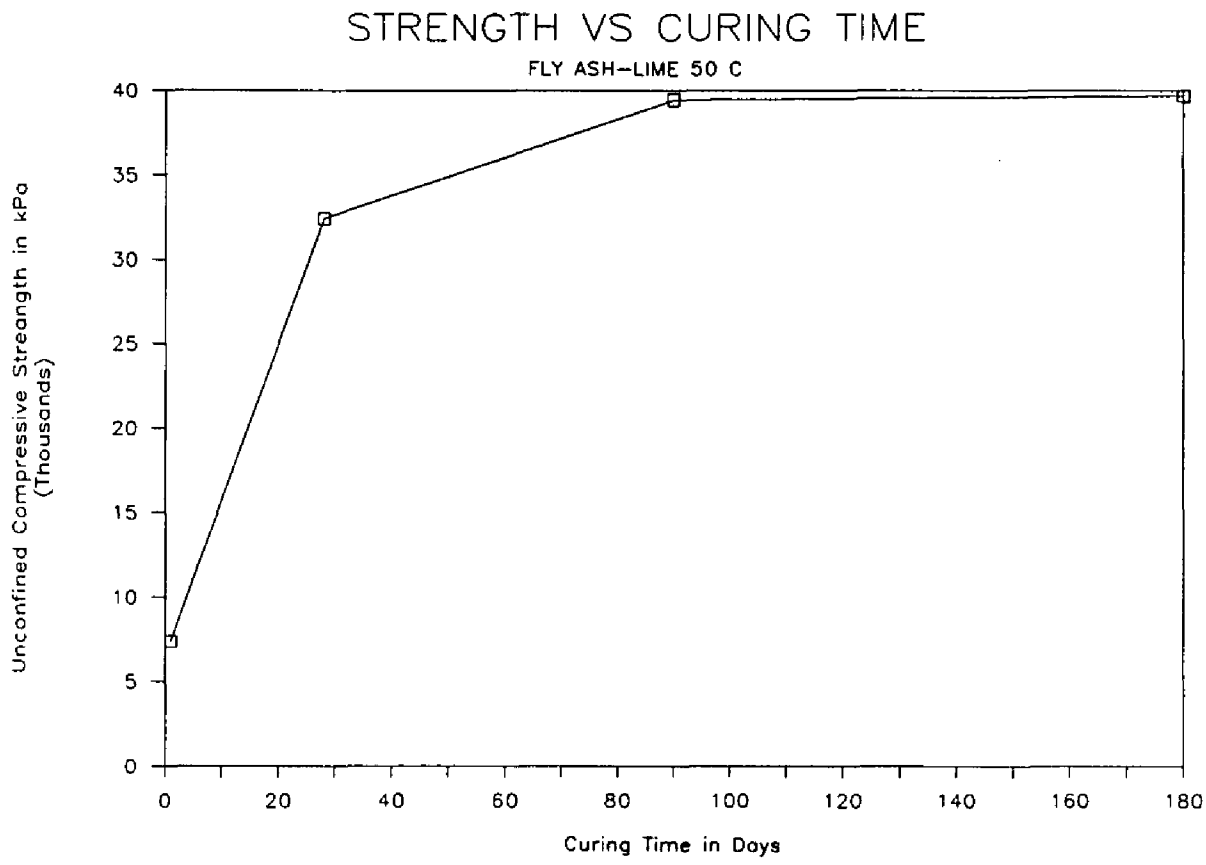

Figure 22. Unconfined Compressive Strength Versus Curing Time for Fly Ash-Lime Cured at 50°C.

Figure 23. Scanning electron micrographs of the fly ash-lime samples cured at 50°C. A) There are two dominant features in the one day cured samples: The matrix (M) which is composed of roughly spherical grains and edge-to-face oriented hexagonal plates (P). B) A representative fracture surface of the 90-day cured sample at intermediate magnification. The outlines of the most of the fly ash grains are not distinct indicating more through participation in the reactions. C) The hexagonal plates (P) are seen at high magnification after 90 days of curing. There are fibrous crystals on their edges which may suggest the beginning of a transformation to a different phase. D) A fracture surface of the 28 day-cured sample at intermediate magnification. The outlines of the fly ash grains are less distinct an dthe pores are spanned with hexagonal crystals (P).

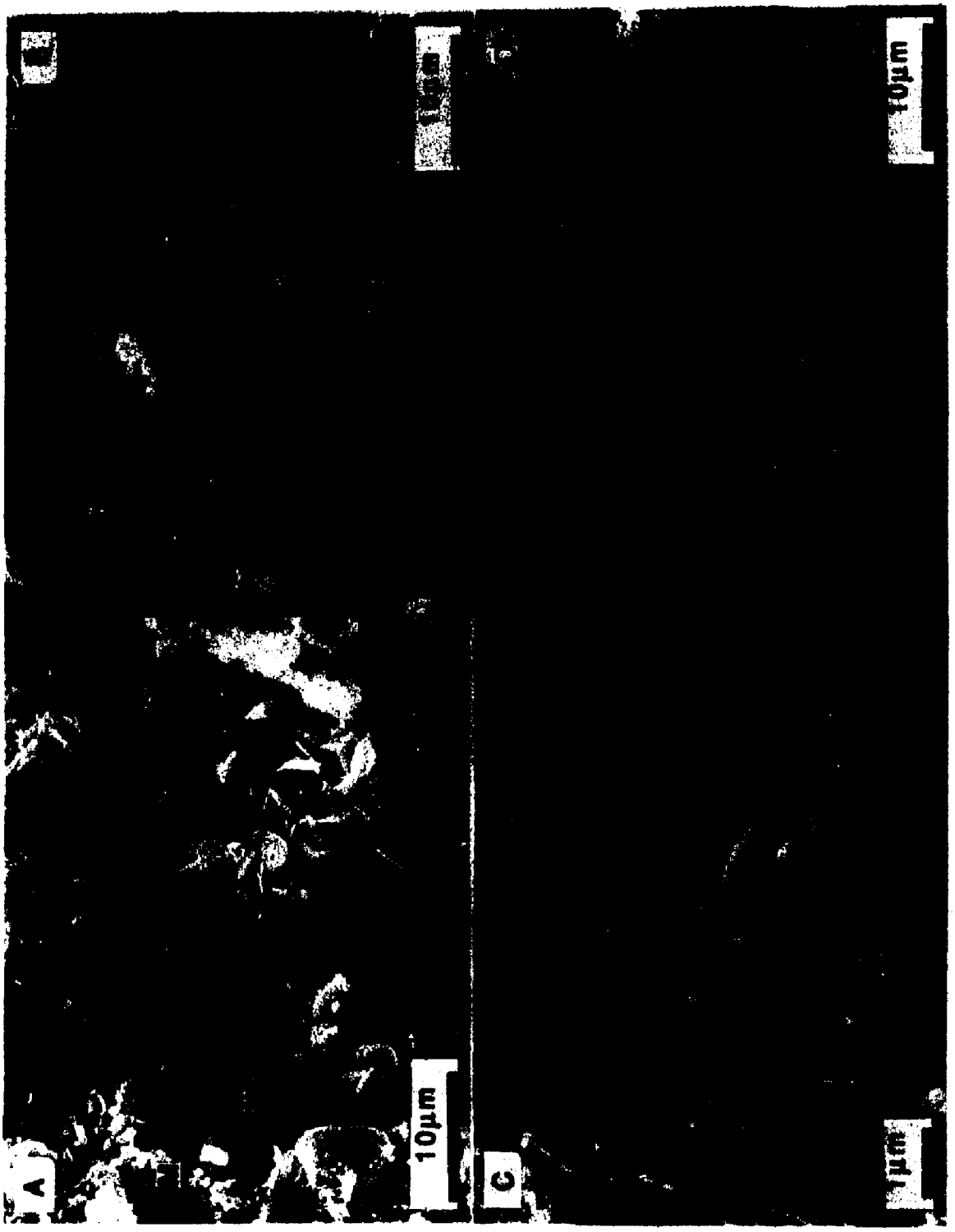
A
10µm
C
10µm

ratio of 1.03 and an Al/Si ratio of 0.44 .

Figure 23C illustrates the hexagonal plates at higher magnification after 90 days of curing. The plates are five to six micrometers across and roughly 0.3 to 0.4 micrometers thick, and they have fibrous crystals on their edges. This may be the beginning of a transformation to a different phase. Note the hexagonal shape of the plate at (P). EDS analyses of these plates yield a Ca/Si ratio of 2.21 and an Al/Si ratio of 1.00 . These plates have less Ca than the plates seen in the one day-cured sample.

Figure 23D illustrates a fractured surface of the 28 day-cured sample at intermediate magnification. Major strength increase occured between one and twenty eight days and this figure demonstrates again, that the pores are spanned with hexagonal crystals (P) and the outlines of the fly ash grains are less distinct. The most significant observations that can be used to relate the strength increase to the changes in the morphology are the densification of the matrix and the presence of hexagonal crystals in the pores. Their relative importance is hard to judge but the densification of the matrix appears to be the more dominant factor in the strength improvement of this mixture. The hexagonal crystals are identified as C_4AH_{13}. Sulphur is present in these hexagonal plates. When the 180 day-cured samples are compared no difference is seen between the morphology of the cementitous materials in the elevated

temperature cured sample and the room temperature cured sample.

X-Ray Diffractograms

The powder X-Ray diffractograms of the 50°C cured fly ash-lime mixtures are presented in Figure 24. The major differences from the 23°C cured sample are discussed below. The intensities of the portlandite peaks (R) are lower at the 50°C cured sample. The 4.08A and 2.87A peaks (G) are assigned to C_4AH_{13}. Their intensities increase after 28 days. C_3AH_6 is tentatively identified from 2.76A and 2.03A peaks (J). The intensity of the 2.76A peak increases after 28 days. The 2.76A peak was not present in the 23°C cured sample after one day. The 3.07 CSH Type I peak (C) appears as a hump on the 3.10 A portlandite peak (R) after 28 days of curing and its intensity increases after 90 days of curing. The unidentified peaks are presented below.

Figure 24. Powder X-Ray Diffraction Patterns of the 50°C Cured Fly Ash-Lime Mixture. R=portlandite, Q=quartz, P=periclase, T=tricalcium aluminate, H=hematite, J= C_3AH_6, G= C_4AH_{13}. For d-spacings represented by numbers refer to the text.

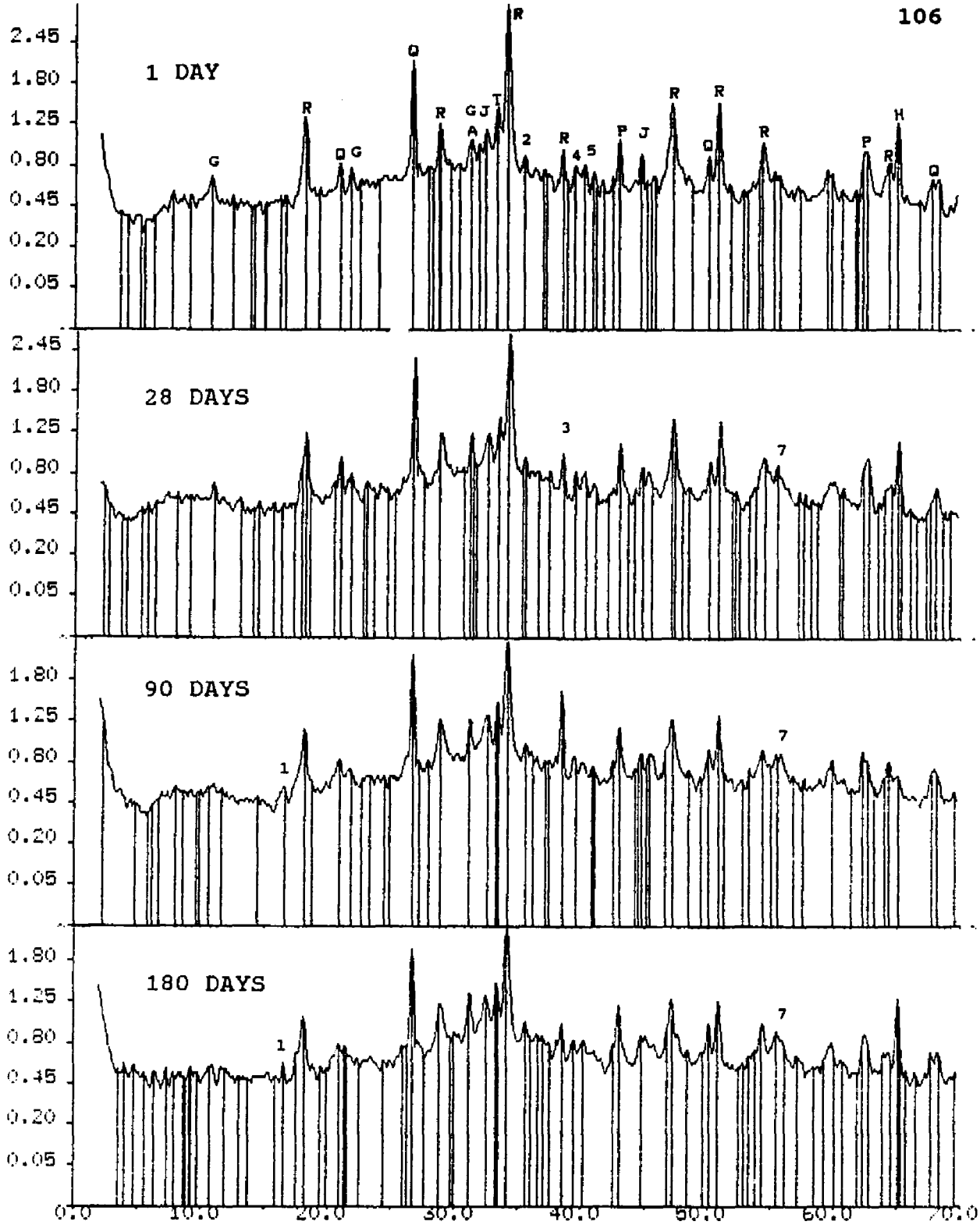
1 DAY
28 DAYS
90 DAYS
180 DAYS
2.45
1.80
1.25
0.80
0.45
0.20
0.05
0.0
10.0
20.0
30.0
40.0
50.0
60.0
70.0
2-Theta Angle (Degrees)

TABLE 9

UNIDENTIFIED PEAKS IN FLY ASH-LIME CURED AT 50°C.

D-spacing	Remarks
5.34 (1)	Appears after 90 days.
2.53 (2)	Unchanged.
2.33 (3)	Intensity is high only at 90 days.
2.28 (4)	Unchanged.
2.24 (5)	Unchanged.
1.99 (6)	Appears after 28 days of curing.
1.66 (7)	Appears after one day and its intensity increases after 28 days.
1.43 (8)	Intensity is high after one day of curing and same at other curing times except its intensity is low after 90 days.

At 50°C C_3AH_6 peaks (J) appeared after one day whereas the same peaks appeared only after 28 days of curing at 23°C. The intensities of the 4.08A (G), 2.76A (J), 1.99A (6) and 1.66A (7) increased considerably after 28 days of curing at 50°C when a major increase in compressive strength was observed.

Bentonite-Fly Ash (Cured at 23°C)

The stress-strain diagrams with zero confining pressure and with 100 kPa confining pressure are presented in Figures 25A and 25B. The major strength increase occurs between one and 28 days. The strengths fluctuate slightly following this period. The one day average strength is 906 kPa (131 psi) and it increases to 1414 kPa (205 psi) after 28 days. The average strain at failure for the one day cured sample is 0.016 and decreases to approximately 0.007 for the 28,90, and 180 day-cured samples. The confining pressure affects the strain at failure for the one day-cured sample by increasing it to 0.0353 but at longer curing periods after cementitious products have formed its effect on strain at failure becomes smaller. The average strain at failure for the 28,90 and 180 day samples is 0.0078. Despite some variation the 28,90 and 180 day stress strain curves plot in a narrow region. When an average curve is used in that region to compute the elastic modulus value , 240000 kPa (34752 psi) is obtained. This is a three fold increase compared to that of the one day-cured sample (80000 kPa). The strain and stress values corresponding to 0.70 times the maximum strength were used to compute the elastic modulus. In stabilized soils the initial portion of the stress-strain curve up to approximately seventy percent of the maximum strength is practically linear.

Figure 26A shows a fractured surface of the one day-

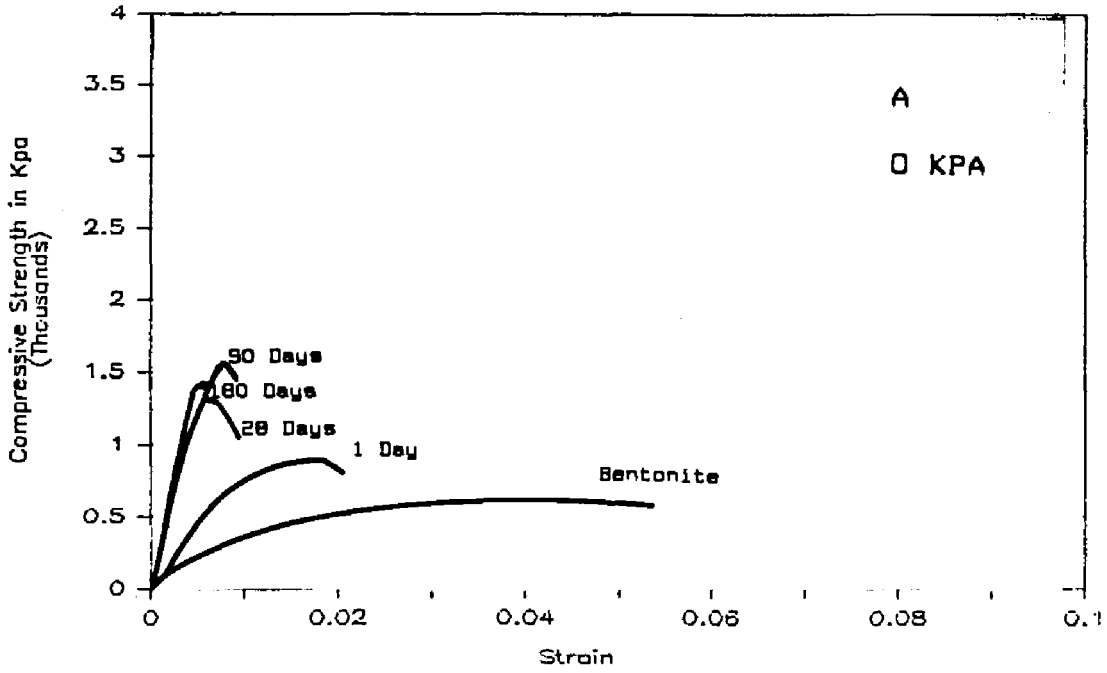

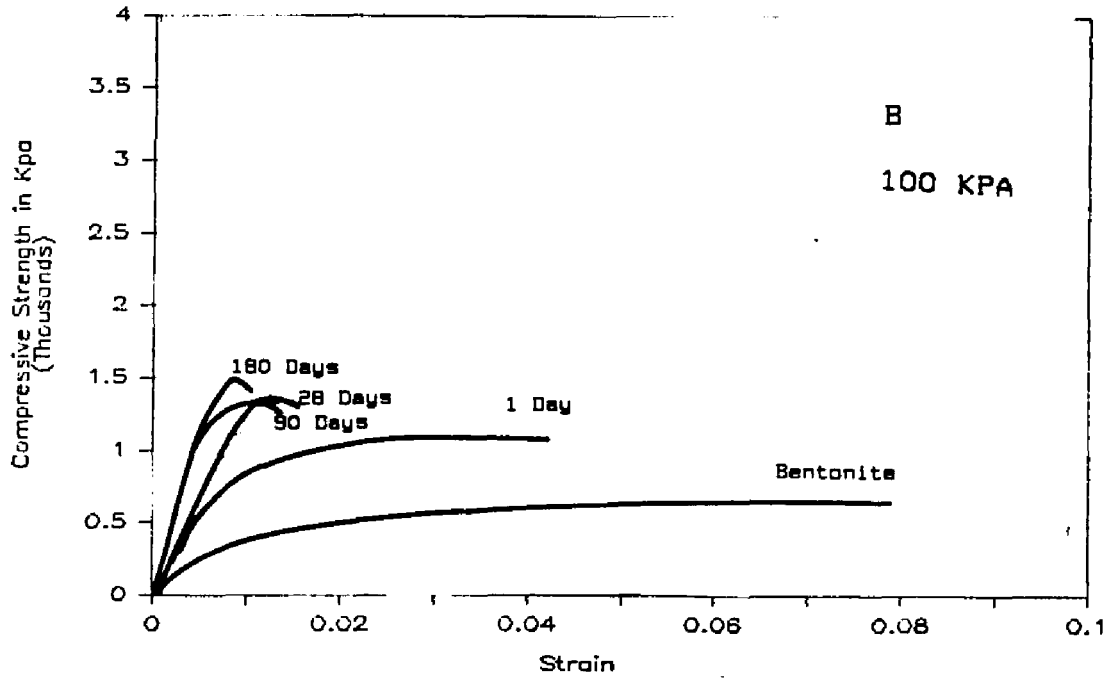

Figure 25. Stress-Strain Curves for Bentonite-Fly Ash Mixture Cured at 23°C. A: Unconfined. B: With 100 kPa Confining Pressure.

Figure 26. Scanning electron micrographs of the bentonite-fly ash samples cured at 23°C. A) A representative fracture surface of the one-day cured sample at low magnification. The outlines of fly ash grains are very smooth and distinct which suggest that these grains have not reacted. B) After 28 days of curing the outlines of the fly ash grains are becoming irregular because of dissolution. C) A fracture surface of the one day cured sample is seen at intermediate magnification. A fly ash grain (S) is supported by montmorillonite aggregates (MA). D) Fly ash spheres (S) with irregular outlines are present in the 28 day-cured sample. The spheres show evidence of dissolution and cementation (R).

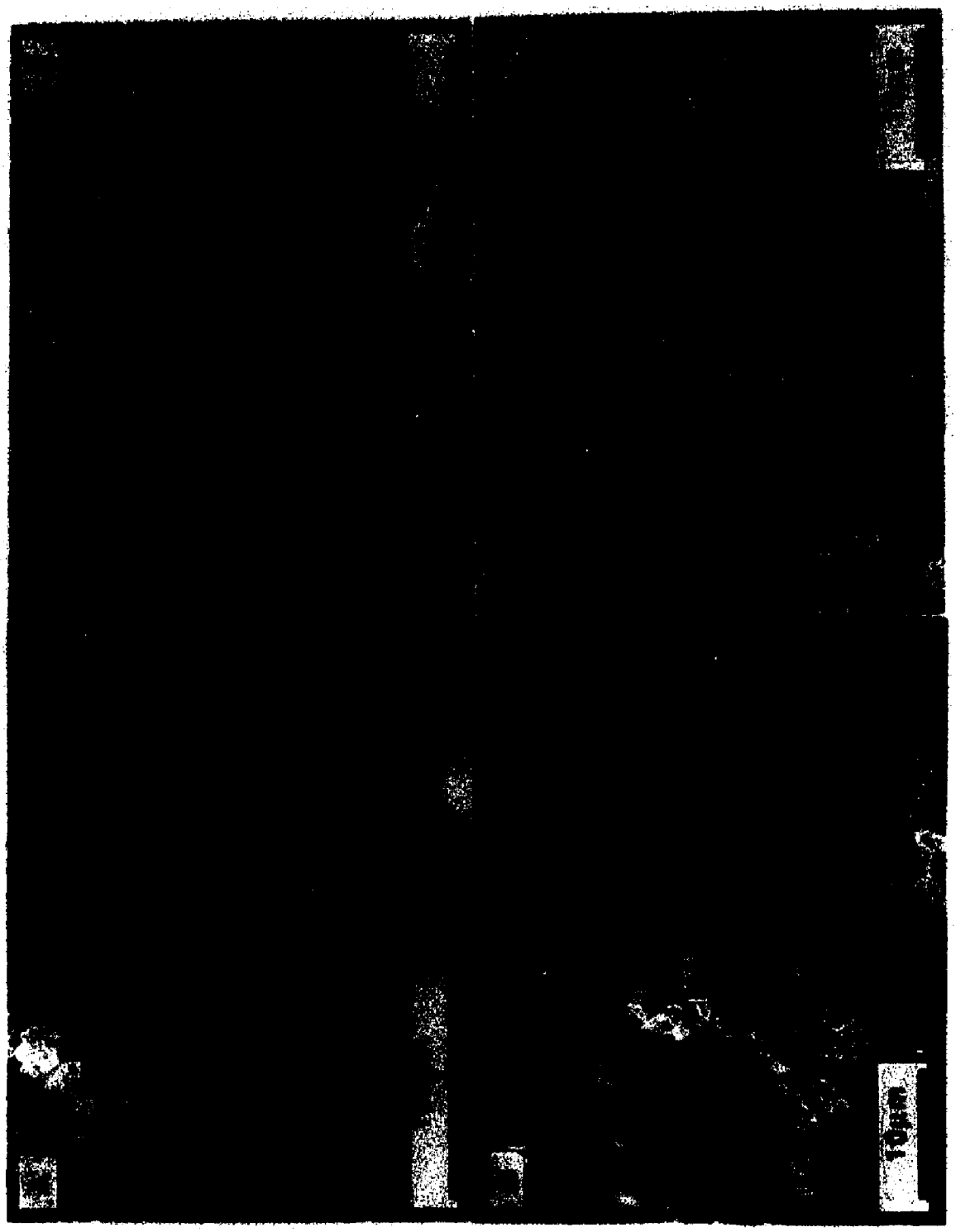

cured sample at low magnification. The outlines of fly ash grains are very smooth and distinct which suggest that these grains have not reacted. Figure 26B shows a fractured surface of the 28 day-cured sample at low magnification. The outlines of some of the fly ash grains are becoming irregular because of dissolution. Comparison of the fly ash spheres is better illustrated in Figures 26C and 26D at intermediate magnification. Figure 26C shows a fracture surface of the one-day cured sample. A 40 micrometer diameter fly ash particle (S) is supported by montmorillonite aggregates (MA). Note that there are no reaction products on the fly ash sphere. Fly ash spheres (S) with irregular outlines are present in the 28 day-cured sample (Figure 26D). The spheres show evidence of dissolution and cementation (R).

Some individual grains affected by hydration reactions are presented in Figures 27A, 27B, 27C and 27D. In Figure 27A, a broken 32 micrometer diameter fly ash particle (S) is seen which is filled with fly ash particles and montmorillonite aggregates after 28 days of curing. The fly ash sphere (S) of Figure 26D is presented in Figure 27B at a higher magnification. After 28 days of curing, hexagonal crystals (H) with varying dimensions are readily apparent. The larger ones are 3.5 micrometers wide and four micrometers long and the smaller ones are 1.5 micrometers wide and two micrometers long. They are randomly oriented. They are only seen on some grains. After 90 days of curing,

Figure 27. Scanning electron micrographs of some reacted grains in bentonite-fly ash samples cured at 23°C. A) A broken fly ash sphere filled with montmorillonite aggregate and other fly ash grains is seen after 28 days of curing. B) Hexagonal crystals (H) are readily apparent on some fly ash grains after 28 days of curing. C) A reacted fly ash grain with needles (N) and hexagonal crystals (H) is seen after 90 days of curing at high magnification. D) Supporting matrix left after either dissolution of fly ash grains or after the fly ash grains were pulled out during fracture after 180 days of curing at intermediate magnification.

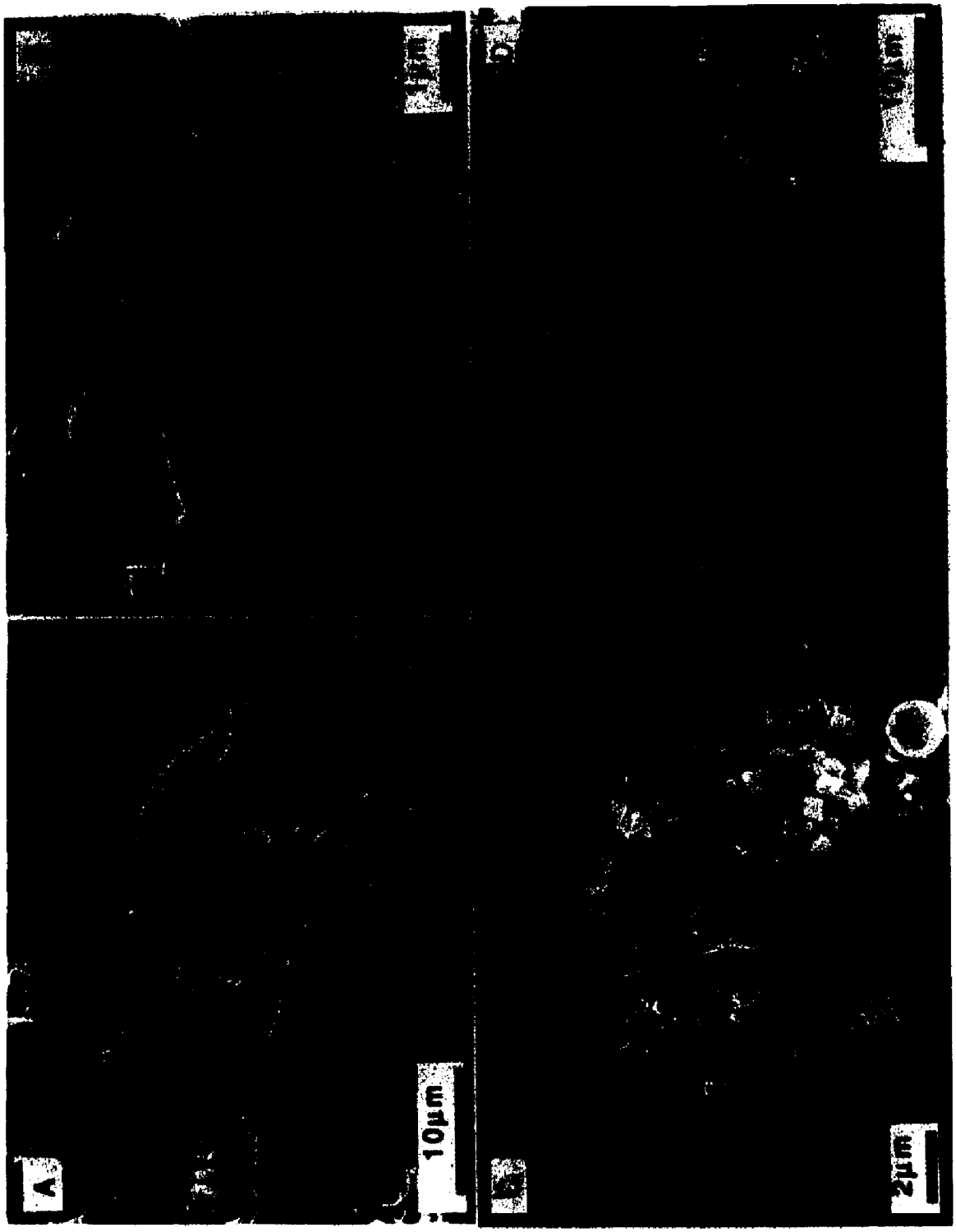
A
10µm
B
2µm

other reaction products are seen on the fly ash grains (Figure 27C) at higher magnification. The fly ash sphere is covered with two types of reaction products, needles (N) and hexagonal crystals (H). The randomly oriented needles are aproximately one micrometer long, 0.2 to 0.4 micrometers in diameter, and have a hexagonal cross section. At (H) hexagonal crystals are present which are two micrometers long. Figure 27D presents a unique material (M) where spherical particles were either pulled out during fracture or were dissolved after 180 days of curing. This feature represents a very localized reaction.

Some of the fly ash particles have reaction products on their surfaces after 28 days of reaction, but dissolution of the fly ash spheres is not observed. Apparently the cementitious products are forming from the finely divided soluble materials, such as anhydrite, in the unreacted fly ash. After 28 days of curing hexagonal crystals appear on some of the fly ash spheres and after 90 days, needles and hexagonal crystals cover some of the particles. The reactions differ on an individual grain level.

X-Ray Diffractograms

The powder X-ray diffractograms for the bentonite-fly ash mixture are presented in Figure 28. The major constituents are montmorillonite (M) and quartz (Q). Calcite (K), tricalcium aluminate (T), periclase (P) and hematite (H) are the minor constituents. The peaks corresponding to these minerals (except hematite) do not change with increasing curing time. The intensity of the hematite peak decreases after 180 days of curing. The 9.84A and 5.61A d-spacings (E) after one day of curing are tentatively assigned to ettringite. The 9.84A peak is present at all curing times but the 5.61A peak dissappears after one day of curing. The strongest peak of CSH Type I , 3.07A (C), appears after 90 days of curing and its intensity increases after 180 days of curing. The unidentified peaks are listed below.

Figure 28. Powder X-Ray Diffraction Patterns of Bentonite-Fly Ash Mixture Cured at 23°C. Q=quartz, M=montmorillonite, P=periclase, T=tricalcium aluminate, K=calcite, E=ettringite, H=hematite, C= CSH I. For d-spacings represented by numbers refer to the text.

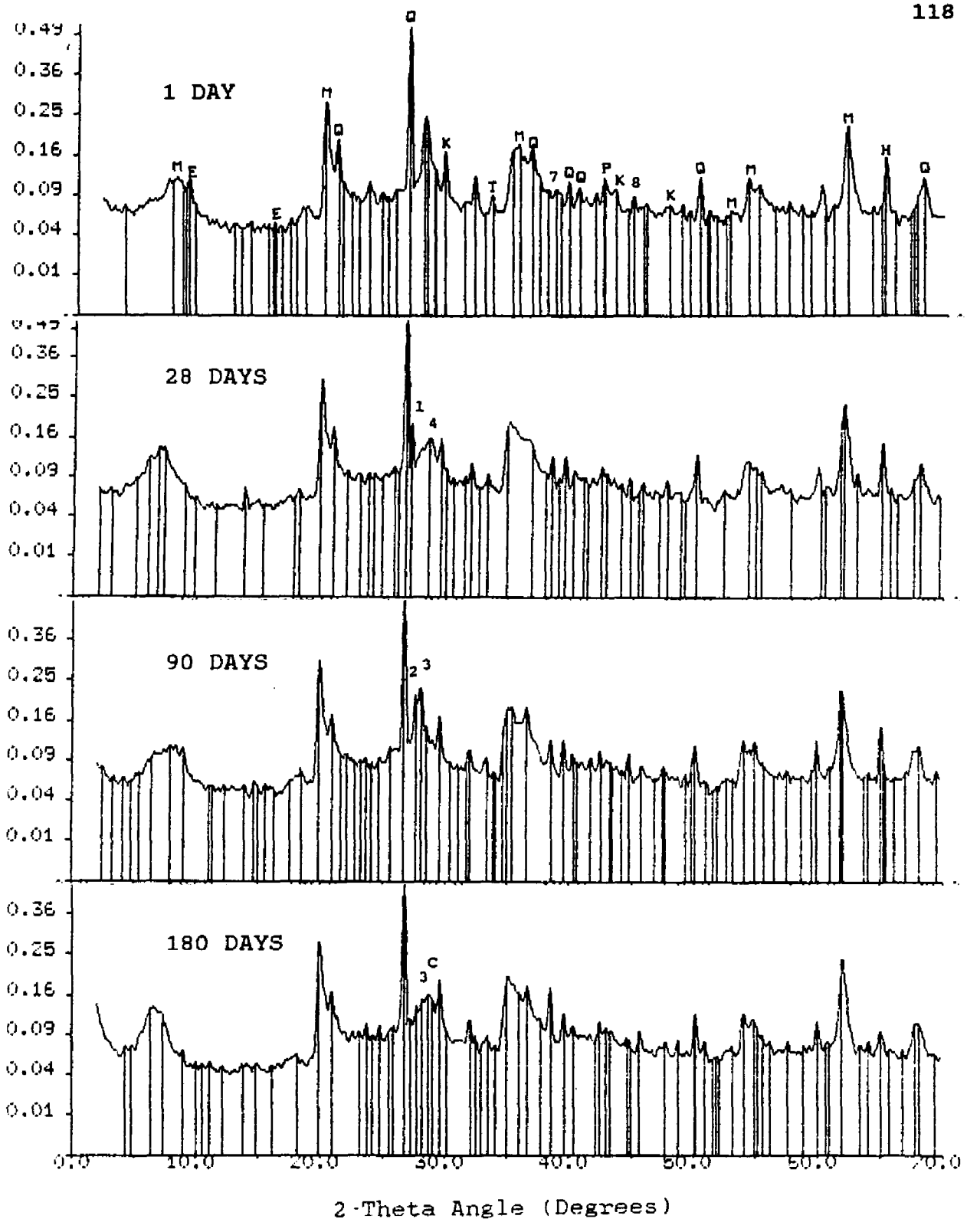
1 DAY
28 DAYS
90 DAYS
180 DAYS
0.49
0.36
0.25
0.16
0.09
0.04
0.01
0.0
10.0
20.0
30.0
40.0
50.0
60.0
70.0
2-Theta Angle (Degrees)

TABLE 10

UNIDENTIFIED PEAKS IN BENTONITE-FLY ASH CURED AT 23°C.

D-spacing	Remarks
3.28 (1)	Appears after 28 days of curing, is not seen after 90 days,has a very low intensity after 180 days.
3.21 (2)	Appears after 90 days and its intensity decreases in the 180 day cured sample, probably afwillite.
3.17 (3)	Is present at all times.
3.11 (4)	Is present at all times.
2.75 (5)	Appears after 180 days of curing.
2.63 (6)	Appears after 90 days of curing and is present in the 180 day-cured sample.
2.33 (7)	Intensity increases with time.
2.02 (8)	Is present at all times.

Bentonite-Fly Ash (Cured at 50°C)

The stress-strain curves for the 50°C cured bentonite-fly ash mixture are presented in Figures 29A and 29B. The bentonite-fly ash mixture developes an unconfined compressive strength of 1234 kPa (179 psi) after one day of curing. It increases to 1327 kPa (192 psi) after 28 days. The unconfined compressive strength increases further to 1525 kPa (221 psi) after 90 days and to 1915 kPa (277 psi) after 180 days of curing. The strain at failure for the one day-cured sample is 0.015 (unconfined) and decreases to 0.011 after 180 days. Five out of six stress strain curves for samples cured longer than 28 days plot in a narrow range. Although there is an increase in unconfined compressive strength , no distinctive change of elastic modulus is obtained after 28 days of curing. With 100 kPa confining pressure the strain at failure after one day is 0.022 . With increased curing time the soil becomes less sensitive to 100 kPa confining pressure.

Mineralogical features found in the 50°C cured samples are similar to those in the 23°C cured samples. Figure 30A illustrates a fracture surface of the 90 day-cured sample at low magnification. The outlines of some of the fly ash grains (S) are irregular suggesting that they have reacted. At intermediate magnification (Figure 30B) the fly ash particles (S) are supported by montmorillonite aggregates (MA). A major strength increase occured between 90 and 180

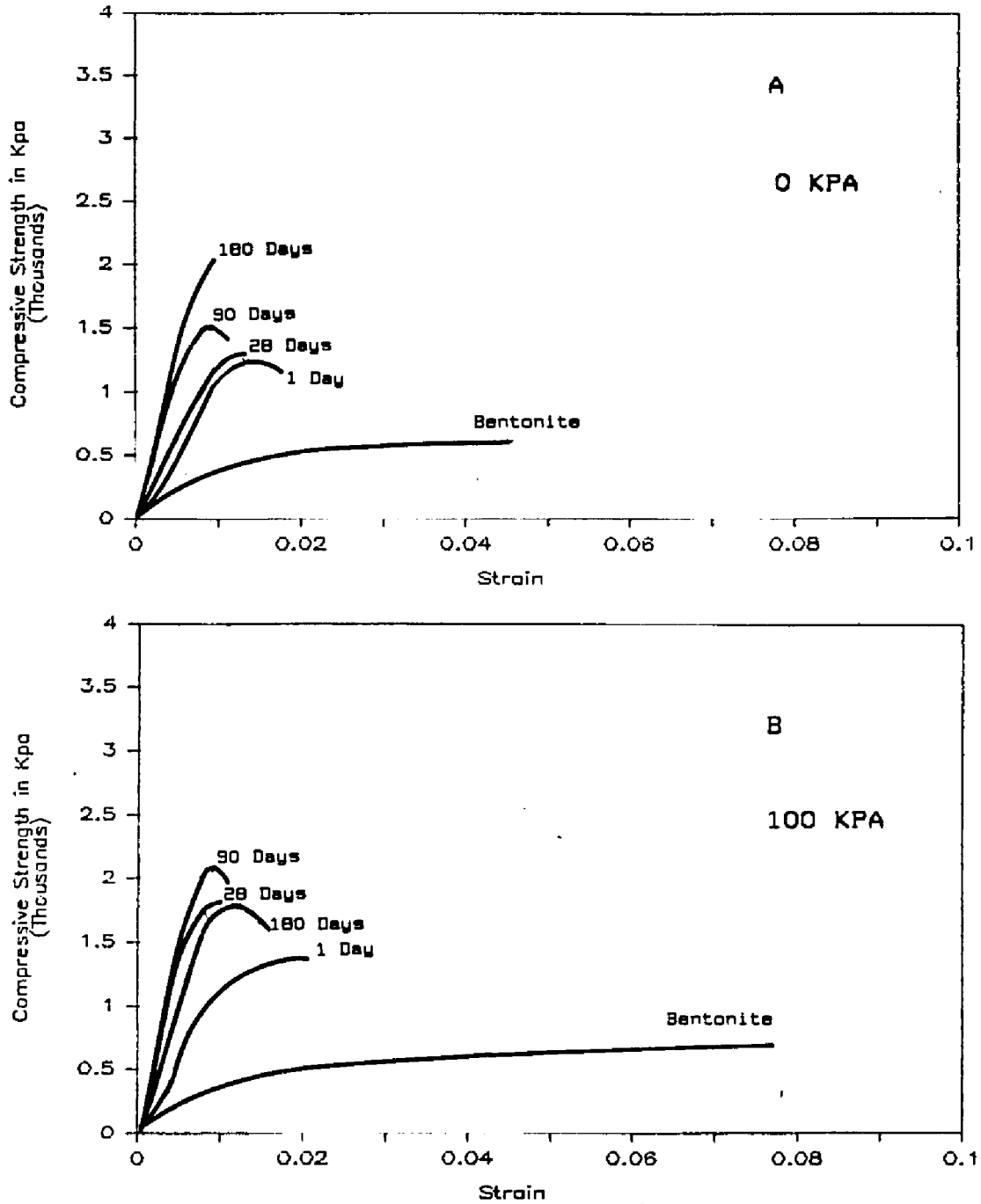

Figure 29. Stress-Strain Curves for Bentonite-Fly Ash Cured at 50°C. A: Unconfined. B: With 100 kPa Confining Pressure.

Figure 30. Scanning electron micrographs of bentonite-fly ash samples cured at 50°C. A) A representative fracture surface of the 90 day-cured sample at low magnification. The outlines of some of the fly ash grains (S) are irregular suggesting that they have reacted. B) The fly ash grains (S) are supported by montmorillonite aggregates (MA) (90 day-cured). C) After 180 days of curing there are more reacted fly ash grains (R) present. The reacted fly ash sphere at location (1) has imprints of crystals on its surface.
D) Hexagonal crystals (H) and needles (N) are seen on a reacted fly ash grain at high magnification after 180 days of curing.

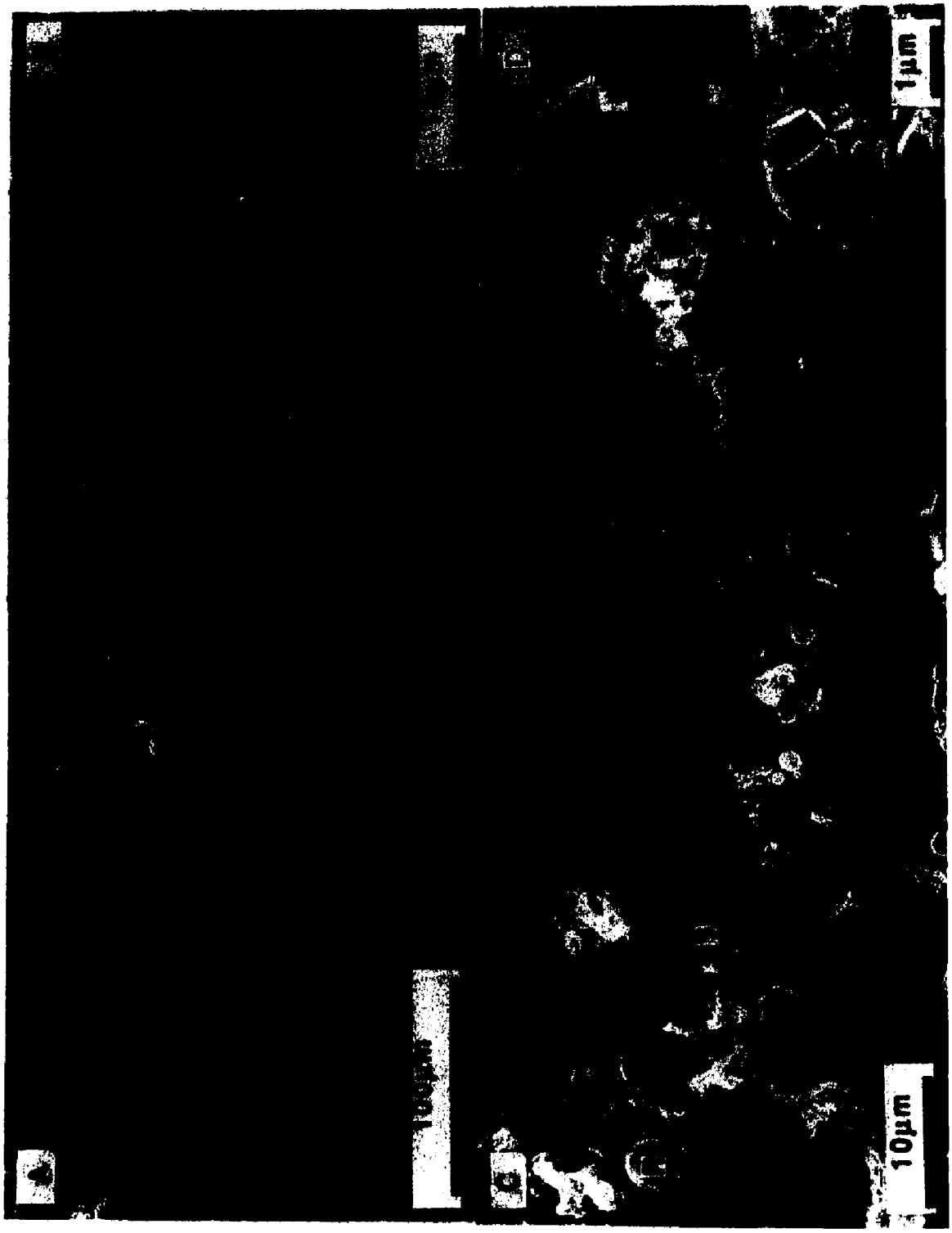
1μm
10μm

days of curing and there are proportionately more reacted fly ash spheres in these samples. Figure 30C illustrates a fractured surface of the 180 day-cured sample at an intermediate magnification. A reacted, six micrometer diameter fly ash particle (R) is seen with the imprints of crystals on its surface. EDS analyses of this sphere yield a Ca/Si ratio of 0.11 and an Al/Si ratio of 0.87 . Note that Ca is very low relative to silicon. A nine micrometer diameter reacted fly ash particle after 180 days of curing is presented in Figure 30D at high magnification. The features at this curing period are similar to the ones present in the 23°C cured sample. Hexagonal crystals (H) of varying sizes are well developed. Their lengths vary between one and four micrometers. An aggregate of small needles (N) is present. EDS analyses of these needles give a Ca/Si ratio of 1.90 and an Al/Si ratio of 1.09. EDS analyses of the prisms give higher Ca/Si ratio of 3.05 and an Al/Si ratio of 1.19 .

At 50°C , the reaction products are similar to the ones observed at lower temperature. The only reaction products observed are hexagonal crystals and needles on some of the fly ash grains.

X-Ray Diffractograms

The powder X-ray diffractograms of the 50°C cured bentonite-fly ash mixture are presented in Figure 31. Only the major differences from the 23°C cured sample will be discussed below. Ettringite (E) is present after one day of curing (9.83A, 5.58A). After 28 days of curing the 9.83A peak shifts to 9.94A . A 3.07A CSH I (C) peak is present after one day of curing and its intensity increases after 180 days of curing. The unidentified peaks are listed below.

TABLE 11

UNIDENTIFIED PEAKS IN BENTONITE-FLY ASH CURED AT 50°C.

D-spacing	Remarks
3.24 (1)	Is present at all times.
3.21 (2)	Appears after one day and its intensity increases after 28 and 90 days and decreases after 180 days of curing, probably afwillite.
3.17 (3)	Intensity decreases after 180 days of curing.
3.12 (4)	Is present at all times.
2.95 (5)	Appears after 28 days of curing.
2.79 (6)	Is present at all times.
2.63 (7)	Appears after one day of curing and dissappears after 180 days.
2.33 (8)	Unchanged.

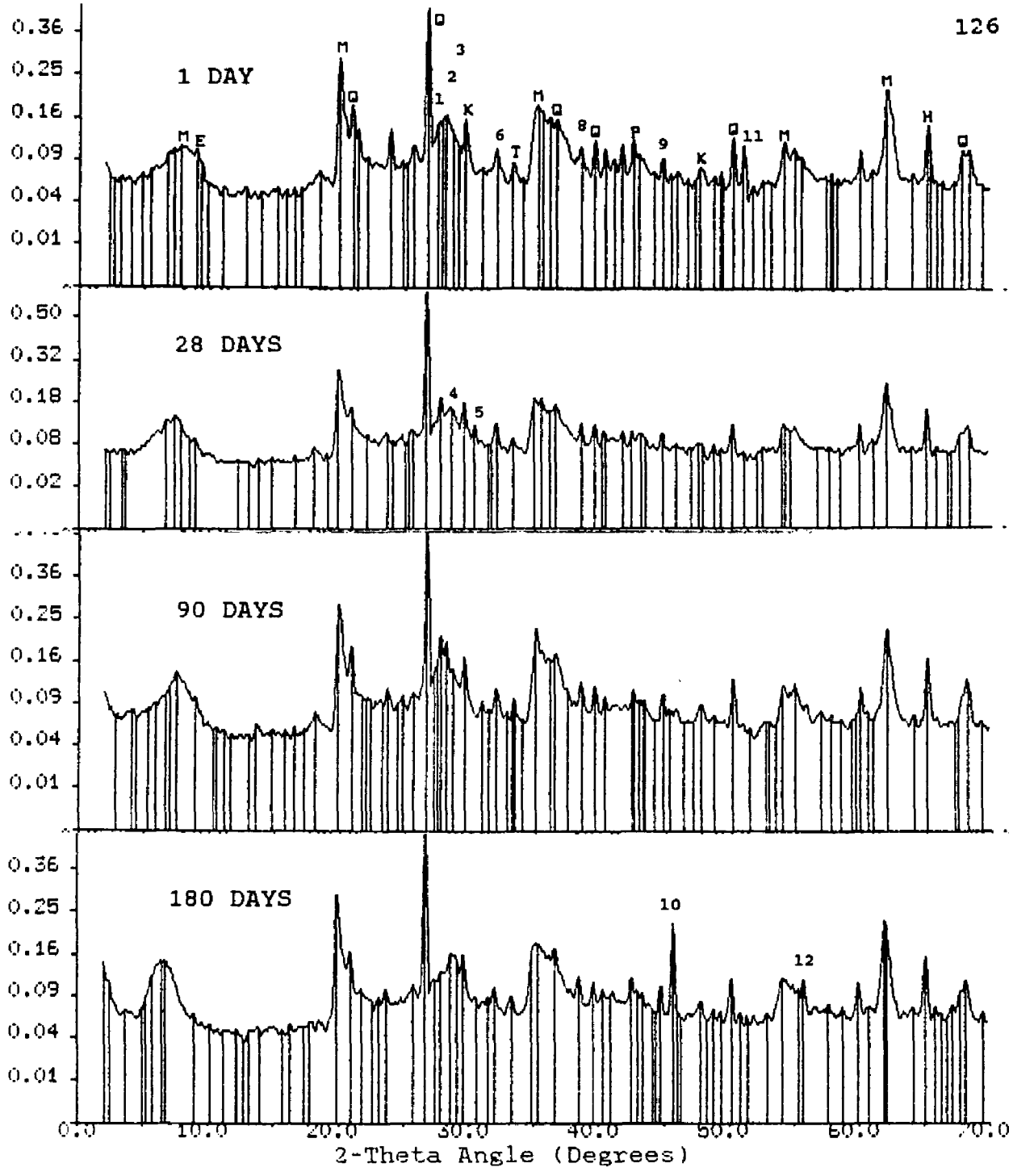

Figure 31. Powder X-Ray Diffraction Patterns of the 50°C Cured Bentonite-Fly Ash. Q=quartz, M=montmorillonite, E=ettringite, K=calcite, H=hematite, P=periclase, C= CSH I. For d-spacings represented by numbers, refer to the text.

2.02 (9)	Unchanged.
1.99 (10)	Appears after 180 days with a high intensity peak.
1.79 (11)	Is present after one day of curing and dissappears after 28 days.
1.65 (12)	Appears after 180 days.

At 50°C more CSH formation is suggested because of the higher intensity of the 3.07A peak when compared to the lower temperature samples. The strength increase continues up to 180 days of curing. The 3.21A may be the strongest peak of afwillite.

Bentonite-Lime (Cured at 23°C)

The stress strain curves for the bentonite and lime mixture cured at 23°C are presented in Figures 32A and 32B. The major increase in strength occurred after 28 days of curing and after this curing period all stress-strain curves plot in a narrow range. The unconfined compressive strength increases from 610 kPa (88 psi) after one day to 996 kPa (144 psi) after 28 days of curing and approximately to 1300 kPa (188 psi) for 90 and 180 day-cured samples. The elastic modulus for the one day-cured sample is 52300 kPa (7573 psi) and it increases to an average of 219697 kPa (31812 psi) for the remaining test samples. The axial strain at failure decreases from 0.0144 for one day to an average value of 0.007 for the 28,90 and 180 day-cured samples. A similar trend is observed with 100 kPa confining pressure. The strength (with confining pressure) increases from 746 kPa (108 psi) after one day to 1108 kPa (160 psi) for 28 days of curing and to approximately 1375 kPa (199 psi) for the 90 and 180 day-cured samples. The elastic modulus value after one day is 55850 kPa (8087 psi), 116000 kPa (16797 psi) after 28 days and increases to approximately 253150 kPa (36656 psi) for the 90 and 180 day-cured samples. One hundred kPa confining pressure resulted in a higher elastic modulus after 28 days of curing. The reactions that are causing the strength increase are happening between 1 and 90 days .

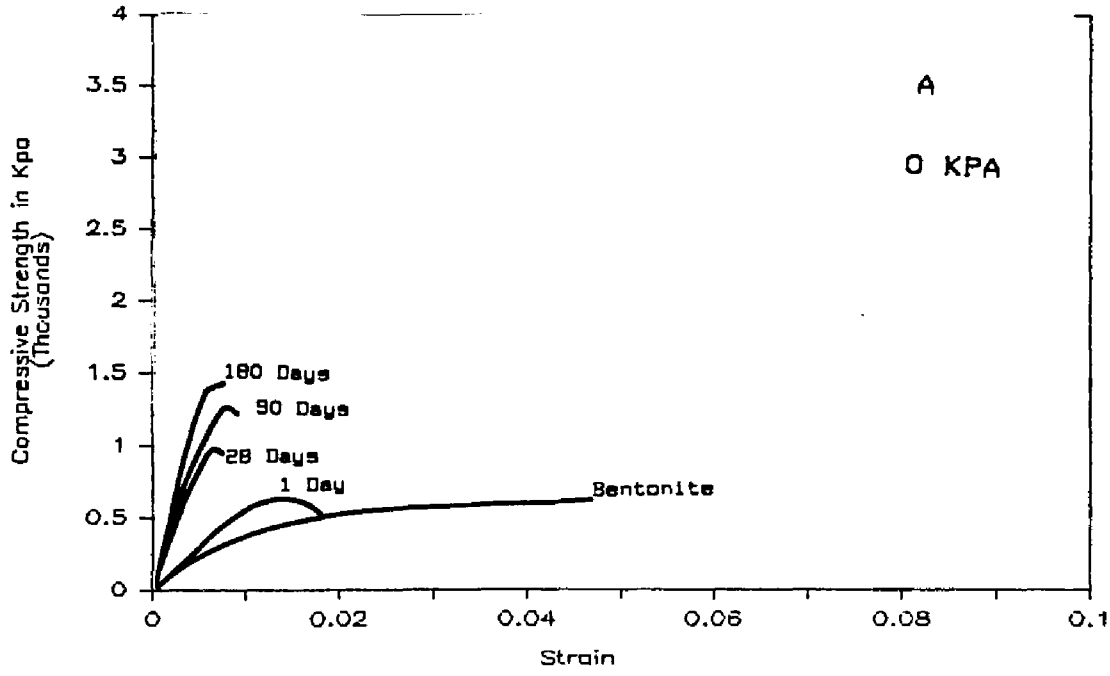

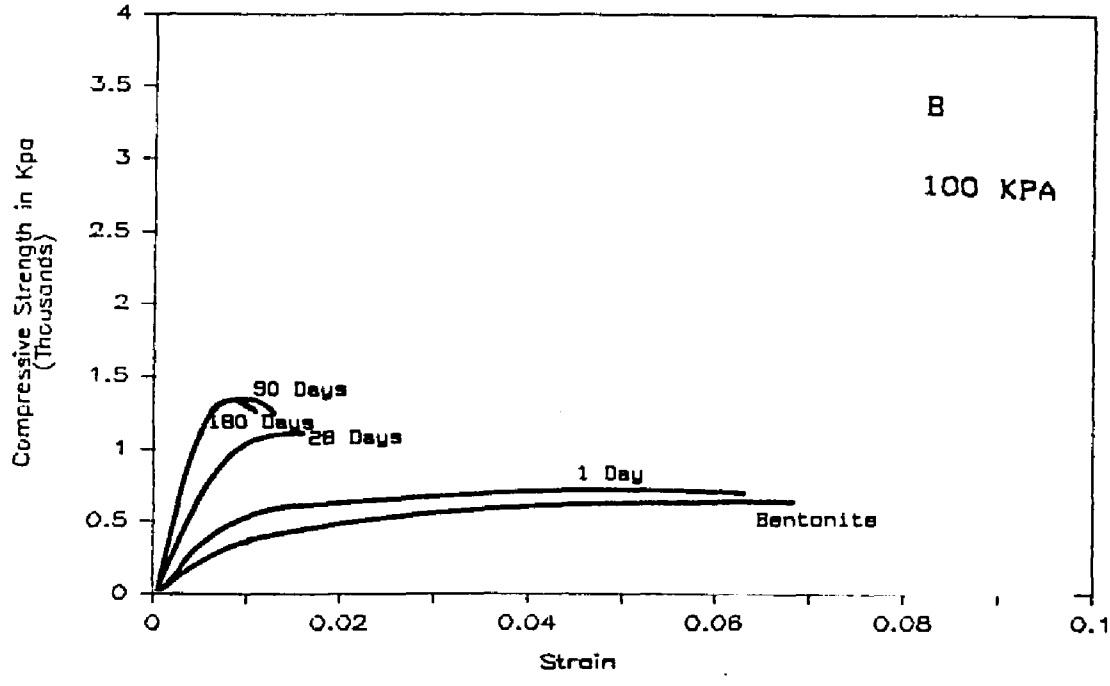

Figure 32. Stress-Strain Curves for Bentonite-Lime Mixture. A: Unconfined. B: With 100 kPa Confining Pressure.

Figures 33A, 33B, 33C, and 33D represent the fracture surfaces of one to 180 day-cured samples at low magnification. In the one day-cured sample, the grain boundaries are hard to find which is typical for plastic, clay-rich material (Figure 33A). The boundaries of the clay aggregates are better defined after 28 days of curing and the overall morphology is more typical of brittle material (Figure 33B). Clay behaves as coarser grained aggregates after 28 days. The aggregation may be seen in Figure 33C after 90 days and in Figure 33D after 180 days of curing. The brittle behavior is better illustrated at intermediate magnifications when Figures 34A and 34B are compared . In Figure 34A the aggregates are formed of face- to-face oriented bundles of montmorillonite flakes (one day-cured). Some of the montmorillonite flakes (MO) are curled as a result of water loss during drying. Figure 34B shows a reacted montmorillonite aggregate where the reacted montmorillonite flakes (RM) are seen as laths and blades. At this magnification their details are not fully apparent. More recognizable aggregates of grains are present after longer curing times.

The reaction products of bentonite and lime are clearly shown in Figures 35A, 35B, 35C, and 35D. Montmorillonite flakes after 28 days of curing are illustrated in Figure 35A at high magnification. There are laths (L) and blades up to two micrometers long and approximately 0.2 micrometers wide. It appears from this picture that the montmorillonite flakes

Figure 33. Scanning electron micrographs of bentonite-lime samples cured at 23°c at low magnification. A) In one-day cured sample the grain boundaries are hard to find which is typical for plastic, clay-rich material. B) The boundaries of the clay aggregates are better defined after 28 days of curing and the overall morphology is more typical of brittle material. Clay behaves as coarser grained aggregates. C) The aggregations can be seen in this 90 day-cured sample. D) A representative fracture surface after 180 days of curing demonstrating the brittle behavior.

A
100μm
B
100μm
C
100μm
D
100μm

Figure 34. Scanning electron micrographs of representative fracture surfaces of bentonite-lime samples at intermediate magnification. A) The aggregates are formed of face-to-face oriented bundles of montmorillonite flakes (one day-cured). Some of the montmorillonite flakes (MO) are curled as a result of water loss during drying. B) A reacted montmorillonite aggregate with reacted flakes (RM) as laths and blades is seen after 28 days of curing. At intermediate magnification their details are not fully apparent. The boundaries of the clay aggregate is better defined.


10µm
10µm

Figure 35. Scanning electron micrographs of the reaction products in bentonite-lime samples cured at 23°C. A) Laths and blades (L) are forming on the edges of the montmorillonite flakes after 28 days of curing, visible at high magnification. B) An example of final stages of lath and blade (L) formation after 90 days of curing at high magnification. C) An aggregation of equant crystals (E) is seen after 90 days of curing at intermediate magnification. D) After 180 days of curing similar aggregations of equant crystals (E) are present.

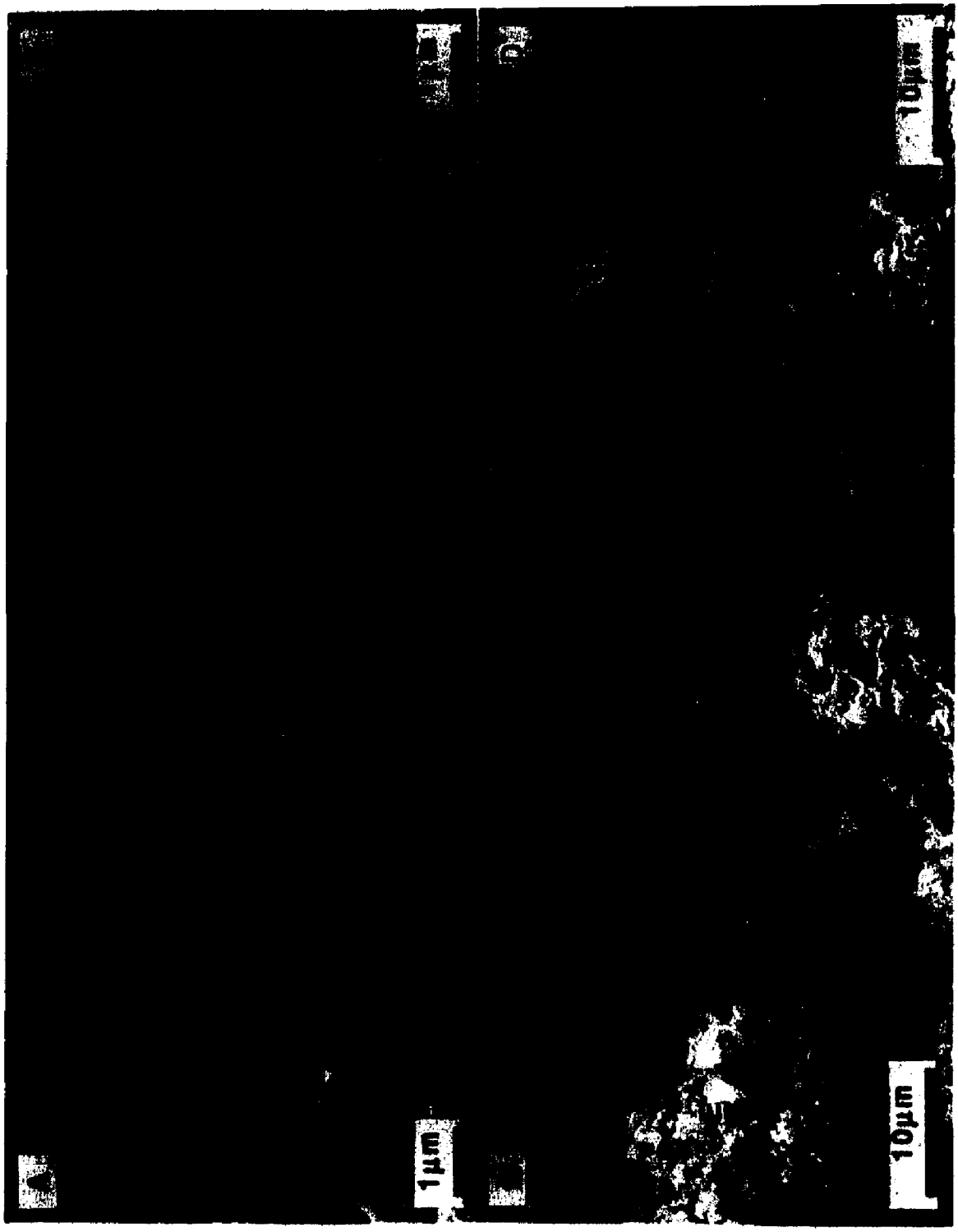
1µm
10µm
1µm
10µm

are attacked by lime and are etched longitudinally every 0.1 to 0.2 micrometers and then seperated along these lines. EDS analyses (L) reveal a high Ca/Si ratio of 1.05 and an Al/Si ratio of 0.54 . These crystals are identified as CSH Type I. The lath and blade type features are more common after 90 days of reaction at 23°C. Figure 35B shows an excellent example of the final stages of lath (L) and blade formation. These crystals are localized. After 90 days of curing aggregations of approximately 0.8 micrometers wide equant crystals (E) are present (Figure 35C). EDS analyses produce a high Al, low Si and no Ca X-ray peak for these features. Figure 35D illustrates a similar feature after 180 days of curing. EDS analyses (E) at high magnification yield a Ca/Si ratio of 0.36 and an Al/Si ratio of 1.83 , which shows that Al is the dominant component of this feature.

In summary, no reaction products are observed after one day curing time. Major changes in the microstructure and strength occur at 28 days by the formation of blade and lath like crystals. Clay behaves as lumps after 28 days and the aggregate boundaries are more distinct. CSH Type I lath and blade-like acicular crystals develop with increased curing time. After 90 days of curing, a blocky crystal morphology is present which has Al as its dominant component.

X-Ray Diffractograms

The X-Ray diffractograms of bentonite-lime mixtures are presented in Figure 36. A complete list of peaks is presented in Appendix B. The major mineral is montmorillonite and its peaks (M) are labeled on the one day-cured sample. The montmorillonite peaks remain unchanged at all curing periods. The second major mineral is quartz (Q) and it does not show any change. Calcite (K) is present in bentonite and the intensity of its peaks appears to be the same at all curing times. The major cementitious mineral is CSH Type I as identified from 3.07A and 1.79A peaks (C). The 1.79A peak is present after one day with a low intensity and its intensity increases after 28 days of curing. The 3.07A peak appears as a hump on calcite peak after 28 days and its intensity increases after 90 and 180 days of curing. The presence of CSH Type I is supported by the needles seen in the scanning electron micrographs. The unidentified peaks are presented below.

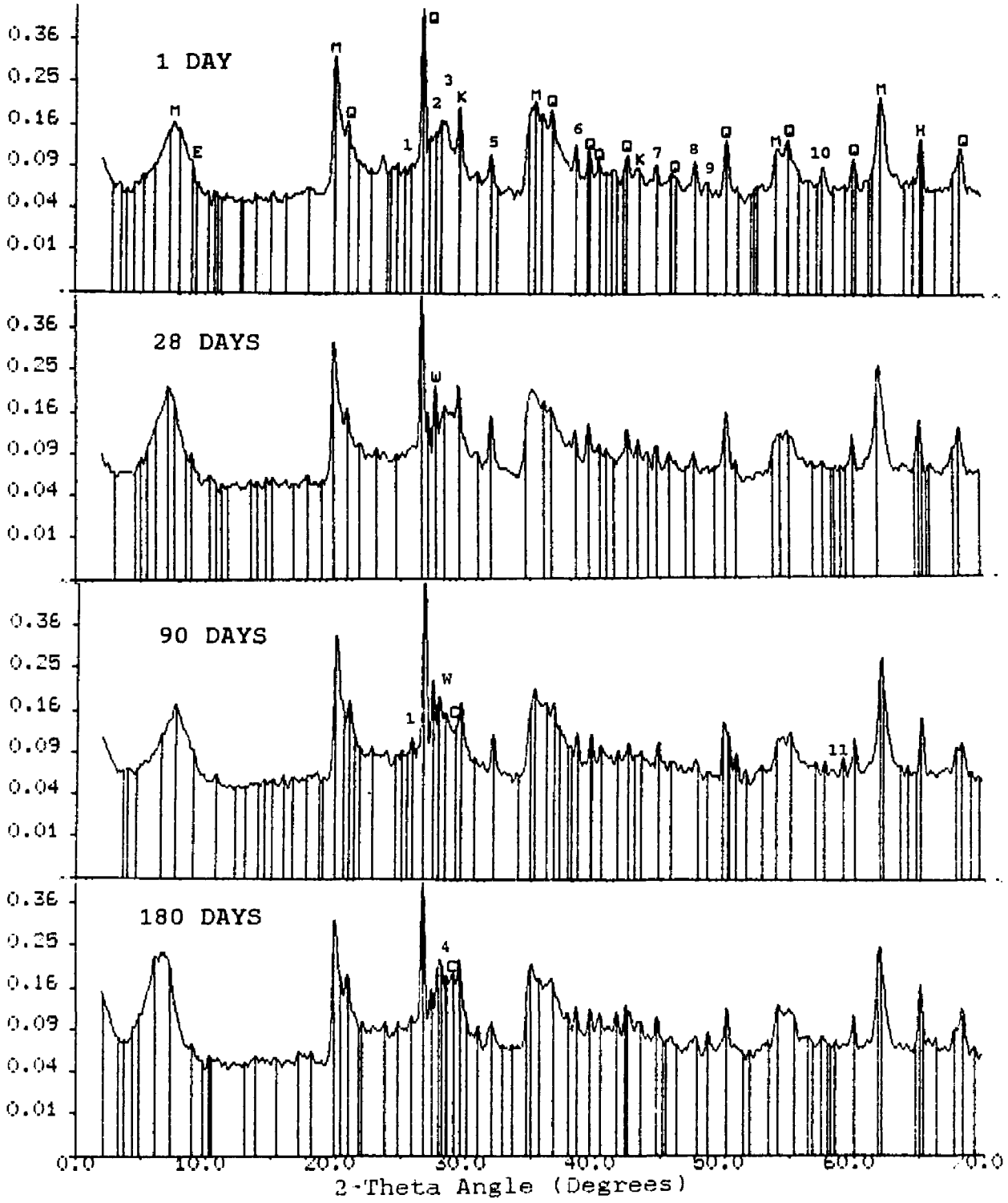

Figure 36. Powder X-Ray Diffraction Patterns of Bentonite-Lime Cured at 23°C . Q=quartz, M=montmorillonite, K=calcite, H=hematite, E=ettringite, C= CSH I, W=afwillite. For d-spacings represented by numbers refer to the text.

TABLE 12

UNIDENTIFIED PEAKS IN BENTONITE-LIME CURED AT 23°C.

D-spacing	Remarks
3.45 (1)	Appears after 1 day and its intensity increases after 90 days.
3.27 (2)	Is present in bentonite and its intensity increases till 90 days and decreases.
3.21 (3)	Is not present in bentonite, appears after one day and its intensity increases, probably afwillite.
3.12 (4)	Appears after 180 days.
2.79 (5)	Intensity increases after 28 days and decreases with increasing curing time.
2.33 (6)	Unchanged.
2.02 (7)	Intensity increases slightly after 90 days.
1.90 (8)	Intensity decreases with time.
1.87 (9)	Intensity is higher after one and 180 days and low at 28 and 90 days of curing.
1.60 (10)	Intensity decreases with time.
1.56 (11)	Is present after 90 days of curing.
1.43 (12)	Intensity slightly increases after 180 days.

The major change is the formation of CSH Type I and the increase in strength appears to be due to the formation of this mineral.

Bentonite-Lime (Cured at 50°C)

The stress-strain curves for the bentonite-lime mixture cured at 50°C are shown in Figures 37A and 37B. The unconfined compressive strength of the one day-cured sample at 50 ° C is 1084 kPa (157 psi) which is higher than the unconfined compressive strength of the 28 day, 23 ° C cured sample . The stress strain curves for the remaining time periods plot in a narrow range with an average unconfined compressive strength of 1316 kPa (191 psi). The elastic modulus for the one day-cured sample is 100000 kPa (14480 psi) and it increases to an average of 207292 kPa (30016 psi) for the 28, 90, and 180 day-cured samples. With 100 kPa confining pressure, the stress strain curve of the one day-cured sample is steeper (Figure 37B). The elastic modulus for the one-day cured sample is 157407 kPa (22793 psi). The stress-strain curves for the 28, 90, and 180 day-cured samples plot in a region where the elastic modulus changes from 157407 kPa (22793 psi) to 243902 kPa (35317 psi). The strain at failure for the one day-cured sample with no confining pressure is 0.0142 and decreases to approximately 0.0075 for the 28, 90 and 180 day-cured samples.

Overall the morphology of the samples cured at 50°C is similar to those cured at 23°C, however needle like crystals were not observed. Figure 38A shows a fractured surface of the one day-cured sample at low magnification. The aggregate boundaries (B) are well defined which is typical for brittle

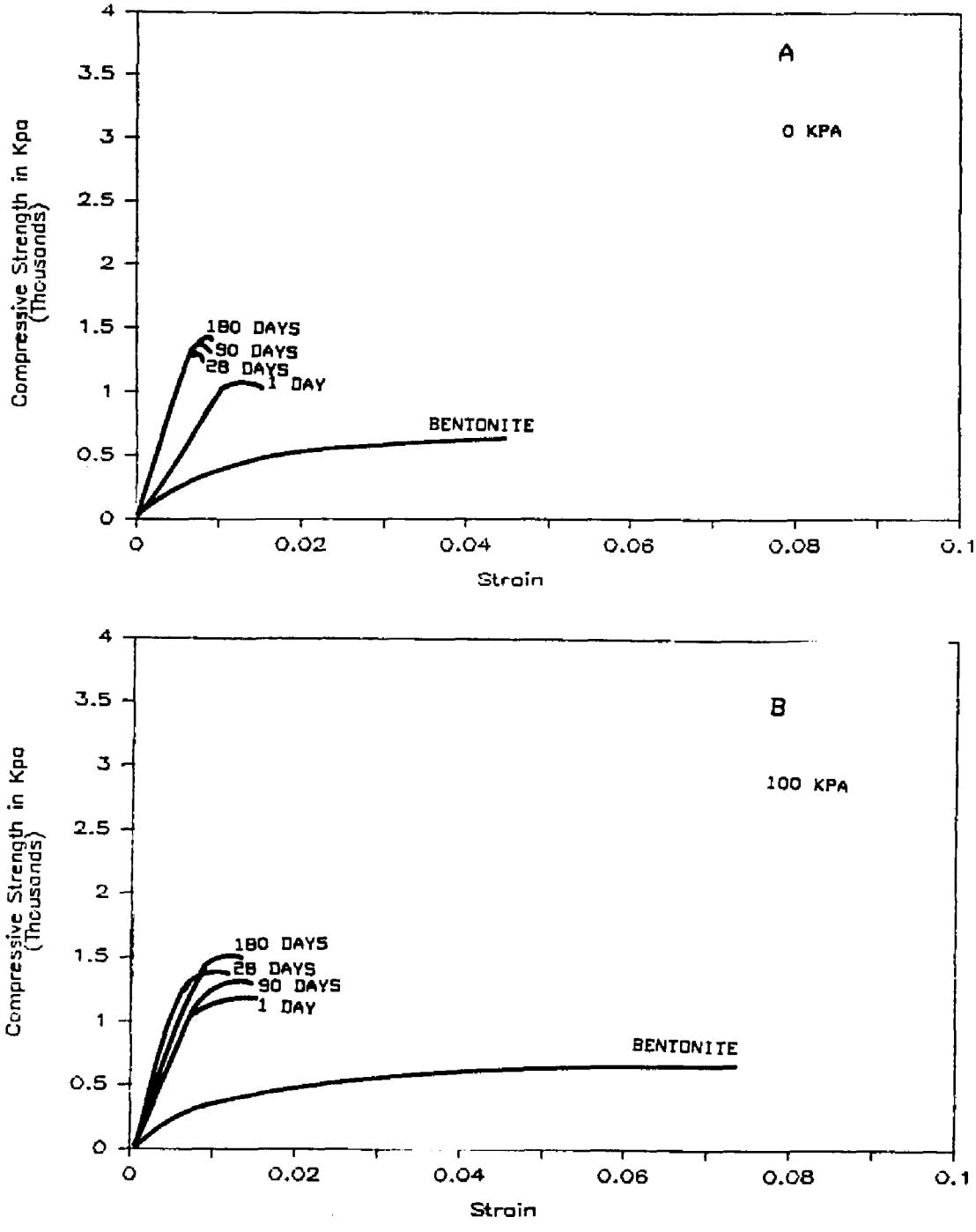

Figure 37. Stress-Strain Curves for Bentonite-Lime Mixture Cured at 50°C. A: Unconfined. B: With 100 kPa Confining Pressure.

Figure 38. Scanning electron micrographs of bentonite-lime samples cured at 50°C. A) The aggregate boundaries are well defined after one day of curing which is typical for brittle material. B) The equant crystal morphology is seen at intermediate magnification after 90 days of curing. C) The reaction products are local and they are not present everywhere (180 day-cured). D) Equant crystal morphology after 180 days of curing at high magnification.

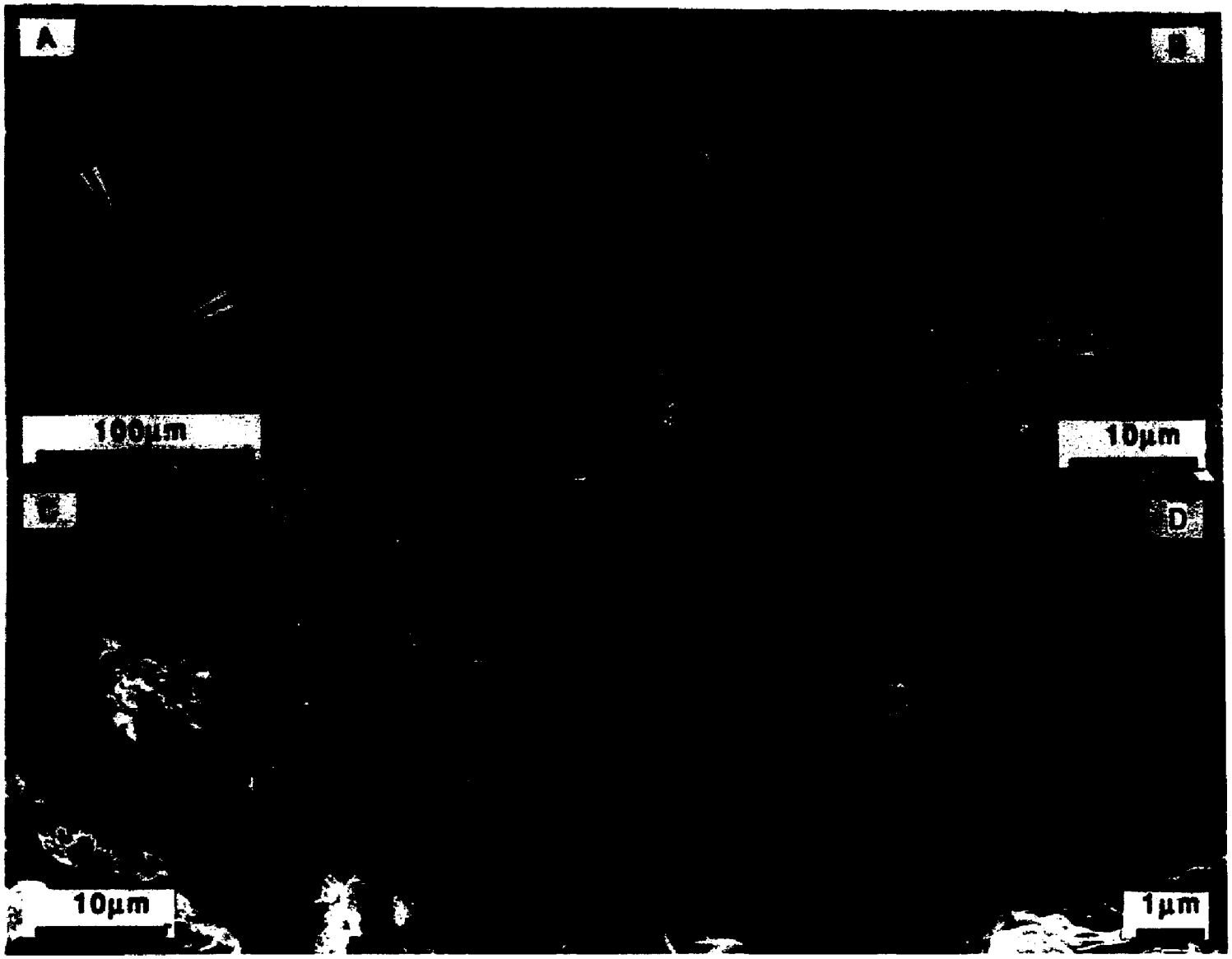
A
B
100µm
10µm
C
D
10µm
1µm

material. The dominant reaction product at this elevated temperature is the equant crystal morphology (E) illustrated in Figure 38B after 90 days of curing time. From morphological criteria this feature (E) appears to be CSH Type III. Figure 38C shows that these reaction products are local. Other CSH Type III crystals are illustrated in Figure 38D after 180 days of curing. EDS analyses of these crystals give a Ca/Si ratio of 0.04 and an Al/Si ratio of 0.19 .

X-Ray Diffractograms

The powder X-Ray patterns of the bentonite-lime mixture cured at 50°C are presented in Figure 39. A list of all the peaks may be found in Appendix B. The X-Ray patterns of samples cured at 50°C are similar to the X-Ray patterns of those cured at 23°C. The 3.07A CSH Type I peak (C) appears after one day of curing instead of after 28 days as in the lower temperature samples, and its intensity increases with time. The second peak assigned to CSH Type I is the 1.79A (C) peak which is present at all times. Higher curing temperature increased the rate of formation of CSH Type I which also increased the rate of strength gain during this period. The unidentified peaks are listed below.

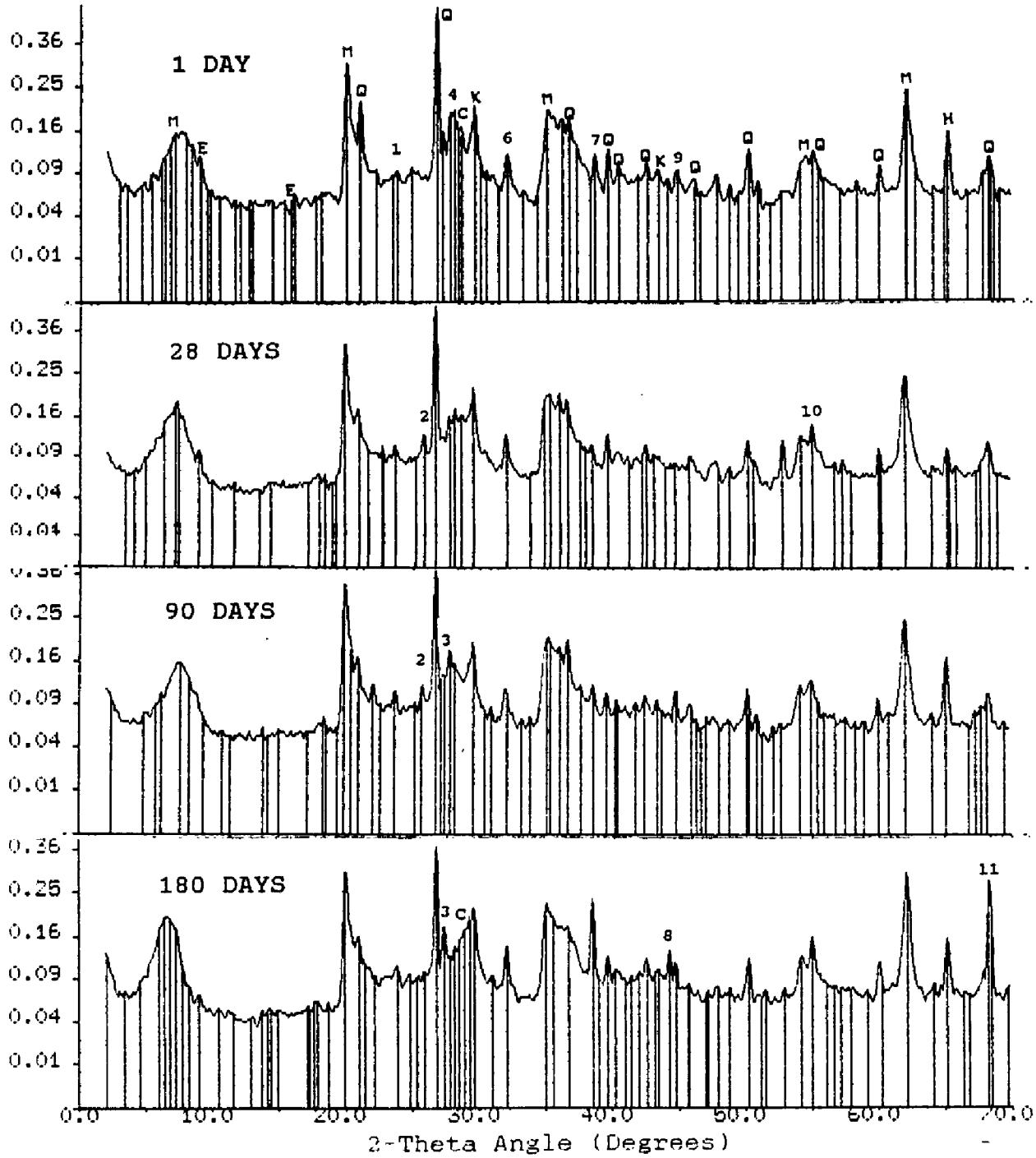

Figure 39. Powder X-Ray Diffraction Patterns of Bentonite-Lime Cured at 50°C. Q=quartz, M=montmorillonite, K=calcite, E=ettringite, H=hematite, C= CSH I. For d-spacings represented by numbers refer to the text.

TABLE 13

UNIDENTIFIED PEAKS IN BENTONITE-LIME CURED AT 50°C.

D-spacing	Remarks
9.86 (E)	Appears after one day,shifts to 9.92 after 28 days and to 9.83 after 180 days (possibly ettringite).
5.60 (E)	Is present after one day, then it dissappears.
3.74 (1)	Is present after one day and its intensity increases slightly after 28 days.
3.45 (2)	Appears after 28 days.
3.24 (3)	Appears after 90 days of curing .
3.21 (4)	Is present at all times, its intensity decreases after 180 days of curing, possibly afwillite.
2.89 (5)	Is present after 90 days.
2.79 (6)	Is present at all times.
2.33 (7)	Is present at all times, its intensity increases sharply after 180 days.
2.04 (8)	Its intensity increases sharply after 180 days of curing.
2.02 (9)	Is present at all times.
1.67 (10)	Is present at all times. Its intensity increases after 28 days, it is highest after 180 days of curing.
1.37 (11)	Appears after 180 days.

The higher curing temperature increased the rate of reaction as seen from the earlier formation of the CSH Type I mineral. The 3.27A peak dissappeared after 28 days at 23°C curing temperature where at 50°C 3.27A peak dissappeared after one day of curing. The intensity of the 3.45 peak increased after 90 days in the case of 23°C curing instead of 28 days for 50°C curing temperature.

Bentonite-Fly Ash-Lime (Cured at 23°C)

The stress-strain curves of bentonite-fly ash-lime mixture are presented in Figures 40A and 40B. The unconfined compressive strength of the one day-cured sample is 1061 kPa (154 psi). The stress-strain curves of the 28, 90 and 180 day-cured samples plot in a narrow region with the 28 day-cured sample having a lower unconfined compressive strength (1800 kPa-261 psi) than the 90 and 180 day- cured samples (2300 kPa-333 psi). The elastic modulus value for the one day-cured sample is 137931 kPa (19972 psi) and increases to 346667 kPa (50197 psi) after 28 days and to 426667 kPa (61781 psi) for the 90 and 180 day-cured samples. The strain at failure decreases from 0.012 for the one day to 0.006 for the 180 day-cured sample. One hundred kPa confining pressure causes an increase in strain at failure, thus a decrease in the elastic modulus in the initial stages. The elastic modulus for the one day-cured sample is 116667 kPa (16893 psi), after 28 days it increases to 201493 kPa (29176 psi) and for 90 days it is 345238 kPa (49990 psi). A higher elastic modulus of 500000 kPa (72400 psi) is obtained with 100 kPa confining pressure for the 180 day-cured sample. Strain at failure after one day is 0.0275 and it decreases to 0.006 after 180 days.

The major change in strength and elastic modulus occurs between one and 28 days. The rate of strength increase is lower between 28 and 90 days of curing. The strength

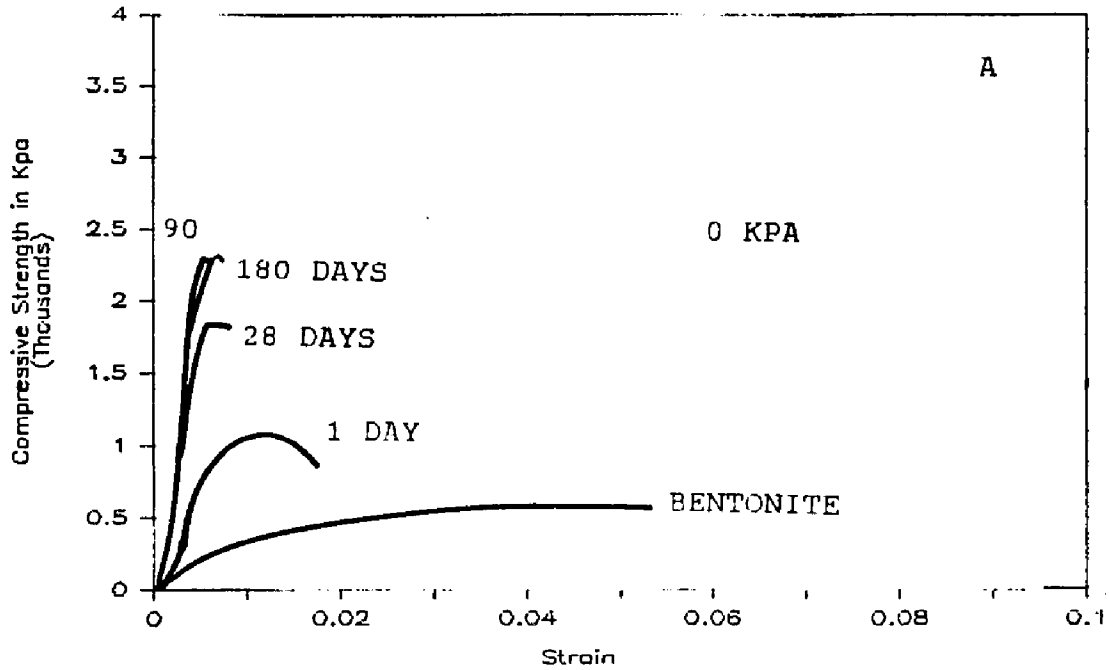

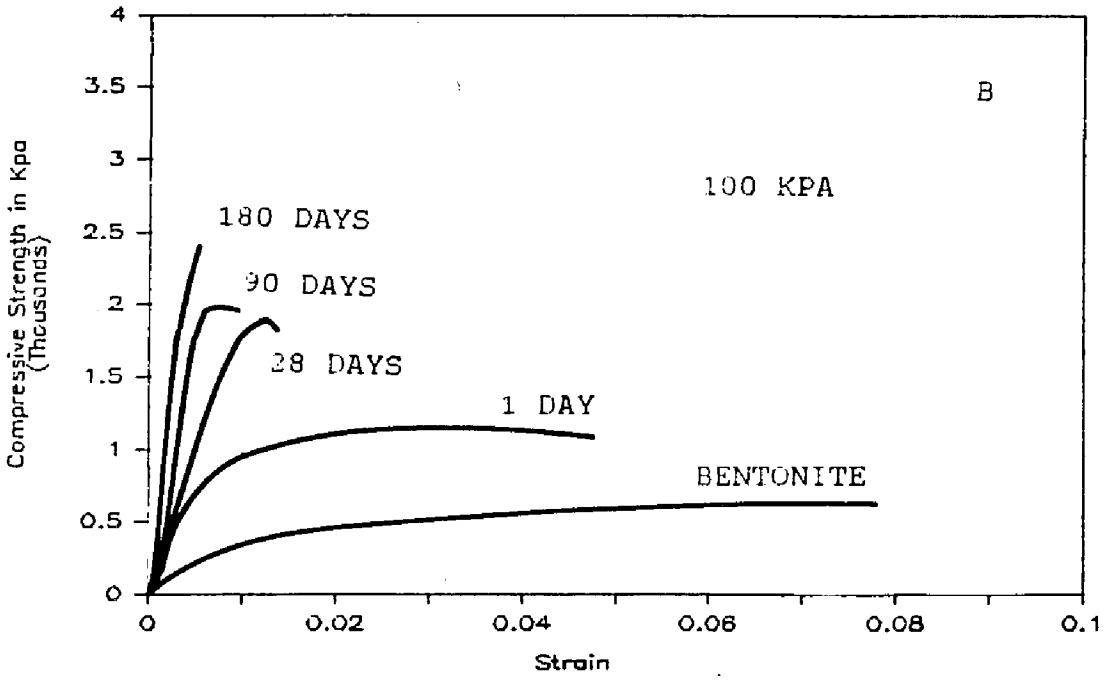

Figure 40. Stress-Strain Curves for Bentonite-Fly Ash-Lime Cured at 23°C. A: Unconfined. B: With 100 kPa Confining Pressure.

remains essentially constant between 90 and 180 days. With no confining pressure an elastic modulus value of 427,000 kPa (61830 psi) is reached after 90 days of curing which reflects a 3.1 fold increase relative to the elastic modulus of the one-day cured sample.

A fractured surface of the one day-cured sample is presented in Figure 41A at an intermediate magnification. This fracture surface contains mostly clay particles which suggests that the fractured surface is passing through the clay matrix. Some of the fly ash spheres have irregular outlines indicating that they are beginning to react chemically. As seen earlier, the boundaries of clay aggregates are not distinct which is a feature typical for plastic materials such as montmorillonite-rich clays.

Figure 41B presents a fractured surface of the 180 day-cured sample at low magnification. Abundant reaction products are typical of this long curing period. Pull out features (PO) and needles (N) along the pores are the dominant features. The major reaction products are acicular crystals with varying crystal forms and dimensions. The development stages of the acicular crystals are presented in Figures 42A, 42B, 42C and 42D. Figure 42A represents (high magnification) the initial stages of formation of ettringite needles (ET) (one day). The reaction products are so small that they are only visible at high magnifications. They are generally seen on montmorillonite aggregate surfaces and are composed of acicular crystals which are two to three

Figure 41. Scanning electron micrographs of bentonite-fly ash-lime samples cured at 23°C. A) A representative fracture surface of the one day-cured sample is seen at intermediate magnification. The fracture surface contains mostly clay particles which suggests that the fracture surface is passing through the clay matrix. B) A representative fracture surface of the 180 day-cured sample at low magnification. The reaction products are abundant. Pull out features (PO) and needles (N) are dominant.

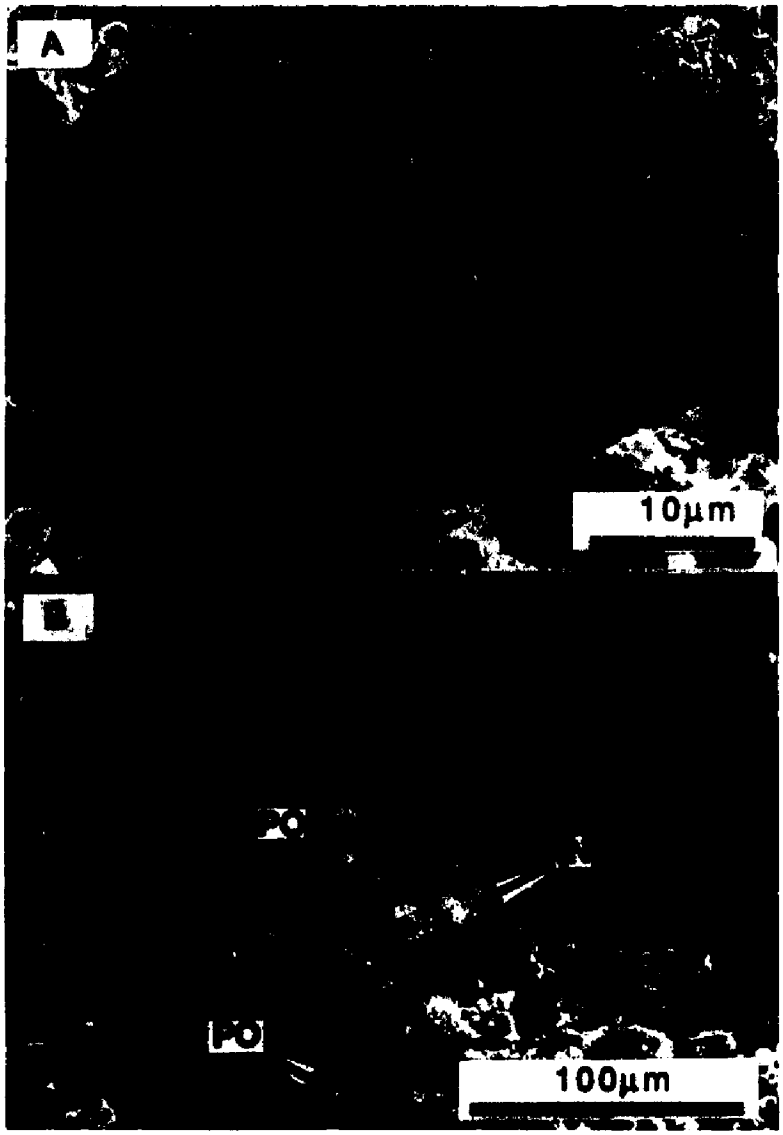
A
10μm
B
C
D
100μm

Figure 42. Scanning electron micrographs showing the development stages of the acicular crystals found in bentonite-fly ash-lime samples cured at 23°C. A) The initial stages of formation of ettringite (E) needles (one day-cured) at high magnification. B) After 28 days of curing a network of needles (N) dominate the microstructure of the fracture surface. C) Another representative fracture surface of the 28 day cured sample is seen at intermediate magnification. Acicular crystals with parallel sides (ET) are present. Their morphology resembles ettringite. D) The acicular crystals are less abundant after 90 days of curing.

A
2μm
B
10μm
C
10μm
D
10μm

micrometers long with diameters ranging from 0.3 to 0.4 micrometers. Their sides are parallel. They do not branch, distinguishing them from CSH Type I needles. Four to six of these crystals form bundles. They are oriented parallel to the montmorillonite aggregate surface and the bundles are randomly oriented relative to each other. They protrude into the pores. It is apparent that the montmorillonite flakes are participating in the reactions because needles are seen at the edges of the montmorillonite flakes. They become wider and flatter towards the origination point which is most probably a montmorillonite flake (they are less than one micrometer long) suggesting that portlandite is attacking the edges of the clay where calcium silicate hydrate gel begins to form as needles. The reaction products are more numerous at certain areas which may be aggregate contact points.

After 28 days of curing, a network of needles dominates the microstructure of the fracture surface as presented in Figures 42B and 42C at intermediate magnification. The radiating needles (N) are more numerous in or near the pores (Figure 42B) and their sizes vary. The types of needles present at this time may be grouped in two morphological categories. (1-) Three to six micrometer long, 0.2 to 0.4 micrometer diameter needles (N) with pointed ends. They form radiating bundles (Figure 42B). They are identified as CSH Type I by comparision to the morphologies described by Diamond (23) in cured cement pastes. In this case longer

needles have formed. The presence of CSH gel is confirmed by the X-ray powder patterns (Figure 44) which will be presented later in this section. (2-) Five to six micrometer long , 0.5 to 0.6 micrometer diameter rods with parallel sides and better defined crystal form (ET) relative to the first type (Figure 42C). They are randomly oriented and they span the pores. The morphology of these rods resembles ettringite.

The ettringite and CSH Type I crystals co-exist. The formation and increased abundance of the acicular crystals (rods and needles) are accompanied by a major strength increase and decrease in the strain at failure. The more rigid behavior may be attributed to the three dimensional network of rods and needles that supports the montmorillonite aggregates and the fly ash spheres and restricts their relative displacement.

Figure 42D presents a fractured surface of the 90 day-cured sample at intermediate magnification. The acicular crystals are less abundant at this curing period. They are three to four micrometers long and 0.3 to 0.5 micrometers in diameter. They are being transformed into other reaction products. The outlines of most of the fly ash grains are irregular indicating that they are reacting. A two micrometer diameter fly ash sphere is seen with a crust of small crystals completely encasing it. Square imprints of crystals which were pulled out when the sample was fractured, are readily apparent.

Figures 43A and 43B illustrate representative fracture surfaces of the 180 day-cured sample at intermediate magnification. The acicular crystals (CSH Type I and ettringite) are still present although they are less abundant relative to the 28 day-cured sample. EDS analyses on the acicular crystals yield a Ca/Si ratio of 1.25 and an Al/Si ratio of 0.66 typical of CSH Type I.

Figure 43A illustrates reacted fly ash particles. Needles (N) form a crust on a 7.5 micrometer diameter fly ash sphere. During fracture one part of this reacted crust was pulled out which suggests that this coating acted as a binder to the neighboring feature. A broken reacted (R) five micrometer fly ash sphere is seen. The whole fly ash sphere is eaten away and is replaced by a three dimensional network of needles. A pull out feature (PO) (20 micrometers long and 10 micrometers wide) illustrates that montmorillonite is participating in the reaction. Tiny needles less than one micrometer long are present on the edges of the montmorillonite flakes. In Figure 43B the remnant of a 45 micrometer fly ash sphere (S) is filled with reacted fly ash spheres and other reaction products. One of the flyash spheres (R) has a reacted crust displaying the typical morphology of CSH Type IV "inner product" . EDS analyses of this product give a Ca/Si ratio of 0.12 and an Al/Si ratio of one. Different aggregates of equant crystals (E) less than 0.4 micrometer in all dimensions are apparent. EDS analyses yield a Ca/Si ratio of 0.58 and an Al/Si ratio of

Figure 43. Scanning electron micrographs of representative fracture surfaces of the 180 day-cured bentonite-fly ash-lime samples cured at 23°C at intermediate magnification. A) A fly ash grain is seen with a coating of needles (N). A pullout feature (P) has tiny needles on the edges of the montmorillonite flakes illustrating that montmorillonite is participating in the reaction. A broken fly ash sphere (R) is eaten away and replaced by three dimensional network of needles. B) The remnant of a reacted fly ash sphere (S) is filled with ather fly ash spheres and reaction products. Aggregations of equant crystals (E) are present engulfing the fly ash sphere.

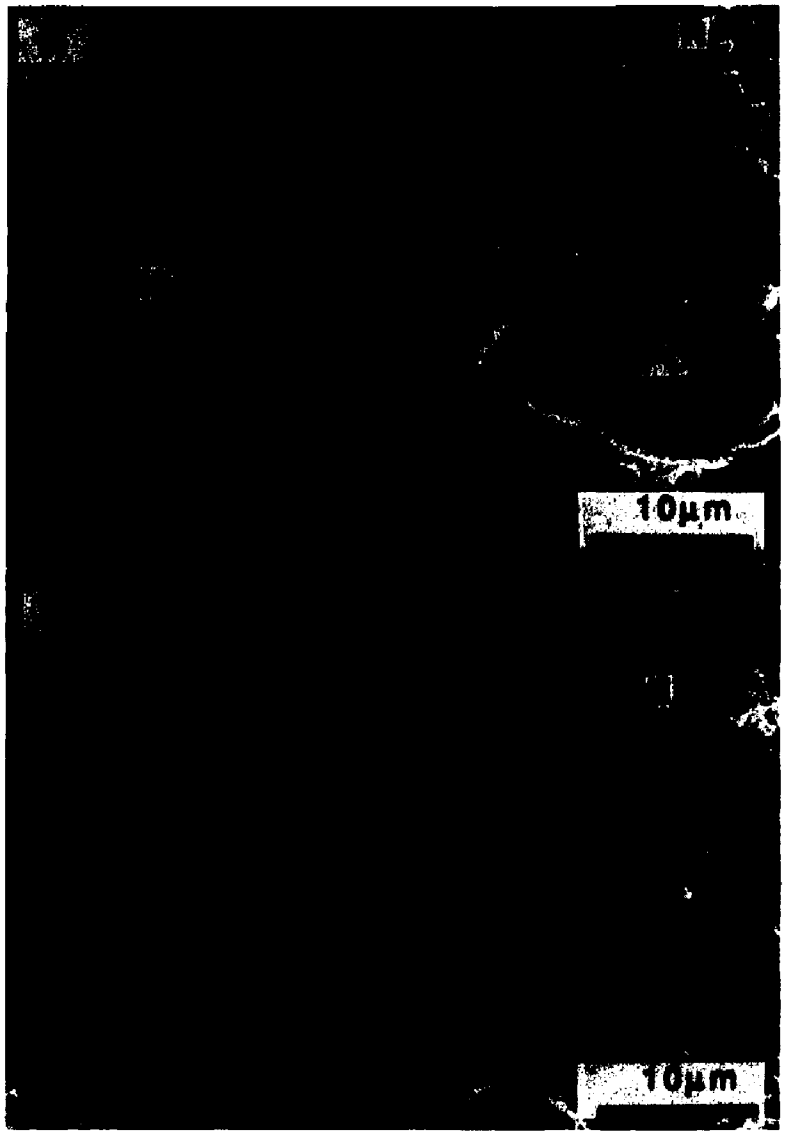
10µm
10µm

0.54 . These features are CSH Type III crystals.

X-Ray Diffractograms

XRD powder patterns for the cured samples are presented in Figure 44. A complete list of all peaks is presented in Appendix B. The major mineral is montmorillonite and no change is observed in the relative intensities of its peaks (M). Quartz (Q) and calcite (K) are present. The relative intensity of the major calcite peak changes with time; it is lowest after 180 days of curing. The intensity of tricalcium aluminate (T) which is one of the abundant minerals in fly ash is drastically reduced because of the small quantity of fly ash in the mixture. Portlandite peaks are not present even after one day of curing. The intensity of the periclase peak (P) does not change with increasing curing time. The intensity of the hematite peak (H) increases after 28 days and then does not change. The strongest peak of CSH Type I (C) appears after 28 days of curing (3.07A) which corresponds to a major strength increase. The intensity of the 3.07A peak increases and it is highest after 180 days of curing. The other peaks that can be assigned to CSH Type I are at 1.79A or 1.83A (C). The relative intensity of the 1.83A peak increases after 28 days and then does not change. The 1.79A peak is present at all times and its relative intensity decreases with time. Another d-spacing for CSH Type I varies between 2.76A and

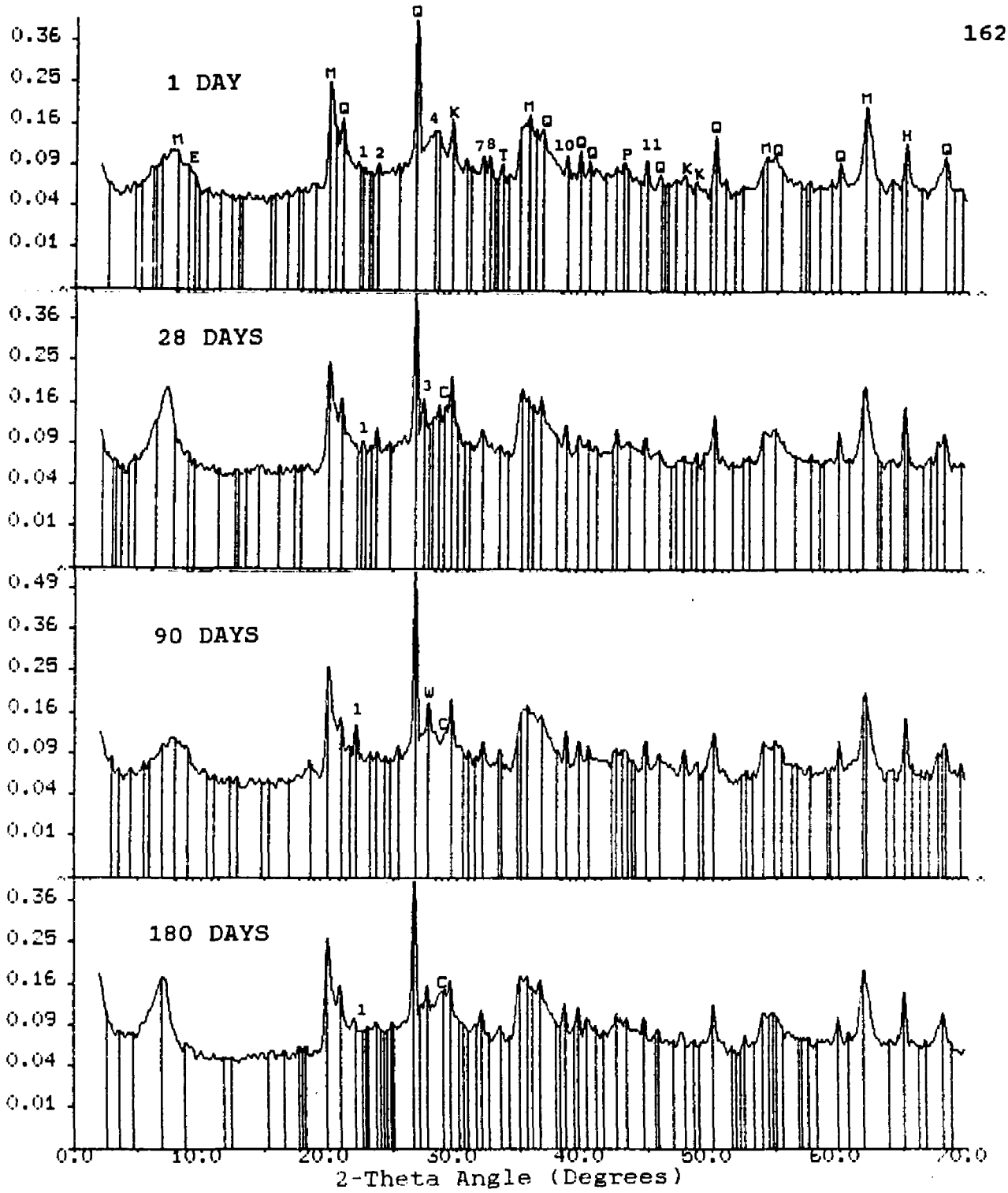

Figure 44. Powder X-Ray Diffraction Patterns of Bentonite-Fly Ash-Lime Cured at 23°C. Q=quartz, M=montmorillonite, K=calcite, T=tricalcium aluminate, P=periclase, H=hematite, C= CSH I, W=afwillite, E=ettringite. For d-spacings represented by numbers refer to the text.

2.81A (C), and is overlapped by the 2.79A montmorillonite peak. The presence of CSH Type I needles is confirmed by the scanning electron micrographs. Even though crystals of ettringite are readily identifiable in the scanning electron micrographs, its presence is not always obvious in XRD results. The major ettringite peak (E) at 10A appears to shift with time from 9.91A to 9.89A and 10.09A. The relative intensities of these peaks decrease with time. The 5.66A peak (E) is not present after 28 days of curing. Afwillite (3.21A peak) appears after 28 days of curing and its major peak (W) increases with time. The other strong peaks reported for afwillite are at 2.84A and 2.74A peaks. The first appears after 90 days of curing and the latter is seen after 180 days of curing. The other peaks, which represent minerals that could not be readily identified because of, low peak intensities, or severe overlaps by other minerals are tabulated below.

TABLE 14

UNIDENTIFIED PEAKS IN BENTONITE-FLY ASH-LIME CURED AT 23°C.

D-spacing	Remarks
4.00-4.03 (1)	Is present after one day of curing, its intensity increases with time; highest after 90 days then decreases.
3.74 (2)	Is present at all times; its intensity is

	higher after 28 days.
3.25 (3)	Appears after 28 days of curing with high intensity.
3.17 (4)	Is present at all times.
2.91-2.93 (5)	Appears after 28 days of curing, and present after 90 and 180 days.
2.88-2.89 (6)	Is present at all times.
2.79 (7)	Is present at all times, and its intensity increases after 28 days and decreases after 180 days.
2.76 (8)	Is present after one day, dissappears after 28 days.
2.64 (9)	Its intensity decreases with time.
2.33 (10)	Its intensity increases after 28 days and decreases after 90 days.
2.02 (11)	Unchanged.
1.90 (12)	Its intensity is higher after 90 and 180 days of curing.

Afwillite, CSH Type I and ettringite are identified as newly forming cementitious minerals. Their appearance in the X-Ray pattern or changes in their peak intensities correspond to an increase in the compressive strength of the bentonite-fly ash-lime mixture. The scanning electron microscopy study confirms the formation of CSH Type I and ettringite. The X-Ray diffraction patterns show that the newly forming minerals are very low in quantity and most

probably they are poorly crystallized. The crystal structure of montmorillonite is not noticebly altered.

Bentonite-Fly Ash-Lime (Cured at 50°C)

The stress-strain curves for the 50°C cured bentonite-fly ash-lime mixture are presented in Figures 45A and 45B. The one day unconfined compressive strength of the bentonite-fly ash-lime mixture is 2100 kPa (304 psi) which is higher than the 28 day unconfined compressive strength of the 23°C cured sample. After 28 days of curing the UCS increases to 2639 kPa (382 psi). An average value of 2900 kPa (420 psi) is typical for the 90 and 180 day-cured samples. The elastic modulus value for the one day-cured sample is 246032 kPa (35625 psi), it increases to 370,000 kPa (53576 psi) for the 90 and 180 day-cured samples. The strain at failure is 0.011 for the one day-cured sample and it decreases to 0.009 after 180 days. One hundred kPa confining pressure increased the elastic modulus to 296296 kPa (42904 psi) for the one day-cured sample. The stress strain curves for the 90 and 180 day-cured samples yield an elastic modulus of 505434 kPa (73187 psi) (confined). The strain at failure decreases from 0.015 for one day to 0.009 for 180 days.

Figure 46A illustrates a representative fracture surface of the one day-cured bentonite-fly ash-lime sample at intermediate magnification. Acicular and lathlike crystals (N) with well developed crystal forms span the pores and support the fly ash spheres and the montmorillonite aggregates. These ettringite crystals are

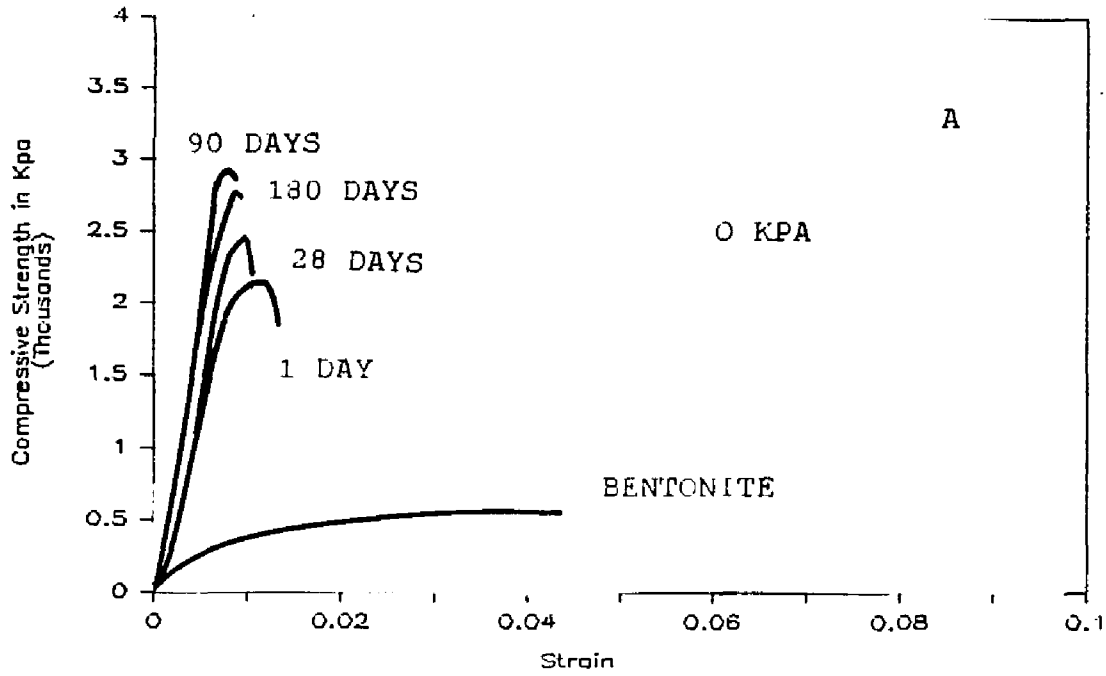

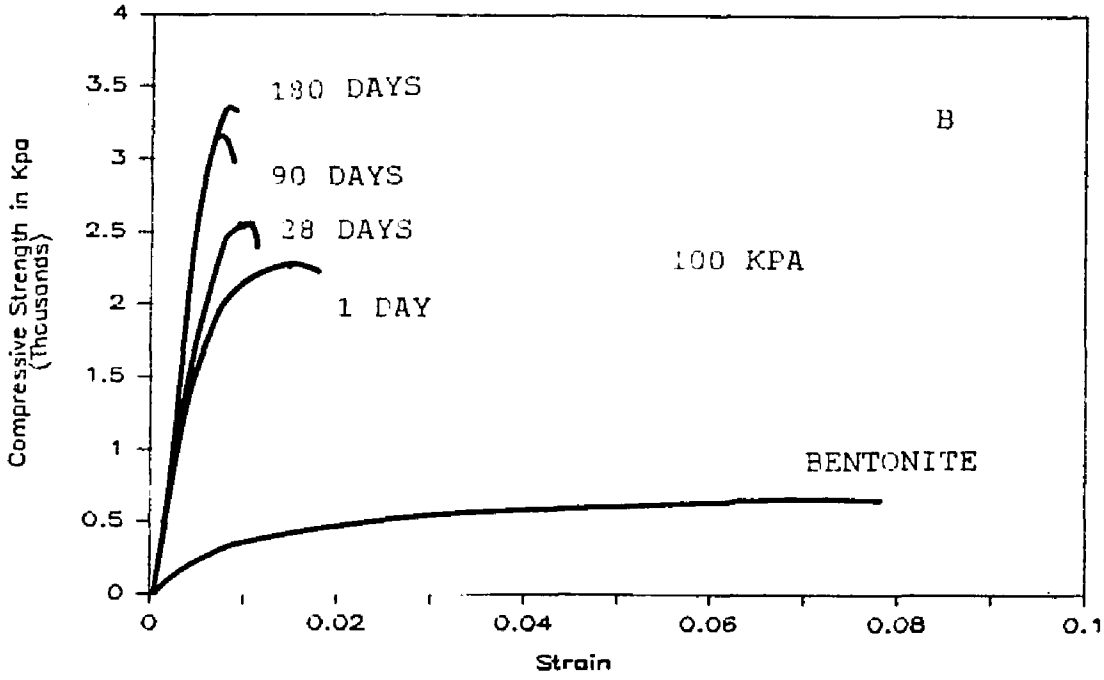

Figure 45. Stress-Strain Curves for Bentonite-Fly Ash-Lime Mixture Cured at 50°C. A: Unconfined. B: With 100 kPa Confining Pressure.

Figure 46. Scanning electron micrographs of bentonite-fly ash-lime samples cured at 50°C. A) A representative fracture surface of the one day-cured sample at intermediate magnification. Acicular and lathlike (N) crystals span the pores and support the fly ash spheres and the montmorillonite aggregates. B) A fracture surface of the 28 day-cured sample at low magnification. The aggregate boundaries are well defined which is typical for brittle material. C) After 28 days of curing the acicular crystals are less abundant and they are seen mostly in the pores (N). A reacted crust of a fly ash sphere is seen at (PO). A fly grain is replaced by a three-dimensional network of needles (R). D) Acicular crystals with better developed crystal forms and hexagonal cross section are seen after 90 days of curing. The hexagonal cross section is typical for secondary ettringite.

A
10μm
B
100μm
C
10μm
D
1μm

four to five micrometers long and 0.4 to 0.5 micrometers wide with parallel sides. Because of the support of the acicular crystals, the fly ash particles and montmorillonite aggregates have a higher strength and become more rigid after only one day of curing. The fly ash particles have irregular outlines which suggests that they are being corroded. Figure 46B illustrates a fracture surface of the 28 day-cured sample at low magnification. The aggregate boundaries are well defined which is typical for brittle material. The fly ash particles have irregular outlines. Figure 46C presents a fracture surface of the 28 day-cured sample at intermediate magnification. There are fewer acicular crystals (N) present at this curing time and they are seen in the pores. There is a 7.5 micrometer diameter completely reacted broken fly ash particle (R) which is filled with a three dimensional network of needles, most probably CSH Type I. A "pull out" feature is present with a reacted crust.

After 90 days of curing the acicular crystals are still present in varying developmental stages. Acicular crystals with better developed crystal forms and hexagonal cross section are seen in Figure 46D. The hexagonal cross section is typical for secondary ettringite. They are up to ten micrometers long and one to three micrometers wide prisms and their Ca/Si ratio is 0.72 and Al/Si ratio is 1.03 . Hexagonal prisms bundle together to form wider rods. CSH Type I co-exist with ettringite at this curing period

(figure not shown). Equant crystals (E), less than 0.5 micrometers in each direction, are the dominant features in Figure 47A at intermediate magnification after 90 days of curing. EDS analyses of these features reveal a Ca/Si ratio of 0.85 and an Al/Si ratio of 0.75 . This is most probably CSH Type III. A fly ash sphere is engulfed by the equant grains. The compressive strength is highest at this curing period. Figure 47B illustrates the crust of a reacted 25 micrometer diameter fly ash sphere (R) after 180 days of curing at intermediate magnification. During fracture this hollow sphere (cenosphere) was broken exposing the inside of the reacted crust. This crust is composed of a mat of interlocking one micrometer long, tiny needles. The crust is approximately two micrometers which means that at least eight to ten layers of needles are present . EDS analyses yield a Ca/Si ratio of 0.33 and an Al/Si ratio of 0.70 . Another reacted, ten micrometer diameter, hollow fly ash sphere is present. The reacted crust (RC) of a 13 micrometer fly ash sphere is evident in Figure 50C, at intermediate magnification after 180 days of curing. The imprint of a 15 micrometer diameter fly ash sphere is seen. Sharp-edged blades (eight micrometers long, one micrometer wide) appear for the first time. Figure 47D illustrates a fracture surface of the 180 day cured sample at high magnification. A reacted 14 micrometer fly ash sphere is seen. It has a reacted crust (RC) and an etched interior (EI). A seven micrometer diameter fly ash particle is

Figure 47. Scanning electron micrographs of bentonite-fly ash-lime samples cured at 50°C. A) Blocky aggregation of equant crystals (E) is seen engulfing a fly ash grain after 90 days of curing. B) A fracture surface of the 180 day-cured sample at intermediate magnification. A reacted crust (R) of a fly ash grain is present. C) Reacted fly ash grains after 180 days of curing at intermediate magnification. A reacted crust (RC) of a fly ash grain is present and sharp edged blades are seen in the imprint of a pulled out (PO) fly ash sphere. D) A fly ash grain with reacted crust (RC) and etched interior (EI) is seen after 180 days of curing at high magnification.

A
10μm
B
10μm
C
10μm
RC
D
2μm
RC

covered with a film.

In summary, major strength development is observed after one day of curing. Overall there are fewer needles than in the 23°C cured sample. The crystal forms are better developed at 50°C relative to 23°C curing temperature. The acicular crystals appear in the pores and on some of the reacted spheres. The Ca/Si ratio is roughly 1.8 and the Al/Si ratio is 1.1 for these acicular crystals. Most of the fly ash spheres are covered with a one to two micrometer thick reacted crust which is rich in aluminum. CSH Type III grains are present after 90 days of curing.

X-Ray Diffractograms

The powder X-ray diffraction patterns for bentonite-fly ash-lime mixture cured at 50°C are presented in Figure 48. A complete listing of the peaks is presented in Appendix B. The XRD patterns of the 50°C and the 23°C cured bentonite-fly ash-lime mixtures are very similar, so to avoid repetition only some highlights will be presented below.

The relative intensity of the calcite (K) peak decreases after 90 days of curing similar to those of samples cured at 23°C. There are no changes in the montmorillonite (M) and quartz (Q) peak intensities. The intensity of the hematite peak (H) increases after 180 days of curing. CSH Type I (C), ettringite (E) and afwillite (W)

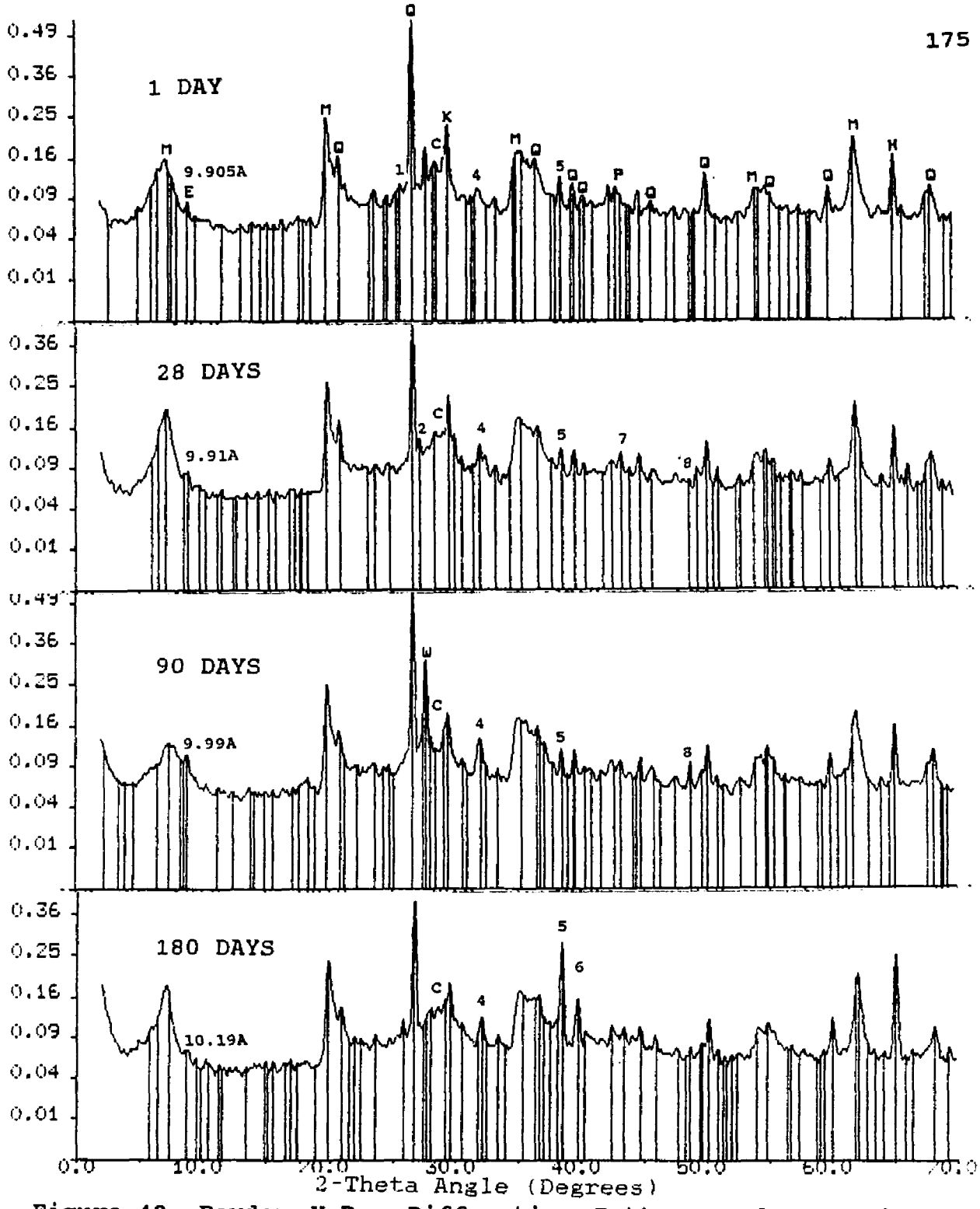

Figure 48. Powder X-Ray Diffraction Patterns of Bentonite-Fly Ash-Lime Cured at 50°C. Q=quartz, M=montmorillonite, K=calcite, P=periclase, H=hematite, C= CSH I, W=afwillite, E=ettringite. For d-spacings represented by numbers refer to the text.

are identified. The high curing temperature increased the rate of the reactions. CSH Type I appears after one day of curing in the 50°C cured sample instead of after 28 days at 23°C. Overall the relative intensities of the 1.84A and 1.79A peaks are higher than in the 23°C cured samples. The ettringite 9.905A d-spacing shifts to 9.91A, 9.99A and 10.19A after 28, 90 and 180 days of curing respectively. The relative intensity of the ettringite peaks corresponding to 90 days of reaction is the highest; the intensity is lower after 180 days of curing. The 5.60A peak dissappears between one and 28 days. The 3.21A, 2.84A and 2.74A d-spacings are assigned to afwillite and appears after one day of curing. After 28 days of curing the 3.21A peak is not seen because of an overlap. The relative intensity of the 3.21A afwillite peak increases considerably after 90 days of curing when this mixture attained its highest strength. A remarkable decrease in the relative intensity of 3.21A afwillite peak after 180 days of curing is accompanied by a slight decrease in compressive strength. The unidentified peaks are presented in the table below.

TABLE 15

UNIDENTIFIED PEAKS IN BENTONITE-FLY ASH-LIME CURED AT 50°C.

D-spacing	Remarks
3.45 (1)	Is present after one and 180 days.
3.26 (2)	Appears after 28 days with a high intensity, is present after 90 and 180 days with very low intensity; similar to the 23°C cured sample.
2.92 (3)	Appears after 28 days of curing and stays unchanged.
2.79 (4)	Its intensity increases after 28 days.
2.33 (5)	Is present at all times, its relative intensity increases sharply after 180 days.
2.27 (6)	Is present at all times, its relative intensity increases after 180 days.
2.08 (7)	Its intensity increases after 28 days and then stays constant.
1.87 (8)	Is present at all times with the highest intensity after 90 days.

The same minerals are observed at 50°C and 23°C temperatures. The higher curing temperature increases the rate of the reactions as observed by the early formation of CSH Type I. The formation of new minerals such as ettrigite, CSH Type I, CHS Type III and afwillite is accompanied by improved compressive strength.

CHAPTER VI

SUMMARY AND DISCUSSION OF RESULTS

In all of the mixtures studied, at both curing temperatures, the unconfined compressive strengths of the treated soils are higher than the unconfined compressive strengths of the untreated bentonite (Tables 16 and 17). The elastic moduli of the bentonite-fly ash-lime mixtures are higher than the elastic moduli of the bentonite-fly ash and bentonite-lime mixtures. After 180 days of curing at 23°C the elastic modulus of the bentonite-fly ash-lime (S) mixture is approximately fifteen times greater than the elastic modulus of bentonite (the elastic modulus of untreated bentonite is 30500 kPa-4416 psi). The unconfined compressive strength of bentonite-fly ash-lime (S) mixture increased four times relative to UCS of bentonite (UCS of bentonite is 592 kPa-86 psi) after 180 days of curing. At 50°C curing temperature the UCS of bentonite-fly ash-lime (S), is 500 kPa (72 psi) higher than the UCS of the 23°C cured sample after 180 days of curing. The maximum values for unconfined compressive strengths and elastic moduli were observed after 90 days of curing and a decrease was observed between 90 and 180 days of curing (Figures 49 and 50). Fly ash and fly ash-lime mixtures have UCS one order of magnitude higher than the UCS of mixtures with bentonite.

TABLE 16

SUMMARY OF COMPRESSIVE STRENGTH TESTS
23°C

	FA	FL	F	L	S
1 Day					
UCS	10237	7189	906	610	1061
CS			1059	746	1107
E(U)			93404	77460	144045
E(C)			155590	70707	118700
28 Days					
UCS	18367	18265	1414	996	1800
CS			1277	1108	1957
E(U)			278289	217945	386882
E(C)			237267	140063	402751
90 Days					
UCS	19745	26492	1467	1252	2444
CS			1299	1323	2144
E(U)			210059	218087	647407
E(C)			137893	265269	399049
180 Days					
UCS	26030	32236	1387	1344	2295
CS			1525	1342	2530
E(U)			261050	252500	460823
E(C)			318471	281449	587259

Note: UCS=Unconfined compressive strength, CS=Confined strength (100 kPa confining pressure), E(U)= Elastic modulus from unconfined test, E(C)= Elastic modulus from confined test. All values presented in the table are in kPa.
UCS of untreated bentonite=590 kPa, CS of untreated bentonite=597 kPa, E(U) of untreated bentonite=30500 kPa, E(C) of untreated bentonite=23064 kPa. To convert to psi multiply by 0.1448 . FA=Fly ash, FL=Fly ash-lime, F=Bentonite-Fly ash, L=Bentonite-lime, S=Bentonite-fly ash-lime.

TABLE 17

SUMMARY OF COMPRESSIVE STRENGTH TESTS
50°C

	FA	FL	F	L	S
1 Day					
UCS	10923	7372	1234	1084	2099
CS			1343	1144	2220
E(U)			140950	85861	349250
E(C)			56697	207692	358066
28 Days					
UCS	18877	32398	1327	1309	2639
CS			1775	1341	2691
E(U)			185954	263589	456193
E(C)			291291	251960	494513
90 Days					
UCS	26949	39472	1525	1386	3102
CS			2052	1318	3178
E(U)			116883	243546	614514
E(C)			301117	146857	667697
180 Days					
UCS	22630	39724	1915	1254	2793
CS			1785	1528	3401
E(U)			284450	201538	398135
E(C)			230392	140030	443735

Note: UCS=Unconfined compressive strength (kPa), CS= Confined compressive strength (kPa) (100 kPa confining pressure), E(U)= Elastic modulus (kPa) from unconfined test, E(C)= Elastic modulus from confined test (kPa). To convert to psi multiply by 0.1448 . FA=Fly ash, FL=Fly ash-lime, F=Bentonite-fly ash, L=Bentonite-lime, S=Bentonite-fly ash-lime.

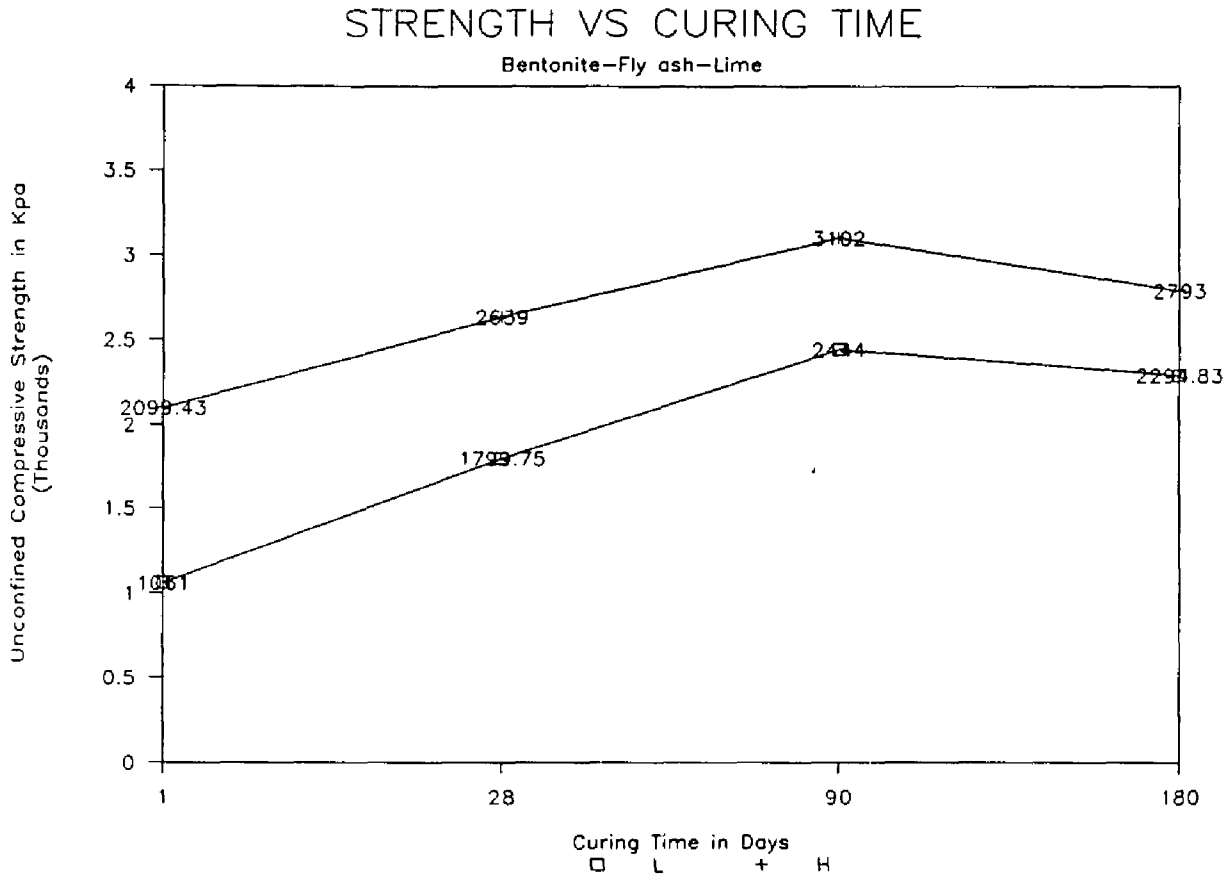

Figure 49. Unconfined Compressive Strength Versus Curing Time for 23°C and 50°C cured Bentonite-Fly Ash-Lime Mixtures.

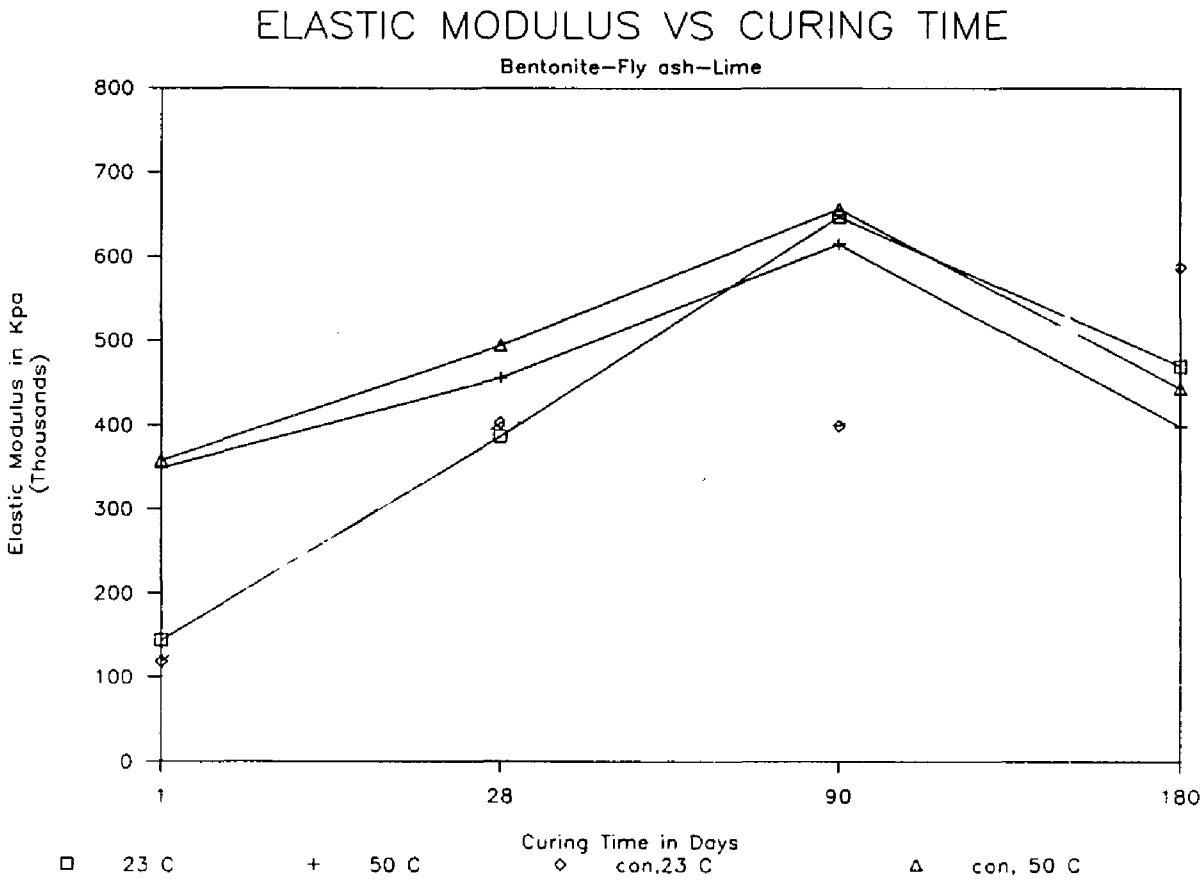

Figure 50. Elastic Modulus Versus Curing Time for 23°C and 50°C Cured Bentonite-Fly Ash-Lime Mixtures.

The addition of fly ash to bentonite-lime makes the mixture more rigid than the original mixture. The elastic moduli obtained for bentonite-fly ash-lime are approximately twice the elastic moduli of bentonite-lime mixtures.

The maximum strength obtained for bentonite-fly ash-lime mixture is satisfactory considering that most of the material in the mixture is fine material without a mechanically stable matrix. The increase in strength is directly related to the formation of cementitous minerals. X-Ray powder diffractograms suggest that these new minerals are forming in minute quantities and they are poorly crystalline.

The minerals identified by X-Ray diffraction techniques are summarized in Tables 18 and 19. Each mixture contained different starting materials and produced different cementitious mineral products. The hydrated calcium aluminates of the fly ash dominated samples were not detected in the montmorillonite dominated samples. The change in bulk composition may have created favorable conditions for the precipitation of ettringite and afwillite instead. Alternatively, the calcium aluminum hydrates may not be abundant enough to be detected. The most consistent reaction product in the mixtures was CSH gel. Its appearance is coincident with the curing times after which considerable compressive strength increases are observed. Ettringite is present in bentonite-fly ash, bentonite-lime and bentonite-fly ash-lime mixtures after one day of curing. The

TABLE 18
THE IDENTIFIED MINERALS IN THE X-RAY POWDER PATTERNS
($23^{o}C$)

	FA	FL	F	L	S
1 Day	Quartz TCA Periclase Alite Anhydrite Lime C_4AH_{13} * CSH I *	Portlan. Quartz TCA Periclase Hematite C_3AH_6 * C_4AH_{13} *	Montmo. Quartz Calcite TCA Periclase Hematite Ettrin. * Afwil. *	Montmo. Quartz Calcite Hemeatite Afwil. * Ettrin. *	Montmo. Quartz Calcite TCA Periclase Hematite Ettrin. *
28 Days	Same	Same	Same	Same+ CSH I *	Same+ CSH I * Afwil. *
90 Days	Same	Same	Same+ CSH I *	Same	Same
180 Days	Same	Same	Same	Same	Same

Note: (*) indicates the newly forming cementitious minerals. (Same) indicates that no change was observed in mineral identifications relative to the previous curing period. Montmo.=Montmorillonite, Afwil.=Afwillite, Ettrin.=Ettringite, Lime=CaO. FA=Fly ash, FL=Fly ash-lime, F=Bentonite-fly ash, L=Bentonite-lime, S=Bentonite-fly ash-lime.

TABLE 19

THE IDENTIFIED MINERALS IN THE X-RAY PATTERNS
50°C

	FA	FL	F	L	S
1 Day	Quartz TCA Periclase Hematite C_4AH_{13} * CSH I *	Portlan. Quartz TCA Periclase C_4AH_{13} * C_3AH_6 * Hematite	Montmo. Quartz Calcite TCA Periclase Hematite CSH I * Etrin. *	Montmo. Quartz Calcite Hematite Afwil. * CSH I * Ettrin. *	Montmo. Quartz Calcite Hematite CSH I * Ettrin. * Afwil. *
28 Days	Same	Same	Same	Same	Same
90 Days	Same	Same	Same	Same	Same
180 Days	Same	Same	Same	Same	Same

Note: (*) indicates the newly forming cementitious minerals. (Same) shows that no change was observed in the identified minerals at that curing period. Montmo.= montmorillonite, Afwil.=afwillite, Ettrin.=ettringite, Portlan.= portlandite. FA=Fly ash, FL=Fly ash-lime, F=Bentonite-fly ash, L=Bentonite-lime, S=Bentonite-fly ash-lime.

ettringite minerals are readily seen in micrographs. The complete transformation of ettringite to monosulphoaluminate as expected by comparision with portland cement is not observed in any of the mixtures. Ettringite is the first stable hydration product of Portland cement when there is an ample supply of calcium sulphate. The source of the sulphur is the anhydrite from the fly ash. There is competition between ettringite and calcium silicate hydrates for sulphur. Sulphates are incorporated into the structure of CSH thus decreasing the availability of sulphates for other reactions. Ettringite reacts and dissolves contributing SO_4 and other elements for the formation of CSH gel and afwillite.

With the scanning electron microscope the development of needles, hexagonal plates and equant crystals and the participation of montmorillonite flakes and fly ash grains in the reactions were observed. Needles are observed at the initial stages of curing (1 day), forming on the edges of montmorillonite flakes at high magnifications (the length of the needles was approximately 2 micrometers). After 28 days of curing the needles became more abundant and their lengths increased to approximately six micrometers. The needles were observed in the pores, on the fly ash grains and on montmorillonite aggregates. Blocky aggregates of 0.5 micrometer equant crystals were observed engulfing the fly ash grains after 90 days of curing. Hexagonal plates were observed only in fly ash and fly ash-lime mixtures. They

span the pores and their sizes increased from approximately two micrometers to approximately ten micrometers with increased curing time.

Montmorillonite participates in the reaction. Even after one day of curing, tiny fibrous crystals form at the edges of the montmorillonite flakes. After longer curing periods, the imprints of the pull out features are full of reacted montmorillonite flakes. Lime appears to be the dominant material that reacts with the montmorillonite flakes because the altered montmorillonite flakes are most evident in the simple mixture of bentonite and lime. This observation supports Stocker's (92) and Ormsby and Bolz's (78) suggestions about participation of clay flakes in the pozzolanic reactions and demonstrates it directly with the micrographs.

The participation of the fly ash grains in the reactions appear to occur in three stages. In the first the smaller soluble phases (some glass and anhydrite) dissolve immediately promoting the formation of acicular crystals (ettringite and CSH Type I). In the next stage, acicular crystals (CSH Type I) are found as coatings on fly ash grains. These radiating crystals increase the contact points between grains thus increasing the compressive strength. At the third stage some fly ash particles have a reacted crust while others are completely replaced by cementitious products. The deterioration of some of the fly ash grains create weak spots in the matrix which appears to be the

reason for the decrase observed in elastic moduli after longer curing periods. This is particularly evident after longer curing periods such as 180 days. The reactions are at the individual particle level as expected because of the wide range of chemical compositions of the particles. Some fly ash spheres do not react and behave as inert fillers as reported by Diamond (21). Duplex film morphology is not seen as much as it is reported in cement fly ash mixtures. All stages of reaction can be found together.

A general qualitative theory of strength modification can be developed from the SEM, XRD and UCS data. In a plastic clay the failure occurs through the slippage of clay flakes. The addition of fly ash and lime to plastic clay results in the formation of cementious crystals that bond the aggregates and grains to each other thus they behave as larger units. After curing the failure plane passes through the cementitious crystals and failure occurs when the ultimate strength of the cementitious crystals are reached. The failure mechanism is similar to that of brittle material. The aggregates and grains are connected to each other with needles and equant crystals. When fly ash and lime are added to bentonite the pH of the mixture increases and the soluble phases in fly ash dissolve. Lime attacks to the edges of the montmotrillonite flakes at early curing periods (1 day) and needles begin to form on the edges. After 28 days of curing fly ash grains are involved more in the formation of cementitious crystals and needles are seen

on fly ash grains, in pores and in montmorillonite aggregates when a major strength increase is observed. Increased contact points due to the formation of needles increase the compressive strength and decrease the strain at failure. At longer curing periods (90 and 180 days) these needles are less abundant and blocky aggregates of equant crystals appear engulfing the fly ash grains. There are more reacted fly ash grains after 180 days of curing. Some of the fly ash grains dissolve and create weak spots in the matrix which appears to be the reason for the decrease in the compressive strength and increase in strain at failure thus a decrease in the elastic moduli. The decrease in elastic moduli is expected to level off after longer curing periods and the amount of decrease is most probably limited to the number of deteriorating fly ash grains.

The major effect of the increased curing temperature (50°C) was increasing the rate and degree of the reaction. The same cementitious minerals are present. In bentonite-fly ash-lime samples, CSH Type I and ettringite crystals are dominant after one day of curing at 50°C instead of after 28 days at 23°C. The elastic modulus of the higher temperature one day-cured sample is close to the elastic modulus of the lower temperature 28 day cured sample. The major peak of CSH Type I appears after one day at 50°C instead of 28 days at 23°C. Fully reacted spheres and spheres with reacted crusts are present after 28 days at 50°C instead of 180 days at the lower temperature.

Fifty degrees centigrate curing increases the rate of the reactions, and the UCS. The UCS of the higher temperature samples is typically 500 to 1000 kPa (72 to 144 psi) higher (Figure 50). The difference decreases with increased curing time.

The 90 and 180 day-cured UCS and elastic moduli are higher than the 28 day-cured UCS and elastic modulus. However a decrease in UCS and elastic is evident after 180 days of curing and if this rate of decrease is extrapolated it may be concluded that it will level off at values higher than UCS and elastic moduli of the 28 day-cured sample (23°C). For design the most suitable UCS and elastic modulus appears to be the 23°C, 28 day-cured values. One day, 50°C curing yields comparable UCS and elastic modulus to the lower temperature 28 day-cured sample. As a design procedure the UCS and elastic modulus corresponding to either 23°C, 28 day-cured sample or 50°C one day cured sample should be used.

The fly ash-lime stabilization of bentonite resulted in an increased elastic modulus aproximately seventeen times the elastic modulus of bentonite. This has important applications regarding the behavior of pavement. The ratios of elastic modulus of bentonite-fly ash-lime to the elastic modulus of bentonite at different curing times were 4.5, 13, 17 and 15 for 1, 28, 90 and 180 day-cured samples respectively. Theoretical analyses reported in the literature stated: " in a layered pavement system,

substantial flexural stresses are developed in the layer containing the lime-soil mixture" (100). Therefore the stabilized soil layer does not behave as a flexible pavement. Thompson's work (99) indicated that lime-soil mixtures have tensile strength properties capable of resisting the flexural stresses developed. The stabilized layer behaves as a slab on the untreated soil. In the design of pavements the slab action of the stabilized layer should be considered. If the slab action of the stabilized layer is not considered and the flexural stresses in this layer are larger than the flexural strength of the stabilized layer, cracks will form. In all of the mixtures studied the strain at failure was less than one percent which may be an important design consideration because the deformation capabilities of these mixtures are limited.

The results of this study may be extrapolated to naturally occuring mixed soils as follows. The addition of fly ash-lime in the stabilization of fine grained soils increases the elastic moduli considerably due to the formation of cementitious minerals. These minerals form at normal temperatures (field) and in compacted soils. It is expected that the formation of the cementitious minerals will not be limited to the type of the soil because all of the necessary constituents to form cementitious compounds are supplied by fly ash and lime. With natural soils higher strengths and elastic moduli will be obtained because of the

presence of non-clay constituents like quartz which may provide a mechanically stable matrix: cementitious minerals will bond these particles and improve the strength. One major application which will be directly related to the materials used in this study may be fly ash-lime-bentonite injection. This study has demonstrated that cementitous minerals are forming and they are improving the strength considerably. This may be successfully used to cure the existing foundation problems. Lime columns have been popular in stabilization of highly plastic clays. Gypsum is added to lime to improve the immediate strength increase through the formation of ettringite. Fly ash can be injected with lime to form fly ash-lime columns which will have improved initial strengths relative to lime columns. Fly ash has excellent flow properties for injection.

CHAPTER VII

CONCLUSIONS AND RECOMMENDATIONS

Conclusions

The micromorphological changes occuring in fly ash-lime stabilized bentonite with increased curing time are related to changes in the elastic moduli of the stabilized mixtures. These conclusions are based on results obtained from fly ash-lime stabilized bentonite but should be valid for other soils where the dominant mineral is montmorillonite. The general conclusions of this study are listed below:

1- Addition of fly ash and lime to bentonite resulted in an increase in elastic modulus relative to untreated bentonite up to 90 days of curing, however at longer curing times (180 days) a decrease was observed. The increase in elastic modulus is related to the formation of cementitious reaction products between fly ash spheres and aggregates of montmorillonite. The decrease in elastic modulus is related to the observed dissolution of some of the fly ash grains which created weak spots in the supporting matrix after longer curing periods. The decrease in elastic modulus is expected to level off because it will be limited to the number of dissolved fly ash grains. The general concept in the stabilization of soils is that the increase in elastic modulus will continue for long terms, however this study showed that in case of fly ash-lime stabilization of fine

grained soils the elastic modulus decreases after a certain curing period and is related to the dissolution of the fly ash grains.

2- The reaction products were more dominant where combined fly ash and lime stabilization was used relative to where only fly ash or only lime stabilization of bentonite was used. This resulted in higher elastic moduli and compressive strengths in fly ash-lime stabilized soils.

3- Strength and elastic modulus increases are associated with the formation of new minerals. Ettringite, CSH gel and afwillite form after curing for various lengths of time and the detection of these minerals corresponds to curing times when increases in elastic modulus and strength occur. The most consistent reaction product which was observed in most of the mixtures was CSH gel.

4- Ettringite is a source of early strength increase in fly ash and lime stabilized bentonite. This is similar to portland cement hydration. In the bentonite-fly ash-lime mixture acicular ettringite crystals were seen spanning the pores thus providing support to the montmorilonite aggregates and the fly ash grains. With increased curing time they were less frequently observed.

5- Strength and elastic modulus increases are associated with the changes in microstructure. Two typical morphologies are attributed to CSH gel: Acicular crystals and blocky aggregates of equant crystals. (a) Acicular crystals were

observed on some fly ash grains increasing contact points and in pores bracing the pore walls thus increasing the compressive strength and decreasing the strain at failure. (b) Equant crystals which appeared after longer curing periods engulfed some of the fly ash grains providing increased support to those grains.

6- Fly ash contributes to increases in the elastic moduli of bentonite-fly ash-lime mixture by affecting it physically and chemically. Physically the fly ash grains provide support in the form of a matrix between montmorillonite aggregates. Chemically, a variety of aluminosilicates and other glasses and mineral phases found in fly ash react with free lime and bentonite to form cementitious products. After long curing periods the partial dissolution of some fly ash grains create weak spots in the matrix and decreases the unconfined compressive strength and elastic modulus.

8- Montmorillonite participates in the pozzolanic reactions. Tiny fibrous crystals form at the edges of the montmorillonite flakes providing increased bond between aggregates and grains. The direct observation of the fibrous crystals forming on montmorillonite flakes supports the findings of Stocker (92) about the attack of lime to edges of 2:1 clay minerals. A complete deterioration of the crystal structure of montmorillonite as proposed by Eades and Grim (28) is not observed.

9- The 50°C curing temperature increased the rate of the

reactions. The same cementitious minerals formed at both curing temperatures. At 50°C, all identified cementitious crystals were present after one day of curing where in case of 23°C curing temperature the formation of cementious minerals were observed after 1, 28 and 90 days. Major strength increases occured after one day of curing. The unconfined compressive strengths and the elastic moduli of samples cured at 50°C are higher than those of the samples cured at 23°C.

10- The increased rigidity of the fly ash-lime stabilized layer should be considered in pavement design. The elastic modulus corresponding to 28 days of curing should be used in design because at this curing time a major portion of the strength increase occurs. One day, 50°C curing may be used to obtain elastic moduli for pavement design instead of 28 days, 23°C curing.

Recommendations

The following suggestions for further investigation were developed as a result of this study:

1- Fly ash-lime stabilization of natural soils should be investigated to determine whether same types of cementitious minerals will form. A comparision of stabilized natural soils with variable contents of kaolinite, illite, chlorite and montmorilonite will bring a more thorough understanding

of the cementation in stabilized natural soils.

2- Cores from existing fly ash-lime stabilized fine grained soils should be studied using the same microscopic and X-Ray diffraction techniques to observe the formation of the cementitous minerals under field conditions. If cores are not available a field test section should be prepared and cored to observe the formation of cementitous minerals under field curing conditions. Potential development of calcite should be considered in field conditions.

3- It would be desirable to investigate methods such as density and magnetic concentration procedures to isolate the reaction products and define them more precisely. A miniature loading frame may be designed which can be fitted in the sample chamber of the scanning electron microscope and the deformation of the stabilized soil may be directly observed. This will provide a better understanding of how the acicular and platy cementitious crystals behave under loading.

BIBLIOGRAPHY

1. Anday, M.C., " Curing Lime Stabilized Soils," HRB Record No. 29, 1963, pp. 13-26.

2. Anday, M.C., " Accelarated Curing for Lime Stabilized Soil," HRB Bulletin No. 304, 1961, pp. 1-13.

3. Arman, A., and Munfakh, G.A., " Lime Stabilization of Organic Soils," Louisiana State University, Engineering Research Bulletin No. 103, 1970.

4. Barden, L., and Sides, G., "Sample Disturbance in the Investigation of Clay Structure, Vol. 21, No. 3, 1971, pp. 211-222.

5. Barnes, B.D., Diamond, S., and Dolch, W.L., "The Contact Zone Between POrtland Cement Paste and Glass "Aggregate" Surfaces," Cement and Concrete Research, Vol. 8, 1978, pp. 233-244.

6. Barnes, P., "Structure and Performance of Cements," Applied Science Publishers, New York, 1983.

7. Barnes, B., " Morphology of the Paste-Aggregate Interface," PhD Thesis, Purdue University, 1975, 290 pp.

8. Berger, R. L., Young, J. F., and Lawrence, F.V., " Discussion of the Paper: Morphology and the Surface Properties of Hydrated Tricalcium Silicate Paste , by M. Colleparti and B. Marchese," Cement and Concrete Research, Vol. 2, No. 5, September 1972, pp. 633-636.

9. Bergeson, R.L., Pitt, J.M., and Demirel, T.," Increasing the Cementitious Products of a Class C Fly Ash." TRB 998, pp. 41-46.

10. Brandl, H., "Alteration of Soil Parameters by Stabilization With Lime," Improvement of Ground, Proceedings of the 8th European Conference on SMFE (Helsinki 1983), pp. 587-594.

11. Brewer, Roy, " Fabric and Mineral Analysis of Soils," John Wiley and Sons, Inc., 1964.

12. Burmister, D.M., " The Theory of Stresses and Displacements in Layered Systems and Applications to the Design of Airport Runways." HRB Proc. Vol. 23, 1948, pp. 126-148.

13. Collins, R.J., and Emery, J.J.," Kiln Dust-Fly Ash Systems for Highway Bases and Subbases," FHWA Report No. 82/167, September 1983.

14. Crawley, A.B., "The Use of Fly Ash in Highway Construction," FHWA Interim Report, March 1984.

15. Croft, J.B., " The Structures Stabilized with Cementitious Agents," Engineering Geology, Vol. 2, No. 2, 1967, pp. 63-80.

16. Croft, J.B., "The processes Involved in the Lime Stabilization of Clay Soils," Proceedings, Conference, Australian Road Research Board, 2nd, 2, 1964, pp. 1169-1203 .

17. Croft, J.B., " The Pozzolanic Reactivities of Some New South Wales Fly Ashes and their Applications to Soil Stabilizations." Australian Research Board Proceedings, Vol. 2, Part 2, 1964, pp. 1144-1168.

18. Demirel, T., Pitt, J.M., Mings, M.L., and Schlorholtz, S.M., "Characterization of Fly Ash for Use in Concrete Interim Report," Iowa State University, 1982.

19. Diamond, S., "The Utilization Of Fly Ash," Cement and Concrete Research, 1984, pp. 763-766 .

20. Diamond, S., Ravina, D., and Lovell, J., "The Occurence of Duplex Films on Fly Ash Surfaces," Cement and Concrete Research, Vol. 10, 1980, pp. 297-300.

21. Diamond, S., "Characterization of Fly Ashes," Proceedings, Effect of Fly Ash Incorporation in Cement and Concrete, Symposium N, Material Research Society, 1981, pp.12-23.

22. Diamond, S., "Hydration Reactions of Tricalcium Aluminate Contained in an Unusual Fly Ash," Proceedings, 7th International Congress on the Chemistry of Cement, (Paris,1980), Vol. III, pp. IV-19 to IV-23.

23. Diamond, S., " Cement Paste Microstructure- An Overview at Several Levels," Proceedings of Conference Held in University of Sheffield, 8-9 April 1976.

24. Diamond, S., Young, J.F., and Lawrence, F.V., "Scanning Electron Microscopy-Energy Dispersive X-Ray Analysis of Cement Constituents- Some Cautions ," Cement and Concrete Research, Vol. 4, 1974, pp. 899-914.

25. Diamond, S., White, J.L., and Dolch, W.L., " Transformation of Clay Minerals by Calcium Hydroxide Attack, " Proceedings, 12th National Conferenceon Clays and Clay Minerals, New York, 1964, pp. 359-379.

26. Diamond, S., and Kinter, E.B., " Mechanisms of Soil-Lime Stabilization: An Interpretive Review, " HRB Record No. 92, 1965, pp. 83-101.

27. Eades, J.L., and Grim, R.E., "A Quick Test to Determine Lime Requirements for Lime Stabilization," HRB Record No. 139, 1963, pp. 61-72.

28. Eades, J.L., and Grim, R.E., "Reaction of Hydrated Lime with Pure Clay Minerals in Soil Stabilization," HRB Bulletin 262, 1960, pp. 51-63.

29. Eades, J.L., Nichols, F.P., and Grim, R.E., " Formation of New Minerals with Lime Stabilization as Proven by Field Experiments in Virginia," HRB Bulletin No. 335, 1962, pp. 31-39.

30. Evstatiev, D., and Todorov, K., "Microstructural Investigations of Cement-Lagooned Ash Mixtures," Improvement of Ground, Proceedings of 8th European Conference of SMFE (Helsinki 1983), pp. 763-766.

31. Fossberg, P.E., " Some Fundamental Engineering Properties of Lime Stabilized Clay," HRB Record No. 263, 1969, pp. 19-26.

32. Ghose, A., Pratt, P.L., "Studies of the Hydration Reactions and the Microstructure of Cement-Fly Ash Pastes," Proceedings, Effects of Fly Ash Incorporation in Cement and Concrete, Symposium N, Material Research Society, 1981, pp. 82-91.

33. Gillott, J.E., " Study of the Fabric of Fine Grained Sediments with the Scanning ELectron Microscope," Journal of Sedimentary Petrology, Vol. 39, No. 1, 1969, pp. 90-105 .

34. Glenn, G.R., and Handy, R.L., " Lime Clay Mineral Reaction Products," HRB Record 29, 1963, pp.70-82.

35. Goldberg, I., and Klein, A., " Some Effects of Treating Expansive Soils With Calcium Hydroxide, " ASTM Special Technical Report No. 142, 1952.

36. Gray, D.H., and Lin, Y.K., " Engineering Properties of Compacted Fly Ash ," Journal of the Soil Mechanics and Foundation Division, ASCE, Vol. 98, No. SM4, 1972.

37. Gregory, C.A., Saylak, D., and Ledbetter, W.B.," The Use of By-Product Phosphogypsum for Road Bases and Subbases." TRB 998, pp. 47-51.

38. Grim, R.E., " Applied Clay Mineralogy," McGraw Hill Book Co., Inc., New York, 1962.

39. Grim, R.E., " Clay Mineralogy," McGraw Hill Book Co., Inc., New York, 1968.

40. Grutzcek, M.W., Roy, D.M., Scheetz, B.E., " Hydration Mechanism of High-Lime Fly Ash in Portland Cement Composites, " Proceedings, Effects of Fly Ash Incorporation in Cement and Concrete, Symposium N, Material Research Society, 1981, pp. 92-101.

41. Halse, Y., Pratt, P.L., Dalziel, J.A., and Gutteridge, W.A., "Development of Microstructure and Other Properties in Fly Ash OPC Systems," Cement and Concrete Research, 1984, pp. 491-498.

42. Hecht, N.L., Duval, D.S., "Characterization and Utilization of Municipal and Utility Sludges and Ashes: Vol III - Utility Coal Ash," National Environm ental Research Center Report, EPA, May 1975.

43. Herzog, A., and Brock, R.," Some Factors Influincing the Strength of Soil Lime Fly Ash Mixtures." Australian Road Research Proceedings, Vol. 2, paper 139, 1964, pp.1226-1232.

44. Hilt, G.H., and Davidson, D.T., "Isolation and Investigation of a Lime-Montmorillonite Crystalline Product," HRB Bulletin 304, 1961, pp. 51-64.

45. Hilt, G.H., and Davidson, D.T., "Lime Fixation in Clayey Soils," HRB Bulletin 262, 1960, pp. 20-32 .

46. Houwink, R., and de Decker, H.K.," Elasticity, Plasticity and Structure of Matter." Cambridge at the University Press, 1971.

47. Idorn, G.M., " International Aspects of Development of the Uses of Fly Ashes in Cement and Concrete, Symposium N, Material Research Society, 1981, pp. 244- 259.

48. Joshi, R.C., Natt, G.S., and Wright, P.J., "Soil Improvement by Lime-Fly Ash Slurry Injection," Improvement of Ground, Proceedings of 8th European Conference on SMFE (Helsinki 1983), pp. 707-712.

49. Jun-Yuan H., Sheetz, B.E., and Roy, D.M., "Hydration of Fly Ash-Portland Cements," Cement and Concrete Research, 1984, pp. 505-511.

50. Kawam, A., and Smith, L.M. et al.,"Feasibilty of Using Sewage Sludge in Highway Embankment Construction," FHWA, Report No. RD-75-38, February 1975.

51. Kezdi, A., " Stabilized Earth Roads." Elsevier Scientific Publishing Company, 1979.

52. Kinter, E.B.," Development and Evaluation of Chemical Soil Stabilizers," FHWA Report No. RD-75-17, March 1975.

53. Klement, K.," Disposal and Utilisation of Neutralisation Sludges Based on Calcium Sulphate, from the Chemical Polishing of Glass, for the Manufacture of Anorganic Insulation Slabs," Building Materials, Edited by V.M. Bhatnagar, The Construction Press, 1981, pp.33-41.

54. Kobubu, M., " Fly Ash and Fly Ash Cement," Proceedings 5th International Symposium on the Chemistry of Cements,(Tokyo 1968), Cement Association of Japan, Tokyo 1969, Vol IV-2, pp. 75-105.

55. Krauskopf, K.B., "Introduction to Geochemistry," New York, McGraw Hill Book Co., 1967.

56. Kronert, W. and Wetzel, K., " Reactions of Alkaline Earth Hydroxides With Clay Minerals," Ziegelindustrie, Vol. 25, 1972, pp. 562-567 .

57. Ladd, C.C., Moh, Z.C., and Lambe, T.W., " Recent Soil-Lime Research at the Massachusets Institute of Technology," HRB Bulletin No. 262, 1960, pp. 64-85.

58. Laguros, J.G., and Baker, M., "Fly Ash Concrete: A Study on the Reaction Products Using X-Ray Diffraction and SEM," Oklahoma Department of Transportation Research Report No. 155-088, 1984.

59. Lea, F.M., "The Chemistry of Cement and Concrete," Great Britain: Edward Arnold Publishers Ltd., 1970.

60. Leonard, R. J., and Davidson, P.I.," Pozzolanic Reactivity Study of Fly Ash," HRB Bulletin No. 231, 1959, pp. 1-17.

61. Marusin, S.L., " Investigation of the Shale Brick Cement-Lime Mortar Bond Using SEM." Pro. of the 5th Int. Clay Conference on Cement Microscopy, Tennesse, March 1983, pp. 180-188.

62. Mateos, M., and Davidson, D.T.," Lime and Fly Ash Proportion in Soil, Lime and Fly Ash Mixtures, and Some Aspects of Soil Lime Stabilization." HRB Bulletin 335, 1962, pp. 40-64.

63. Matsuo, S., and Kamon, M., "Soil Stabilization by Multivalent Cations," Improvement of Ground, Proceedings of 8th European Conference on SMFE (Helsinki 1983), pp. 735-738.

64. Matsuo, S., and Sung, Y. K., " Fabric of Lime Stabilized Soils by X-Ray and Electron MIcroscopy," Doboku Gakkai Ronbushu (Japaneese Society of Civil Engineers), No. 193, September 1971, pp. 59-68.

65. McCarthy, G.J., "Qualitative X-Ray Phase Analysis of Lignite Gasification Ash. Illustration of a Strategy for Analysis of Very Complex Solids," Powder Diffraction, Vol.1, No. 1, 1986, pp. 50-55.

66. McCarthy, G.J., and et al., "Mineralogy of Western Fly Ash," Cement and Concrete Research, 1984, pp. 471-478.

67. McDowell, C., " Stabilization of Soils With Lime, Lime-Fly Ash, and Other Lime Reactive Materials ," HRB Bulletin No. 231, 1959, pp. 60-66.

68. McHardy, W.J., "Application of Scanning Electron Microscopy and Microanalysis to the Study of Soil Mineralogy," Geologica Applicata Idrogeologica, Vol. 12, No.2 , 1977, pp. 213-233.

69. McKerall, W.C., Ledbetter, W.B., and Teague, D.J., " Analysis of Fly Ashes Produced in Texas," FHWA Report No. TX-81/21+240-1, January 1981.

70. McMannis, K.L., Ferrell, R.E., and Arman, A.," Interpreting the Physical Properties of a Clay Using Microanalysis Techniques," Geotechnical Testing Journal, GTJODJ, Vol. 6, No. 2, June 1983, pp. 87-92.

71. Meyers, J.F., Pichumain, R., Kapples, B.S., " Fly Ash as a Construction Material for Highways," Federal Highway Administration, FHWA-IP-76-16, June 1976.

72. Mings, M.L., Schlorholtz, S.M., Pitt, J.M., and Demirel, T.," Characterization of Fly Ash by X-Ray Analysis Methods." TRB 941, pp. 5-12.

73. Minnick, L.J., " Fundamental Characteristics of Pulverized Coal Fly Ashes," Proceedings, ASTM, Vol 59, 1959, pp. 1155-77.

74. Minnick, L.J., " Reactions of Hydrated Lime with Pulverized Coal Fly Ash," Proceedings, Fly Ash Utilization Conference, Bureau of Mines Information Circular 8348, 1967.

75. Mitchell, J.K., "Soil Improvement - State of the Art Report,"

76. Mitchell, J.K., "The Properties of Cement Stabilized Soils," Residential Workshop on Materials and Methods for Low Cost Road, Rail and Reclamation Works (Australia 1976), pp. 365-404.

77. Mitchell, J.K., and El Jack, A.," The Fabric of Soil-Cement and Its Formation," Proccedings of 14th National Conference on Clays and Clay Minerals, 1964, pp.297-305.

78. Ormsby, W.C. and Bolz, L.H., "Microtexture and Composition of Reaction Products in the System Kaolin-Lime-Water." Journal of the American Ceramic Society, Vol. 49, No.7, 1966, pp. 364-366.

79. Pachowski, J. et al.," The Application of Brown Coal Fly Ash to Road Base Courses," FHWA Report No. RD-79-101, September 1979.

80. Pierre, J.J., and Thompson, C.M.," User's Manual: Coal-Mine Refuse in Highway Embankments," FHWA Report No. TS-80-213, December 1979.

81. Pitt, J.M., Mings, M.L., and Schlorholtz, S.M.," Characterization and Techniques for Rapid Evaluation of Iowa Fly Ashes." TRB 941, pp. 12-17.

82. Postek, M.T., Howard, K.S., Johnson, A.H., and McMichael, K.L., "Scanning Electron Microscopy: A Student's Handbook," Ladd Research Industries Inc.

83. Queiroz De Carvalho J.B., "Amorphous Materials and Lime Stabilized Soils," Improvement of Ground, Proceedings of 8th European Conference on SMFE (Helsinki 1983), pp. 761-764.

84. Ravina, D., " Production and Collection of Fly Ash for Use in Concrete," Proceedings, Effects of Fly Ash Incorporation in Cement and Concrete , Symposium N, Material Research Society, 1981, pp. 2-11.

85. Richartz, W., " Electron Microscopic Investigations About the Relations Between Structure and Strength of Hardened Cement," Proc. 5th Int. Symposium on the Chemistry of Cement, Tokyo, Vol. III, 1969, pp. 119-128.

86. Ruff, C. G., and Clara, Ho, " Time-Temperature Strength-Reaction Product Relationships in Lime-Bentonite-Water Mixtures," HRB Record, No. 139, 1966, pp.42-60.

87. Sabry, M.M., " Mineralogical and Engineering Properties of Compacted Soil-Lime Mixes," PhD Thesis, Oklahoma State University, 1977.

88. Schlorholtz, S., and Demirel, T.," Quick Lime-Gypsum Interactions in Stabilized Soil Bases for Concrete Highways," Cement and Concrete Research, 1983, pp. 529-532.

89. Smith, R.L., and Raba, C.F., "The Basic Chemistry of Fly Ash Pozzolanic Reactions," Paper Presented to 1980 Spring Meeting of the ASCE, San Antonio, Texas.

90. ASTM C618, "Standard Specification For Fly Ash and Raw or Calcined Natural Pozzolan for Use as a Mineral Admixture in Portland Cement Concrete," 1980 Annual Book for ASTM Standards, Part 14, American Society for Testing and Materials, Philadelphia, 1980, p.370 .

91. "State of the Art: Lime Stabilization, Reaction, Properties, Design, Construction," TRB Circular No. 180, September 1976.

92. Stocker, P.T., "Diffusion and Diffuse Cementation in Lime and Cement Stabilized Clayey Soils-Studies of Plasticity and Aggregation ," Australian Road Research, Vol. 5, No. 6, 1974, pp. 51-75.

93. Stocker, P.T., "Diffusion and Diffuse Cementation in Lime and Cement Stabilized Clayey Soils-Chemical Aspects," Australian Road Research, Vol. 5, No. 9, 1975, pp. 6-47.

94. Takemoto, K., Uchitawa, H., "Hydration of Pozzolanic Cement," Proceedings, 7th International Congress on the Chemistry of the Cement, (Paris 1980), Vol. 1, pp. IV-2/1 to IV-2/29 .

95. Taylor, W. H., "Modern Chemistry of Cements," Chemistry and Industry , 1981, pp. 620-625.

96. Taylor, W. H., " The Chemistry of Cements," Vols. 1 and 2, Academic Press, New York, 1964.

97. Taylor, W.H., and Arman, A.," Lime Stabilization Using Preconditioned Soils." HRB Bulletin.

98. Thompson, M.R., "Lime Reactivity of Illinois Soils," Journal of the Soil Mechanics and Foundation Division, ASCE, Vol. 92, No. SM5, 1966, pp. 67-92.

99. Thompson, M.R., "Shear Strength and Elastic Properties of Lime Soil Mixtures," HRB record 139, 1966, pp. 1-15.

100. Thompson, M.R.," Lime Treated Soils For Pavement Construction," ASCE Journal of the Highway Division, Vol. 94, No. HW2, Nov. 1968.

101. Thornton, S., and Parker, D.G.," Construction Procedures Using Self-Hardening Fly Ash," FHWA Report No. AR-80/004 , July 1980.

102. Thornton, S., and Parker, D.G.," Fly Ash as Fill and Base Material in Arkansas Highways," Report, Arkansas State Highway Department, October 1975.

103. Uppal, H.L., and Chadda, L.R.," Physico-Chemical Changes in the Lime Stabilization of Blackcotton Soil." Engineering Geology, 2, 1967/68, pp.179-189.

104. Vivian, H.E., "Effect of Particle Size on the Properties of Cement Paste," Proceedings, Symposium o the Structure of Portland Cement Paste and Concrete, Highway Research Board, Special Report 90, 1966, pp. 18-25 .

105. Wild, S., Arabi, M., and Leng-Ward, G., " Soil-Lime Reaction and Microstructural Development at Elevated Temperatures." Clay Minerals, Vol. 21, No. 3, September 1986, pp. 279-292.

106. Williamson, R.B., and Tewari, R.P., "Effects of Microstructure on Deformation and Fracture of Portland Cement Paste," Electron Microscopy and Structure of Materials, 1972, pp. 1223-1233.

107. Williamson, R.B., " Solidification of POrtland Cement," Progress in Materials Science, Vol. 15, No. 3, 1972, pp. 189-286.

108. Winterkorn, H.F., "Soil Stabilization," Foundation Engineering Handbook, Chapter 8, 1975, pp. 312-336.

109. Zimmie, T. F. and Almaleh, L. J., "Shrinkage of Soil Specimens During Preparation for Porositometry Tests," Soil Specimen Preparation for Laboratory Testing, ASTM STP 599, 1976, pp. 202-215.

APPENDIX A

UNCONFINED COMPRESSIVE STRENGTH AND DRY DENSITY VS WATER CONTENT CURVES FOR BENTONITE-FLY ASH-LIME, BENTONITE-FLY ASH, AND BENTONITE-LIME

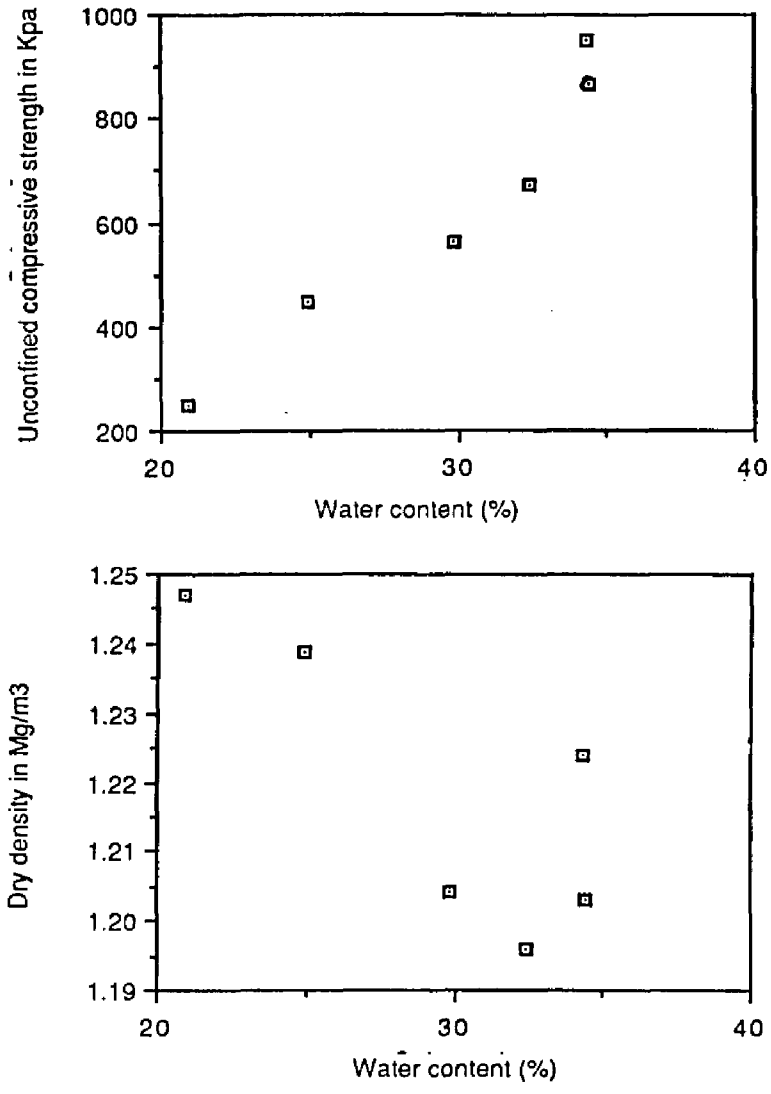

Figure A1. Unconfined Compressive Strength and Dry Density Versus Water Content Relationship for Bentonite-Fly Ash-Lime (82% : 12.3% : 5.7% by dry weight) Cured for 1 Day at 23°C.

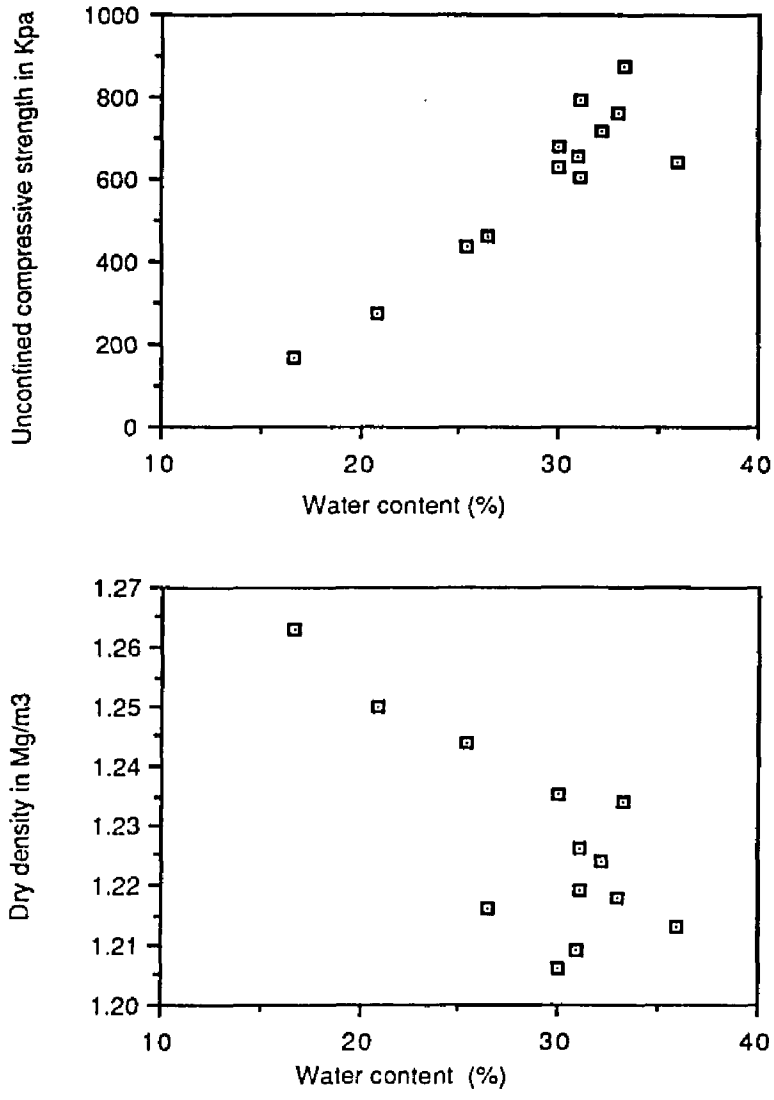

Figure A2. Unconfined Compressive Strength and Dry Density Versus Water Content Relationship for Bentonite-Fly Ash-Lime (79% : 15.5% : 5.5% by dry weight) Cured for 1 Day at 23°C.

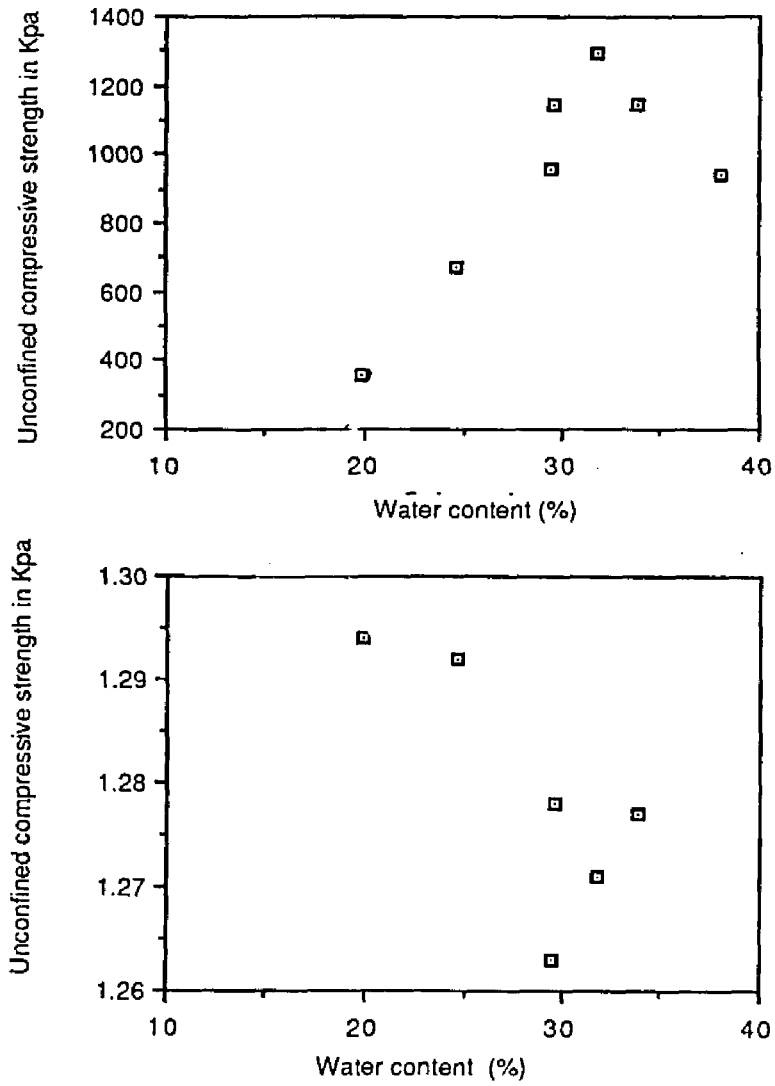

Figure A3. Unconfined Compressive Strength and Dry Density Versus Water Content Relationship for Bentonite-Fly Ash-Lime (75% : 20% : 5% by dry weight) Cured for 1 Day at 23°C.

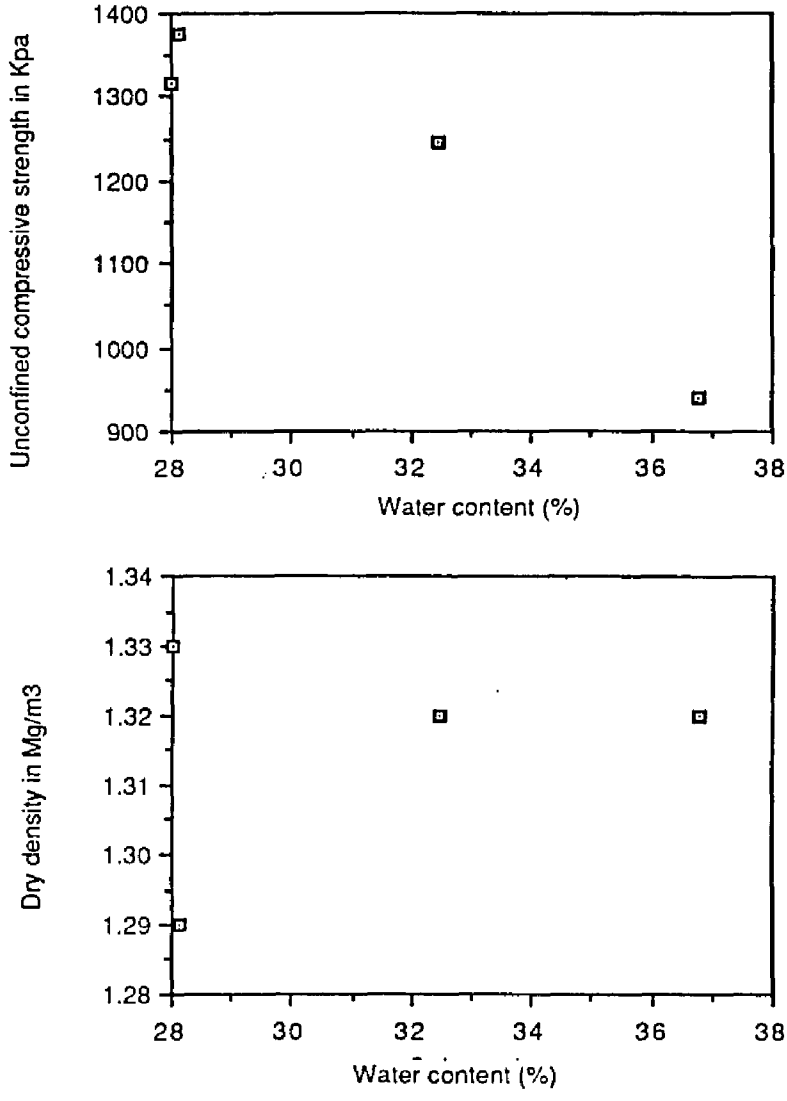

Figure A4. Unconfined Compressive Strength and Dry Density Versus Water Content Relationship for Bentonite-Fly Ash-Lime (65% : 30% : 5% by dry weight) Cured for 1 Day at 23°C.

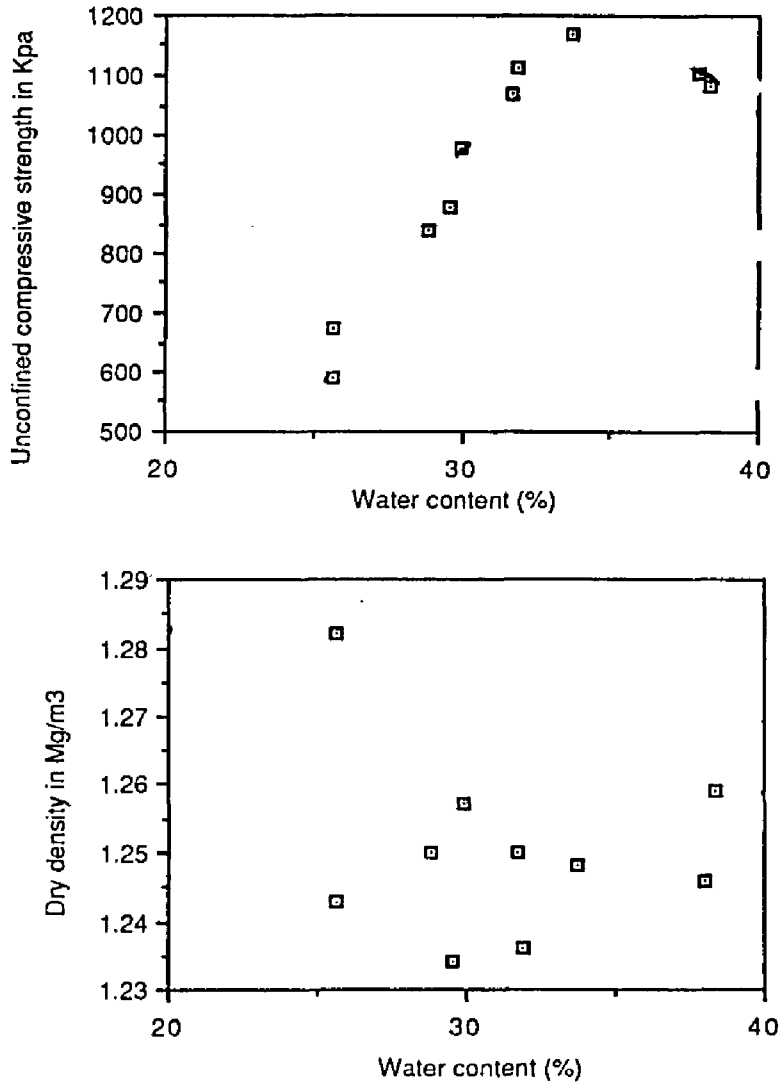

Figure A5. Unconfined Compressive Strength and Dry Density Versus Water Content Relationship for Bentonite-Fly Ash-Lime (75% : 20% : 5% by dry weight) Cured for 1 Day at 23°C.

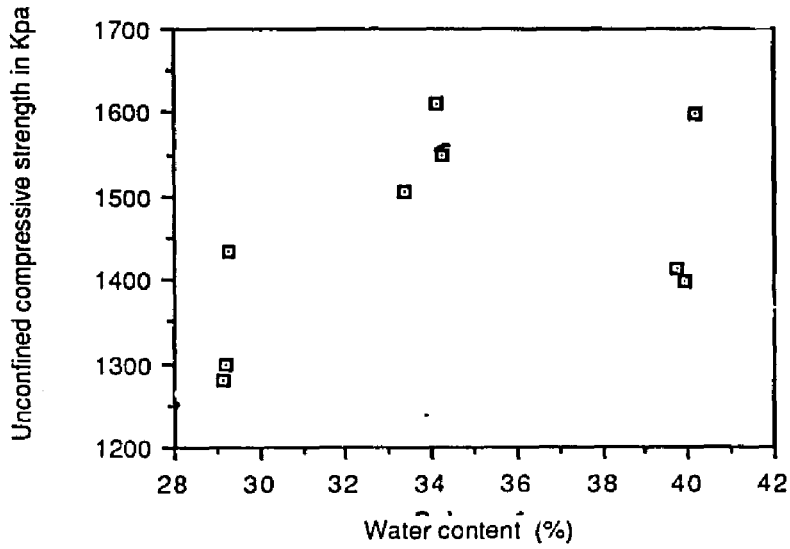

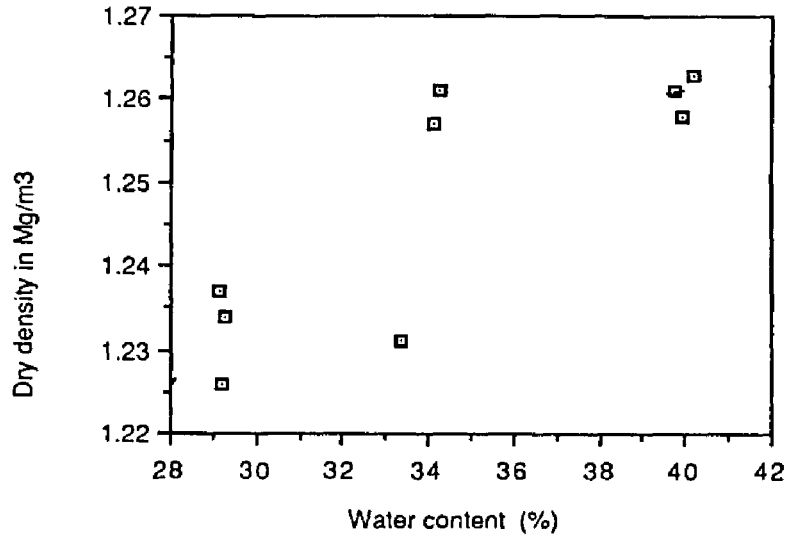

Figure A6. Unconfined Compressive Strength and Dry Density Versus Water Content Relationship for Bentonite-Fly Ash-Lime (75% : 20% : 5% by dry weight) Cured for 7 Days at 23°C.

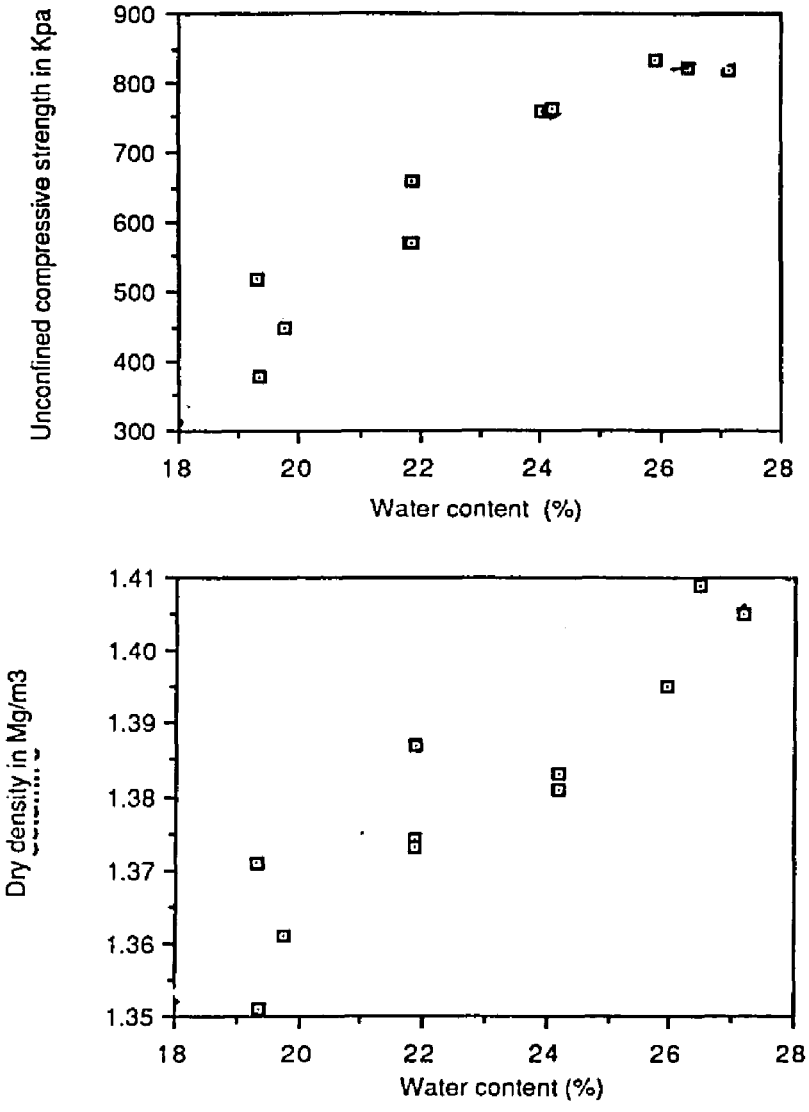

Figure A7. Unconfined Compressive Strength and Dry Density Versus Water Content Relationship for Bentonite-Fly Ash (79% : 21% by dry weight) Cured for 1 Day at 23°C.

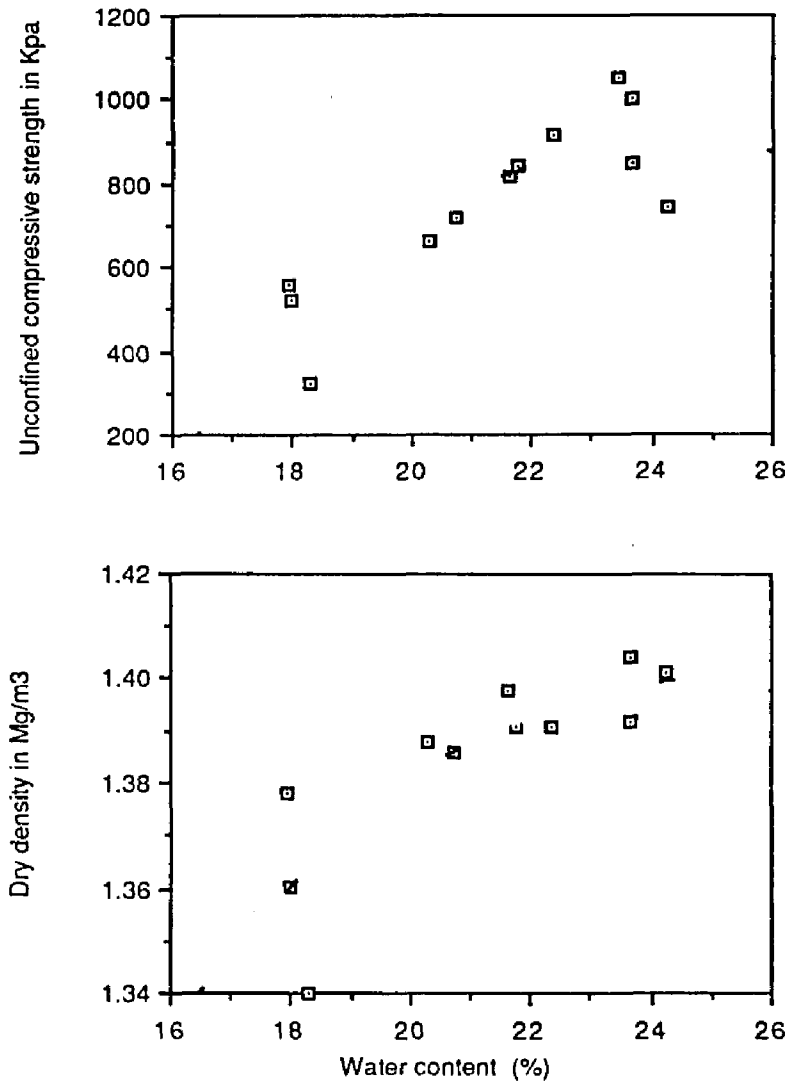

Figure A8. Unconfined Compressive Strength and Dry Density Versus Water Content Relationship for Bentonite-Fly Ash (79% : 21% by dry weight) Cured for 7 Days at 23°C.

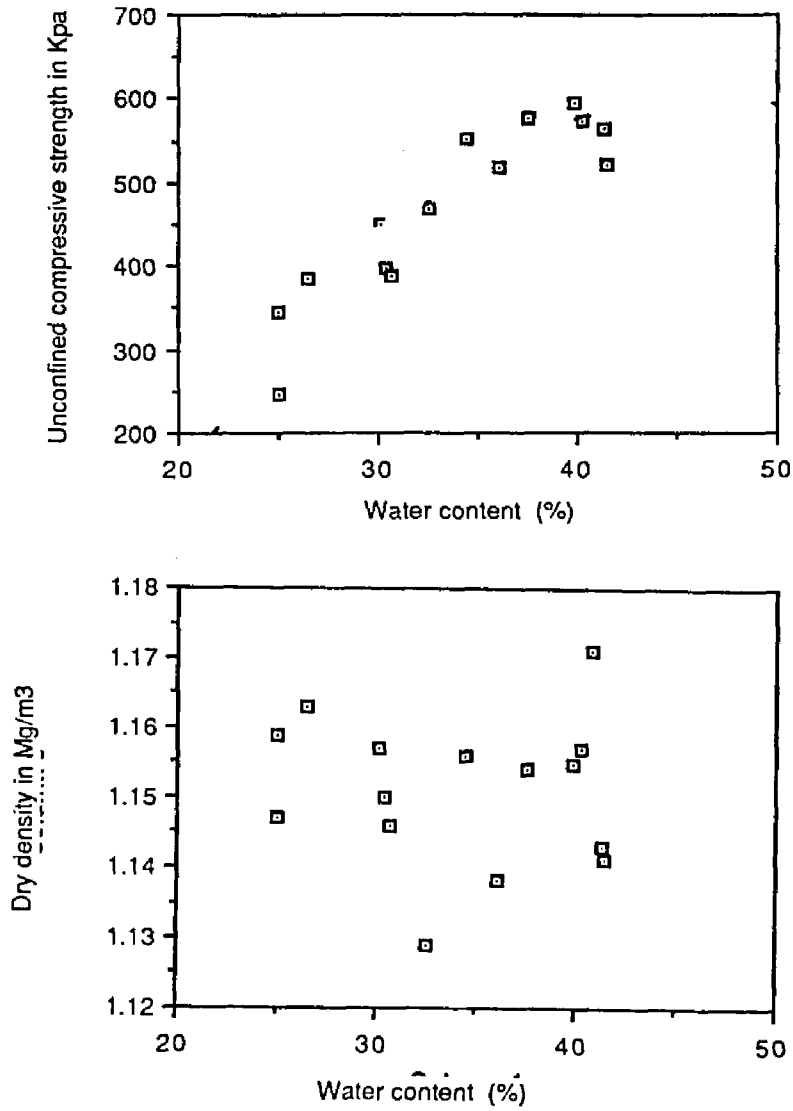

Figure A9. Unconfined Compressive Strength and Dry Density Versus Water Content Relationship for Bentonite-Lime (93.7 : 6.3% by dry weight) Cured for 1 Day at 23°C.

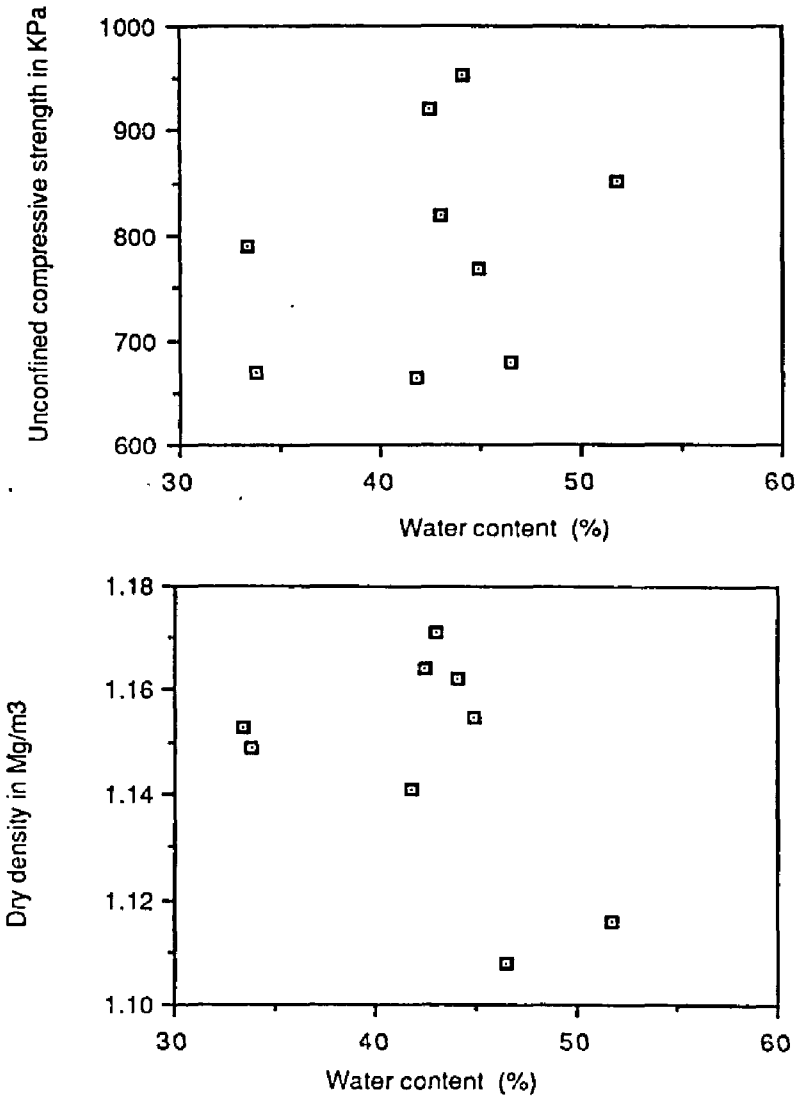

Figure A10. Unconfined Compressive Strength and Dry Density Versus Water Content Relationship for Bentonite-Lime (93.7 : 6.3% by dry weight) Cured for 7 Days at 23°C.

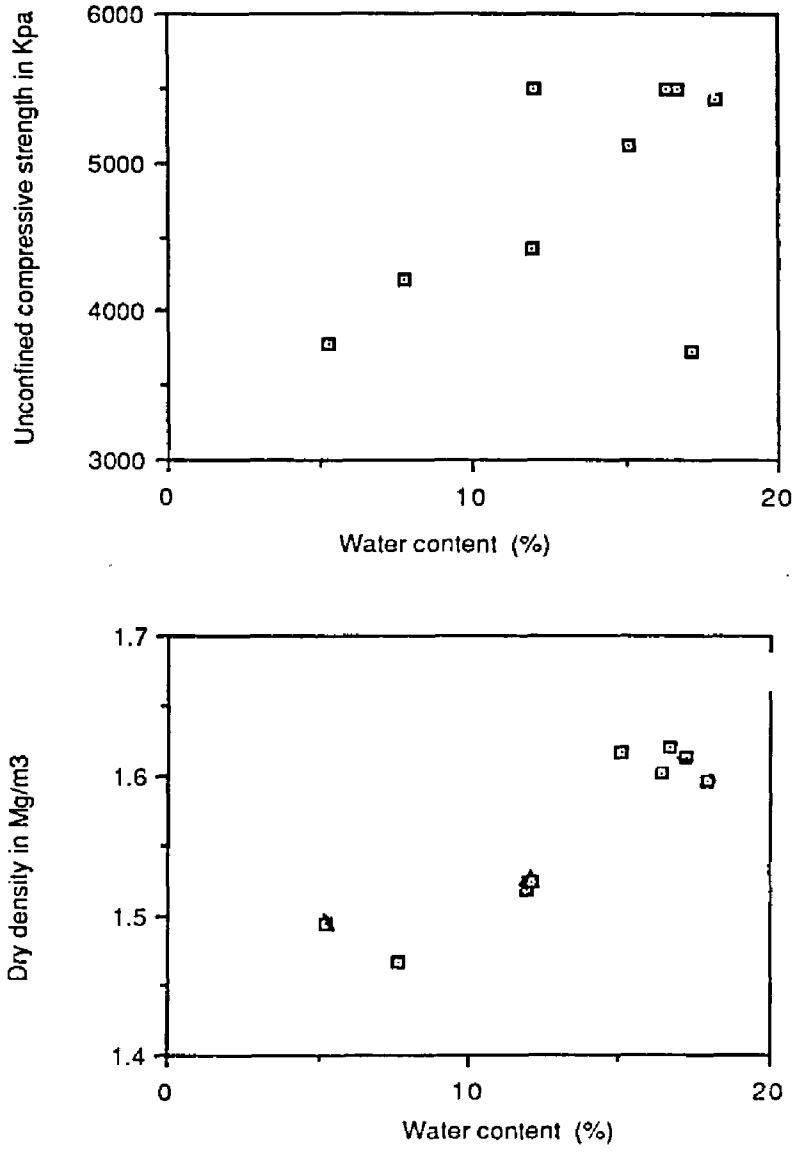

Figure A11. Unconfined Compressive Strength and Dry Density Versus Water Content Relationship for Fly Ash-Lime (80% : 20% by dry weight) Cured for 1 Day at 23°C.

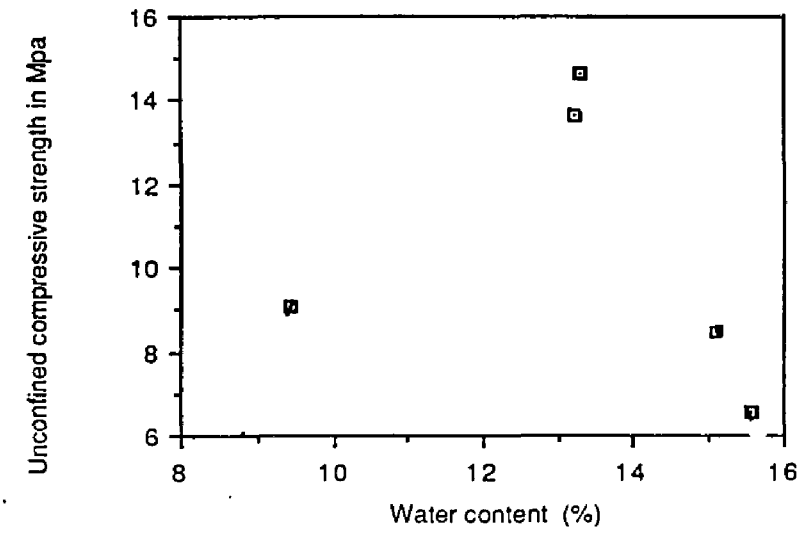

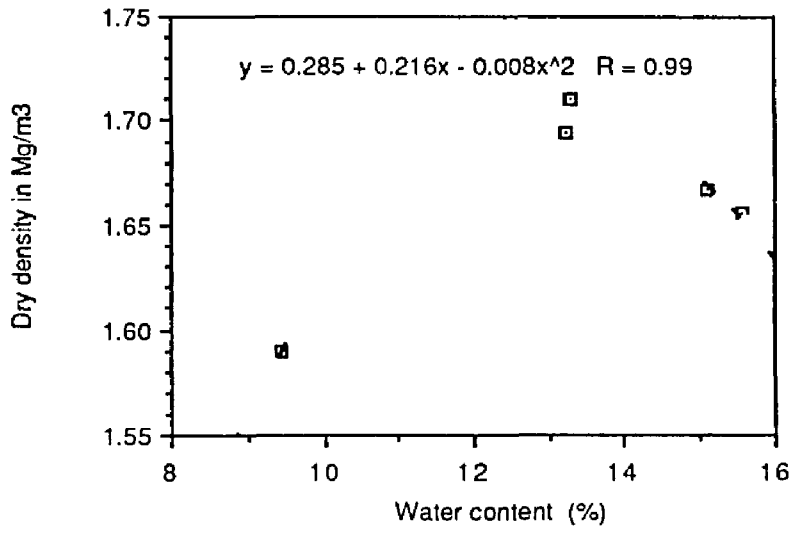

Figure A12. Unconfined Compressive Strength and Dry Density Versus Water Content Relationship for Fly Ash-Lime (80% : 20% by dry weight) Cured for 7 Days at 23°C.

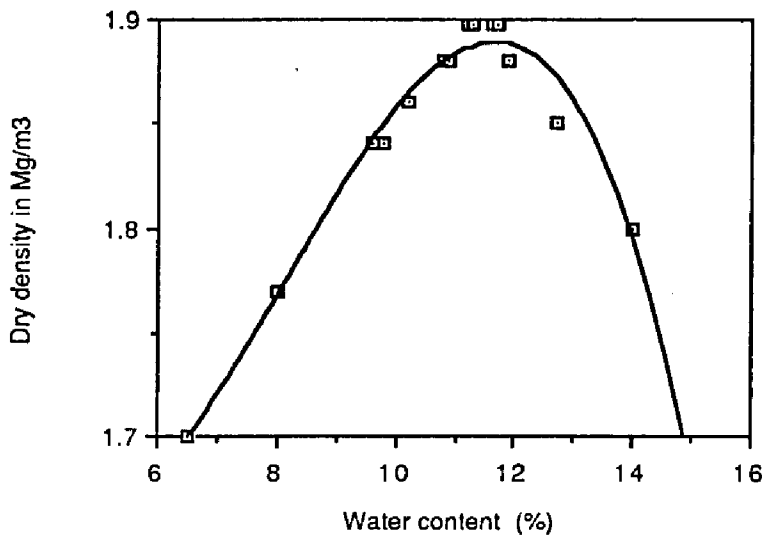

Figure A13. Water Content-Dry Density Relationship for Fly Ash as Determined by Harvard Miniature Compaction Device.

APPENDIX B

COMPLETE LIST OF X-RAY DIFFRACTION PEAKS OF THE STUDIED MIXTURES

Peak no	Angle (deg)	Tip width (deg)	Peak (cts)	Backg (cts)	D spac (Ang)	I/Imax (%)	Type A1	Type M2	Type Ot	Sign
1	3.5300	0.12	10.	156.	25.0090	1.60	X	X		0.19
2	4.7175	0.12	10.	98.	18.7160	1.60	X	X		0.10
3	5.3850	0.24	10.	85.	16.3974	1.60	X	X		0.11
4	6.4750	0.12	50.	76.	13.6393	7.88	X	X		0.17
5	7.4400	0.08	67.	79.	11.8723	10.50	X	X		0.15
6	8.0325	0.48	10.	102.	10.9978	1.60	X	X		0.11
7	9.0400	0.32	10.	102.	9.7743	1.60	X	X		0.12
8	9.7875	0.24	10.	92.	9.0294	1.60	X	X		0.23
9	11.0000	0.08	10.	50.	8.0367	1.60	X	X		0.24
10	11.4575	0.12	10.	49.	7.7168	1.60	X	X		0.18
11	11.8575	0.12	10.	48.	7.4573	1.60	X	X		0.20
12	12.8400	0.08	10.	41.	6.8888	1.60	X	X		0.15
13	13.2350	0.12	10.	41.	6.6841	1.60	X	X		0.24
14	13.9025	0.12	10.	41.	6.3647	1.60	X	X		0.32
15	14.2400	0.12	14.	41.	6.2146	2.14	X	X		0.10
16	14.3200	0.16	11.	41.	6.1800	1.70	X	X		0.16
17	14.8900	0.12	18.	40.	5.9447	2.89	X	X		0.22
18	15.3125	0.12	14.	40.	5.7816	2.14	X	X		0.20
19	16.7750	0.24	10.	44.	5.2807	1.60	X	X		0.14
20	17.4900	0.24	14.	44.	5.0664	2.26	X	X		0.13
21	18.4150	0.80	14.	49.	4.8139	2.14	X	X		0.62
22	19.8950	0.20	313.	59.	4.4590	48.94	X	X		3.02
23	20.5200	0.08	119.	58.	4.3246	18.56	X	X		0.10
24	20.9775	0.16	142.	69.	4.2313	22.12	X	X		1.02
25	23.7450	0.12	41.	88.	3.7441	6.40	X	X		0.54
26	24.7450	0.12	13.	83.	3.5950	2.02	X	X		0.17
27	26.7225	0.16	640.	76.	3.3333	100.00	X	X		5.75
28	27.3500	0.12	96.	74.	3.2582	15.00	X	X		0.62
29	27.7600	0.08	74.	72.	3.2110	11.55	X	X		0.15
30	28.1375	0.12	190.	72.	3.1688	29.75	X	X		0.83
31	28.5725	0.12	128.	71.	3.1215	19.95	X	X		0.28
32	29.6025	0.16	207.	66.	3.0152	32.40	X	X		2.45
33	30.0400	0.08	42.	66.	2.9723	6.60	X	X		0.15
34	30.5600	0.08	16.	62.	2.9229	2.50	X	X		0.16
35	32.0800	0.08	50.	58.	2.7878	7.88	X	X		0.16
36	34.1075	0.12	12.	52.	2.6265	1.91	X	X		0.30
37	35.0525	0.20	207.	50.	2.5579	32.40	X	X		1.07
38	36.1225	0.24	142.	56.	2.4845	22.12	X	X		0.33
39	36.6275	0.20	142.	58.	2.4514	22.12	X	X		0.91
40	38.5550	0.20	77.	64.	2.3332	12.10	X	X		1.51
41	39.5400	0.16	67.	67.	2.2773	10.50	X	X		0.91
42	40.3725	0.16	37.	71.	2.2322	5.81	X	X		0.34
43	42.4950	0.12	55.	77.	2.1255	8.56	X	X		0.55
44	43.3850	0.12	25.	79.	2.0840	3.91	X	X		0.26
45	44.7625	0.16	19.	79.	2.0230	3.02	X	X		0.56
46	45.8800	0.24	10.	76.	1.9763	1.60	X	X		0.51
47	47.5950	0.12	21.	66.	1.9090	3.31	X	X		0.18
48	48.7050	0.32	10.	64.	1.8680	1.60	X	X		0.68
49	49.3950	0.24	23.	59.	1.8435	3.60	X	X		0.79
50	50.1875	0.16	86.	58.	1.8163	13.51	X	X		1.00
51	50.9125	0.12	31.	55.	1.7921	4.90	X	X		0.32
52	51.3825	0.12	35.	59.	1.7768	5.44	X	X		0.66
53	52.8000	0.32	17.	50.	1.7324	2.63	X	X		0.29
54	53.7525	0.12	35.	53.	1.7039	5.44	X	X		0.23
55	54.0150	0.12	81.	53.	1.6963	12.65	X	X		0.22
56	54.8900	0.12	76.	64.	1.6713	11.82	X	X		0.17
57	56.2650	0.16	10.	72.	1.6336	1.60	X	X		0.13
58	56.7200	0.16	10.	72.	1.6216	1.60	X	X		0.13
59	57.4300	0.16	10.	71.	1.6032	1.60	X	X		0.28
60	58.7600	0.08	13.	61.	1.5701	2.02	X			0.11
61	58.9600	0.32	10.	61.	1.5652	1.60	X	X		0.11
62	59.9400	0.16	67.	61.	1.5420	10.50	X	X		0.85
63	61.9175	0.20	250.	69.	1.4974	39.00	X	X		2.09
64	65.0525	0.12	85.	67.	1.4326	13.22	X			0.63
65	65.2400	0.08	55.	64.	1.4324	8.56		X		0.13
66	65.7925	0.12	18.	62.	1.4183	2.76	X	X		0.23
67	67.2100	0.12	12.	61.	1.3917	1.81	X	X		0.19
68	68.0225	0.12	62.	59.	1.3771	9.75	X	X		0.16

Table B1. Bentonite.

Peak no	Angle (deg)	Tip width (deg)	Peak (cts)	Backg (cts)	D spac (Ang)	I/Imax (%)	Type A1	Type m2	Type Ot	Sign
1	3.9200	0.08	14.	46.	22.5217	2.39	X	X		0.10
2	4.7050	0.32	36.	48.	18.7657	5.95	X	X		0.27
3	5.9200	0.08	46.	48.	14.9167	7.64	X	X		0.11
4	6.7100	0.12	64.	49.	13.1622	10.58	X	X		0.30
5	8.5175	0.12	56.	50.	10.3726	9.30	X	X		0.20
6	8.9725	0.12	52.	50.	9.8476	8.57	X	X		0.29
7	10.5600	0.08	52.	52.	8.3705	8.57	X	X		0.11
8	11.5100	0.24	49.	52.	7.6817	8.10	X	X		0.11
9	12.2050	0.24	58.	53.	7.2458	9.54	X	X		0.18
10	13.4475	0.16	52.	55.	6.5790	8.57	X	X		0.25
11	13.8400	0.16	44.	55.	6.3933	7.20	X	X		0.10
12	14.8800	0.08	45.	55.	5.9487	7.42	X	X		0.14
13	15.3525	0.32	41.	56.	5.7666	6.77	X	X		0.30
14	16.4800	0.08	58.	56.	5.3746	9.54	X	X		0.11
15	17.7275	0.12	50.	58.	4.9991	8.33	X	X		0.13
16	18.3600	0.08	50.	58.	4.8282	8.33	X	X		0.13
17	18.8350	0.12	55.	58.	4.7075	9.05	X	X		0.13
18	19.6400	0.08	64.	59.	4.5164	10.58	X	X		0.11
19	20.9100	0.12	137.	59.	4.2448	22.62	X	X		0.55
20	21.2000	0.08	74.	61.	4.1874	12.22	X	X		0.14
21	21.6350	0.24	72.	61.	4.1042	11.94	X	X		0.20
22	22.9650	0.24	90.	62.	3.8694	14.91	X	X		0.12
23	23.7075	0.24	112.	62.	3.7499	18.57	X	X		0.55
24	24.5525	0.40	94.	62.	3.6227	15.55	X	X		0.31
25	25.5000	0.16	219.	64.	3.4902	36.20	X	X		1.26
26	26.6150	0.12	605.	64.	3.3465	100.00	X	X		2.24
27	27.4400	0.32	114.	66.	3.2477	18.92	X	X		0.22
28	28.0375	0.12	125.	66.	3.1798	20.73	X	X		0.16
29	28.2950	0.12	119.	66.	3.1515	19.63	X	X		0.16
30	28.5600	0.08	139.	66.	3.1228	23.01	X	X		0.12
31	30.0400	0.08	151.	67.	2.9723	25.00	X	X		0.12
32	31.1850	0.12	188.	69.	2.8657	31.01	X	X		0.11
33	32.3600	0.08	188.	69.	2.7643	31.01	X	X		0.11
34	33.3450	0.28	313.	71.	2.6848	51.77	X	X		3.63
35	33.8750	0.12	146.	71.	2.6440	24.19	X	X		0.22
36	34.6200	0.24	88.	71.	2.5888	14.60	X	X		0.16
37	35.5175	0.20	128.	72.	2.5254	21.10	X	X		0.79
38	36.1200	0.12	79.	72.	2.4847	13.09	X	X		0.11
39	36.4800	0.12	106.	72.	2.4610	17.53	X	X		0.10
40	36.9675	0.12	74.	72.	2.4296	12.22	X	X		0.10
41	37.4800	0.16	164.	74.	2.3976	27.07	X	X		1.82
42	38.4775	0.16	110.	74.	2.3377	18.22	X	X		0.72
43	39.3150	0.12	74.	76.	2.2898	12.22	X			0.19
44	39.4975	0.12	74.	76.	2.2796	12.22	X	X		0.15
45	40.3175	0.12	71.	76.	2.2351	11.66	X	X		0.11
46	40.8475	0.24	96.	76.	2.2074	15.87	X	X		0.35
47	41.3500	0.12	83.	77.	2.1817	13.68	X	X		0.31
48	41.8750	0.12	62.	77.	2.1555	10.31	X	X		0.13
49	42.3450	0.24	69.	77.	2.1327	11.38	X	X		0.15
50	42.9150	0.16	228.	77.	2.1057	37.68	X	X		2.40
51	44.7000	0.24	90.	79.	2.0257	14.91	X	X		1.66
52	45.6200	0.32	52.	81.	1.9869	8.57	X	X		0.32
53	46.5600	0.08	76.	81.	1.9490	12.51	X	X		0.11
54	47.7150	0.24	79.	81.	1.9045	13.09	X	X		0.31
55	48.5650	0.12	64.	83.	1.8731	10.58	X	X		0.18
56	50.1050	0.20	112.	83.	1.8191	18.57	X	X		0.95
57	51.2875	0.12	34.	85.	1.7739	5.56	X	X		0.27
58	52.1650	0.32	40.	85.	1.7520	6.56	X	X		0.23
59	54.0500	0.16	100.	86.	1.6952	16.52	X	X		0.93
60	54.8400	0.08	42.	88.	1.6727	6.98	X	X		0.15
61	55.7600	0.08	44.	88.	1.6472	7.20	X	X		0.11
62	57.0000	0.48	38.	90.	1.6143	6.35	X	X		0.63
63	58.5475	0.12	40.	90.	1.5753	6.56	X			0.13
64	58.8125	0.12	44.	90.	1.5688	7.20	X	X		0.18
65	59.1950	0.12	48.	90.	1.5596	7.87	X	X		0.17
66	59.8000	0.56	77.	92.	1.5452	12.80	X	X		2.34
67	60.6625	0.24	48.	92.	1.5253	7.87	X	X		0.26
68	62.2400	0.08	128.	94.	1.4904	21.10	X			0.14
69	62.4400	0.08	96.	94.	1.4861	15.87	X	X		0.14
70	63.9200	0.08	32.	94.	1.4552	5.37	X			0.15
71	64.2325	0.12	35.	96.	1.4524	5.75		X		0.12
72	64.5200	0.08	44.	96.	1.4431	7.20	X	X		0.10
73	65.0225	0.12	164.	96.	1.4332	27.07	X			1.32
74	65.2400	0.08	58.	96.	1.4324	9.54		X		0.11
75	67.5525	0.24	40.	98.	1.3855	6.56	X	X		0.11
76	68.0925	0.12	49.	98.	1.3758	8.10	X	X		0.22
77	68.9750	0.12	10.	100.	1.3604	1.69	X	X		0.15

Table B2. Fly Ash.

Peak no	Angle (deg)	Tip width (deg)	Peak (cts)	Backg (cts)	D spac (Ang)	I/Imax (%)	Type A1	A2	Ot	Sign
1	8.8750	1.60	10.	22.	9.9550	0.78	X	X		0.25
2	18.0050	0.12	493.	34.	4.9228	37.61	X	X		2.75
3	28.6300	0.18	320.	21.	3.1154	24.45	X	X		8.32
4	34.0225	0.16	1310.	37.	2.6330	100.00	X			6.17
5	34.1075	0.06	1282.	37.	2.6266	97.80	X	X		0.81
6	38.3300	0.14	164.	26.	2.3464	12.50	X	X		3.16
7	42.8950	0.20	18.	18.	2.1067	1.41	X	X		0.78
8	44.5600	0.16	22.	22.	2.0317	1.69	X	X		0.79
9	47.0900	0.12	557.	29.	1.9293	42.50	X	X		2.00
10	50.7175	0.14	581.	29.	1.7986	44.32	X	X		4.27
11	54.2850	0.22	279.	24.	1.6885	21.28	X	X		5.75
12	56.1750	0.48	11.	21.	1.6361	0.83	X	X		0.79
13	59.3450	0.40	58.	17.	1.5560	4.41	X	X		7.03
14	62.5525	0.28	190.	19.	1.4827	14.52	X	X		4.07
15	64.2325	0.24	151.	18.	1.4489	11.54	X	X		2.45
16	65.0100	0.24	50.	17.	1.4335	3.85	X	X		1.12

Table B3. Hydrated Lime.

Peak no	Angle (deg)	Tip width (deg)	Peak (cts)	Backg (cts)	D spac (Ang)	I/Imax (%)	Type A1	Type A2	Type Ot	Sign
1	2.9600	0.08	10.	88.	29.8235	3.46	X	X		0.10
2	4.4150	0.16	10.	38.	19.9976	3.46	X	X		0.12
3	4.7575	0.16	10.	32.	18.5587	3.46	X	X		0.11
4	5.5825	0.24	10.	31.	15.8178	3.46	X	X		0.19
5	6.4975	0.12	18.	30.	13.5922	6.25	X	X		0.36
6	8.1550	0.12	15.	40.	10.8329	5.14	X	X		0.12
7	8.4400	0.16	18.	40.	10.4677	6.25	X	X		0.36
8	9.1675	0.12	10.	46.	9.6386	3.46	X	X		0.12
9	10.7525	0.48	13.	48.	8.2211	4.38	X	X		1.02
10	11.4550	0.24	10.	46.	7.7185	3.46	X	X		0.51
11	13.0275	0.24	10.	41.	6.7901	3.46	X	X		0.13
12	13.4850	0.16	10.	41.	6.5608	3.46	X	X		0.33
13	14.5425	0.16	12.	45.	6.0860	3.91	X	X		0.24
14	15.0925	0.32	10.	45.	5.8654	3.46	X	X		0.25
15	16.4200	0.24	10.	48.	5.3941	3.46	X	X		0.18
16	17.1825	0.32	10.	48.	5.1564	3.46	X	X		0.20
17	17.6000	0.08	10.	48.	5.0350	3.46	X	X		0.11
18	17.6800	0.16	10.	48.	5.0124	3.46	X	X		0.11
19	18.1950	0.12	12.	48.	4.8717	3.91	X	X		0.22
20	18.7400	0.24	10.	48.	4.7312	3.46	X	X		0.23
21	19.3000	0.24	12.	49.	4.5952	3.91	X	X		0.22
22	20.2475	0.12	15.	52.	4.3822	5.14	X	X		0.19
23	20.8900	0.16	53.	53.	4.2489	18.01	X	X		0.98
24	21.8000	0.08	27.	56.	4.0735	9.14	X	X		0.13
25	25.4350	0.16	25.	71.	3.4990	8.45	X	X		0.54
26	26.6600	0.20	296.	69.	3.3409	100.00	X	X		5.50
27	27.3800	0.24	17.	77.	3.2547	5.68	X	X		0.10
28	28.0250	0.12	26.	79.	3.1812	8.79	X			0.16
29	28.1325	0.16	22.	79.	3.1693	7.47	X	X		0.11
30	28.6800	0.08	24.	85.	3.1100	8.12	X	X		0.11
31	29.0800	0.16	28.	85.	3.0682	9.49	X	X		0.28
32	30.1600	0.08	28.	90.	2.9607	9.49	X	X		0.15
33	31.2125	0.48	24.	92.	2.8632	8.12	X	X		0.47
34	33.4700	0.12	72.	104.	2.6751	24.42	X	X		0.38
35	35.2875	0.12	10.	100.	2.5414	3.46	X	X		0.13
36	35.6375	0.12	23.	83.	2.5172	7.79	X	X		0.16
37	36.5450	0.24	10.	77.	2.4567	3.46	X	X		0.19
38	37.5050	0.16	10.	81.	2.3960	3.46	X	X		0.59
39	37.9600	0.08	10.	77.	2.3684	3.46	X	X		0.10
40	38.3825	0.20	204.	67.	2.3433	69.12	X	X		5.25
41	39.4725	0.16	34.	69.	2.2810	11.37	X	X		0.72
42	39.9200	0.08	14.	69.	2.2565	4.63	X	X		0.15
43	40.9200	0.12	27.	66.	2.2036	9.14	X	X		0.14
44	42.1200	0.08	10.	79.	2.1436	3.46	X	X		0.15
45	42.9525	0.16	88.	67.	2.1039	29.87	X	X		1.51
46	44.6250	0.12	36.	71.	2.0289	12.17	X	X		0.42
47	45.0800	0.16	10.	69.	2.0095	3.46	X	X		0.19
48	45.7475	0.12	18.	64.	1.9917	6.25	X	X		0.19
49	46.5225	0.24	10.	67.	1.9505	3.46	X	X		0.13
50	47.8200	0.24	18.	67.	1.9005	5.96	X	X		0.23
51	49.4400	0.08	10.	69.	1.8420	3.46	X	X		0.11
52	50.0475	0.16	59.	62.	1.8210	20.04	X	X		0.68
53	51.9750	0.48	10.	61.	1.7579	3.46	X	X		0.28
54	53.0575	0.24	10.	61.	1.7246	3.46	X	X		0.10
55	53.6350	0.16	12.	59.	1.7074	3.91	X	X		0.35
56	54.0375	0.24	13.	59.	1.6956	4.38	X	X		0.27
57	55.3475	0.12	18.	62.	1.6585	6.25	X	X		0.11
58	55.7200	0.16	10.	66.	1.6483	3.46	X	X		0.29
59	56.1500	0.12	10.	66.	1.6367	3.46	X	X		0.13
60	57.1375	0.12	19.	58.	1.6107	6.54	X	X		0.19
61	57.9675	0.12	16.	59.	1.5896	5.41	X	X		0.11
62	58.9000	0.24	10.	64.	1.5667	3.46	X	X		0.18
63	59.8975	0.32	31.	62.	1.5430	10.60	X	X		0.76
64	60.7100	0.12	10.	62.	1.5242	3.46	X	X		0.17
65	61.2400	0.08	10.	66.	1.5123	3.46	X	X		0.16
66	62.2000	0.08	40.	62.	1.4913	13.42	X			0.11
67	62.4400	0.08	38.	58.	1.4861	12.99	X	X		0.14
68	62.6400	0.08	27.	58.	1.4855	9.14		X		0.13
69	63.4600	0.16	10.	59.	1.4646	3.46	X	X		0.30
70	65.0050	0.16	213.	56.	1.4335	72.05	X	X		2.63
71	66.1675	0.12	10.	59.	1.4111	3.46	X	X		0.20
72	66.5975	0.12	10.	58.	1.4031	3.46	X	X		0.12
73	67.2750	0.16	14.	55.	1.3906	4.88	X	X		0.45
74	68.1725	0.12	38.	52.	1.3744	12.99	X	X		0.23
75	68.6775	0.12	10.	52.	1.3655	3.46	X	X		0.14

Table B4. Fly Ash Cured at 23°C For 1 Day.

Peak no	Angle (deg)	Tip Width (deg)	Peak (cts)	Backg (cts)	D spac (Ang)	I/Imax (%)	Type A1	A2	Qt	Sign
1	2.2950	0.24	10.	28.	38.4634	2.96	X	X		0.46
2	2.7650	0.16	10.	27.	31.9263	2.96	X	X		0.33
3	3.3925	0.12	10.	27.	26.0223	2.96	X	X		0.14
4	4.0400	0.08	10.	27.	21.8530	2.96	X	X		0.10
5	4.9375	0.24	18.	26.	17.8925	5.34	X	X		0.17
6	6.2100	0.24	21.	34.	14.2208	6.12	X	X		0.11
7	7.3300	0.12	34.	36.	12.0502	9.72	X	X		0.19
8	7.8400	0.08	29.	37.	11.2674	8.43	X	X		0.13
9	8.1525	0.32	28.	37.	10.8362	8.12	X	X		0.24
10	9.4275	0.12	21.	40.	9.3734	6.12	X	X		0.17
11	9.7200	0.08	34.	41.	9.0919	9.72	X	X		0.11
12	10.7775	0.32	18.	42.	8.2021	5.34	X	X		0.22
13	11.4100	0.12	14.	45.	7.7488	4.17	X	X		0.19
14	12.5575	0.12	21.	46.	7.0432	6.12	X	X		0.34
15	12.9600	0.08	14.	48.	6.8253	3.96	X	X		0.16
16	14.2625	0.16	10.	50.	6.2048	2.96	X	X		0.37
17	15.7875	0.12	10.	46.	5.6087	2.96	X	X		0.19
18	16.2700	0.12	10.	49.	5.4435	2.96	X	X		0.19
19	17.3500	0.16	10.	49.	5.1070	2.96	X	X		0.26
20	18.6825	0.16	22.	52.	4.7456	6.39	X	X		0.59
21	19.1325	0.12	14.	55.	4.6350	4.17	X	X		0.11
22	19.9725	0.32	16.	56.	4.4419	4.62	X	X		0.22
23	20.9275	0.16	72.	61.	4.2413	20.88	X	X		1.32
24	23.6350	0.48	10.	67.	3.7612	2.96	X	X		0.10
25	26.6850	0.16	346.	81.	3.3379	100.00	X	X		3.63
26	27.5775	0.24	18.	81.	3.2318	5.10	X	X		0.16
27	27.9600	0.08	24.	81.	3.1885	6.94	X	X		0.12
28	29.4700	0.12	29.	79.	3.0284	8.43	X	X		0.17
29	29.8400	0.08	27.	79.	2.9917	7.82	X	X		0.11
30	30.2100	0.16	36.	77.	2.9559	10.41	X	X		0.13
31	31.0975	0.12	59.	77.	2.8736	17.14	X	X		0.18
32	31.6000	0.08	49.	77.	2.8290	14.16	X	X		0.13
33	31.8200	0.12	50.	77.	2.8099	14.57	X	X		0.17
34	33.4375	0.20	114.	76.	2.6776	33.09	X	X		1.10
35	34.1325	0.16	31.	76.	2.6247	9.06	X	X		0.23
36	35.6400	0.32	28.	74.	2.5170	8.12	X	X		0.83
37	36.6000	0.08	27.	72.	2.4532	7.82	X	X		0.11
38	37.0800	0.08	16.	72.	2.4225	4.62	X	X		0.11
39	37.5500	0.16	17.	72.	2.3933	4.86	X	X		0.38
40	38.2025	0.12	12.	72.	2.3539	3.34	X	X		0.21
41	38.5300	0.16	50.	71.	2.3346	14.57	X	X		1.10
42	39.4700	0.16	29.	71.	2.2812	8.43	X	X		0.85
43	40.1600	0.08	16.	69.	2.2435	4.62	X	X		0.15
44	40.9325	0.24	27.	66.	2.2030	7.82	X	X		0.41
45	42.5600	0.08	32.	67.	2.1224	9.39	X	X		0.11
46	42.9400	0.12	98.	67.	2.1045	28.33	X	X		0.55
47	44.7575	0.16	36.	66.	2.0232	10.41	X	X		0.81
48	45.4000	0.08	10.	64.	1.9960	2.96	X	X		0.11
49	45.8000	0.08	22.	64.	1.9795	6.39	X	X		0.15
50	47.7475	0.32	23.	64.	1.9032	6.66	X	X		0.58
51	50.2100	0.12	40.	61.	1.8155	11.47	X	X		0.22
52	54.0925	0.48	16.	59.	1.6940	4.62	X	X		0.36
53	55.2200	0.12	23.	59.	1.6621	6.66	X	X		0.30
54	55.6225	0.12	46.	59.	1.6510	13.37	X			0.69
55	55.8400	0.08	22.	59.	1.6491	6.39		X		0.15
56	56.1500	0.12	12.	59.	1.6367	3.34	X	X		0.30
57	57.2800	0.12	14.	59.	1.6071	4.17	X	X		0.10
58	59.7150	0.24	46.	59.	1.5472	13.37	X	X		0.98
59	60.5925	0.16	15.	59.	1.5269	4.40	X	X		0.23
60	61.0100	0.12	14.	58.	1.5175	4.17	X	X		0.20
61	62.2675	0.12	48.	56.	1.4898	13.76	X			0.54
62	62.5175	0.12	34.	56.	1.4881	9.72		X		0.14
63	63.6000	0.16	11.	55.	1.4618	3.15	X	X		0.10
64	63.9250	0.12	13.	55.	1.4551	3.75	X	X		0.12
65	64.6725	0.12	25.	53.	1.4401	7.23	X	X		0.23
66	65.0200	0.12	85.	53.	1.4332	24.47	X			0.63
67	65.2400	0.08	50.	52.	1.4324	14.57		X		0.16
68	67.6450	0.20	40.	49.	1.3838	11.47	X	X		0.81
69	68.3550	0.16	18.	49.	1.3712	5.34	X	X		0.17
70	69.5600	0.08	15.	49.	1.3504	4.40	X	X		0.14

Table B5. Fly Ash Cured at 23°C for 28 Days.

Peak no	Angle (deg)	Tip width (deg)	Peak (cts)	Backg (cts)	D spac (Ang)	I/Imax (%)	Type A1	Type A2	Type Ot	Sign
1	2.9200	0.08	13.	40.	30.2319	6.47	X	X		0.15
2	4.3275	0.12	10.	40.	20.4018	3.59	X	X		0.21
3	4.6175	0.12	10.	40.	19.1211	3.59	X	X		0.13
4	7.5025	0.12	12.	40.	11.7735	4.29	X	X		0.12
5	7.8075	0.12	18.	40.	11.3143	6.47	X	X		0.14
6	9.4400	0.16	12.	42.	9.3610	4.05	X	X		0.11
7	9.9200	0.16	14.	44.	8.9091	5.06	X	X		0.10
8	10.9325	0.12	17.	45.	8.0861	5.89	X	X		0.10
9	11.4400	0.08	10.	46.	7.7285	3.59	X	X		0.12
10	11.9125	0.12	10.	46.	7.4230	3.59	X	X		0.17
11	12.6350	0.12	10.	46.	7.0001	3.59	X	X		0.28
12	12.9050	0.48	10.	46.	6.8543	3.59	X	X		0.13
13	14.3075	0.12	14.	46.	6.1854	5.06	X	X		0.36
14	14.7475	0.24	10.	48.	6.0018	3.59	X	X		0.11
15	16.0100	0.20	10.	50.	5.5313	3.59	X	X		0.56
16	16.6100	0.12	10.	49.	5.3328	3.59	X	X		0.22
17	17.1475	0.12	10.	48.	5.1668	3.59	X	X		0.11
18	17.4500	0.12	10.	48.	5.0779	3.59	X	X		0.11
19	18.0525	0.12	18.	46.	4.9098	6.18	X	X		0.16
20	18.3800	0.12	14.	46.	4.8230	5.06	X	X		0.11
21	18.8400	0.08	23.	48.	4.7063	8.07	X	X		0.25
22	19.4525	0.12	14.	50.	4.5595	4.79	X	X		0.14
23	20.2000	0.08	20.	50.	4.3924	7.09	X	X		0.10
24	20.8800	0.08	66.	53.	4.2509	22.97	X	X		0.19
25	23.4100	0.12	18.	66.	3.7969	6.18	X	X		0.22
26	24.6725	0.12	20.	64.	3.6054	7.09	X	X		0.20
27	24.9200	0.08	24.	64.	3.5701	8.41	X	X		0.16
28	26.6275	0.20	286.	64.	3.3449	100.00	X	X		5.89
29	27.3200	0.24	35.	64.	3.2617	12.19	X	X		0.32
30	27.7200	0.08	36.	64.	3.2155	12.60	X	X		0.10
31	27.8850	0.32	36.	64.	3.1969	12.60	X	X		0.18
32	28.0800	0.32	35.	64.	3.1751	12.19	X	X		0.13
33	29.5950	0.12	49.	64.	3.0159	17.16	X	X		0.18
34	30.1450	0.24	49.	62.	2.9622	17.16	X	X		0.26
35	31.3925	0.12	66.	62.	2.8472	22.97	X	X		0.22
36	31.9600	0.12	55.	62.	2.7980	19.17	X	X		0.14
37	32.5475	0.32	48.	62.	2.7488	16.67	X	X		0.12
38	33.2175	0.12	117.	62.	2.6948	40.84	X			0.31
39	33.3700	0.20	128.	62.	2.6829	44.71	X	X		0.91
40	34.4000	0.08	30.	62.	2.6049	10.59	X	X		0.18
41	35.5475	0.16	49.	61.	2.5234	17.16	X	X		0.69
42	35.9200	0.08	29.	61.	2.4980	10.21	X	X		0.13
43	36.5850	0.12	38.	61.	2.4542	13.46	X	X		0.48
44	37.5175	0.12	25.	61.	2.3953	8.75	X	X		0.18
45	38.4750	0.24	49.	61.	2.3378	17.16	X	X		1.74
46	38.8750	0.12	15.	61.	2.3147	5.33	X	X		0.22
47	39.4700	0.12	31.	61.	2.2812	10.98	X	X		0.22
48	40.2300	0.24	19.	61.	2.2398	6.79	X	X		0.16
49	40.9825	0.24	28.	61.	2.2004	9.84	X	X		0.38
50	41.4375	0.16	14.	59.	2.1773	4.79	X	X		0.31
51	42.9150	0.16	92.	59.	2.1057	32.27	X	X		1.10
52	43.9025	0.24	13.	59.	2.0606	4.54	X	X		0.10
53	44.6975	0.12	38.	59.	2.0258	13.46	X	X		0.25
54	45.5125	0.16	14.	59.	1.9914	4.79	X	X		0.17
55	46.8300	0.12	20.	59.	1.9384	7.09	X	X		0.26
56	47.9175	0.80	16.	58.	1.8969	5.60	X	X		0.55
57	49.2375	0.40	16.	58.	1.8470	5.60	X	X		0.72
58	50.0350	0.20	59.	58.	1.8214	20.76	X	X		0.83
59	50.4800	0.08	12.	58.	1.8064	4.05	X	X		0.11
60	50.8875	0.24	10.	58.	1.7929	3.59	X	X		0.18
61	52.8300	0.12	10.	56.	1.7315	3.59	X	X		0.12
62	54.4800	0.08	16.	56.	1.6829	5.60	X	X		0.11
63	54.8850	0.48	14.	56.	1.6714	5.06	X	X		0.21
64	56.8000	0.08	18.	56.	1.6195	6.47	X	X		0.11
65	57.5150	0.16	17.	56.	1.6011	5.89	X	X		0.24
66	58.4300	0.12	15.	55.	1.5782	5.33	X	X		0.27
67	59.9025	0.12	49.	55.	1.5428	17.16	X	X		0.50
68	60.6075	0.16	19.	55.	1.5266	6.78	X	X		0.18
69	62.2450	0.16	58.	55.	1.4903	20.22	X			0.93
70	62.5625	0.12	30.	55.	1.4871	10.59		X		0.15
71	64.2025	0.24	12.	53.	1.4495	4.29	X	X		0.16
72	64.6800	0.08	19.	53.	1.4399	6.78	X			0.10
73	64.9850	0.12	81.	53.	1.4339	28.36	X	X		0.63
74	66.1200	0.16	10.	53.	1.4120	3.59	X	X		0.14
75	66.5600	0.08	14.	53.	1.4037	5.06	X	X		0.15
76	67.1200	0.08	10.	53.	1.3934	3.59	X	X		0.14
77	67.5675	0.24	22.	52.	1.3852	7.73	X	X		0.22
78	68.0375	0.12	36.	53.	1.3768	12.60	X	X		0.18

Table B6. Fly Ash Cured at 23°C for 90 Days.

Peak no	Angle (deg)	Tip width (deg)	Peak (cts)	Backg (cts)	D spac (Ang)	I/Imax (%)	Type A1	Type A2	Type Ot	Sign
1	3.4325	0.12	10.	72.	25.7191	3.34	X	X		0.16
2	3.8400	0.08	10.	72.	22.9907	3.34	X	X		0.10
3	4.9425	0.48	10.	46.	17.8645	3.34	X	X		0.25
4	5.9375	0.40	10.	42.	14.8728	3.34	X	X		0.46
5	7.1375	0.12	36.	34.	12.3748	8.49	X	X		0.30
6	8.1175	0.32	10.	40.	10.8829	3.34	X	X		0.24
7	8.6800	0.08	12.	42.	10.1798	4.00	X	X		0.11
8	8.9900	0.12	10.	48.	9.8285	3.34	X	X		0.22
9	9.6050	0.48	10.	46.	9.2005	3.34	X	X		0.26
10	10.9250	0.32	12.	46.	8.0917	3.77	X	X		0.31
11	12.0000	0.08	10.	46.	7.3691	3.34	X	X		0.17
12	12.5375	0.24	10.	50.	7.0544	3.34	X	X		0.14
13	13.0950	0.24	10.	46.	6.7553	3.34	X	X		0.21
14	14.0650	0.12	20.	41.	6.2915	6.61	X	X		0.41
15	14.3225	0.12	17.	41.	6.1789	5.49	X	X		0.18
16	14.5850	0.12	14.	41.	6.0683	4.47	X	X		0.18
17	15.0175	0.12	10.	41.	5.8945	3.34	X	X		0.18
18	16.4400	0.08	14.	44.	5.3875	4.72	X	X		0.12
19	17.3150	0.16	10.	48.	5.1172	3.34	X	X		0.32
20	17.6550	0.12	10.	48.	5.0194	3.34	X	X		0.23
21	18.1975	0.12	10.	48.	4.8710	3.34	X	X		0.10
22	19.0825	0.16	12.	49.	4.6470	3.77	X	X		0.28
23	19.5600	0.12	10.	52.	4.5347	3.34	X	X		0.15
24	20.2750	0.12	11.	56.	4.3763	3.56	X	X		0.16
25	20.9650	0.16	61.	53.	4.2338	19.87	X	X		1.10
26	22.8450	0.24	10.	71.	3.8895	3.34	X	X		0.16
27	23.3500	0.12	10.	71.	3.8065	3.34	X	X		0.17
28	24.0400	0.08	20.	64.	3.6988	6.61	X	X		0.16
29	24.5200	0.16	18.	64.	3.6274	6.04	X	X		0.32
30	24.9200	0.08	14.	72.	3.5701	4.72	X	X		0.13
31	26.7600	0.16	306.	74.	3.3287	100.00	X	X		3.72
32	27.6750	0.16	14.	85.	3.2207	4.47	X	X		0.32
33	28.2350	0.12	10.	92.	3.1580	3.34	X	X		0.19
34	29.1550	0.16	12.	86.	3.0604	3.77	X	X		0.23
35	29.7975	0.16	14.	86.	2.9959	4.47	X	X		0.11
36	30.1975	0.24	22.	86.	2.9571	7.21	X	X		0.26
37	31.1450	0.24	23.	96.	2.8693	7.52	X	X		0.19
38	33.4025	0.28	74.	98.	2.6803	24.15	X	X		2.00
39	33.9600	0.08	10.	96.	2.6376	3.34	X	X		0.16
40	34.8025	0.12	10.	94.	2.5757	3.34	X	X		0.13
41	35.6650	0.12	29.	81.	2.5153	9.52	X	X		0.21
42	36.1225	0.12	10.	81.	2.4845	3.34	X	X		0.20
43	36.7175	0.16	22.	72.	2.4456	7.21	X	X		0.15
44	37.0125	0.12	14.	72.	2.4268	4.72	X	X		0.21
45	37.5175	0.12	16.	72.	2.3953	5.22	X	X		0.11
46	37.9200	0.08	14.	72.	2.3708	4.72	X	X		0.14
47	38.5200	0.16	125.	66.	2.3352	40.96	X	X		1.29
48	39.5600	0.08	27.	66.	2.2762	8.83	X	X		0.12
49	39.8400	0.08	10.	66.	2.2608	3.34	X	X		0.11
50	40.9200	0.08	28.	62.	2.2036	9.17	X	X		0.11
51	41.1600	0.16	26.	62.	2.1913	8.49	X	X		0.48
52	42.5025	0.12	34.	62.	2.1252	10.98	X	X		0.22
53	42.9900	0.16	85.	62.	2.1022	27.64	X	X		1.23
54	44.0800	0.12	17.	62.	2.0527	5.49	X	X		0.13
55	44.5600	0.08	31.	62.	2.0317	10.24	X	X		0.10
56	44.8075	0.12	37.	62.	2.0210	12.15	X	X		0.34
57	46.8250	0.40	19.	62.	1.9386	6.32	X	X		0.62
58	47.5600	0.08	22.	59.	1.9103	7.21	X	X		0.11
59	47.9450	0.24	25.	59.	1.8959	8.16	X	X		0.21
60	48.3225	0.16	26.	59.	1.8819	8.49	X	X		0.38
61	48.7900	0.12	10.	59.	1.8650	3.34	X	X		0.13
62	49.2400	0.08	20.	59.	1.8490	6.61	X	X		0.14
63	50.1125	0.12	44.	59.	1.8198	14.22	X	X		0.26
64	50.7025	0.12	14.	58.	1.7990	4.47	X	X		0.42
65	52.0925	0.40	10.	58.	1.7542	3.34	X	X		0.35
66	52.8000	0.16	10.	58.	1.7324	3.34	X	X		0.11
67	54.1900	0.12	17.	58.	1.6912	5.49	X	X		0.18
68	54.8200	0.12	18.	58.	1.6732	6.04	X	X		0.23
69	55.3275	0.24	22.	56.	1.6591	7.21	X	X		0.28
70	56.2325	0.12	12.	56.	1.6345	4.00	X	X		0.13
71	57.1475	0.40	19.	56.	1.6105	6.32	X	X		0.66
72	57.7525	0.24	13.	56.	1.5951	4.23	X			0.56
73	58.0000	0.08	10.	56.	1.5888	3.34	X	X		0.13
74	58.3900	0.12	13.	56.	1.5791	4.23	X	X		0.11
75	59.6000	0.08	42.	56.	1.5499	13.80	X	X		0.17

Table B7. Fly Ash Cured at 23°C For 180 Days.

Peak no	Angle (deg)	Tip width (deg)	Peak (cts)	Backg (cts)	D spac (Ang)	I/Imax (%)	Type A1	A2	Ot	Sign
1	2.2475	0.48	35.	36.	39.2762	10.74	X	X		0.38
2	3.6075	0.12	10.	36.	24.4719	3.16	X	X		0.29
3	3.7750	0.24	10.	36.	23.3864	3.16	X	X		0.30
4	4.5500	0.12	10.	36.	19.4046	3.16	X	X		0.14
5	4.9875	0.12	10.	36.	17.7034	3.16	X	X		0.32
6	7.3200	0.24	13.	36.	12.0666	4.00	X	X		0.26
7	8.5225	0.16	19.	37.	10.3666	5.98	X	X		0.50
8	9.9100	0.16	12.	37.	8.9180	3.57	X	X		0.12
9	10.8800	0.08	30.	38.	8.1250	9.34	X	X		0.13
10	12.4550	0.12	13.	40.	7.1009	4.00	X	X		0.17
11	12.9275	0.24	10.	40.	6.8424	3.16	X	X		0.15
12	14.8525	0.20	14.	41.	5.9596	4.23	X	X		0.49
13	15.5200	0.08	14.	41.	5.7048	4.23	X	X		0.13
14	15.9725	0.16	18.	41.	5.5442	5.71	X	X		0.51
15	16.4000	0.16	13.	42.	5.4006	4.00	X	X		0.11
16	17.2400	0.08	20.	42.	5.1393	6.25	X	X		0.19
17	17.5250	0.12	12.	42.	5.0564	3.57	X	X		0.12
18	18.0000	0.08	15.	42.	4.9240	4.69	X	X		0.11
19	19.6600	0.24	20.	44.	4.5118	6.25	X	X		0.29
20	20.8900	0.16	76.	45.	4.2489	23.36	X	X		1.17
21	21.8475	0.16	41.	45.	4.0648	12.64	X	X		0.30
22	22.2775	0.12	34.	45.	3.9873	10.38	X	X		0.20
23	22.8100	0.12	34.	46.	3.8954	10.38	X	X		0.18
24	24.1425	0.16	45.	46.	3.6833	13.85	X	X		0.60
25	24.4000	0.08	36.	48.	3.6450	11.11	X	X		0.11
26	25.2275	0.24	37.	48.	3.5273	11.48	X	X		0.15
27	25.6800	0.08	45.	48.	3.4662	13.85	X	X		0.12
28	26.6425	0.16	324.	48.	3.3431	100.00	X	X		3.72
29	27.3075	0.12	48.	49.	3.2632	14.69	X	X		0.15
30	27.7700	0.12	50.	49.	3.2099	15.56	X	X		0.13
31	28.2800	0.32	49.	49.	3.1531	15.12	X	X		0.22
32	29.1100	0.12	52.	50.	3.0651	16.00	X	X		0.10
33	30.5775	0.16	67.	50.	2.9212	20.75	X	X		0.40
34	31.0400	0.16	72.	52.	2.8788	22.30	X	X		0.43
35	32.4800	0.12	77.	52.	2.7543	23.90	X	X		0.17
36	33.2400	0.08	110.	53.	2.6931	34.03	X	X		0.15
37	33.4675	0.12	121.	53.	2.6753	37.35	X	X		0.52
38	34.0400	0.32	42.	53.	2.6316	13.04	X	X		0.13
39	34.8800	0.08	32.	53.	2.5701	10.03	X	X		0.13
40	35.5450	0.12	61.	55.	2.5235	18.78	X	X		0.29
41	36.5225	0.24	30.	55.	2.4582	9.34	X	X		0.36
42	37.0700	0.24	24.	55.	2.4232	7.41	X	X		0.19
43	37.5600	0.08	31.	56.	2.3927	9.68	X	X		0.12
44	37.9975	0.16	32.	56.	2.3661	10.03	X	X		0.39
45	38.5100	0.20	156.	56.	2.3358	48.23	X	X		3.98
46	38.9600	0.08	21.	56.	2.3098	6.53	X	X		0.14
47	39.2000	0.08	24.	56.	2.2963	7.41	X	X		0.13
48	39.4600	0.16	40.	56.	2.2817	12.25	X	X		0.76
49	40.3400	0.16	27.	58.	2.2340	8.35	X	X		0.50
50	40.9575	0.20	38.	58.	2.2017	11.86	X	X		0.68
51	41.7600	0.16	14.	58.	2.1612	4.23	X	X		0.11
52	42.9575	0.16	121.	59.	2.1037	37.35	X	X		2.19
53	44.6850	0.16	28.	61.	2.0263	8.67	X	X		0.26
54	45.2450	0.12	10.	61.	2.0025	3.16	X	X		0.13
55	45.7325	0.16	18.	61.	1.9823	5.71	X	X		0.23
56	46.0450	0.12	12.	61.	1.9696	3.57	X	X		0.19
57	47.2800	0.12	17.	61.	1.9210	5.19	X	X		0.11
58	47.9075	0.12	28.	62.	1.8972	8.67	X	X		0.22
59	50.0800	0.12	35.	64.	1.8199	10.74	X			0.12
60	50.1950	0.12	30.	64.	1.8160	9.34	X	X		0.19
61	50.6925	0.12	10.	64.	1.7994	3.16	X	X		0.13
62	51.8725	0.12	18.	58.	1.7612	5.44	X	X		0.16
63	52.9600	0.08	15.	61.	1.7275	4.69	X	X		0.20
64	53.4800	0.08	12.	61.	1.7120	3.57	X			0.11
65	53.5600	0.08	13.	61.	1.7096	4.00	X	X		0.11
66	54.1250	0.32	14.	55.	1.6931	4.46	X	X		0.43
67	54.7600	0.08	16.	59.	1.6749	4.94	X	X		0.11
68	55.4025	0.24	14.	59.	1.6570	4.46	X	X		0.29
69	57.5525	0.16	18.	58.	1.6001	5.44	X	X		0.25
70	59.8625	0.12	38.	61.	1.5438	11.86	X	X		0.25
71	60.6500	0.32	10.	61.	1.5256	3.16	X	X		0.19
72	61.7675	0.12	17.	61.	1.5007	5.19	X	X		0.24
73	62.3000	0.20	56.	61.	1.4891	17.36	X	X		1.29
74	63.4100	0.12	10.	61.	1.4657	3.16	X	X		0.16
75	63.8400	0.08	10.	61.	1.4568	3.16	X	X		0.10
76	64.6000	0.08	25.	56.	1.4415	7.72	X	X		0.10
77	65.0300	0.12	28.	56.	1.4330	8.67	X	X		0.31
78	65.7200	0.08	10.	59.	1.4196	3.16	X	X		0.13
79	67.6225	0.16	37.	53.	1.3843	11.48	X	X		0.56
80	68.1125	0.16	31.	55.	1.3755	9.68	X	X		0.20

Table B8. Fly Ash Cured at 50°C for 1 Day.

Peak no	Angle (deg)	Tip width (deg)	Peak (cts)	Backg (cts)	D spac (Ang)	I/Imax (%)	Type A1	Type A2	Type Ot	Sign
1	3.9600	0.08	10.	30.	22.2943	3.46	X	X		0.13
2	4.8125	0.12	16.	30.	18.3467	5.41	X	X		0.17
3	5.3300	0.08	21.	31.	15.0181	7.15	X	X		0.11
4	6.0800	0.12	22.	32.	14.5245	7.47	X	X		0.14
5	6.4725	0.12	25.	32.	13.6446	8.45	X	X		0.21
6	6.9550	0.16	23.	34.	12.6991	7.79	X	X		0.12
7	7.2650	0.32	25.	34.	12.1579	8.45	X	X		0.15
8	7.6800	0.08	29.	35.	11.5018	9.86	X	X		0.14
9	8.9550	0.12	25.	36.	9.8668	8.45	X	X		0.17
10	9.4000	0.08	30.	36.	9.4007	10.23	X	X		0.13
11	10.3125	0.12	28.	37.	8.5709	9.49	X	X		0.17
12	10.6900	0.20	21.	38.	8.2690	7.15	X	X		0.38
13	11.9125	0.12	24.	41.	7.4230	8.12	X	X		0.25
14	12.6275	0.12	19.	41.	7.0043	6.54	X	X		0.22
15	12.9650	0.20	19.	42.	6.8227	6.54	X	X		0.76
16	13.4975	0.24	12.	42.	6.5547	4.14	X	X		0.14
17	13.6800	0.32	11.	42.	6.4677	3.68	X	X		0.10
18	14.8500	0.48	10.	45.	5.9606	3.46	X	X		0.15
19	16.4425	0.24	18.	46.	5.3867	5.96	X	X		0.27
20	18.9250	0.24	18.	50.	4.6853	5.96	X	X		0.20
21	20.9450	0.12	58.	58.	4.2378	19.52	X	X		0.63
22	21.5800	0.12	18.	59.	4.1145	5.96	X	X		0.12
23	23.0400	0.08	30.	61.	3.8570	10.23	X	X		0.12
24	23.5700	0.12	26.	61.	3.7715	8.79	X	X		0.19
25	24.3900	0.12	28.	61.	3.6465	9.49	X	X		0.19
26	25.2950	0.24	31.	61.	3.5180	10.60	X	X		0.20
27	26.6825	0.16	296.	61.	3.3382	100.00	X	X		3.47
28	27.5900	0.12	37.	61.	3.2304	12.58	X	X		0.19
29	27.8500	0.12	45.	61.	3.2008	15.17	X	X		0.19
30	28.3750	0.12	53.	61.	3.1428	18.01	X	X		0.32
31	28.9500	0.24	41.	61.	3.0816	13.85	X	X		0.11
32	30.2400	0.08	52.	61.	2.9531	17.52	X	X		0.11
33	30.9925	0.16	69.	61.	2.8831	23.29	X	X		0.36
34	31.7200	0.08	58.	61.	2.8186	19.52	X	X		0.10
35	31.8800	0.08	62.	61.	2.8048	21.10	X	X		0.10
36	32.1200	0.08	69.	61.	2.7844	23.29	X	X		0.19
37	32.3600	0.08	74.	61.	2.7643	25.00	X	X		0.18
38	32.6000	0.08	66.	61.	2.7445	22.18	X	X		0.11
39	32.8550	0.12	64.	61.	2.7237	21.63	X	X		0.13
40	33.3125	0.16	123.	61.	2.6874	41.65	X	X		0.66
41	33.4775	0.16	110.	61.	2.6745	37.27	X	X		0.33
42	34.4800	0.08	27.	62.	2.5990	9.14	X	X		0.11
43	35.6025	0.32	46.	62.	2.5196	15.63	X	X		0.81
44	36.5575	0.16	44.	62.	2.4559	14.72	X	X		0.20
45	37.0650	0.16	24.	62.	2.4235	8.12	X	X		0.42
46	37.5175	0.12	24.	62.	2.3953	8.12	X	X		0.14
47	38.5250	0.16	37.	62.	2.3349	12.58	X	X		0.79
48	39.5175	0.48	22.	62.	2.2785	7.47	X	X		1.35
49	40.2050	0.24	17.	62.	2.2411	5.68	X	X		0.39
50	40.9050	0.12	41.	61.	2.2044	13.85	X	X		0.30
51	41.8925	0.12	10.	62.	2.1547	3.46	X	X		0.13
52	42.3200	0.08	22.	62.	2.1339	7.47	X	X		0.10
53	42.5350	0.12	27.	62.	2.1236	9.14	X	X		0.12
54	42.9375	0.12	90.	62.	2.1046	30.51	X	X		0.73
55	44.7075	0.12	37.	62.	2.0253	12.58	X	X		0.43
56	45.7175	0.16	18.	64.	1.9829	5.96	X	X		0.16
57	46.5175	0.12	18.	64.	1.9507	5.96	X			0.21
58	46.6550	0.24	18.	64.	1.9452	5.96	X	X		0.30
59	47.8650	0.64	17.	62.	1.8988	5.68	X	X		0.43
60	50.0875	0.16	58.	64.	1.8197	19.52	X	X		0.76
61	51.0975	0.12	10.	64.	1.7860	3.46	X			0.25
62	51.2000	0.16	10.	64.	1.7827	3.46	X	X		0.10
63	51.9450	0.16	11.	62.	1.7589	3.68	X	X		0.50
64	52.9350	0.32	10.	61.	1.7283	3.46	X	X		0.29
65	53.5750	0.24	10.	61.	1.7091	3.46	X	X		0.18
66	54.2400	0.08	22.	59.	1.6897	7.47	X	X		0.13
67	54.9375	0.16	14.	61.	1.6699	4.63	X	X		0.25
68	55.5225	0.12	18.	61.	1.6537	5.96	X	X		0.19
69	56.0950	0.24	10.	59.	1.6392	3.46	X	X		0.17
70	56.6000	0.12	10.	59.	1.6248	3.46	X	X		0.11
71	57.5600	0.08	24.	59.	1.5999	8.12	X	X		0.15
72	58.3225	0.12	14.	58.	1.5808	4.63	X			0.11
73	58.4600	0.24	11.	58.	1.5774	3.68	X	X		0.10
74	59.4025	0.24	29.	58.	1.5546	9.86	X	X		0.21
75	59.9200	0.08	49.	58.	1.5424	16.56	X	X		0.13
76	61.1600	0.08	18.	56.	1.5141	5.96	X	X		0.13

Table B9. Fly Ash Cured at 50°C for 28 Days.

Peak no	Angle (deg)	Tip width (deg)	Peak (cts)	Backg (cts)	D spac (Ang)	I/Imax (%)	Type A1	Type A2	Type Ot	Sign
1	3.3600	0.16	10.	62.	26.2739	3.16	X	X		0.11
2	4.6850	0.48	10.	44.	18.8457	3.16	X	X		0.19
3	5.9200	0.16	10.	46.	14.9167	3.16	X	X		0.12
4	6.5300	0.12	10.	46.	13.5246	3.16	X	X		0.26
5	7.0000	0.08	12.	45.	12.6175	3.57	X	X		0.13
6	8.6700	0.16	11.	41.	10.1905	3.36	X	X		0.14
7	10.5675	0.12	12.	48.	8.3646	3.57	X	X		0.19
8	12.2000	0.08	10.	49.	7.2487	3.16	X	X		0.12
9	12.7525	0.12	10.	49.	6.9359	3.16	X	X		0.25
10	13.2300	0.20	10.	45.	6.6866	3.16	X	X		0.18
11	14.0325	0.48	10.	45.	6.3060	3.16	X	X		0.13
12	15.5875	0.24	10.	46.	5.6802	3.16	X	X		0.18
13	16.3950	0.32	10.	48.	5.4022	3.16	X	X		0.15
14	17.7600	0.08	12.	50.	4.9900	3.78	X	X		0.11
15	18.6000	0.08	10.	50.	4.7665	3.16	X	X		0.11
16	19.1800	0.24	14.	50.	4.6236	4.23	X	X		0.16
17	20.9600	0.08	45.	58.	4.2348	13.85	X	X		0.15
18	21.6850	0.12	23.	61.	4.0948	7.11	X	X		0.22
19	22.4825	0.12	16.	59.	3.9514	4.94	X	X		0.10
20	23.5625	0.12	28.	59.	3.7726	8.67	X	X		0.22
21	25.0425	0.12	28.	59.	3.5529	8.67	X	X		0.17
22	26.7000	0.12	324.	59.	3.3360	100.00	X	X		1.86
23	27.6700	0.12	42.	59.	3.2212	13.04	X	X		0.23
24	27.8850	0.12	45.	59.	3.1969	13.85	X	X		0.17
25	28.4375	0.32	38.	59.	3.1360	11.86	X	X		0.21
26	29.0025	0.16	42.	59.	3.0762	13.04	X	X		0.26
27	29.6300	0.16	53.	59.	3.0125	16.45	X	X		0.21
28	29.9800	0.16	45.	59.	2.9781	13.85	X	X		0.22
29	30.6950	0.12	58.	59.	2.9103	17.83	X	X		0.10
30	31.2350	0.32	71.	59.	2.8612	21.78	X	X		0.59
31	31.9050	0.24	59.	59.	2.8026	18.30	X	X		0.12
32	32.7200	0.08	67.	59.	2.7347	20.75	X	X		0.12
33	33.4125	0.16	125.	59.	2.6796	38.72	X	X		0.78
34	34.9125	0.16	26.	58.	2.5678	8.03	X	X		0.14
35	35.6400	0.08	58.	58.	2.5170	17.83	X	X		0.25
36	36.4025	0.12	36.	58.	2.4660	11.11	X	X		0.11
37	36.9250	0.16	32.	58.	2.4323	10.03	X	X		0.32
38	37.5175	0.32	21.	58.	2.3953	6.53	X	X		0.35
39	38.2250	0.16	19.	58.	2.3525	5.98	X	X		0.25
40	38.5100	0.16	36.	58.	2.3358	11.11	X	X		0.62
41	39.3200	0.08	32.	58.	2.2895	10.03	X	X		0.11
42	39.5075	0.12	34.	58.	2.2791	10.38	X	X		0.22
43	40.3000	0.24	16.	58.	2.2361	4.94	X	X		0.16
44	40.9200	0.16	38.	58.	2.2036	11.86	X	X		0.59
45	41.5575	0.12	16.	58.	2.1713	4.94	X	X		0.11
46	42.9975	0.16	104.	58.	2.1018	32.11	X	X		1.38
47	43.6050	0.12	18.	58.	2.0739	5.71	X	X		0.19
48	43.9350	0.16	25.	58.	2.0591	7.72	X	X		0.32
49	44.7600	0.16	35.	58.	2.0231	10.74	X	X		0.54
50	45.6625	0.12	18.	58.	1.9852	5.71	X			0.13
51	45.8800	0.08	22.	58.	1.9763	6.82	X	X		0.17
52	46.7400	0.16	29.	58.	1.9419	9.00	X	X		0.32
53	47.1725	0.12	18.	58.	1.9251	5.71	X	X		0.13
54	47.8200	0.32	24.	56.	1.9005	7.41	X	X		0.33
55	48.9875	0.12	12.	56.	1.8579	3.78	X	X		0.14
56	49.4675	0.12	22.	56.	1.8410	6.82	X	X		0.33
57	50.1525	0.24	71.	56.	1.8175	21.78	X	X		1.86
58	50.4150	0.12	26.	56.	1.8086	8.03	X	X		0.11
59	50.8400	0.08	10.	56.	1.7945	3.16	X	X		0.11
60	53.6325	0.12	16.	55.	1.7074	4.94	X	X		0.14
61	54.2725	0.12	19.	55.	1.6888	5.98	X	X		0.11
62	55.2800	0.08	30.	55.	1.6604	9.34	X	X		0.15
63	56.0000	0.08	16.	55.	1.6407	4.94	X	X		0.12
64	56.9150	0.32	19.	55.	1.6165	5.98	X	X		0.41
65	57.5900	0.12	21.	55.	1.5992	6.53	X	X		0.22
66	58.2000	0.12	16.	55.	1.5838	4.94	X	X		0.13
67	58.5050	0.12	28.	55.	1.5763	8.67	X	X		0.42
68	58.9325	0.12	21.	55.	1.5659	6.53	X	X		0.22
69	59.9300	0.16	52.	55.	1.5422	16.00	X	X		0.58
70	60.6025	0.16	28.	55.	1.5267	8.67	X	X		0.71
71	62.2800	0.08	48.	55.	1.4895	14.69	X	X		0.20
72	64.0175	0.24	14.	55.	1.4532	4.46	X	X		0.25
73	65.0400	0.08	83.	55.	1.4328	25.56	X			0.23
74	65.8500	0.24	10.	55.	1.4172	3.16	X	X		0.19
75	66.5525	0.24	10.	55.	1.4039	3.16	X	X		0.10
76	67.6625	0.12	26.	55.	1.3835	8.03	X	X		0.20

Table B10. Fly Ash Cured at 50°C for 90 Days.

Peak no	Angle (deg)	Tip width (deg)	Peak (cts)	Backg (cts)	D spac (Ang)	I/Imax (%)	Type A1	A2	Ot	Sign
1	2.8800	0.08	18.	44.	30.6517	4.55	X	X		0.10
2	4.0875	0.12	16.	44.	21.5991	4.12	X	X		0.27
3	5.5400	0.12	10.	44.	15.9390	2.64	X	X		0.45
4	6.0200	0.12	13.	44.	14.6692	3.34	X	X		0.32
5	6.9450	0.12	10.	44.	12.7173	2.64	X	X		0.24
6	7.1950	0.16	10.	44.	12.2760	2.64	X	X		0.37
7	7.5425	0.16	11.	44.	11.7112	2.81	X	X		0.49
8	8.0400	0.08	11.	44.	10.9876	2.81	X	X		0.12
9	9.1200	0.08	20.	44.	9.6887	5.22	X	X		0.16
10	9.7700	0.12	10.	44.	9.0455	2.64	X	X		0.11
11	10.8525	0.24	14.	44.	8.1456	3.72	X	X		0.11
12	11.3300	0.20	10.	44.	7.8033	2.64	X	X		0.13
13	11.6000	0.08	13.	44.	7.6223	3.34	X	X		0.12
14	12.7800	0.32	10.	44.	6.9210	2.64	X	X		0.33
15	13.4725	0.24	13.	44.	5.7222	3.34	X	X		0.25
16	17.4000	0.08	12.	45.	5.0924	3.16	X	X		0.11
17	17.6400	0.08	10.	45.	5.0237	2.64	X	X		0.17
18	18.3050	0.24	16.	45.	4.8426	4.12	X	X		0.18
19	19.0875	0.12	21.	45.	4.6458	5.45	X	X		0.23
20	19.4400	0.08	19.	45.	4.5624	4.99	X	X		0.16
21	20.1200	0.08	25.	45.	4.4097	6.44	X	X		0.12
22	20.8550	0.12	61.	46.	4.2559	15.68	X	X		0.49
23	21.5175	0.12	41.	46.	4.1263	10.55	X	X		0.24
24	21.8375	0.24	35.	46.	4.0666	8.97	X	X		0.12
25	23.5250	0.12	34.	46.	3.7786	8.67	X	X		0.25
26	23.8750	0.16	37.	48.	3.7240	9.59	X	X		0.23
27	24.5175	0.16	36.	48.	3.6278	9.28	X	X		0.18
28	25.0325	0.32	36.	48.	3.5543	9.28	X	X		0.23
29	25.6375	0.12	45.	48.	3.4718	11.57	X	X		0.10
30	26.6475	0.16	388.	48.	3.3425	100.00	X	X		4.57
31	28.0000	0.08	53.	49.	3.1840	13.73	X	X		0.11
32	28.6200	0.16	55.	49.	3.1164	14.11	X	X		0.32
33	29.6850	0.12	61.	49.	3.0070	15.68	X	X		0.12
34	30.0100	0.16	62.	49.	2.9752	16.08	X	X		0.40
35	31.1000	0.24	76.	50.	2.8733	19.50	X	X		0.26
36	31.9375	0.12	64.	50.	2.7999	16.49	X	X		0.17
37	32.4650	0.12	76.	50.	2.7556	19.50	X	X		0.13
38	33.2250	0.12	117.	50.	2.6943	30.05	X	X		0.22
39	33.4000	0.12	121.	50.	2.6805	31.18	X	X		0.12
40	33.9275	0.20	50.	50.	2.6401	12.99	X	X		0.13
41	34.4125	0.24	38.	52.	2.6040	9.90	X	X		0.14
42	35.6300	0.12	55.	52.	2.5177	14.11	X	X		0.25
43	36.5700	0.12	52.	52.	2.4551	13.36	X	X		0.42
44	36.8875	0.12	32.	52.	2.4347	8.37	X	X		0.17
45	37.4525	0.12	40.	52.	2.3993	10.23	X	X		0.25
46	37.9675	0.12	44.	53.	2.3679	11.22	X	X		0.20
47	38.3925	0.16	219.	53.	2.3427	56.44	X	X		2.38
48	39.3575	0.32	37.	53.	2.2874	9.59	X	X		0.74
49	40.2400	0.16	24.	53.	2.2393	6.19	X	X		0.11
50	40.9125	0.16	41.	53.	2.2040	10.55	X	X		0.27
51	41.4475	0.12	27.	53.	2.1768	6.97	X	X		0.33
52	42.3750	0.12	30.	55.	2.1313	7.79	X	X		0.11
53	42.9225	0.16	94.	55.	2.1053	24.24	X	X		1.55
54	43.4000	0.08	30.	55.	2.0833	7.79	X	X		0.14
55	43.8350	0.12	24.	55.	2.0636	6.19	X	X		0.11
56	44.5200	0.08	34.	55.	2.0334	8.67	X	X		0.12
57	45.7525	0.12	22.	56.	1.9815	5.69	X	X		0.13
58	47.6400	0.24	23.	56.	1.9073	5.94	X	X		0.11
59	48.4425	0.12	22.	56.	1.8775	5.69	X	X		0.18
60	48.7000	0.12	10.	56.	1.8682	2.64	X	X		0.17
61	50.1075	0.20	59.	58.	1.8190	15.28	X	X		1.51
62	51.6250	0.24	11.	58.	1.7690	2.81	X	X		0.19
63	52.4400	0.08	10.	58.	1.7434	2.64	X	X		0.11
64	52.9275	0.24	12.	58.	1.7285	3.16	X	X		0.35
65	53.4050	0.12	13.	59.	1.7142	3.34	X	X		0.12
66	53.8000	0.08	22.	53.	1.7025	5.69	X			0.12
67	54.0400	0.08	20.	53.	1.6955	5.22	X	X		0.10
68	54.4000	0.08	19.	53.	1.6852	4.99	X	X		0.16
69	54.8950	0.12	16.	59.	1.6711	4.12	X	X		0.10
70	55.6050	0.12	29.	59.	1.6515	7.51	X	X		0.29
71	56.6150	0.12	10.	59.	1.6244	2.64	X	X		0.19
72	57.8000	0.08	10.	61.	1.5939	2.64	X	X		0.11
73	59.1575	0.12	13.	61.	1.5605	3.34	X	X		0.17
74	59.7200	0.08	35.	59.	1.5471	8.97	X	X		0.11
75	62.2700	0.12	42.	62.	1.4897	10.89	X	X		0.27
76	63.9700	0.32	10.	61.	1.4542	2.64	X	X		0.26
77	64.9700	0.12	125.	59.	1.4342	32.32	X	X		0.74

Table B11. Fly Ash Cured at 50°C for 180 Days.

Peak no	Angle (deg)	Tip width (deg)	Peak (cts)	Backg (cts)	D spac (Ang)	I/Imax (%)	Type A1	Type A2	Type Ot	Sign
1	2.1050	0.20	74.	30.	41.9348	30.39	X	X		0.54
2	4.7350	0.20	10.	30.	18.4137	4.21	X	X		0.38
3	5.6450	0.12	10.	27.	15.6428	4.21	X	X		0.27
4	5.8800	0.08	12.	27.	15.0181	4.75	X	X		0.18
5	7.8650	0.48	11.	35.	11.2317	4.47	X	X		0.21
6	9.2175	0.24	12.	37.	9.5864	4.75	X	X		0.13
7	10.3100	0.12	17.	40.	8.5729	6.91	X	X		0.22
8	10.8475	0.24	25.	40.	8.1493	10.27	X	X		0.91
9	11.9825	0.20	15.	42.	7.3798	6.25	X	X		0.60
10	12.6975	0.32	10.	42.	6.9658	4.21	X	X		0.23
11	13.3125	0.12	12.	41.	6.6454	5.03	X	X		0.25
12	14.2575	0.24	10.	42.	6.2070	4.21	X	X		0.12
13	14.9600	0.08	10.	42.	5.9170	4.21	X	X		0.13
14	16.3350	0.12	13.	44.	5.4219	5.33	X	X		0.33
15	18.2150	0.12	121.	45.	4.8663	49.72	X	X		0.79
16	19.0925	0.12	10.	55.	4.6446	4.21	X	X		0.15
17	19.3600	0.08	10.	55.	4.5810	4.21	X	X		0.12
18	19.6000	0.08	10.	56.	4.5255	4.21	X	X		0.14
19	20.2025	0.24	10.	56.	4.3919	4.21	X	X		0.22
20	20.9700	0.24	48.	50.	4.2328	19.56	X	X		1.78
21	21.4575	0.12	17.	52.	4.1377	6.91	X	X		0.18
22	21.7500	0.12	27.	52.	4.0828	11.11	X	X		0.44
23	22.9475	0.24	10.	58.	3.8723	4.21	X	X		0.28
24	24.1600	0.16	11.	58.	3.6807	4.47	X	X		0.13
25	25.3850	0.12	15.	61.	3.5058	6.25	X	X		0.23
26	26.0950	0.16	22.	62.	3.4120	9.08	X	X		0.26
27	26.7150	0.16	188.	66.	3.3342	77.12	X	X		2.14
28	28.8025	0.20	72.	72.	3.0971	29.69	X	X		1.45
29	29.6650	0.12	17.	71.	3.0090	6.91	X	X		0.23
30	31.1550	0.12	48.	71.	2.8684	19.56	X	X		0.19
31	31.8100	0.12	29.	71.	2.8108	11.98	X	X		0.11
32	33.5750	0.16	94.	69.	2.6670	38.66	X	X		0.72
33	34.1750	0.24	243.	69.	2.6215	100.00	X	X		2.34
34	34.3450	0.12	210.	69.	2.6089	86.39	X	X		0.23
35	35.6000	0.32	16.	69.	2.5198	6.57	X	X		0.13
36	36.6025	0.24	26.	69.	2.4530	10.69	X	X		0.39
37	37.5775	0.12	12.	67.	2.3916	4.75	X	X		0.16
38	37.8800	0.12	10.	67.	2.3732	4.21	X	X		0.10
39	38.6400	0.08	32.	67.	2.3282	13.35	X	X		0.12
40	39.5050	0.24	10.	67.	2.2792	4.21	X	X		0.18
41	39.9300	0.12	10.	64.	2.2559	4.21	X	X		0.23
42	41.1025	0.12	19.	58.	2.1943	7.96	X	X		0.30
43	42.0800	0.08	10.	66.	2.1455	4.21	X	X		0.12
44	42.9925	0.16	76.	59.	2.1021	31.10	X	X		0.98
45	43.4750	0.12	12.	59.	2.0798	4.75	X	X		0.12
46	44.7325	0.12	10.	64.	2.0243	4.21	X	X		0.10
47	45.4775	0.12	10.	62.	1.9928	4.21	X	X		0.19
48	46.2225	0.12	12.	62.	1.9624	4.75	X	X		0.18
49	47.2000	0.16	108.	61.	1.9240	44.44	X	X		0.79
50	49.5275	0.12	10.	62.	1.8389	4.21	X	X		0.19
51	50.2250	0.16	40.	62.	1.8150	16.31	X	X		0.59
52	50.8350	0.16	128.	52.	1.7946	52.47	X	X		1.20
53	53.2300	0.12	14.	52.	1.7194	5.63	X	X		0.17
54	54.4275	0.12	66.	53.	1.6844	26.96	X	X		0.44
55	57.3100	0.12	10.	56.	1.6063	4.21	X	X		0.19
56	58.0400	0.08	12.	53.	1.5878	5.03	X	X		0.11
57	59.4500	0.12	36.	49.	1.5535	14.79	X	X		0.19
58	60.0475	0.12	23.	49.	1.5395	9.47	X	X		0.17
59	60.4850	0.12	12.	52.	1.5294	5.03	X	X		0.26
60	61.5900	0.12	10.	52.	1.5045	4.21	X	X		0.11
61	62.2950	0.12	45.	50.	1.4892	18.45	X			0.38
62	62.5500	0.48	48.	50.	1.4837	19.56	X	X		1.29
63	64.1350	0.32	29.	50.	1.4508	11.98	X	X		0.40
64	65.8575	0.12	10.	49.	1.4170	4.21	X	X		0.26
65	67.6000	0.08	21.	46.	1.3847	8.69	X	X		0.10
66	68.2100	0.40	21.	46.	1.3738	8.69	X	X		0.59
67	69.6400	0.03	10.	48.	1.3490	4.21	X	X		0.12

Table B12. Fly Ash-Lime Cured at 23°C for 1 Day.

Peak no	Angle (deg)	Tip width (deg)	Peak (cts)	Backg (cts)	D spac (Ang)	I/Imax (%)	Type A1	A2	Ot	Sign
1	2.2400	0.16	10.	64.	39.4077	3.27	X	X		0.11
2	2.6175	0.12	10.	64.	33.7251	3.27	X	X		0.14
3	2.7200	0.16	10.	61.	32.4544	3.27	X	X		0.14
4	4.1600	0.16	10.	34.	21.2229	3.27	X	X		0.10
5	4.5600	0.08	10.	34.	19.3621	3.27	X	X		0.17
6	4.6400	0.16	10.	34.	19.0294	3.27	X	X		0.15
7	6.4500	0.24	20.	37.	13.6921	6.46	X	X		0.35
8	6.8400	0.12	14.	44.	12.9123	4.61	X	X		0.15
9	7.3900	0.12	19.	46.	11.9525	6.18	X	X		0.22
10	8.2625	0.12	15.	49.	10.6922	4.85	X	X		0.30
11	8.9600	0.08	10.	53.	9.8614	3.27	X	X		0.11
12	9.4800	0.08	10.	55.	9.3216	3.27	X	X		0.13
13	10.5950	0.12	19.	55.	8.3430	6.18	X	X		0.16
14	10.9125	0.16	24.	52.	8.1009	7.66	X	X		0.19
15	11.7500	0.12	11.	55.	7.5253	3.48	X	X		0.27
16	12.4225	0.12	12.	52.	7.1194	3.91	X	X		0.40
17	13.6275	0.16	10.	49.	6.4925	3.27	X	X		0.41
18	15.6275	0.20	10.	50.	5.6658	3.27	X	X		0.28
19	15.9200	0.08	10.	48.	5.5623	3.27	X	X		0.12
20	16.9200	0.08	12.	48.	5.2358	3.69	X	X		0.10
21	18.1625	0.16	125.	52.	4.8803	40.04	X	X		1.23
22	19.6700	0.12	10.	62.	4.5095	3.27	X	X		0.14
23	19.9225	0.12	10.	62.	4.4530	3.27	X	X		0.20
24	20.2325	0.12	10.	62.	4.3854	3.27	X	X		0.12
25	20.9500	0.12	32.	59.	4.2368	10.37	X	X		0.33
26	21.7850	0.16	38.	56.	4.0763	12.27	X	X		0.51
27	22.3600	0.12	12.	62.	3.9727	3.69	X	X		0.10
28	22.5975	0.12	10.	64.	3.9315	3.27	X	X		0.11
29	22.8425	0.12	10.	64.	3.8899	3.27	X	X		0.14
30	23.4150	0.24	10.	64.	3.7961	3.27	X	X		0.22
31	24.8600	0.32	10.	64.	3.5786	3.27	X	X		0.40
32	25.9925	0.12	26.	61.	3.4252	8.30	X	X		0.30
33	26.7200	0.16	313.	67.	3.3336	100.00	X	X		3.72
34	28.7900	0.20	72.	69.	3.0984	23.06	X	X		1.17
35	30.1200	0.08	24.	67.	2.9646	7.66	X	X		0.13
36	31.1050	0.12	52.	67.	2.8729	16.55	X	X		0.28
37	32.4175	0.12	44.	66.	2.7595	13.90	X	X		0.32
38	33.3375	0.12	90.	66.	2.6854	28.91	X	X		0.44
39	34.1925	0.28	289.	64.	2.6202	92.25	X	X		5.01
40	35.3350	0.12	21.	64.	2.5381	6.75	X	X		0.17
41	35.6300	0.12	31.	64.	2.5177	10.01	X	X		0.19
42	37.5925	0.12	27.	61.	2.3907	8.63	X	X		0.28
43	38.4975	0.12	41.	61.	2.3365	13.07	X	X		0.28
44	39.3950	0.12	19.	59.	2.2853	6.18	X			0.10
45	39.5600	0.20	14.	59.	2.2313	4.37		X		0.40
46	40.8950	0.12	18.	59.	2.2049	5.90	X	X		0.15
47	42.9700	0.20	64.	58.	2.1031	20.43	X	X		1.32
48	44.2450	0.12	12.	56.	2.0454	3.31	X	X		0.20
49	44.7200	0.08	32.	58.	2.0248	10.37	X	X		0.15
50	47.1725	0.24	112.	61.	1.9251	35.86	X	X		2.00
51	47.6000	0.08	44.	61.	1.9088	13.90	X	X		0.10
52	48.9750	0.24	10.	59.	1.8584	3.27	X	X		0.17
53	49.4800	0.08	10.	59.	1.8406	3.27	X	X		0.12
54	50.1375	0.12	38.	58.	1.8180	12.27	X	X		0.28
55	50.8125	0.20	104.	58.	1.7954	33.21	X			1.51
56	50.9700	0.12	85.	58.	1.7902	27.02	X	X		0.11
57	52.6250	0.12	10.	56.	1.7377	3.27	X	X		0.34
58	53.4175	0.32	10.	55.	1.7138	3.27	X	X		0.22
59	54.3675	0.16	64.	53.	1.6861	20.43	X	X		0.49
60	57.0775	0.20	12.	53.	1.6123	3.91	X	X		0.52
61	57.5200	0.08	10.	53.	1.6009	3.27	X	X		0.14
62	58.3675	0.16	10.	53.	1.5797	3.27	X	X		0.25
63	59.2400	0.08	15.	52.	1.5585	4.85	X	X		0.18
64	59.9100	0.32	28.	49.	1.5427	8.97	X	X		0.85
65	60.6150	0.24	10.	50.	1.5264	3.27	X	X		0.11
66	61.0525	0.16	10.	50.	1.5165	3.27	X	X		0.15
67	62.3600	0.16	52.	50.	1.4878	16.55	X	X		0.35
68	63.9650	0.12	25.	49.	1.4543	7.98	X	X		0.11
69	64.5200	0.08	36.	49.	1.4431	11.49	X	X		0.13
70	65.0500	0.12	114.	49.	1.4326	36.54	X	X		1.02
71	66.4175	0.12	10.	48.	1.4064	3.27	X	X		0.11
72	66.8400	0.08	10.	48.	1.3985	3.27	X	X		0.10
73	67.5325	0.32	18.	42.	1.3859	5.90	X	X		0.30
74	68.2300	0.80	18.	42.	1.3734	5.90	X	X		1.26
75	69.8100	0.12	10.	46.	1.3461	3.27	X			0.22

Table B13. Fly Ash-Lime Cured at 23°C for 28 Days.

Peak no	Angle (deg)	Tip width (deg)	Peak (cts)	Backg (cts)	D spac (Ang)	I/Imax (%)	Type A1	Type A2	Type Ot	Sign
1	2.2350	0.20	59.	48.	39.4959	21.74	X	X		0.40
2	5.2400	0.12	10.	46.	16.8509	3.85	X	X		0.15
3	6.1475	0.24	10.	46.	14.3652	3.85	X	X		0.10
4	7.2000	0.16	12.	45.	12.2675	4.35	X	X		0.10
5	7.7750	0.24	16.	45.	11.3615	6.02	X	X		0.16
6	10.9800	0.32	13.	48.	8.0513	4.88	X	X		0.41
7	11.7575	0.12	14.	48.	7.5205	5.43	X	X		0.20
8	12.5200	0.08	11.	49.	7.0642	4.10	X	X		0.11
9	13.5600	0.08	10.	49.	6.5246	3.85	X	X		0.11
10	14.2875	0.24	10.	45.	6.1940	3.85	X	X		0.24
11	15.6575	0.24	10.	45.	5.6550	3.85	X	X		0.44
12	16.1825	0.24	10.	45.	5.4727	3.85	X	X		0.20
13	16.6650	0.24	11.	44.	5.3153	4.10	X	X		0.14
14	18.1600	0.16	100.	50.	4.8810	37.64	X	X		1.20
15	20.9475	0.16	48.	55.	4.2373	17.92	X	X		0.68
16	21.6575	0.12	26.	55.	4.1000	9.79	X	X		0.19
17	23.4400	0.16	22.	58.	3.7921	8.31	X	X		0.49
18	23.7600	0.08	13.	58.	3.7417	4.88	X	X		0.17
19	26.7025	0.12	188.	61.	3.3357	70.64	X	X		1.23
20	27.0800	0.08	20.	61.	3.2901	7.62	X	X		0.11
21	27.7150	0.12	20.	61.	3.2161	7.62	X	X		0.15
22	28.7600	0.08	74.	61.	3.1016	27.84	X	X		0.17
23	30.0400	0.08	38.	59.	2.9723	14.47	X	X		0.20
24	30.6800	0.08	30.	59.	2.9117	11.39	X	X		0.11
25	31.0400	0.08	66.	59.	2.8788	24.69	X	X		0.11
26	31.2525	0.24	79.	59.	2.8597	29.81	X	X		1.55
27	32.4350	0.12	53.	59.	2.7581	20.06	X	X		0.20
28	33.3675	0.12	98.	59.	2.6831	36.89	X	X		0.30
29	34.2000	0.24	266.	58.	2.6196	100.00	X	X		3.72
30	35.5625	0.12	44.	58.	2.5223	16.40	X	X		0.22
31	36.1700	0.16	36.	58.	2.4814	13.55	X	X		0.17
32	37.4225	0.12	29.	58.	2.4011	10.98	X			0.21
33	37.5200	0.16	27.	58.	2.3951	10.18	X	X		0.13
34	38.4975	0.20	222.	58.	2.3365	83.56	X	X		5.13
35	39.4075	0.12	30.	56.	2.2846	11.39	X	X		0.12
36	39.9200	0.08	18.	56.	2.2565	6.64	X	X		0.11
37	41.2400	0.08	18.	56.	2.1873	6.64	X	X		0.12
38	42.9625	0.16	86.	56.	2.1035	32.55	X	X		1.38
39	43.7800	0.24	17.	55.	2.0661	6.33	X	X		0.22
40	44.5900	0.16	48.	55.	2.0304	17.92	X			0.35
41	44.8000	0.08	50.	55.	2.0214	18.97	X	X		0.12
42	45.7825	0.16	26.	55.	1.9802	9.79	X	X		0.32
43	46.3925	0.12	25.	55.	1.9556	9.41	X	X		0.21
44	47.0850	0.12	94.	55.	1.9285	35.41	X			0.16
45	47.2400	0.16	110.	55.	1.9225	41.50	X	X		0.56
46	48.7100	0.16	20.	53.	1.8679	7.62	X	X		0.34
47	49.3000	0.12	18.	53.	1.8469	6.96	X	X		0.14
48	50.0875	0.16	56.	53.	1.8197	21.17	X	X		0.79
49	50.7850	0.24	96.	53.	1.7963	36.15	X			1.38
50	50.9725	0.16	98.	53.	1.7901	36.89	X	X		0.72
51	52.0075	0.12	12.	53.	1.7569	4.35	X	X		0.15
52	53.3175	0.40	14.	52.	1.7168	5.15	X	X		0.47
53	54.4050	0.28	55.	52.	1.6850	20.61	X	X		1.66
54	55.3600	0.08	46.	52.	1.6592	17.40	X	X		0.15
55	56.0575	0.12	19.	52.	1.6392	7.29	X	X		0.14
56	57.3500	0.16	12.	50.	1.6053	4.35	X	X		0.22
57	57.8950	0.12	10.	50.	1.5915	3.85	X	X		0.16
58	58.6625	0.16	12.	50.	1.5725	4.61	X	X		0.21
59	59.7600	0.08	37.	49.	1.5462	14.01	X			0.10
60	59.9850	0.12	37.	49.	1.5409	14.01	X	X		0.20
61	60.8400	0.08	11.	49.	1.5213	4.10	X	X		0.11
62	62.4800	0.08	46.	49.	1.4852	17.40	X			0.12
63	62.7775	0.32	36.	49.	1.4789	13.55	X	X		0.46
64	64.0625	0.12	29.	49.	1.4523	10.98	X	X		0.14
65	64.4300	0.24	34.	49.	1.4449	12.66	X	X		0.25
66	65.0475	0.12	108.	49.	1.4327	40.71	X			0.56
67	65.2800	0.08	59.	48.	1.4317	22.32		X		0.15
68	65.8025	0.12	14.	48.	1.4181	5.43	X	X		0.17
69	66.7050	0.12	10.	48.	1.4010	3.85	X	X		0.12
70	67.9325	0.12	30.	48.	1.3787	11.39	X	X		0.28
71	69.0800	0.08	10.	48.	1.3596	3.85	X	X		0.14

Table B14. Fly Ash-Lime Cured at 23°C for 90 Days.

Peak no	Angle (deg)	Tip width (deg)	Peak (cts)	Backg (cts)	D spac (Ang)	I/Imax (%)	Type A1	Type A2	Type Ot	Sign
1	3.5625	0.24	10.	125.	24.7809	4.74	X	X		0.19
2	4.6300	0.48	10.	62.	19.0695	4.74	X	X		0.12
3	5.9525	0.32	10.	55.	14.8354	4.74	X	X		0.21
4	7.1400	0.32	10.	52.	12.3704	4.74	X	X		0.26
5	8.6975	0.64	10.	53.	10.1584	4.74	X	X		0.21
6	10.0550	0.48	10.	52.	8.7898	4.74	X	X		0.30
7	10.8225	0.32	10.	50.	8.1681	4.74	X	X		0.16
8	12.2450	0.40	10.	52.	7.2222	4.74	X	X		0.17
9	14.7600	0.24	10.	49.	5.9968	4.74	X	X		0.11
10	16.1025	0.24	10.	49.	5.4997	4.74	X	X		0.12
11	18.0925	0.32	83.	53.	4.8990	38.32	X	X		1.35
12	19.1875	0.40	10.	58.	4.6218	4.74	X	X		0.15
13	20.2300	0.40	10.	59.	4.3860	4.74	X	X		0.25
14	20.8800	0.16	29.	59.	4.2509	13.49	X	X		0.11
15	21.4750	0.24	20.	62.	4.1344	9.37	X	X		0.17
16	23.3975	0.24	10.	66.	3.7989	4.74	X	X		0.16
17	25.1600	0.24	10.	66.	3.5366	4.74	X	X		0.14
18	26.6425	0.32	146.	67.	3.3431	67.75	X	X		3.16
19	28.7525	0.24	42.	76.	3.1024	19.55	X	X		0.37
20	30.2475	0.48	17.	76.	2.9523	7.78	X	X		0.54
21	31.1975	0.32	59.	74.	2.8646	27.44	X	X		0.89
22	32.4500	0.24	38.	74.	2.7568	17.79	X	X		0.17
23	33.3225	0.24	86.	72.	2.6866	40.02	X	X		0.54
24	34.1650	0.32	216.	72.	2.6222	100.00	X	X		2.34
25	35.6375	0.24	16.	71.	2.5172	7.40	X	X		0.14
26	36.5300	0.32	15.	69.	2.4577	7.04	X	X		0.12
27	37.4825	0.24	13.	69.	2.3974	6.00	X	X		0.19
28	38.4800	0.32	102.	67.	2.3375	47.21	X	X		2.45
29	39.3600	0.32	13.	66.	2.2873	6.00	X	X		0.39
30	40.1275	0.24	10.	66.	2.2453	4.74	X	X		0.12
31	40.7900	0.32	10.	64.	2.2103	4.74	X	X		0.33
32	42.9575	0.32	53.	62.	2.1037	24.66	X	X		1.45
33	44.6275	0.32	10.	66.	2.0288	4.74	X	X		0.25
34	47.1925	0.32	77.	69.	1.9243	35.84	X	X		0.93
35	48.9975	0.24	10.	67.	1.8576	4.74	X	X		0.13
36	50.0850	0.32	29.	66.	1.8197	13.49	X	X		0.68
37	50.8775	0.32	85.	64.	1.7932	39.17	X	X		1.58
38	54.3225	0.48	41.	59.	1.6874	18.96	X	X		1.20
39	55.3575	0.32	24.	59.	1.6583	11.11	X	X		0.42
40	58.7450	0.24	10.	58.	1.5704	4.74	X	X		0.11
41	59.6100	0.40	18.	56.	1.5497	8.56	X	X		0.39
42	62.3300	0.40	34.	53.	1.4885	15.57	X	X		0.74
43	62.7375	0.32	31.	53.	1.4798	14.51	X	X		0.25
44	64.2300	0.48	23.	52.	1.4489	10.66	X	X		0.51
45	65.0750	0.24	36.	52.	1.4321	16.66	X	X		0.35
46	65.8150	0.32	10.	52.	1.4178	4.74	X	X		0.10
47	67.7275	0.48	20.	50.	1.3824	9.37	X	X		0.76

Table B15. Fly Ash-Lime Cured at 23°C for 180 Days.

Peak no	Angle (deg)	Tip width (deg)	Peak (cts)	Backg (cts)	D spac (Ang)	I/Imax (%)	Type A1	Type A2	Type Ot	Sign
1	3.6000	0.08	10.	38.	24.5228	3.85	X	X		0.11
2	4.1450	0.40	10.	42.	21.2996	3.85	X	X		0.18
3	5.1475	0.16	10.	38.	17.1535	3.85	X	X		0.15
4	5.5200	0.08	10.	38.	15.9967	3.85	X	X		0.10
5	6.2525	0.12	10.	34.	14.1242	3.85	X	X		0.14
6	7.6700	0.12	22.	37.	11.5168	8.31	X	X		0.25
7	9.0925	0.12	16.	45.	9.7179	6.02	X	X		0.37
8	10.7850	0.12	26.	46.	8.1964	9.79	X	X		0.20
9	12.4675	0.12	10.	48.	7.0938	3.85	X	X		0.12
10	13.9125	0.12	10.	45.	6.3601	3.85	X	X		0.18
11	14.1200	0.08	10.	45.	6.2671	3.85	X	X		0.10
12	14.9425	0.12	10.	44.	5.9239	3.85	X	X		0.28
13	15.0400	0.16	10.	44.	5.8857	3.85	X	X		0.11
14	16.1600	0.08	12.	46.	5.4803	4.35	X	X		0.19
15	16.6125	0.12	12.	46.	5.3320	4.35	X	X		0.22
16	18.1775	0.12	96.	48.	4.8763	36.15	X	X		0.33
17	19.2625	0.12	10.	58.	4.6040	3.85	X	X		0.31
18	20.9225	0.24	26.	55.	4.2423	9.79	X	X		0.55
19	21.7925	0.12	27.	58.	4.0749	10.18	X	X		0.26
20	22.5225	0.16	12.	59.	3.9444	4.61	X	X		0.35
21	23.9950	0.12	13.	61.	3.7056	4.88	X	X		0.18
22	26.6800	0.16	199.	64.	3.3385	74.83	X	X		2.75
23	27.9600	0.08	23.	64.	3.1885	8.67	X	X		0.10
24	28.2000	0.08	23.	64.	3.1619	8.67	X	X		0.14
25	28.7300	0.12	71.	64.	3.1047	26.56	X			0.46
26	28.8500	0.12	64.	64.	3.0921	24.09	X	X		0.18
27	29.6500	0.12	27.	62.	3.0105	10.18	X	X		0.32
28	30.2900	0.32	20.	62.	2.9483	7.62	X	X		0.21
29	31.2250	0.40	44.	62.	2.8621	16.40	X	X		0.72
30	31.8625	0.12	46.	62.	2.8063	17.40	X	X		0.27
31	32.4275	0.12	71.	62.	2.7587	26.56	X	X		0.46
32	33.2750	0.16	86.	62.	2.6903	32.55	X	X		0.32
33	34.1400	0.24	266.	61.	2.6241	100.00	X	X		3.55
34	35.4700	0.24	29.	61.	2.5287	10.98	X	X		0.25
35	36.9950	0.16	22.	61.	2.4279	8.31	X	X		0.25
36	37.2000	0.32	14.	61.	2.4150	5.15	X	X		0.10
37	38.5200	0.16	55.	59.	2.3352	20.61	X	X		1.23
38	38.8775	0.20	11.	59.	2.3146	4.10	X	X		0.36
39	39.4700	0.24	20.	59.	2.2812	7.62	X	X		0.23
40	40.1600	0.08	24.	59.	2.2435	9.04	X	X		0.13
41	40.8500	0.12	28.	59.	2.2072	10.57	X	X		0.59
42	41.1375	0.12	14.	59.	2.1925	5.15	X	X		0.11
43	41.6775	0.16	10.	59.	2.1653	3.85	X	X		0.13
44	42.4475	0.24	15.	53.	2.1278	5.72	X	X		0.19
45	42.9475	0.16	74.	53.	2.1042	27.34	X	X		1.38
46	44.7125	0.16	46.	58.	2.0251	17.40	X	X		1.10
47	45.1725	0.20	12.	58.	2.0056	4.35	X	X		0.39
48	45.5200	0.08	15.	56.	1.9910	5.72	X	X		0.15
49	45.8200	0.32	14.	56.	1.9787	5.15	X	X		0.34
50	47.2125	0.32	94.	56.	1.9235	35.41	X	X		1.55
51	48.7575	0.12	13.	56.	1.8661	4.88	X	X		0.22
52	50.0800	0.16	41.	56.	1.8199	15.42	X	X		0.59
53	50.8225	0.20	102.	55.	1.7951	38.39	X	X		1.32
54	51.8150	0.12	14.	55.	1.7630	5.15	X	X		0.41
55	52.7900	0.24	10.	55.	1.7327	3.85	X	X		0.15
56	53.2000	0.08	12.	53.	1.7203	4.61	X	X		0.17
57	54.0325	0.16	24.	52.	1.6957	9.04	X	X		0.25
58	54.3150	0.16	58.	52.	1.6876	21.74	X	X		0.62
59	55.2200	0.16	20.	53.	1.6621	7.62	X	X		0.14
60	55.7475	0.24	15.	53.	1.6476	5.72	X	X		0.12
61	57.2800	0.08	10.	53.	1.6071	3.85	X	X		0.12
62	59.4250	0.24	24.	52.	1.5541	9.04	X	X		0.31
63	59.7950	0.16	27.	52.	1.5454	10.18	X	X		0.50
64	60.6250	0.16	11.	52.	1.5262	4.10	X	X		0.42
65	61.6625	0.12	10.	50.	1.5030	3.85	X			0.24
66	61.8800	0.08	10.	50.	1.4982	3.85	X	X		0.11
67	62.2650	0.12	44.	50.	1.4899	16.40	X	X		0.26
68	62.6650	0.24	42.	50.	1.4813	15.90	X	X		0.50
69	64.3600	0.08	41.	49.	1.4463	15.42	X	X		0.15
70	65.0175	0.12	106.	49.	1.4333	39.93	X	X		1.17
71	66.8075	0.24	10.	48.	1.3991	3.85	X	X		0.15
72	67.7700	0.12	24.	46.	1.3816	9.04	X	X		0.28
73	68.3425	0.32	21.	45.	1.3714	7.96	X	X		0.79
74	69.8075	0.12	10.	45.	1.3462	3.85	X			0.16

Table B16. Fly Ash-Lime Cured at 50°C for 1 Day.

Peak no	Angle (deg)	Tip width (deg)	Peak (cts)	Backg (cts)	D spac (nng)	I/Imax (%)	Type A1	A2	Ot	Sign
1	2.2850	0.40	15.	50.	39.6319	5.72	X	X		0.29
2	2.7200	0.08	10.	48.	32.4544	3.85	X	X		0.11
3	3.6725	0.16	10.	48.	24.0389	3.85	X	X		0.25
4	4.0725	0.12	10.	48.	21.6736	3.85	X	X		0.15
5	5.2250	0.24	10.	42.	16.3992	3.85	X	X		0.19
6	5.7125	0.16	14.	42.	15.4581	5.15	X	X		0.25
7	6.3375	0.24	11.	44.	13.9349	4.10	X	X		0.19
8	8.0050	0.12	16.	48.	11.0355	6.02	X	X		0.17
9	9.0900	0.12	18.	48.	9.7206	6.64	X	X		0.11
10	10.9975	0.12	25.	48.	8.0385	9.41	X	X		0.10
11	13.0800	0.16	12.	48.	6.7630	4.35	X	X		0.26
12	14.0000	0.16	10.	48.	6.3205	3.85	X	X		0.11
13	14.4825	0.40	10.	48.	6.1110	3.85	X	X		0.65
14	15.6375	0.24	10.	48.	5.6622	3.85	X	X		0.21
15	16.3200	0.08	12.	48.	5.4269	4.35	X	X		0.11
16	17.2800	0.12	10.	48.	5.1275	3.85	X	X		0.11
17	17.8400	0.08	49.	48.	4.9679	18.44	X	X		0.13
18	18.2175	0.24	77.	48.	4.8657	29.15	X	X		1.82
19	18.5325	0.12	31.	48.	4.7837	11.80	X	X		0.18
20	20.4650	0.24	25.	48.	4.3361	9.41	X	X		0.16
21	20.9325	0.16	66.	48.	4.2403	24.69	X	X		1.32
22	21.7850	0.24	32.	48.	4.0763	12.23	X	X		0.32
23	22.7650	0.12	17.	48.	3.9030	6.33	X	X		0.13
24	23.0550	0.32	25.	48.	3.8545	9.41	X	X		0.42
25	23.6275	0.12	18.	48.	3.7624	6.96	X	X		0.16
26	24.6775	0.12	22.	48.	3.6046	8.31	X	X		0.14
27	25.2425	0.12	18.	48.	3.5252	6.96	X	X		0.17
28	26.7000	0.12	266.	48.	3.3360	100.00	X	X		1.86
29	27.5250	0.12	44.	48.	3.2379	16.40	X	X		0.35
30	28.7625	0.16	85.	46.	3.1013	31.86	X	X		0.49
31	30.6750	0.12	44.	46.	2.9122	16.40	X	X		0.12
32	31.1200	0.08	79.	46.	2.8715	29.81	X	X		0.11
33	31.3775	0.12	61.	46.	2.8486	22.90	X	X		0.15
34	31.6400	0.08	49.	46.	2.8255	18.44	X	X		0.12
35	32.5750	0.40	76.	46.	2.7465	28.49	X	X		0.83
36	33.4250	0.12	106.	46.	2.6786	39.93	X	X		0.28
37	34.1725	0.20	253.	46.	2.6217	95.15	X	X		2.57
38	35.2800	0.08	49.	46.	2.5419	18.44	X	X		0.10
39	35.5325	0.12	55.	46.	2.5244	20.61	X	X		0.37
40	36.5450	0.12	46.	46.	2.4567	17.40	X	X		0.43
41	37.4050	0.48	31.	46.	2.4022	11.80	X	X		0.25
42	38.5250	0.20	66.	46.	2.3349	24.69	X	X		1.35
43	39.4725	0.16	42.	46.	2.2810	15.90	X	X		0.46
44	40.2825	0.16	36.	46.	2.2370	13.55	X	X		0.29
45	41.0000	0.08	28.	46.	2.1995	10.57	X	X		0.12
46	42.0675	0.16	23.	46.	2.1461	8.67	X	X		0.42
47	42.9625	0.16	79.	46.	2.1035	29.81	X	X		1.07
48	43.6400	0.08	19.	46.	2.0724	7.29	X	X		0.16
49	44.0725	0.12	21.	46.	2.0530	7.96	X	X		0.14
50	44.7450	0.12	50.	46.	2.0237	18.97	X	X		0.30
51	45.5200	0.08	31.	46.	1.9910	11.80	X	X		0.10
52	47.1325	0.12	106.	46.	1.9266	39.93	X			0.38
53	47.3650	0.12	77.	46.	1.9224	29.15		X		0.17
54	47.8800	0.08	34.	46.	1.8983	12.66	X	X		0.15
55	48.3825	0.12	25.	46.	1.8797	9.41	X	X		0.20
56	50.1050	0.16	52.	46.	1.8191	19.51	X	X		0.54
57	50.8525	0.24	100.	46.	1.7941	37.64	X	X		1.91
58	51.8750	0.12	23.	46.	1.7611	8.67	X	X		0.16
59	52.1625	0.16	20.	46.	1.7521	7.62	X	X		0.19
60	52.5150	0.12	12.	46.	1.7411	4.61	X	X		0.18
61	53.2425	0.12	18.	46.	1.7190	6.96	X	X		0.14
62	53.6875	0.12	31.	46.	1.7058	11.80	X	X		0.26
63	54.4600	0.12	58.	46.	1.6834	21.74	X	X		0.32
64	55.4525	0.12	46.	46.	1.6556	17.40	X	X		0.11
65	57.1200	0.16	17.	46.	1.6112	6.33	X	X		0.11
66	57.5200	0.08	17.	45.	1.6009	6.33	X	X		0.15
67	58.1725	0.24	11.	45.	1.5845	4.10	X	X		0.15
68	58.6750	0.12	14.	45.	1.5722	5.15	X	X		0.13
69	60.3600	0.08	17.	45.	1.5322	6.33	X			0.11
70	60.6125	0.12	25.	45.	1.5265	9.41	X	X		0.28
71	62.2800	0.08	55.	45.	1.4895	20.61	X	X		0.24
72	62.7150	0.32	49.	45.	1.4802	18.44	X	X		0.81
73	63.4500	0.12	11.	45.	1.4649	4.10	X	X		0.17
74	63.9525	0.32	17.	45.	1.4545	6.33	X	X		0.26
75	64.5250	0.12	34.	45.	1.4430	12.66	X	X		0.19

Table B17. Fly Ash-Lime Cured at 50°C for 28 Days.

Peak no	Angle (deg)	Tip width (deg)	Peak (cts)	Backg (cts)	D spac (Ang)	I/Imax (%)	Type A1	A2	Ot	Sign
1	2.2525	0.40	86.	44.	39.1891	37.44	X	X		0.41
2	4.8400	0.08	10.	44.	18.2426	4.43	X	X		0.13
3	5.8000	0.08	10.	40.	15.2251	4.43	X	X		0.13
4	6.1625	0.12	10.	40.	14.3303	4.43	X	X		0.12
5	6.6550	0.96	10.	40.	13.2708	4.43	X	X		0.35
6	7.9625	0.32	15.	42.	11.0944	6.58	X	X		0.28
7	8.6000	0.08	15.	44.	10.2733	6.58	X	X		0.13
8	9.6375	0.12	14.	45.	9.1696	5.93	X	X		0.23
9	9.8800	0.08	14.	45.	8.9451	5.93	X	X		0.12
10	10.6400	0.08	18.	45.	8.3078	7.64	X	X		0.15
11	11.6275	0.24	12.	45.	7.6043	5.00	X	X		0.18
12	14.4625	0.24	10.	45.	6.1194	4.43	X	X		0.11
13	16.5950	0.24	16.	41.	5.3376	6.93	X	X		0.22
14	18.1625	0.20	81.	44.	4.8803	35.06	X	X		1.26
15	18.7775	0.12	22.	45.	4.7218	9.56	X	X		0.32
16	20.9600	0.08	41.	53.	4.2348	17.73	X	X		0.13
17	21.8800	0.08	26.	53.	4.0588	11.26	X	X		0.14
18	22.6625	0.12	12.	56.	3.9204	5.00	X	X		0.23
19	23.3725	0.32	10.	58.	3.8029	4.43	X	X		0.17
20	24.5200	0.08	12.	59.	3.6274	5.00	X	X		0.13
21	24.9600	0.08	14.	59.	3.5645	6.25	X	X		0.12
22	26.7200	0.16	231.	62.	3.3336	100.00	X	X		3.72
23	27.2125	0.16	27.	66.	3.2743	11.70	X	X		0.47
24	28.0350	0.16	15.	72.	3.1801	6.58	X	X		0.25
25	28.8750	0.12	64.	72.	3.0895	27.70	X	X		0.21
26	31.1850	0.16	53.	81.	2.8657	23.07	X	X		0.52
27	32.6250	0.40	52.	81.	2.7424	22.44	X	X		1.02
28	33.3350	0.16	66.	81.	2.6856	28.40	X	X		0.54
29	33.5150	0.12	67.	79.	2.6716	29.10	X	X		0.17
30	34.2075	0.20	182.	79.	2.6191	78.88	X	X		1.74
31	35.6050	0.32	20.	77.	2.5194	8.76	X	X		0.43
32	36.2000	0.08	20.	77.	2.4794	8.76	X	X		0.14
33	37.2075	0.12	12.	77.	2.4145	5.00	X	X		0.26
34	37.5025	0.12	10.	76.	2.3962	4.43	X	X		0.26
35	38.5225	0.16	119.	74.	2.3351	51.42	X	X		1.91
36	39.5825	0.16	10.	74.	2.2749	4.43	X	X		0.43
37	40.8800	0.16	10.	69.	2.2057	4.43	X			0.22
38	41.0400	0.32	10.	69.	2.1974	4.43	X	X		0.11
39	42.5175	0.12	18.	69.	2.1244	7.64	X	X		0.13
40	42.9950	0.16	79.	62.	2.1019	34.28	X	X		1.38
41	44.2750	0.16	10.	71.	2.0441	4.43	X	X		0.39
42	44.5200	0.08	11.	71.	2.0334	4.71	X	X		0.12
43	44.7750	0.24	18.	71.	2.0224	8.00	X	X		0.33
44	45.1950	0.12	14.	69.	2.0046	5.93	X	X		0.18
45	45.4800	0.08	27.	69.	1.9927	11.70	X	X		0.10
46	46.6825	0.12	28.	69.	1.9441	12.16	X	X		0.20
47	47.2150	0.12	67.	67.	1.9234	29.10	X	X		0.15
48	48.5175	0.12	14.	67.	1.8748	6.25	X	X		0.17
49	49.4700	0.20	10.	66.	1.8409	4.43	X	X		0.37
50	50.1200	0.12	32.	66.	1.8186	14.06	X	X		0.16
51	50.9150	0.12	76.	59.	1.7920	32.76	X	X		0.19
52	51.3250	0.12	10.	64.	1.7787	4.43	X	X		0.16
53	52.7800	0.24	10.	62.	1.7330	4.43	X	X		0.16
54	53.3275	0.12	13.	61.	1.7165	5.61	X	X		0.10
55	54.3875	0.16	38.	56.	1.6855	16.64	X	X		0.15
56	55.0400	0.08	22.	61.	1.6671	9.56	X	X		0.11
57	55.5200	0.08	32.	61.	1.6538	14.06	X	X		0.11
58	56.8375	0.16	10.	59.	1.6185	4.43	X	X		0.12
59	57.5750	0.12	10.	58.	1.5995	4.43	X	X		0.12
60	59.9075	0.12	34.	56.	1.5427	14.56	X	X		0.16
61	61.3925	0.24	10.	53.	1.5089	4.43	X	X		0.15
62	62.2975	0.12	48.	52.	1.4892	20.61	X	X		0.44
63	62.7100	0.12	34.	52.	1.4803	14.56	X	X		0.11
64	63.1675	0.12	11.	52.	1.4707	4.71	X	X		0.11
65	63.9950	0.12	19.	50.	1.4537	8.38	X	X		0.11
66	64.3625	0.24	30.	49.	1.4463	13.09	X	X		0.41
67	65.0950	0.32	18.	49.	1.4318	7.64	X	X		0.44
68	67.7550	0.32	27.	44.	1.3819	11.70	X	X		0.31
69	68.1400	0.24	27.	44.	1.3750	11.70	X	X		0.12
70	69.5750	0.24	10.	44.	1.3501	4.43	X	X		0.24

Table B18. Fly Ash-Lime Cured at 50°C for 90 Days.

Peak no	Angle (deg)	Tip width (deg)	Peak (cts)	Backg (cts)	D spac (Ang)	I/Imax (%)	Type A1	Type A2	Type Ot	Sign
1	3.5200	0.16	10.	114.	25.0300	5.38	X	X		0.11
2	4.0000	0.16	10.	64.	22.0714	5.38	X	X		0.16
3	4.7275	0.32	10.	56.	18.6764	5.38	X	X		0.33
4	5.6050	0.12	10.	50.	15.7543	5.38	X	X		0.23
5	6.3450	0.24	10.	50.	13.9185	5.38	X	X		0.23
6	7.3075	0.12	14.	46.	12.0872	7.58	X	X		0.36
7	7.9050	0.12	13.	44.	11.1749	6.81	X	X		0.13
8	8.6275	0.12	10.	46.	10.2406	5.38	X	X		0.21
9	8.8400	0.08	10.	46.	9.9949	5.38	X	X		0.12
10	9.1000	0.12	10.	46.	9.7100	5.38	X	X		0.12
11	9.2375	0.16	10.	46.	9.5657	5.38	X	X		0.13
12	9.7300	0.24	10.	48.	9.0826	5.38	X	X		0.14
13	10.7450	0.48	10.	49.	8.2268	5.38	X	X		0.46
14	11.9200	0.08	18.	44.	7.4184	9.26	X	X		0.11
15	13.0325	0.12	10.	46.	6.7875	5.38	X	X		0.19
16	13.6750	0.12	10.	49.	6.4700	5.38	X	X		0.11
17	15.8750	0.12	12.	46.	5.5780	6.07	X	X		0.26
18	16.5075	0.12	18.	46.	5.3657	9.26	X	X		0.25
19	17.5300	0.12	23.	46.	5.0549	12.10	X	X		0.13
20	18.1850	0.16	64.	45.	4.8743	33.61	X	X		0.54
21	19.4800	0.08	17.	46.	4.5531	8.83	X	X		0.14
22	19.9600	0.08	14.	48.	4.4447	7.19	X	X		0.14
23	20.9325	0.24	30.	48.	4.2403	15.88	X	X		0.21
24	21.3700	0.12	30.	48.	4.1545	15.88	X	X		0.13
25	21.5600	0.08	28.	48.	4.1183	14.75	X	X		0.10
26	22.4800	0.08	19.	48.	3.9518	10.17	X	X		0.11
27	24.4550	0.12	18.	48.	3.6369	9.26	X	X		0.18
28	25.9750	0.12	31.	48.	3.4275	16.47	X	X		0.10
29	26.2900	0.12	32.	49.	3.3871	17.06	X	X		0.17
30	26.7200	0.16	185.	49.	3.3336	97.12	X	X		2.09
31	27.6725	0.12	25.	49.	3.2209	13.13	X	X		0.13
32	28.8100	0.16	71.	49.	3.0963	37.05	X	X		0.12
33	29.6950	0.12	45.	49.	3.0060	23.57	X	X		0.23
34	30.0125	0.12	44.	49.	2.9749	22.87	X	X		0.20
35	31.1775	0.12	92.	49.	2.8664	48.39	X	X		0.34
36	32.5950	0.16	85.	49.	2.7449	44.44	X	X		0.35
37	33.2950	0.20	92.	50.	2.6888	48.39	X	X		0.54
38	33.4900	0.16	92.	50.	2.6735	48.39	X	X		0.34
39	34.1600	0.24	190.	50.	2.6226	100.00	X	X		2.14
40	35.5925	0.24	49.	50.	2.5203	25.73	X	X		0.19
41	36.0250	0.12	40.	50.	2.4910	20.84	X	X		0.10
42	36.6525	0.12	48.	50.	2.4498	25.00	X	X		0.43
43	37.0800	0.08	40.	50.	2.4225	20.84	X	X		0.11
44	37.5300	0.12	30.	50.	2.3945	15.88	X	X		0.11
45	38.5675	0.16	59.	50.	2.3324	31.13	X	X		0.89
46	39.4450	0.12	35.	52.	2.2826	18.28	X	X		0.20
47	40.2300	0.32	31.	52.	2.2398	16.47	X	X		0.40
48	42.5525	0.12	29.	52.	2.1228	15.31	X	X		0.17
49	43.0100	0.20	83.	52.	2.1012	43.48	X	X		1.86
50	44.7300	0.24	27.	58.	2.0244	14.20	X	X		0.23
51	46.8400	0.08	32.	66.	1.9380	17.06	X	X		0.14
52	47.2950	0.12	58.	67.	1.9204	30.33	X	X		0.13
53	48.4225	0.12	10.	66.	1.8733	5.38	X	X		0.18
54	49.6225	0.16	10.	66.	1.8356	5.38	X	X		0.15
55	50.1375	0.12	42.	62.	1.8180	22.19	X	X		0.32
56	50.8400	0.08	64.	64.	1.7945	33.61	X	X		0.11
57	52.4550	0.12	10.	62.	1.7430	5.38	X	X		0.14
58	52.8700	0.12	10.	59.	1.7303	5.38	X	X		0.19
59	53.3275	0.12	14.	58.	1.7165	7.58	X	X		0.22
60	53.8400	0.12	21.	56.	1.7014	11.11	X	X		0.15
61	54.2850	0.12	40.	56.	1.6885	20.84	X	X		0.12
62	55.4875	0.24	30.	59.	1.6547	15.88	X	X		0.19
63	56.1375	0.16	20.	59.	1.6370	10.63	X	X		0.22
64	57.1250	0.24	10.	58.	1.6111	5.38	X	X		0.12
65	58.5025	0.12	10.	56.	1.5764	5.38	X	X		0.22
66	59.2000	0.12	14.	55.	1.5595	7.58	X	X		0.15
67	60.0275	0.16	23.	55.	1.5399	12.10	X	X		0.25
68	60.6850	0.12	11.	55.	1.5248	5.72	X	X		0.11
69	61.3800	0.08	10.	53.	1.4992	5.38	X	X		0.10
70	62.2850	0.12	29.	52.	1.4894	15.31	X	X		0.14
71	62.7675	0.24	26.	52.	1.4791	13.66	X	X		0.17
72	63.9025	0.12	22.	52.	1.4556	11.60	X	X		0.29
73	64.4800	0.08	20.	52.	1.4439	10.63	X	X		0.15
74	65.0800	0.08	90.	52.	1.4320	47.39	X			0.21
75	65.2800	0.08	40.	50.	1.4317	20.84		X		0.10

Table B19. Fly Ash-Lime Cured at 50°C for 180 Days.

Peak no	Angle (deg)	Tip Width (deg)	Peak (cts)	Backg (cts)	D spac (Ang)	I/Imax (%)	Type A1	A2	Ot	Sign
1	3.3150	0.12	17.	66.	23.1413	2.69	X	X		0.30
2	7.6800	0.08	37.	81.	11.5018	5.95	X	X		0.11
3	8.4400	0.08	35.	77.	10.4677	5.57	X	X		0.10
4	8.7125	0.12	29.	74.	10.1409	4.67	X	X		0.21
5	8.9600	0.08	64.	71.	9.8614	10.24	X	X		0.21
6	9.4550	0.12	13.	67.	9.3462	2.07	X	X		0.11
7	12.6275	0.32	10.	52.	7.0043	1.64	X	X		0.15
8	13.2000	0.08	10.	45.	6.7018	1.64	X	X		0.11
9	13.9825	0.24	10.	45.	6.3284	1.64	X	X		0.19
10	15.3925	0.12	12.	46.	5.7517	1.96	X	X		0.26
11	15.7600	0.08	10.	46.	5.6184	1.64	X	X		0.14
12	15.9600	0.08	10.	46.	5.5485	1.64	X	X		0.16
13	16.4525	0.24	10.	44.	5.3835	1.64	X	X		0.13
14	17.1675	0.32	14.	44.	5.1608	2.31	X	X		0.28
15	17.6450	0.12	14.	45.	5.0222	2.31	X	X		0.12
16	18.3250	0.96	25.	46.	4.8374	4.00	X	X		1.95
17	19.9175	0.24	269.	48.	4.4541	43.03	X	X		4.47
18	20.9875	0.12	180.	48.	4.2293	28.73	X	X		1.05
19	21.3600	0.08	71.	48.	4.1564	11.29	X	X		0.12
20	22.0875	0.12	62.	48.	4.0211	9.99	X	X		0.39
21	22.6400	0.08	42.	49.	3.9242	6.76	X	X		0.11
22	23.4800	0.08	77.	49.	3.7857	12.39	X	X		0.25
23	24.4875	0.16	53.	49.	3.6322	8.53	X	X		0.48
24	25.0400	0.08	49.	49.	3.5533	7.84	X	X		0.19
25	25.6575	0.32	50.	49.	3.4691	8.07	X	X		0.18
26	26.7225	0.16	625.	50.	3.3333	100.00	X	X		5.62
27	27.8700	0.12	243.	50.	3.1986	38.94	X	X		1.07
28	28.1200	0.08	231.	50.	3.1707	36.97	X	X		0.38
29	28.7125	0.12	88.	50.	3.1066	14.14	X			0.15
30	28.8000	0.16	81.	50.	3.0974	12.96	X	X		0.10
31	29.6125	0.16	142.	50.	3.0142	22.66	X	X		1.66
32	31.1675	0.32	29.	52.	2.8673	4.67	X	X		0.16
33	32.0050	0.16	77.	52.	2.7941	12.39	X	X		0.63
34	32.8050	0.12	18.	52.	2.7278	2.96	X	X		0.23
35	33.4325	0.16	42.	52.	2.6780	6.76	X	X		0.37
36	35.0750	0.12	130.	53.	2.5563	20.79	X	X		0.22
37	35.6000	0.16	137.	53.	2.5198	21.90	X	X		0.68
38	36.6525	0.16	132.	53.	2.4498	21.16	X	X		0.79
39	37.1850	0.12	74.	53.	2.4159	11.83	X	X		0.30
40	37.8800	0.08	52.	55.	2.3732	8.29	X	X		0.10
41	38.5725	0.12	53.	55.	2.3322	8.53	X	X		0.21
42	38.9175	0.20	45.	55.	2.3123	7.18	X	X		0.68
43	39.6000	0.20	64.	55.	2.2740	10.24	X	X		1.20
44	40.4075	0.20	50.	55.	2.2304	8.07	X	X		0.56
45	41.7050	0.12	50.	56.	2.1639	8.07	X	X		0.49
46	42.3150	0.12	67.	56.	2.1341	10.76	X			0.32
47	42.4800	0.32	55.	56.	2.1262	8.76	X	X		0.26
48	43.3375	0.24	42.	56.	2.0861	6.76	X	X		0.41
49	44.3350	0.12	18.	56.	2.0415	2.82	X	X		0.19
50	44.7925	0.12	44.	56.	2.0221	6.97	X	X		0.34
51	45.5875	0.12	20.	56.	1.9883	3.24	X	X		0.13
52	45.8800	0.08	29.	56.	1.9763	4.67	X	X		0.17
53	47.7100	0.32	18.	58.	1.9046	2.82	X	X		0.25
54	48.6875	0.24	18.	58.	1.8687	2.82	X	X		0.28
55	49.3000	0.24	10.	58.	1.8469	1.64	X	X		0.29
56	50.1325	0.12	74.	58.	1.8181	11.83	X	X		0.51
57	50.7200	0.08	10.	56.	1.7984	1.64	X			0.10
58	50.8950	0.24	13.	56.	1.7927	2.07	X	X		0.21
59	51.4750	0.24	10.	56.	1.7738	1.64	X	X		0.16
60	52.2825	0.16	13.	56.	1.7483	2.07	X	X		0.39
61	52.6100	0.16	14.	56.	1.7382	2.31	X	X		0.26
62	54.0500	0.24	64.	55.	1.6952	10.24	X	X		0.54
63	54.9275	0.24	44.	61.	1.6702	6.97	X	X		0.22
64	56.2525	0.12	13.	61.	1.6340	2.07	X	X		0.19
65	57.3050	0.24	20.	61.	1.6064	3.24	X	X		0.44
66	58.4250	0.12	21.	61.	1.5783	3.39	X	X		0.40
67	59.0675	0.12	10.	62.	1.5626	1.64	X	X		0.31
68	60.2300	0.12	18.	61.	1.5352	2.96	X	X		0.25
69	60.8525	0.32	13.	62.	1.5210	2.07	X	X		0.22
70	62.0150	0.16	172.	62.	1.4953	27.46	X	X		0.32
71	64.0500	0.12	14.	64.	1.4526	2.19	X	X		0.30
72	64.7600	0.08	21.	64.	1.4383	3.39	X			0.13
73	65.0525	0.12	100.	64.	1.4326	16.00	X	X		0.83
74	65.8225	0.24	10.	64.	1.4177	1.64	X	X		0.17
75	67.0700	0.12	10.	58.	1.3943	1.64	X			0.14
76	67.3300	0.16	19.	58.	1.3930	3.10		X		0.45
77	67.6300	0.16	38.	56.	1.3841	6.15	X	X		0.33
78	68.1550	0.12	64.	56.	1.3747	10.24	X	X		0.19

Table B20. Bentonite-Fly Ash Cured at 23°C for 1 Day.

Peak no	Angle (deg)	Tip width (deg)	Peak (cts)	Backg (cts)	D spac (Ang)	I/Imax (%)	Type A1	Type A2	Type Ot	Sign
1	2.0725	0.12	28.	46.	42.5923	4.60	X	X		0.18
2	3.0800	0.48	24.	46.	28.6618	3.94	X	X		0.19
3	5.0700	0.12	50.	46.	17.4155	8.26	X	X		0.23
4	6.0525	0.32	77.	46.	14.5905	12.69	X	X		0.28
5	6.8325	0.24	92.	46.	12.9265	15.11	X	X		0.23
6	7.3600	0.08	96.	46.	12.0011	15.74	X	X		0.11
7	8.9825	0.24	31.	46.	9.8367	5.14	X	X		0.17
8	9.8450	0.12	16.	46.	8.9768	2.62	X	X		0.21
9	11.4500	0.12	10.	46.	7.7213	1.63	X	X		0.17
10	13.8400	0.08	52.	46.	6.3933	8.50	X	X		0.23
11	15.3250	0.12	12.	46.	5.7769	2.01	X	X		0.24
12	17.7850	0.12	17.	48.	4.9830	2.76	X	X		0.10
13	18.1675	0.40	20.	50.	4.8790	3.32	X	X		0.54
14	19.8750	0.16	269.	58.	4.4635	44.09	X	X		2.09
15	20.9475	0.12	139.	59.	4.2373	22.82	X	X		0.69
16	22.0400	0.16	37.	71.	4.0297	6.10	X	X		0.45
17	23.1250	0.32	15.	77.	3.8430	2.49	X	X		0.21
18	23.7600	0.16	17.	79.	3.7417	2.76	X	X		0.12
19	24.1650	0.16	14.	83.	3.6799	2.37	X	X		0.25
20	24.8075	0.12	13.	83.	3.5861	2.12	X	X		0.26
21	25.8750	0.12	30.	86.	3.4405	4.96	X	X		0.29
22	26.1550	0.12	18.	86.	3.4043	2.89	X	X		0.13
23	26.7200	0.16	610.	86.	3.3336	100.00	X	X		6.46
24	27.1800	0.12	182.	86.	3.2782	29.87	X	X		2.24
25	28.6175	0.48	64.	92.	3.1167	10.49	X	X		1.29
26	29.5500	0.20	58.	110.	3.0204	9.47	X	X		1.32
27	29.9975	0.16	10.	114.	2.9764	1.63	X	X		0.18
28	30.5975	0.16	10.	100.	2.9194	1.68	X	X		0.26
29	31.4725	0.16	15.	81.	2.8402	2.49	X	X		0.23
30	31.9975	0.20	34.	81.	2.7948	5.51	X	X		0.39
31	32.6325	0.12	10.	79.	2.7418	1.68	X	X		0.17
32	33.3300	0.12	17.	79.	2.6860	2.76	X	X		0.12
33	34.8650	0.48	108.	71.	2.5712	17.73	X	X		2.45
34	36.8700	0.24	10.	154.	2.4358	1.68	X	X		0.15
35	37.9625	0.16	10.	151.	2.3682	1.68	X	X		0.12
36	38.4950	0.12	18.	119.	2.3367	3.03	X	X		0.41
37	39.0175	0.16	10.	104.	2.3066	1.68	X	X		0.46
38	39.5150	0.16	49.	88.	2.2797	8.03	X	X		0.95
39	40.2300	0.32	21.	79.	2.2398	3.47	X	X		0.65
40	41.0400	0.08	15.	79.	2.1974	2.49	X	X		0.13
41	41.3475	0.12	10.	76.	2.1818	1.68	X	X		0.16
42	42.4600	0.24	28.	76.	2.1272	4.60	X	X		0.25
43	42.8950	0.12	30.	72.	2.1071	4.96	X	X		0.26
44	44.0000	0.16	10.	72.	2.0562	1.68	X	X		0.10
45	44.7450	0.16	26.	72.	2.0237	4.26	X	X		0.76
46	45.4800	0.08	10.	66.	1.9927	1.68	X	X		0.11
47	45.7200	0.08	21.	66.	1.9828	3.47	X	X		0.11
48	47.1200	0.08	13.	59.	1.9271	2.12	X	X		0.17
49	47.7600	0.08	35.	59.	1.9028	5.71	X	X		0.13
50	48.8400	0.08	12.	59.	1.8632	1.89	X	X		0.12
51	49.1525	0.12	10.	59.	1.8521	1.68	X	X		0.15
52	50.1075	0.16	85.	59.	1.8190	13.87	X	X		0.91
53	52.3100	0.32	19.	50.	1.7475	3.17	X	X		0.47
54	54.3600	0.08	61.	59.	1.6863	9.97	X	X		0.13
55	54.9000	0.16	52.	59.	1.6710	8.50	X	X		0.35
56	55.2725	0.16	42.	59.	1.6606	6.93	X	X		0.17
57	57.6800	0.32	10.	66.	1.5969	1.68	X	X		0.10
58	60.1050	0.12	31.	59.	1.5381	5.14	X	X		0.25
59	60.4875	0.12	18.	59.	1.5293	3.03	X	X		0.19
60	61.7525	0.12	135.	61.	1.5010	22.06	X			0.12
61	61.9150	0.20	185.	61.	1.4974	30.32	X	X		1.17
62	63.0000	0.08	48.	62.	1.4742	7.80	X	X		0.21
63	65.0150	0.12	104.	64.	1.4333	17.05	X	X		1.10
64	65.7200	0.08	12.	66.	1.4196	2.01	X	X		0.12
65	66.2625	0.12	10.	64.	1.4093	1.68	X	X		0.14
66	67.6000	0.16	29.	58.	1.3847	4.78	X	X		0.11
67	68.0850	0.20	53.	59.	1.3760	8.73	X	X		0.49
68	69.6400	0.08	13.	59.	1.3490	2.12	X			0.13
69	69.9050	0.12	10.	59.	1.3445	1.68	X	X		0.27

Table B21. Bentonite-Fly Ash Cured at 23°C for 28 Days.

Peak no	Angle (deg)	Tip width (deg)	Peak (cts)	Backg (cts)	D spac (Ang)	I Imax (%)	Type A1	A2	Ot	Sign
1	2.4350	0.24	29.	53.	36.2523	4.28	X	X		0.15
2	3.2800	0.08	26.	53.	26.9146	4.52	X	X		0.21
3	4.1125	0.40	12.	53.	21.4679	2.13	X	X		0.60
4	4.7125	0.12	15.	53.	18.7358	2.64	X	X		0.32
5	5.3750	0.16	20.	53.	16.4279	3.52	X	X		0.15
6	6.3600	0.80	38.	53.	13.9857	6.67	X	X		0.43
7	7.9400	0.12	61.	53.	11.1257	10.56	X	X		0.14
8	8.9850	0.16	49.	53.	9.8340	8.51	X	X		0.30
9	11.0400	0.08	10.	53.	8.0076	1.78	X	X		0.12
10	11.2800	0.08	10.	53.	7.8378	1.78	X	X		0.10
11	12.2875	0.24	10.	53.	7.1973	1.78	X	X		0.14
12	13.8725	0.24	10.	50.	6.3784	1.78	X	X		0.19
13	14.6250	0.16	14.	50.	6.0518	2.38	X	X		0.54
14	14.9950	0.12	10.	50.	5.9033	1.78	X	X		0.10
15	15.5575	0.12	16.	46.	5.6911	2.78	X	X		0.15
16	16.3075	0.24	10.	48.	5.4310	1.78	X	X		0.11
17	17.5275	0.12	18.	48.	5.0556	3.06	X	X		0.11
18	18.4275	0.32	29.	49.	4.8107	4.88	X	X		0.43
19	19.8550	0.20	266.	53.	4.4679	46.13	X	X		3.80
20	20.9300	0.16	135.	53.	4.2408	23.36	X	X		1.07
21	21.6000	0.08	53.	53.	4.1108	9.25	X	X		0.10
22	22.0800	0.08	55.	53.	4.0225	9.51	X	X		0.17
23	22.7650	0.12	42.	53.	3.9030	7.34	X	X		0.22
24	23.3025	0.12	42.	53.	3.8141	7.34	X	X		0.15
25	23.6800	0.16	41.	53.	3.7542	7.11	X	X		0.11
26	24.0800	0.08	38.	53.	3.6927	6.67	X	X		0.11
27	24.7075	0.32	38.	53.	3.6003	6.67	X	X		0.35
28	25.5875	0.16	64.	53.	3.4785	11.11	X	X		0.18
29	26.6800	0.16	576.	53.	3.3385	100.00	X	X		5.25
30	27.7075	0.12	210.	53.	3.2170	36.50	X	X		1.26
31	28.0400	0.08	256.	53.	3.1796	44.44	X	X		0.43
32	28.4800	0.16	92.	53.	3.1314	16.00	X	X		0.10
33	29.5425	0.16	135.	53.	3.0212	23.36	X	X		1.29
34	30.3850	0.12	41.	53.	2.9393	7.11	X	X		0.22
35	31.0400	0.08	35.	53.	2.8788	6.04	X	X		0.15
36	31.7525	0.12	41.	53.	2.8158	7.11	X	X		0.17
37	31.9950	0.12	64.	53.	2.7950	11.11	X	X		0.27
38	33.3700	0.12	42.	53.	2.6829	7.34	X	X		0.22
39	33.8950	0.20	20.	53.	2.6425	3.52	X			0.45
40	34.0225	0.24	20.	53.	2.6329	3.52	X	X		0.14
41	34.6500	0.12	72.	53.	2.5866	12.54	X	X		0.31
42	34.9425	0.20	135.	53.	2.5657	23.36	X	X		0.74
43	35.3725	0.32	135.	53.	2.5354	23.36	X	X		0.49
44	36.5900	0.20	137.	53.	2.4538	23.77	X	X		0.91
45	38.5325	0.24	86.	53.	2.3345	15.02	X	X		2.14
46	39.5200	0.16	88.	53.	2.2784	15.34	X	X		1.41
47	40.3425	0.12	49.	53.	2.2338	8.51	X	X		0.17
48	40.6300	0.12	45.	53.	2.2187	7.79	X	X		0.32
49	41.7150	0.16	50.	53.	2.1634	8.75	X	X		0.39
50	42.5250	0.20	53.	53.	2.1241	9.25	X	X		0.62
51	43.3125	0.12	37.	53.	2.0873	6.46	X			0.10
52	43.4175	0.12	35.	53.	2.0825	6.04	X	X		0.11
53	44.2000	0.08	28.	53.	2.0474	4.88	X	X		0.10
54	44.7300	0.12	55.	53.	2.0244	9.51	X	X		0.46
55	45.7975	0.24	28.	53.	1.9796	4.88	X	X		0.21
56	46.8775	0.12	18.	53.	1.9365	3.06	X	X		0.17
57	47.4800	0.08	31.	53.	1.9133	5.44	X			0.11
58	47.6900	0.12	31.	53.	1.9054	5.44	X	X		0.32
59	49.3400	0.24	18.	53.	1.8455	3.06	X	X		0.30
60	49.8000	0.08	34.	53.	1.8295	5.84	X	X		0.19
61	50.1150	0.12	66.	53.	1.8187	11.39	X	X		0.29
62	51.0225	0.48	10.	53.	1.7885	1.78	X	X		0.74
63	51.5525	0.16	10.	53.	1.7713	1.78	X	X		0.35
64	51.8750	0.16	10.	53.	1.7611	1.78	X	X		0.25
65	52.6675	0.12	20.	50.	1.7364	3.52	X	X		0.12
66	53.1425	0.24	14.	50.	1.7220	2.38	X	X		0.10
67	54.0450	0.32	74.	53.	1.6954	12.84	X	X		1.91
68	54.8725	0.16	74.	53.	1.6718	12.84	X	X		0.74
69	55.6200	0.12	37.	53.	1.6510	6.46	X	X		0.20
70	56.4800	0.08	22.	53.	1.6279	3.84	X	X		0.14
71	57.4825	0.24	20.	53.	1.6019	3.52	X	X		0.18
72	58.6450	0.12	18.	53.	1.5729	3.06	X	X		0.19
73	59.4575	0.12	26.	53.	1.5533	4.52	X	X		0.13
74	59.8900	0.16	83.	53.	1.5431	14.39	X	X		1.10
75	60.9300	0.24	29.	53.	1.5193	5.06	X	X		0.21
76	61.8050	0.16	172.	53.	1.4998	29.79	X			0.76
77	61.9500	0.12	169.	53.	1.4967	29.34	X	X		0.20

Table B22. Bentonite-Fly Ash Cured at 23°C for 90 Days.

Peak no	Angle (deg)	Tip width (deg)	Peak (cts)	Backg (cts)	D spac (Ang)	I Imax (%)	Type K1	Type K2	Type Ot	Sign
1	4.2650	0.24	10.	66.	20.7006	2.04	X	X		0.19
2	4.7600	0.08	17.	66.	18.5490	3.35	X	X		0.15
3	6.3275	0.40	66.	67.	13.9569	13.08	X	X		0.38
4	7.3125	0.16	56.	67.	12.0790	11.21	X	X		0.29
5	8.9325	0.12	10.	69.	9.8916	2.04	X	X		0.25
6	10.0050	0.12	10.	62.	8.8336	2.04	X	X		0.14
7	10.4800	0.08	10.	50.	8.4342	2.04	X	X		0.14
8	11.0400	0.08	13.	46.	8.0076	2.53	X	X		0.15
9	12.1225	0.24	10.	48.	7.2949	2.04	X	X		0.14
10	13.7600	0.08	10.	45.	6.4302	2.04	X	X		0.11
11	14.8000	0.08	11.	44.	5.9806	2.17	X	X		0.12
12	16.1125	0.24	10.	46.	5.4963	2.04	X	X		0.11
13	18.0800	0.16	14.	49.	4.9024	2.73	X	X		0.11
14	19.8775	0.16	243.	52.	4.4629	48.50	X	X		1.78
15	20.9675	0.16	112.	67.	4.2333	22.39	X	X		0.72
16	23.1450	0.32	15.	79.	3.8397	3.03	X	X		0.32
17	23.7250	0.16	36.	79.	3.7472	7.17	X	X		0.63
18	24.1900	0.12	18.	79.	3.6762	3.52	X	X		0.21
19	24.7400	0.16	28.	77.	3.5957	5.60	X	X		0.42
20	25.5200	0.08	27.	77.	3.4875	5.39	X	X		0.19
21	25.8375	0.12	31.	77.	3.4454	6.25	X	X		0.17
22	26.7225	0.16	502.	76.	3.3333	100.00	X	X		4.90
23	27.2400	0.08	49.	76.	3.2711	9.77	X	X		0.14
24	27.7750	0.20	66.	76.	3.2093	13.08	X	X		1.05
25	28.1500	0.12	81.	76.	3.1674	16.14	X	X		0.24
26	28.6750	0.12	92.	74.	3.1106	18.37	X	X		0.14
27	28.9550	0.16	81.	74.	3.0811	16.14	X	X		0.21
28	29.5850	0.12	139.	74.	3.0169	27.75	X	X		0.79
29	30.1800	0.12	26.	74.	2.9588	5.18	X	X		0.14
30	32.0525	0.12	56.	72.	2.7901	11.21	X	X		0.45
31	32.4800	0.16	15.	72.	2.7543	3.03	X	X		0.11
32	32.9375	0.12	10.	72.	2.7171	2.04	X	X		0.15
33	33.4400	0.08	25.	71.	2.6774	4.98	X	X		0.13
34	34.0550	0.12	10.	71.	2.6305	2.04	X	X		0.22
35	35.0050	0.24	130.	69.	2.5612	25.90	X	X		1.35
36	35.9950	0.16	98.	69.	2.4930	19.53	X	X		0.13
37	36.6150	0.16	117.	69.	2.4522	23.25	X	X		0.63
38	37.6825	0.16	50.	67.	2.3852	10.05	X	X		0.27
39	38.5025	0.20	130.	67.	2.3362	25.90	X	X		2.92
40	39.5800	0.20	71.	66.	2.2751	14.06	X	X		1.29
41	40.3700	0.24	36.	66.	2.2324	7.17	X	X		0.23
42	42.1200	0.08	24.	64.	2.1436	4.79	X	X		0.11
43	42.4750	0.20	50.	64.	2.1265	10.05	X	X		0.93
44	42.9675	0.12	41.	64.	2.1032	8.16	X	X		0.25
45	43.3175	0.48	31.	62.	2.0870	6.25	X	X		0.19
46	44.7200	0.08	34.	62.	2.0248	6.70	X	X		0.19
47	44.9600	0.08	18.	61.	2.0145	3.52	X	X		0.15
48	45.6075	0.12	37.	61.	1.9874	7.42	X	X		0.21
49	47.7025	0.20	23.	59.	1.9049	4.59	X	X		0.40
50	48.7200	0.12	29.	59.	1.8675	5.81	X	X		0.15
51	50.0400	0.08	45.	59.	1.8213	8.95	X			0.10
52	50.1850	0.20	74.	59.	1.8164	14.74	X	X		1.74
53	50.9250	0.24	17.	59.	1.7917	3.35	X	X		0.36
54	51.5300	0.12	10.	59.	1.7721	2.04	X	X		0.25
55	51.8350	0.12	10.	59.	1.7623	2.04	X			0.17
56	52.0800	0.08	10.	59.	1.7546	2.04	X	X		0.16
57	53.1275	0.12	19.	53.	1.7225	3.86	X	X		0.15
58	54.0325	0.24	66.	55.	1.6957	13.08	X	X		0.46
59	54.8550	0.16	58.	58.	1.6722	11.51	X	X		0.39
60	55.1550	0.12	44.	58.	1.6639	8.68	X	X		0.14
61	55.5300	0.24	36.	58.	1.6535	7.17	X	X		0.76
62	56.1750	0.24	19.	58.	1.6360	3.86	X	X		0.14
63	57.5850	0.24	19.	58.	1.5993	3.86	X	X		0.21
64	58.8100	0.12	14.	58.	1.5689	2.88	X	X		0.13
65	59.9450	0.12	61.	58.	1.5418	12.13	X	X		0.46
66	60.6300	0.12	21.	58.	1.5261	4.22	X			0.12
67	60.9450	0.12	23.	58.	1.5212	4.59	X	X		0.12
68	61.8800	0.32	172.	58.	1.4982	34.20	X	X		3.31
69	63.3875	0.40	15.	58.	1.4661	3.03	X	X		0.44
70	64.0375	0.12	24.	58.	1.4528	4.79	X	X		0.11
71	65.0350	0.12	45.	58.	1.4329	8.95	X	X		0.28
72	65.7325	0.12	18.	56.	1.4194	3.69	X	X		0.33
73	66.3000	0.16	10.	56.	1.3993	2.04	X	X		0.12
74	67.7600	0.32	48.	56.	1.3818	9.49	X			0.47
75	68.0875	0.32	49.	56.	1.3759	9.77	X	X		0.36
76	69.3725	0.12	10.	56.	1.3535	2.04	X	X		0.19

Table B23. Bentonite-Fly Ash Cured at 23°C for 180 Days.

Peak no	Angle (deg)	Tip width (deg)	Peak (cts)	Backg (cts)	D spac (Ang)	I/Imax (%)	Type A1	A2	Dt	Sign
1	2.3525	0.12	10.	71.	37.5234	2.04	X	X		0.14
2	2.6700	0.12	10.	71.	33.0621	2.04	X	X		0.20
3	3.1850	0.12	10.	69.	27.7171	2.04	X	X		0.23
4	4.0400	0.08	10.	62.	21.8530	2.04	X	X		0.11
5	4.8175	0.16	16.	59.	18.3277	3.19	X	X		0.33
6	5.4875	0.12	25.	59.	16.0914	4.98	X	X		0.28
7	6.7375	0.12	36.	66.	13.1085	7.17	X	X		0.19
8	7.2250	0.12	45.	66.	12.2251	8.95	X	X		0.15
9	7.7200	0.16	50.	66.	11.4423	10.05	X	X		0.21
10	8.9850	0.12	41.	66.	9.8340	8.16	X	X		0.15
11	9.2925	0.12	28.	66.	9.5092	5.60	X	X		0.27
12	9.7675	0.12	10.	66.	9.0478	2.04	X	X		0.16
13	11.0000	0.08	10.	62.	8.0367	2.04	X	X		0.17
14	12.7825	0.24	10.	49.	6.9197	2.04	X	X		0.13
15	13.9850	0.32	10.	48.	6.3273	2.04	X	X		0.27
16	15.1775	0.24	10.	46.	5.8327	2.04	X	X		0.12
17	15.8825	0.32	10.	50.	5.5754	2.04	X	X		0.27
18	16.5125	0.24	10.	50.	5.3641	2.04	X	X		0.28
19	17.0325	0.12	10.	48.	5.2014	2.04	X	X		0.15
20	18.4375	0.32	28.	48.	4.8081	5.60	X	X		0.20
21	19.8950	0.20	246.	66.	4.4590	49.13	X	X		3.39
22	20.9875	0.12	154.	66.	4.2293	30.64	X	X		0.74
23	21.3375	0.12	100.	66.	4.1607	19.93	X	X		0.74
24	22.0800	0.16	30.	66.	4.0225	6.03	X	X		0.10
25	23.8550	0.12	110.	66.	3.7270	21.97	X	X		1.26
26	24.8000	0.08	32.	66.	3.5871	6.48	X	X		0.11
27	25.1650	0.16	27.	66.	3.5359	5.39	X	X		0.17
28	25.6950	0.40	46.	66.	3.4642	9.22	X	X		1.12
29	26.7200	0.16	502.	66.	3.3336	100.00	X	X		4.90
30	27.5200	0.08	100.	66.	3.2384	19.93	X	X		0.14
31	27.7925	0.12	94.	66.	3.2073	18.75	X	X		0.19
32	28.0400	0.08	110.	66.	3.1796	21.97	X	X		0.12
33	28.6775	0.12	71.	66.	3.1103	14.06	X	X		0.11
34	29.0400	0.08	58.	66.	3.0723	11.51	X	X		0.15
35	29.5950	0.16	106.	66.	3.0159	21.14	X	X		0.85
36	30.8675	0.12	25.	66.	2.8944	4.98	X	X		0.26
37	32.0750	0.12	45.	66.	2.7882	8.95	X	X		0.10
38	33.2150	0.12	21.	66.	2.6950	4.22	X	X		0.27
39	34.0775	0.20	10.	66.	2.6288	2.04	X	X		0.34
40	35.2000	0.08	132.	64.	2.5475	26.36	X	X		0.13
41	35.5475	0.12	119.	64.	2.5234	23.69	X	X		0.17
42	36.1525	0.12	104.	66.	2.4825	20.74	X	X		0.29
43	36.6400	0.08	106.	66.	2.4506	21.14	X	X		0.11
44	38.5075	0.12	69.	66.	2.3359	13.73	X	X		0.55
45	39.5350	0.16	62.	66.	2.2776	12.44	X	X		0.74
46	40.4000	0.08	45.	66.	2.2308	8.95	X	X		0.11
47	41.0150	0.12	36.	66.	2.1987	7.17	X	X		0.35
48	41.6025	0.12	67.	66.	2.1690	13.40	X	X		0.11
49	42.5400	0.16	71.	66.	2.1234	14.06	X	X		0.72
50	42.9550	0.16	42.	66.	2.1038	8.42	X	X		0.47
51	44.1075	0.12	14.	66.	2.0515	2.73	X	X		0.14
52	44.7775	0.12	36.	66.	2.0223	7.17	X	X		0.37
53	45.4400	0.08	12.	66.	1.9944	2.30	X	X		0.11
54	45.8700	0.24	10.	66.	1.9767	2.04	X	X		0.17
55	46.6600	0.24	10.	66.	1.9450	2.04	X	X		0.17
56	47.2700	0.12	10.	62.	1.9213	2.04	X	X		0.17
57	47.6225	0.24	17.	64.	1.9079	3.35	X	X		0.28
58	48.6900	0.24	10.	64.	1.8686	2.04	X	X		0.16
59	49.1975	0.12	23.	59.	1.8505	4.59	X			0.15
60	49.3600	0.08	10.	66.	1.8493	2.04		X		0.10
61	50.1325	0.20	83.	59.	1.8181	16.50	X	X		2.09
62	50.9350	0.12	71.	55.	1.7914	14.06	X	X		0.58
63	51.6500	0.16	10.	62.	1.7682	2.04	X	X		0.17
64	52.4800	0.08	10.	64.	1.7422	2.04	X	X		0.12
65	53.0925	0.12	18.	48.	1.7235	3.52	X	X		0.14
66	54.0425	0.20	67.	56.	1.6955	13.40	X	X		0.74
67	54.9200	0.08	52.	61.	1.6704	10.33	X	X		0.13
68	55.4150	0.24	28.	66.	1.6567	5.60	X	X		0.11
69	57.3275	0.12	10.	66.	1.6059	2.04	X	X		0.19
70	57.6350	0.12	12.	66.	1.5980	2.30	X			0.24
71	57.8000	0.08	10.	66.	1.5939	2.04	X	X		0.11
72	58.1600	0.08	10.	66.	1.5848	2.04	X	X		0.10
73	59.9000	0.24	50.	62.	1.5429	10.05	X	X		1.48
74	60.8325	0.24	14.	66.	1.5215	2.73	X	X		0.28
75	61.8475	0.20	142.	66.	1.4989	28.22	X	X		0.89
76	63.8800	0.24	10.	66.	1.4560	2.04	X	X		0.20

Table B24. Bentonite-Fly Ash Cured at 50°C for 1 Day.

Peak no	Angle (deg)	Tip width (deg)	Peak (cts)	Backg (cts)	D spac (Ang)	I/Imax (%)	Type A1	Type A2	Type Ot	Sign
1	2.1375	0.12	10.	66.	41.2972	1.18	X	X		0.13
2	2.4400	0.08	10.	67.	36.1780	1.19	X	X		0.11
3	3.3450	0.12	10.	66.	26.3917	1.18	X	X		0.25
4	3.5800	0.24	10.	66.	24.6598	1.18	X	X		0.13
5	6.6200	0.16	64.	66.	13.3409	7.40	X	X		0.26
6	7.2800	0.20	85.	64.	12.1328	9.79	X	X		0.44
7	7.8150	0.32	61.	62.	11.3034	7.04	X	X		0.29
8	8.4750	0.12	34.	61.	10.4246	3.89	X	X		0.11
9	8.8800	0.16	31.	59.	9.9500	3.63	X	X		0.11
10	12.2350	0.12	10.	49.	7.2281	1.18	X	X		0.18
11	13.0400	0.32	10.	48.	6.7836	1.18	X	X		0.22
12	13.8000	0.08	12.	48.	6.4117	1.34	X	X		0.10
13	14.8350	0.48	10.	48.	5.9666	1.18	X	X		0.13
14	16.6625	0.48	10.	49.	5.3161	1.18	X	X		0.13
15	18.0000	0.16	26.	50.	4.9240	3.01	X	X		0.31
16	19.1025	0.16	13.	50.	4.6422	1.50	X	X		0.27
17	19.8800	0.16	243.	50.	4.4624	28.15	X	X		1.32
18	20.9400	0.16	130.	52.	4.2388	15.04	X	X		1.07
19	22.1450	0.24	44.	52.	4.0108	5.04	X	X		0.19
20	23.6775	0.12	52.	53.	3.7546	6.00	X	X		0.18
21	24.0675	0.12	38.	53.	3.6946	4.45	X	X		0.25
22	25.1200	0.08	29.	53.	3.5421	3.37	X	X		0.11
23	25.3725	0.12	44.	53.	3.5075	5.04	X	X		0.13
24	25.7025	0.24	52.	53.	3.4632	6.00	X	X		0.11
25	26.7000	0.12	864.	55.	3.3360	100.00	X	X		4.07
26	27.7600	0.08	182.	55.	3.2110	21.08	X	X		0.33
27	28.5550	0.32	108.	55.	3.1234	12.51	X	X		0.50
28	29.5700	0.12	164.	56.	3.0184	18.96	X	X		0.83
29	30.3250	0.12	69.	56.	2.9450	7.97	X	X		0.36
30	31.3775	0.16	26.	56.	2.8486	3.01	X	X		0.24
31	31.6400	0.08	31.	56.	2.8255	3.63	X	X		0.16
32	32.0350	0.12	71.	56.	2.7916	8.16	X	X		0.17
33	33.3175	0.12	37.	58.	2.6870	4.30	X	X		0.15
34	34.8925	0.12	121.	58.	2.5692	14.00	X	X		0.22
35	35.4725	0.12	132.	59.	2.5285	15.30	X	X		0.22
36	36.1650	0.12	102.	59.	2.4817	11.80	X	X		0.18
37	36.5925	0.20	119.	59.	2.4537	13.75	X	X		0.76
38	38.5225	0.16	81.	59.	2.3351	9.37	X	X		1.45
39	39.5350	0.16	62.	61.	2.2776	7.22	X	X		0.63
40	40.1175	0.12	37.	61.	2.2458	4.30	X	X		0.12
41	40.4000	0.32	35.	61.	2.2308	4.03	X	X		0.16
42	41.7250	0.12	50.	61.	2.1629	5.83	X	X		0.39
43	42.3675	0.12	46.	62.	2.1316	5.35	X	X		0.44
44	43.0825	0.40	36.	62.	2.0979	4.16	X	X		0.58
45	43.4675	0.32	26.	62.	2.0802	3.01	X	X		0.21
46	44.7875	0.16	37.	62.	2.0219	4.30	X	X		0.71
47	45.7800	0.12	18.	64.	1.9803	2.04	X	X		0.38
48	46.9075	0.12	14.	64.	1.9353	1.58	X	X		0.26
49	47.4800	0.08	15.	64.	1.9133	1.76	X	X		0.11
50	47.8150	0.32	12.	64.	1.9007	1.34	X	X		0.35
51	48.6825	0.20	16.	64.	1.8688	1.85	X	X		0.81
52	49.2000	0.08	10.	64.	1.8504	1.18	X	X		0.11
53	50.1000	0.16	66.	59.	1.8192	7.59	X	X		0.76
54	50.9850	0.24	10.	61.	1.7897	1.18	X	X		0.22
55	52.0000	0.08	10.	59.	1.7571	1.18	X	X		0.16
56	52.4000	0.16	14.	56.	1.7447	1.67	X	X		0.14
57	53.9200	0.08	49.	61.	1.6990	5.67	X			0.15
58	54.1550	0.12	58.	61.	1.6922	6.68	X	X		0.11
59	54.5325	0.12	48.	61.	1.6814	5.51	X	X		0.21
60	56.6125	0.16	10.	69.	1.6244	1.18	X	X		0.24
61	57.5475	0.12	10.	69.	1.6002	1.18	X	X		0.15
62	58.3600	0.16	10.	67.	1.5799	1.18	X	X		0.40
63	59.9100	0.20	59.	64.	1.5427	6.86	X	X		1.10
64	60.9500	0.12	19.	66.	1.5188	2.24	X	X		0.17
65	61.9375	0.28	180.	64.	1.4969	20.77	X	X		2.57
66	63.8550	0.24	10.	64.	1.4565	1.18	X	X		0.15
67	65.0525	0.12	106.	62.	1.4326	12.27	X	X		0.81
68	65.7900	0.24	10.	62.	1.4183	1.18	X	X		0.27
69	66.7200	0.08	10.	62.	1.4008	1.18	X			0.14
70	66.9725	0.12	10.	62.	1.3961	1.18	X	X		0.18
71	67.5875	0.32	32.	61.	1.3849	3.76	X	X		0.60
72	68.3450	0.12	44.	61.	1.3714	5.04	X	X		0.28

Table B25. Bentonite-Fly Ash Cured at 50°C for 28 Days.

Peak no	Angle (deg)	Tip width (deg)	Peak (cts)	Backg (cts)	D spac (Ang)	I/Imax (%)	Type A1	A2	Ot	Sign
1	2.8025	0.12	10.	94.	31.4992	1.90	X	X		0.17
2	4.0975	0.12	19.	71.	21.5464	3.60	X	X		0.29
3	4.3925	0.12	10.	71.	20.1000	1.90	X	X		0.18
4	5.3125	0.12	23.	69.	16.6211	4.29	X	X		0.23
5	5.8925	0.16	19.	74.	14.9863	3.44	X	X		0.14
6	6.6250	0.12	25.	83.	13.3309	4.64	X	X		0.22
7	6.9525	0.12	38.	83.	12.7036	7.14	X	X		0.13
8	7.5125	0.40	56.	83.	11.7579	10.45	X	X		0.54
9	8.8925	0.12	27.	83.	9.9472	5.02	X	X		0.22
10	10.2900	0.08	10.	83.	8.5979	1.90	X	X		0.11
11	10.5200	0.08	10.	77.	8.4023	1.90	X	X		0.13
12	11.1150	0.32	10.	66.	7.9538	1.90	X	X		0.25
13	11.6650	0.12	10.	56.	7.5800	1.90	X	X		0.12
14	13.0125	0.32	10.	49.	6.7979	1.90	X	X		0.24
15	13.5225	0.12	16.	48.	6.5426	2.97	X	X		0.12
16	14.8050	0.12	12.	49.	5.9786	2.15	X	X		0.12
17	15.7550	0.12	10.	52.	5.6202	1.90	X	X		0.18
18	16.5125	0.16	11.	52.	5.3641	2.02	X	X		0.45
19	17.3100	0.12	14.	48.	5.1187	2.68	X	X		0.17
20	18.0875	0.48	24.	50.	4.9004	4.46	X	X		0.44
21	19.8750	0.16	250.	62.	4.4635	46.38	X	X		1.45
22	20.9250	0.16	159.	61.	4.2418	29.50	X	X		1.62
23	21.6425	0.12	29.	83.	4.1028	5.42	X	X		0.21
24	22.0000	0.08	21.	83.	4.0369	3.93	X	X		0.13
25	22.3100	0.24	13.	83.	3.9815	2.41	X	X		0.15
26	23.2325	0.16	15.	83.	3.8255	2.83	X	X		0.25
27	23.6775	0.12	34.	83.	3.7546	6.25	X	X		0.23
28	24.4350	0.12	17.	83.	3.6399	3.12	X	X		0.25
29	24.8300	0.24	19.	83.	3.5829	3.60	X	X		0.32
30	25.6400	0.32	21.	83.	3.4715	3.93	X	X		0.22
31	26.7150	0.16	538.	83.	3.3342	100.00	X	X		5.01
32	27.2175	0.12	55.	83.	3.2737	10.17	X	X		0.23
33	27.4675	0.12	83.	83.	3.2445	15.39	X	X		0.33
34	27.7600	0.08	182.	83.	3.2110	33.86	X	X		0.35
35	28.1250	0.16	142.	83.	3.1701	26.31	X	X		1.35
36	28.6900	0.24	59.	83.	3.1090	11.02	X	X		0.20
37	29.5725	0.16	104.	83.	3.0182	19.33	X	X		1.05
38	30.8625	0.24	10.	83.	2.8949	1.90	X	X		0.34
39	31.4350	0.12	10.	83.	2.8435	1.90	X	X		0.12
40	31.9600	0.08	41.	74.	2.7980	7.61	X	X		0.12
41	32.8400	0.16	10.	76.	2.7250	1.90	X	X		0.12
42	33.2000	0.08	17.	76.	2.6962	3.12	X	X		0.17
43	33.3900	0.20	20.	76.	2.6813	3.76	X	X		0.60
44	33.9600	0.08	10.	74.	2.6376	1.90	X	X		0.12
45	34.9925	0.12	177.	67.	2.5621	32.36	X	X		0.41
46	36.1575	0.16	83.	83.	2.4822	15.39	X	X		0.19
47	36.4875	0.12	92.	83.	2.4605	17.12	X	X		0.20
48	37.5050	0.12	29.	83.	2.3960	5.42	X	X		0.21
49	38.5525	0.12	49.	83.	2.3333	9.10	X	X		0.39
50	39.5200	0.16	45.	83.	2.2784	8.34	X	X		0.93
51	40.2675	0.12	25.	83.	2.2378	4.64	X	X		0.35
52	42.3300	0.12	19.	83.	2.1334	3.60	X			0.19
53	42.4925	0.32	25.	83.	2.1256	4.64	X	X		0.78
54	42.9750	0.12	21.	83.	2.1029	3.93	X	X		0.26
55	43.2800	0.08	16.	83.	2.0888	2.97	X			0.11
56	43.3600	0.16	12.	83.	2.0902	2.15		X		0.13
57	44.1075	0.12	10.	81.	2.0515	1.90	X	X		0.14
58	44.7550	0.16	34.	81.	2.0233	6.25	X	X		0.89
59	45.2950	0.12	21.	67.	2.0004	3.93	X	X		0.38
60	46.3200	0.08	10.	74.	1.9585	1.90	X	X		0.14
61	47.0700	0.16	10.	74.	1.9290	1.90	X	X		0.23
62	47.6950	0.40	26.	62.	1.9052	4.83	X	X		0.83
63	48.6800	0.16	10.	64.	1.8689	1.90	X	X		0.15
64	50.1150	0.16	74.	67.	1.8187	13.74	X	X		1.05
65	51.4275	0.24	10.	61.	1.7754	1.90	X	X		0.14
66	52.6375	0.12	14.	55.	1.7374	2.68	X	X		0.10
67	52.9050	0.16	12.	55.	1.7292	2.28	X	X		0.13
68	53.3900	0.12	12.	55.	1.7146	2.28	X	X		0.19
69	53.8625	0.12	49.	59.	1.7007	9.10	X	X		0.12
70	54.9225	0.24	50.	62.	1.6704	9.37	X	X		0.38
71	56.9125	0.12	10.	69.	1.6166	1.90	X	X		0.14
72	57.6300	0.24	10.	67.	1.5981	1.90	X	X		0.24
73	58.4100	0.12	10.	66.	1.5787	1.90	X	X		0.22
74	59.1925	0.16	10.	66.	1.5596	1.90	X	X		0.21
75	59.5350	0.12	14.	64.	1.5515	2.54	X	X		0.21
76	59.8975	0.12	58.	61.	1.5430	10.73	X	X		0.56
77	60.4250	0.16	26.	61.	1.5307	4.93	X	X		0.63

Table B26. Bentonite-Fly Ash Cured at 50°C for 90 Days.

Peak no	Angle (deg)	Tip width (deg)	Peak (cts)	Backg (cts)	D spac (Ang)	I/Imax (%)	Type A1	A2	Ot	Sign
1	2.0900	0.08	76.	69.	42.4297	14.06	X	X		0.13
2	2.4800	0.16	44.	67.	35.5946	8.09	X	X		0.12
3	3.7075	0.24	10.	67.	23.8120	1.90	X	X		0.13
4	4.9725	0.12	12.	67.	17.7567	2.28	X	X		0.10
5	5.2875	0.12	27.	66.	16.6996	5.02	X	X		0.15
6	5.7125	0.16	59.	66.	15.4581	11.02	X	X		0.23
7	6.4875	0.12	94.	66.	13.6131	17.48	X	X		0.32
8	6.7300	0.12	85.	67.	13.1231	15.73	X	X		0.13
9	8.8875	0.12	10.	67.	9.9416	1.90	X	X		0.26
10	10.1775	0.32	10.	61.	8.6842	1.90	X	X		0.33
11	11.1675	0.16	10.	50.	7.9165	1.90	X	X		0.31
12	12.1075	0.12	10.	46.	7.3039	1.90	X	X		0.19
13	12.2525	0.24	10.	46.	7.2178	1.90	X	X		0.15
14	12.6800	0.08	10.	45.	6.9754	1.90	X	X		0.10
15	13.1575	0.12	10.	45.	6.7233	1.90	X	X		0.13
16	13.9600	0.12	16.	38.	6.3386	2.97	X	X		0.15
17	15.7175	0.12	10.	45.	5.6335	1.90	X	X		0.13
18	16.2925	0.12	10.	46.	5.4360	1.90	X	X		0.18
19	17.3650	0.12	10.	46.	5.1026	1.90	X	X		0.13
20	17.8050	0.16	12.	45.	4.9775	2.15	X	X		0.17
21	19.8700	0.16	266.	48.	4.4646	49.36	X	X		1.86
22	20.9475	0.16	128.	48.	4.2373	23.72	X	X		1.07
23	21.7425	0.24	46.	52.	4.0841	8.59	X	X		0.13
24	22.5600	0.08	35.	58.	3.9380	6.47	X	X		0.17
25	23.1075	0.24	28.	59.	3.8459	5.22	X	X		0.20
26	23.6450	0.24	52.	62.	3.7597	9.63	X	X		1.74
27	25.7750	0.24	29.	76.	3.4536	5.42	X	X		0.20
28	26.7025	0.12	538.	76.	3.3357	100.00	X	X		2.63
29	27.4425	0.12	45.	76.	3.2474	8.34	X	X		0.17
30	27.8575	0.24	52.	76.	3.2000	9.63	X	X		0.26
31	28.6075	0.32	83.	76.	3.1178	15.39	X	X		0.44
32	29.0775	0.12	79.	76.	3.0684	14.72	X	X		0.16
33	29.5900	0.16	94.	76.	3.0164	17.48	X	X		1.07
34	30.5375	0.12	18.	74.	2.9250	3.28	X	X		0.19
35	31.4600	0.24	12.	74.	2.8413	2.28	X	X		0.19
36	31.9600	0.08	42.	74.	2.7980	7.85	X	X		0.21
37	33.2875	0.48	15.	74.	2.6893	2.83	X	X		1.48
38	34.7675	0.16	90.	64.	2.5782	16.77	X	X		0.42
39	35.2650	0.12	114.	66.	2.5429	21.27	X	X		0.14
40	36.6300	0.16	102.	72.	2.4512	18.95	X	X		0.55
41	38.4875	0.16	55.	71.	2.3371	10.17	X	X		0.74
42	39.4925	0.12	48.	71.	2.2799	8.85	X	X		0.45
43	40.2875	0.24	28.	71.	2.2367	5.22	X	X		0.26
44	40.8400	0.08	24.	71.	2.2077	4.46	X	X		0.11
45	42.4625	0.12	58.	69.	2.1271	10.73	X	X		0.48
46	42.9350	0.12	37.	69.	2.1047	6.91	X	X		0.32
47	43.3600	0.16	23.	69.	2.0851	4.28	X	X		0.12
48	44.0950	0.16	10.	69.	2.0520	1.90	X	X		0.37
49	44.3825	0.12	10.	69.	2.0394	1.90	X	X		0.27
50	44.7200	0.16	40.	69.	2.0248	7.37	X	X		0.47
51	45.6600	0.16	222.	64.	1.9853	41.25	X	X		3.63
52	46.0100	0.12	12.	64.	1.9710	2.15	X	X		0.10
53	46.2875	0.12	10.	64.	1.9598	1.90	X	X		0.17
54	47.7850	0.32	22.	61.	1.9018	4.10	X	X		0.62
55	48.2400	0.08	10.	61.	1.8849	1.90	X	X		0.12
56	48.7350	0.32	10.	61.	1.8670	1.90	X	X		0.54
57	49.3275	0.20	13.	59.	1.8459	2.41	X	X		0.65
58	50.1475	0.12	74.	56.	1.8176	13.74	X	X		0.52
59	50.8400	0.24	10.	56.	1.7945	1.90	X	X		0.21
60	51.4075	0.12	11.	56.	1.7760	2.02	X	X		0.25
61	52.8925	0.32	15.	50.	1.7296	2.83	X	X		0.40
62	54.0500	0.24	61.	53.	1.6952	11.30	X	X		0.25
63	55.2725	0.12	42.	64.	1.6606	7.85	X	X		0.21
64	55.6525	0.12	62.	64.	1.6502	11.60	X	X		0.65
65	57.5625	0.12	20.	62.	1.5999	3.76	X	X		0.17
66	58.7475	0.48	10.	62.	1.5704	1.90	X	X		0.28
67	59.8950	0.16	56.	61.	1.5430	10.45	X	X		0.76
68	60.6750	0.32	13.	61.	1.5250	2.41	X	X		0.12
69	61.8450	0.16	161.	61.	1.4990	29.97	X			0.66
70	62.0075	0.20	156.	61.	1.4954	29.03	X	X		0.46
71	64.0900	0.32	12.	59.	1.4518	2.28	X	X		0.26
72	65.0000	0.08	123.	59.	1.4336	22.89			Ot	0.33
73	65.7850	0.12	22.	59.	1.4184	4.10	X	X		0.34
74	66.2825	0.24	10.	59.	1.4090	1.90	X	X		0.15
75	66.7200	0.08	10.	59.	1.4008	1.90	X	X		0.10

Table B27. Bentonite-Fly Ash Cured at 50°C for 180 Days.

Peak no	Angle (deg)	Tip width (deg)	Peak (cts)	Backg (cts)	D spac (Ang)	I/Imax (%)	Type A1	A2	Ot	Sign
1	2.8300	0.12	20.	52.	31.1032	3.67	X	X		0.17
2	3.4875	0.12	20.	52.	25.3136	3.67	X	X		0.18
3	3.8950	0.12	14.	52.	22.6662	2.48	X	X		0.31
4	4.5300	0.12	18.	52.	19.4902	3.35	X	X		0.13
5	5.2575	0.32	27.	52.	16.7948	4.90	X	X		0.30
6	6.0525	0.12	48.	52.	14.5905	8.62	X	X		0.13
7	7.2400	0.08	106.	52.	12.1998	19.21	X	X		0.15
8	7.9950	0.16	106.	52.	11.0493	19.21	X	X		0.55
9	8.9800	0.12	48.	52.	9.8394	8.62	X	X		0.47
10	9.3150	0.12	22.	52.	9.4863	4.00	X	X		0.11
11	10.2100	0.12	14.	52.	8.6567	2.48	X	X		0.45
12	10.7125	0.12	14.	52.	8.2517	2.48	X	X		0.35
13	10.9600	0.08	11.	52.	8.0659	1.97	X	X		0.17
14	11.2400	0.08	10.	52.	7.8656	1.85	X	X		0.19
15	12.6800	0.08	13.	45.	6.9754	2.35	X	X		0.20
16	12.9200	0.08	10.	48.	6.8464	1.85	X	X		0.13
17	13.9200	0.08	10.	48.	6.3567	1.85	X	X		0.10
18	15.0800	0.12	14.	46.	5.8702	2.61	X	X		0.10
19	16.1675	0.12	10.	50.	5.4777	1.85	X	X		0.14
20	17.9575	0.48	12.	50.	4.9355	2.22	X	X		0.13
21	19.9100	0.24	279.	52.	4.4557	50.50	X	X		4.17
22	20.9825	0.12	132.	52.	4.2303	23.95	X	X		0.65
23	21.7675	0.16	55.	52.	4.0795	9.92	X	X		0.19
24	22.7350	0.24	35.	52.	3.9080	6.30	X	X		0.14
25	23.9850	0.12	32.	52.	3.7071	5.88	X	X		0.11
26	24.2400	0.08	44.	52.	3.6687	7.89	X	X		0.12
27	24.7375	0.16	50.	52.	3.5960	9.13	X	X		0.33
28	25.3300	0.24	38.	52.	3.5133	6.96	X	X		0.19
29	25.8050	0.12	52.	52.	3.4496	9.39	X	X		0.21
30	26.7225	0.16	552.	52.	3.3333	100.00	X	X		5.25
31	27.2600	0.12	92.	52.	3.2687	16.69	X	X		0.25
32	27.7300	0.12	106.	52.	3.2144	19.21	X	X		0.23
33	28.1375	0.12	137.	52.	3.1688	24.79	X	X		0.48
34	29.5950	0.16	169.	52.	3.0159	30.60	X	X		1.62
35	30.8800	0.12	38.	52.	2.8933	6.96	X	X		0.12
36	31.9825	0.16	62.	52.	2.7960	11.30	X	X		0.45
37	32.4800	0.08	18.	52.	2.7543	3.35	X	X		0.13
38	34.8975	0.40	123.	52.	2.5689	22.31	X	X		1.66
39	35.4125	0.12	182.	52.	2.5327	33.00	X	X		0.49
40	35.8800	0.08	139.	52.	2.5007	25.21	X	X		0.14
41	36.6725	0.24	142.	52.	2.4485	25.64	X	X		0.76
42	38.5600	0.16	90.	52.	2.3329	16.34	X	X		1.17
43	39.4800	0.08	64.	52.	2.2806	11.59	X			0.17
44	39.5875	0.12	67.	52.	2.2747	12.18	X	X		0.33
45	40.3525	0.12	52.	52.	2.2333	9.39	X	X		0.22
46	40.8900	0.12	36.	52.	2.2052	6.52	X	X		0.12
47	41.3100	0.12	42.	52.	2.1837	7.65	X	X		0.13
48	41.6525	0.12	38.	52.	2.1665	6.96	X	X		0.19
49	42.2000	0.08	42.	52.	2.1397	7.65	X	X		0.12
50	42.4750	0.12	64.	52.	2.1265	11.59	X	X		0.30
51	43.4400	0.32	36.	52.	2.0814	6.52	X	X		0.15
52	44.7450	0.24	40.	53.	2.0237	7.19	X	X		0.47
53	45.8150	0.12	32.	53.	1.9789	5.88	X			0.22
54	45.9200	0.16	30.	53.	1.9746	5.48	X	X		0.11
55	46.2875	0.12	28.	53.	1.9598	5.09	X	X		0.14
56	47.7350	0.16	52.	53.	1.9037	9.39	X	X		0.30
57	48.7825	0.24	18.	53.	1.8652	3.19	X	X		0.21
58	50.1800	0.20	90.	53.	1.8165	16.34	X	X		1.74
59	51.0700	0.12	11.	53.	1.7869	1.97	X	X		0.25
60	52.0925	0.12	10.	53.	1.7542	1.85	X	X		0.13
61	52.3600	0.12	12.	53.	1.7459	2.22	X			0.11
62	52.6000	0.12	18.	53.	1.7385	3.19	X	X		0.10
63	54.0000	0.32	62.	52.	1.6967	11.30	X	X		0.85
64	54.8750	0.32	79.	53.	1.6717	14.34	X	X		0.81
65	55.7550	0.12	41.	53.	1.6474	7.42	X	X		0.17
66	56.4850	0.40	20.	53.	1.6278	3.67	X	X		0.30
67	57.1600	0.08	24.	53.	1.6102	4.35	X			0.10
68	57.4450	0.12	42.	53.	1.6029	7.65	X	X		0.32
69	58.4300	0.32	10.	53.	1.5782	1.85	X	X		0.21
70	59.3175	0.16	15.	53.	1.5566	2.75	X	X		0.10
71	59.9100	0.12	48.	53.	1.5427	8.62	X			0.18
72	60.1100	0.12	44.	53.	1.5380	7.89	X	X		0.21
73	61.1200	0.08	29.	53.	1.5150	5.28	X			0.15
74	61.3600	0.08	40.	53.	1.5096	7.19	X	X		0.11
75	61.9300	0.24	164.	55.	1.4971	29.67	X	X		0.79

Table B28. Bentonite-Lime Cured at 23°C for 1 Day.

Peak no	Angle (deg)	Tip width (deg)	Peak (cts)	Backg (cts)	D spac (Ang)	I/Imax (%)	Type K1	Type K2	Type Ot	Sign
1	2.9600	0.08	10.	94.	29.8235	2.10	X	X		0.11
2	4.5600	0.08	10.	62.	19.3621	2.10	X	X		0.13
3	5.0150	0.24	22.	62.	17.6064	4.52	X	X		0.23
4	5.5200	0.16	37.	62.	15.9967	7.62	X	X		0.11
5	6.2000	0.08	76.	71.	14.2437	15.50	X	X		0.10
6	7.0775	0.24	125.	81.	12.4795	25.68	X	X		0.38
7	7.5400	0.24	106.	81.	11.7150	21.72	X	X		0.18
8	8.4475	0.20	18.	81.	10.4584	3.79	X	X		0.47
9	8.9400	0.12	18.	81.	9.8834	3.79	X	X		0.47
10	10.3300	0.12	10.	81.	8.5564	2.10	X	X		0.28
11	10.8000	0.08	10.	69.	8.1850	2.10	X	X		0.13
12	11.2200	0.24	10.	56.	7.8796	2.10	X	X		0.23
13	11.7175	0.12	10.	53.	7.5461	2.10	X	X		0.13
14	13.4300	0.24	10.	49.	6.5875	2.10	X	X		0.12
15	13.9875	0.12	10.	48.	6.3262	2.10	X	X		0.17
16	14.6475	0.12	10.	49.	6.0426	2.10	X	X		0.13
17	15.1325	0.16	10.	50.	5.8500	2.10	X	X		0.41
18	16.7425	0.16	10.	52.	5.2909	2.10	X	X		0.35
19	17.8825	0.24	10.	50.	4.9561	2.10	X	X		0.23
20	18.9600	0.08	10.	50.	4.6768	2.10	X	X		0.13
21	19.8900	0.20	296.	50.	4.4602	60.57	X	X		3.39
22	20.9425	0.12	123.	53.	4.2383	25.23	X	X		0.38
23	21.8725	0.12	26.	83.	4.0602	5.33	X	X		0.17
24	23.2000	0.16	19.	83.	3.8308	3.96	X	X		0.41
25	24.7025	0.32	10.	83.	3.6011	2.10	X	X		0.19
26	26.7150	0.16	488.	81.	3.3342	100.00	X	X		4.79
27	27.1850	0.12	108.	83.	3.2776	22.15	X	X		0.85
28	27.7425	0.12	190.	81.	3.2130	38.99	X	X		1.78
29	28.4225	0.12	100.	79.	3.1376	20.47	X	X		0.33
30	29.5550	0.16	166.	77.	3.0199	34.07	X	X		1.95
31	31.0325	0.12	18.	72.	2.8794	3.61	X	X		0.19
32	31.9975	0.24	81.	69.	2.7948	16.58	X	X		1.58
33	34.6800	0.08	83.	61.	2.5845	16.96	X	X		0.16
34	36.0750	0.12	128.	61.	2.4877	26.14	X	X		0.25
35	36.6400	0.16	102.	61.	2.4506	20.89	X	X		0.10
36	38.5125	0.16	79.	59.	2.3356	16.22	X	X		1.05
37	39.4950	0.12	81.	59.	2.2798	16.58	X	X		0.31
38	40.3650	0.24	41.	58.	2.2326	8.39	X	X		0.33
39	40.9025	0.24	34.	58.	2.2045	6.89	X	X		0.17
40	41.4075	0.12	28.	58.	2.1788	5.75	X	X		0.19
41	42.4875	0.12	79.	58.	2.1259	16.22	X	X		0.28
42	43.3025	0.12	55.	58.	2.0877	11.21	X	X		0.44
43	44.0725	0.40	29.	56.	2.0530	5.97	X	X		0.73
44	44.7525	0.12	32.	56.	2.0239	6.75	X	X		0.24
45	45.7500	0.32	30.	56.	1.9816	6.19	X	X		0.58
46	47.0350	0.12	14.	56.	1.9304	2.96	X	X		0.17
47	47.6800	0.20	36.	56.	1.9058	7.37	X	X		0.68
48	49.2900	0.16	14.	55.	1.8476	2.80	X	X		0.14
49	50.0800	0.08	92.	55.	1.8199	19.87	X	X		0.18
50	50.8800	0.16	21.	55.	1.7932	4.33	X	X		0.11
51	53.7675	0.12	45.	53.	1.7035	9.19	X	X		0.26
52	54.2800	0.08	72.	53.	1.6886	14.79	X	X		0.13
53	55.0000	0.64	61.	55.	1.6682	12.46	X	X		0.74
54	56.7900	0.12	23.	56.	1.6198	4.72	X	X		0.25
55	57.5500	0.32	18.	56.	1.6002	3.61	X	X		0.28
56	58.1975	0.12	10.	58.	1.5842	2.10	X			0.14
57	58.4575	0.12	10.	58.	1.5775	2.10	X	X		0.16
58	58.9675	0.12	13.	58.	1.5650	2.65	X	X		0.21
59	59.4175	0.12	16.	59.	1.5543	3.28	X	X		0.24
60	59.9325	0.16	58.	59.	1.5421	11.93	X	X		0.69
61	61.8050	0.24	174.	61.	1.4998	35.67	X	X		1.65
62	64.7250	0.12	12.	62.	1.4390	2.37	X			0.11
63	65.0175	0.12	94.	62.	1.4333	19.26	X	X		1.02
64	65.2400	0.08	50.	62.	1.4289	10.32	X	X		0.16
65	65.5700	0.12	10.	62.	1.4260	2.10		X		0.14
66	65.8350	0.12	18.	61.	1.4174	3.61	X	X		0.22
67	67.6575	0.12	42.	59.	1.3836	8.65	X	X		0.33
68	68.0900	0.12	74.	58.	1.3759	15.14	X	X		0.41
69	69.7600	0.08	10.	59.	1.3470	2.10	X			0.14

Table B29. Bentonite-Lime Cured at 23°C for 28 Days.

Peak no	Angle (deg)	Tip width (deg)	Peak (cts)	Backg (cts)	D spac (Ang)	I Imax (%)	Type A1	Type A2	Type Qt	Sign
1	3.6075	0.12	10.	104.	24.4719	1.87	X	X		0.18
2	3.9525	0.32	10.	66.	22.3366	1.87	X	X		0.11
3	4.5850	0.16	10.	66.	19.2565	1.87	X	X		0.13
4	6.4750	0.12	53.	66.	13.6393	9.73	X	X		0.13
5	7.5600	0.40	104.	66.	11.6841	19.00	X	X		0.95
6	9.0025	0.24	23.	66.	9.8149	4.21	X	X		0.22
7	10.7175	0.12	10.	64.	8.2479	1.87	X	X		0.18
8	12.2450	0.12	10.	53.	7.2222	1.87	X	X		0.10
9	13.0000	0.08	10.	48.	6.8044	1.87	X	X		0.11
10	13.9600	0.08	10.	46.	6.3386	1.87	X	X		0.11
11	14.4400	0.16	10.	49.	6.1289	1.87	X	X		0.34
12	15.0825	0.16	12.	49.	5.8693	2.11	X	X		0.25
13	15.9075	0.32	10.	49.	5.5667	1.87	X	X		0.56
14	16.5900	0.32	10.	52.	5.3392	1.87	X	X		0.25
15	17.7300	0.16	10.	50.	4.9984	1.87	X	X		0.21
16	18.6725	0.12	10.	55.	4.7481	1.87	X	X		0.26
17	18.9650	0.12	10.	55.	4.6756	1.87	X	X		0.17
18	19.8825	0.16	296.	55.	4.4618	54.03	X	X		2.00
19	20.5700	0.12	98.	58.	4.3142	17.90	X	X		0.11
20	20.9475	0.12	149.	58.	4.2373	27.18	X	X		0.71
21	21.3475	0.12	64.	66.	4.1598	11.69	X	X		0.29
22	21.8050	0.12	36.	66.	4.0726	6.57	X	X		0.12
23	22.7550	0.12	38.	66.	3.9047	7.02	X	X		0.14
24	24.5500	0.12	32.	66.	3.6231	5.93	X	X		0.35
25	25.0375	0.16	32.	66.	3.5536	5.93	X	X		0.24
26	25.4400	0.08	30.	66.	3.4983	5.52	X	X		0.10
27	25.8400	0.08	74.	66.	3.4451	13.51	X	X		0.29
28	26.7150	0.16	548.	66.	3.3342	100.00	X	X		4.79
29	27.4250	0.12	256.	66.	3.2494	46.75	X	X		1.86
30	27.8525	0.12	150.	66.	3.2005	28.09	X	X		0.53
31	28.8525	0.12	100.	66.	3.1471	18.26	X	X		0.29
32	29.1925	0.12	74.	66.	3.0566	13.51	X	X		0.10
33	29.5725	0.12	125.	66.	3.0182	22.91	X	X		0.40
34	30.5975	0.16	23.	66.	2.9194	4.21	X	X		0.22
35	32.0350	0.16	67.	66.	2.7916	12.28	X	X		1.00
36	33.9575	0.12	10.	64.	2.6378	1.87	X	X		0.13
37	34.8675	0.20	114.	59.	2.5710	20.91	X	X		0.46
38	35.2050	0.16	156.	58.	2.5471	28.54	X	X		0.40
39	36.1125	0.24	110.	66.	2.4852	20.13	X	X		0.26
40	36.6750	0.12	117.	66.	2.4483	21.30	X	X		0.14
41	37.1450	0.16	67.	66.	2.4184	12.28	X	X		0.19
42	37.8000	0.08	49.	66.	2.3780	8.95	X	X		0.21
43	38.0400	0.08	42.	66.	2.3636	7.72	X	X		0.17
44	38.5400	0.12	74.	66.	2.3340	13.51	X	X		0.49
45	39.5175	0.12	59.	66.	2.2795	10.83	X			0.22
46	39.6025	0.12	55.	66.	2.2738	10.00	X	X		0.20
47	40.4000	0.32	30.	66.	2.2308	5.52	X	X		0.17
48	41.6000	0.16	28.	66.	2.1692	5.13	X	X		0.12
49	42.4800	0.16	38.	66.	2.1262	7.02	X	X		0.10
50	42.9600	0.20	25.	66.	2.1036	4.57	X	X		0.36
51	43.4075	0.24	27.	66.	2.0829	4.94	X	X		0.19
52	44.7600	0.16	50.	66.	2.0231	9.21	X	X		0.81
53	45.7650	0.12	21.	66.	1.9810	3.86	X	X		0.18
54	47.7950	0.16	15.	66.	1.9015	2.78	X	X		0.20
55	48.5550	0.32	10.	66.	1.8735	1.87	X	X		0.25
56	49.7850	0.12	117.	61.	1.8300	21.30	X	X		0.91
57	50.1475	0.12	74.	61.	1.8176	13.51	X			0.42
58	50.2400	0.08	58.	61.	1.8145	10.55	X	X		0.11
59	50.7425	0.12	40.	62.	1.7977	7.25	X	X		0.25
60	51.6000	0.12	10.	64.	1.7698	1.87	X	X		0.17
61	52.8300	0.16	24.	53.	1.7315	4.38	X	X		0.20
62	53.9200	0.08	50.	62.	1.6990	9.21	X	X		0.11
63	54.9375	0.24	56.	64.	1.6699	10.27	X	X		0.39
64	56.9000	0.24	14.	64.	1.6169	2.50	X	X		0.20
65	57.5825	0.12	21.	64.	1.5994	3.86	X	X		0.22
66	59.0300	0.12	35.	61.	1.5635	6.36	X	X		0.45
67	59.9400	0.20	58.	61.	1.5420	10.55	X	X		1.15
68	61.9100	0.12	228.	62.	1.4975	41.64	X			0.62
69	62.1200	0.08	190.	62.	1.4967	34.78		X		0.13
70	63.4725	0.24	12.	62.	1.4644	2.24	X	X		0.19
71	64.0250	0.12	16.	62.	1.4531	2.92	X	X		0.30
72	64.6800	0.08	11.	61.	1.4399	1.99	X	X		0.10
73	65.0550	0.12	92.	61.	1.4325	16.83	X	X		0.69
74	67.7275	0.24	37.	61.	1.3924	6.80	X	X		0.30
75	68.2025	0.16	50.	61.	1.3739	9.21	X	X		0.29
76	68.9625	0.12	12.	59.	1.3606	2.11	X	X		0.20
77	69.5550	0.16	10.	59.	1.3504	1.87	X	X		0.30

Table B30. Bentonite-Lime Cured at 23°C for 90 Days.

Peak no	Angle (deg)	Tip width (deg)	Peak (cts)	Backg (cts)	D spac (Ang)	I/Imax (%)	Type K1	Type K2	Type Qt	Sign
1	2.0750	0.12	103.	44.	42.5410	22.15	X	X		0.15
2	3.2800	0.12	44.	44.	26.9146	8.92	X	X		0.13
3	3.6450	0.12	36.	44.	24.2202	7.37	X	X		0.11
4	4.3525	0.12	55.	44.	20.2846	11.21	X	X		0.17
5	4.8400	0.08	72.	44.	18.2426	14.79	X	X		0.13
6	6.1200	0.08	190.	44.	14.4297	38.99	X	X		0.11
7	7.1950	0.40	161.	44.	12.2760	33.02	X	X		0.78
8	8.9150	0.24	27.	44.	9.9110	5.54	X	X		0.32
9	9.6975	0.24	10.	44.	9.1130	2.10	X	X		0.11
10	10.2000	0.16	14.	44.	8.6651	2.96	X	X		0.29
11	10.3550	0.16	13.	44.	8.5358	2.65	X	X		0.13
12	12.9950	0.12	10.	44.	6.8070	2.10	X	X		0.21
13	13.8225	0.24	11.	44.	6.4013	2.23	X	X		0.13
14	15.4400	0.32	10.	45.	5.7342	2.10	X	X		0.10
15	17.1550	0.24	14.	45.	5.1646	2.80	X	X		0.19
16	18.1100	0.24	15.	46.	4.8943	3.11	X	X		0.28
17	19.8900	0.20	286.	46.	4.4602	58.48	X	X		3.47
18	20.3600	0.08	144.	46.	4.3582	29.48	X	X		0.13
19	20.9600	0.16	151.	46.	4.2348	30.98	X	X		0.87
20	21.2550	0.12	49.	48.	4.0818	10.03	X	X		0.14
21	22.0500	0.12	66.	48.	4.0275	13.43	X	X		0.46
22	23.7600	0.16	52.	48.	3.7417	10.61	X	X		0.11
23	24.7300	0.16	56.	48.	3.5971	11.52	X	X		0.35
24	25.8650	0.16	64.	49.	3.4418	13.10	X	X		0.21
25	26.7225	0.16	488.	49.	3.3333	100.00	X	X		4.68
26	27.4300	0.12	144.	49.	3.2489	29.48	X	X		0.78
27	27.8650	0.12	216.	49.	3.1991	44.24	X	X		1.05
28	28.1600	0.08	256.	49.	3.1663	52.41	X	X		0.54
29	28.4800	0.16	151.	49.	3.1314	30.98	X			1.12
30	28.5600	0.16	135.	49.	3.1228	27.55	X	X		0.27
31	29.0975	0.12	146.	50.	3.0664	29.98	X	X		0.32
32	29.5775	0.12	193.	50.	3.0177	39.56	X	X		0.69
33	30.0750	0.16	61.	50.	2.9689	12.46	X	X		0.22
34	30.9150	0.16	48.	50.	2.8901	9.75	X	X		0.55
35	31.9475	0.48	45.	50.	2.7990	9.19	X	X		1.74
36	32.8000	0.12	23.	52.	2.7282	4.72	X	X		0.13
37	33.5900	0.12	18.	52.	2.6658	3.79	X	X		0.13
38	34.6800	0.08	90.	52.	2.5845	18.48	X	X		0.13
39	34.9500	0.48	149.	52.	2.5651	30.47	X	X		3.16
40	35.6250	0.24	125.	52.	2.5181	25.68	X	X		0.15
41	36.7200	0.08	123.	53.	2.4454	25.23	X	X		0.11
42	37.8800	0.12	61.	53.	2.3732	12.46	X	X		0.10
43	38.5050	0.12	90.	53.	2.3361	18.48	X	X		0.79
44	39.5475	0.12	83.	53.	2.2769	16.96	X	X		0.76
45	40.3650	0.12	62.	55.	2.2326	12.78	X	X		0.25
46	41.6200	0.16	69.	55.	2.1682	14.10	X	X		0.66
47	42.2800	0.08	79.	55.	2.1358	16.22	X			0.16
48	42.4800	0.32	66.	55.	2.1262	13.43	X	X		0.35
49	43.4600	0.40	45.	55.	2.0805	9.19	X	X		0.78
50	44.6925	0.12	56.	56.	2.0260	11.52	X	X		0.36
51	45.1750	0.12	23.	56.	2.0055	4.72	X	X		0.16
52	45.4675	0.12	19.	56.	1.9932	3.96	X	X		0.12
53	46.2725	0.12	16.	56.	1.9604	3.28	X	X		0.17
54	47.7950	0.24	22.	58.	1.9015	4.52	X	X		0.25
55	48.6400	0.08	32.	58.	1.8704	6.65	X	X		0.10
56	50.1275	0.12	72.	58.	1.8183	14.79	X	X		0.44
57	51.4400	0.08	10.	59.	1.7749	2.10	X	X		0.13
58	51.9550	0.16	10.	59.	1.7586	2.10	X	X		0.30
59	53.4000	0.08	21.	56.	1.7143	4.33	X	X		0.11
60	54.0700	0.12	74.	56.	1.6947	15.14	X	X		0.24
61	55.2675	0.12	52.	61.	1.6607	10.61	X	X		0.13
62	56.3900	0.16	22.	61.	1.6303	4.52	X	X		0.12
63	56.6850	0.12	22.	61.	1.6225	4.52	X	X		0.30
64	57.4050	0.24	17.	61.	1.6039	3.44	X	X		0.13
65	57.8550	0.12	14.	61.	1.5925	2.96	X	X		0.22
66	58.1575	0.12	14.	61.	1.5849	2.96	X			0.17
67	58.4400	0.08	12.	61.	1.5779	2.51	X	X		0.12
68	59.9900	0.24	48.	62.	1.5408	9.75	X	X		1.48
69	61.7700	0.12	139.	62.	1.5006	28.51	X			0.22
70	62.0525	0.20	172.	62.	1.4944	35.14	X	X		0.74
71	64.7100	0.16	12.	64.	1.4393	2.37	X			0.15
72	65.0200	0.12	106.	64.	1.4332	21.72	X	X		1.23
73	65.2400	0.08	66.	62.	1.4324	13.43		X		0.14
74	66.3275	0.12	16.	59.	1.4081	3.28	X	X		0.12
75	67.6475	0.12	32.	58.	1.3838	6.65	X	X		0.15
76	68.3600	0.08	71.	56.	1.3711	14.45	X	X		0.19
77	69.2700	0.24	10.	55.	1.3553	2.10	X	X		0.11

Table B31. Bentonite-Lime Cured at 23°C for 180 Days.

Peak no	Angle (deg)	Tip width (deg)	Peak (cts)	Backg (cts)	D spac (Ang)	I/Imax (%)	Type A1	A2	Ot	Sign
1	2.9000	0.12	29.	53.	30.4404	5.28	X	X		0.33
2	3.5125	0.16	38.	53.	25.1335	5.09	X	X		0.44
3	4.5600	0.32	22.	53.	19.3621	4.00	X	X		0.13
4	5.3175	0.32	34.	53.	16.6054	6.09	X	X		0.54
5	6.0800	0.08	64.	53.	14.5245	11.59	X	X		0.13
6	6.3200	0.08	71.	53.	13.9735	12.78	X	X		0.18
7	6.7250	0.12	88.	53.	13.1328	16.00	X	X		0.21
8	7.0575	0.12	110.	53.	12.5148	19.96	X	X		0.28
9	7.9225	0.12	106.	53.	11.1503	19.21	X	X		0.25
10	8.3500	0.24	83.	53.	10.5803	15.00	X	X		0.25
11	8.9600	0.16	59.	53.	9.8614	10.74	X	X		0.10
12	9.4600	0.12	19.	53.	9.3412	3.51	X	X		0.16
13	9.7550	0.12	19.	53.	9.0594	3.51	X	X		0.19
14	10.3600	0.08	14.	53.	8.5317	2.48	X	X		0.13
15	11.5250	0.12	10.	53.	7.6717	1.85	X	X		0.13
16	11.9875	0.16	10.	53.	7.3768	1.85	X	X		0.41
17	12.6600	0.24	10.	52.	6.9864	1.85	X	X		0.15
18	12.9200	0.48	10.	49.	6.8464	1.85	X	X		0.17
19	14.3850	0.24	10.	50.	6.1522	1.85	X	X		0.19
20	15.2725	0.24	10.	50.	5.7967	1.85	X	X		0.11
21	15.8000	0.08	10.	50.	5.6043	1.85	X	X		0.13
22	16.0250	0.32	10.	50.	5.5261	1.85	X	X		0.34
23	17.6400	0.08	15.	49.	5.0237	2.75	X	X		0.11
24	18.0000	0.16	17.	49.	4.9240	3.04	X	X		0.15
25	19.9075	0.16	279.	53.	4.4563	50.50	X	X		1.51
26	20.9800	0.12	240.	53.	4.2308	43.50	X	X		1.62
27	22.1600	0.16	42.	53.	4.0081	7.65	X	X		0.13
28	23.4275	0.12	38.	53.	3.7941	6.96	X	X		0.17
29	23.7675	0.16	42.	53.	3.7406	7.65	X	X		0.10
30	24.8800	0.08	50.	53.	3.5758	9.13	X	X		0.12
31	26.7225	0.16	552.	53.	3.3333	100.00	X	X		5.01
32	27.2000	0.08	146.	53.	3.2758	26.51	X	X		0.32
33	27.7450	0.12	174.	53.	3.2127	31.55	X	X		0.60
34	28.0675	0.12	193.	53.	3.1765	34.99	X	X		0.69
35	28.3600	0.08	123.	53.	3.1444	22.31	X	X		0.13
36	28.5950	0.24	108.	53.	3.1191	19.59	X	X		0.17
37	29.5550	0.16	185.	53.	3.0199	33.49	X	X		1.62
38	30.0000	0.08	71.	53.	2.9761	12.78	X	X		0.16
39	30.4175	0.24	41.	53.	2.9362	7.42	X	X		0.26
40	31.2800	0.08	29.	53.	2.8572	5.28	X	X		0.18
41	32.0225	0.12	79.	53.	2.7926	14.34	X	X		0.58
42	33.1575	0.32	14.	53.	2.6996	2.48	X	X		0.21
43	34.2000	0.08	14.	53.	2.6196	2.48	X	X		0.13
44	34.9725	0.12	151.	53.	2.5635	27.40	X	X		0.35
45	36.1600	0.08	142.	53.	2.4820	25.64	X	X		0.13
46	36.6400	0.16	142.	53.	2.4506	25.64	X	X		0.83
47	37.2225	0.24	81.	53.	2.4136	14.67	X	X		0.13
48	38.1925	0.12	37.	53.	2.3545	6.74	X	X		0.14
49	38.5500	0.12	86.	53.	2.3335	15.66	X	X		0.46
50	39.5275	0.16	83.	53.	2.2780	15.00	X	X		0.87
51	40.3975	0.12	50.	53.	2.2309	9.13	X	X		0.12
52	41.7350	0.12	37.	53.	2.1624	6.74	X	X		0.11
53	42.5150	0.12	61.	53.	2.1246	11.02	X	X		0.19
54	43.3650	0.12	49.	53.	2.0849	8.87	X	X		0.21
55	44.0450	0.16	38.	53.	2.0542	6.96	X	X		0.60
56	44.7800	0.12	50.	53.	2.0222	9.13	X	X		0.26
57	46.0925	0.16	31.	53.	1.9676	5.68	X	X		0.31
58	46.5175	0.12	18.	53.	1.9507	3.19	X	X		0.15
59	47.7200	0.16	38.	53.	1.9043	6.96	X	X		0.28
60	48.6875	0.16	20.	53.	1.8687	3.67	X	X		0.32
61	49.3600	0.08	15.	53.	1.8448	2.75	X	X		0.17
62	50.1925	0.24	74.	53.	1.8161	13.39	X	X		1.82
63	50.8525	0.12	26.	53.	1.7941	4.71	X	X		0.12
64	51.7725	0.16	10.	53.	1.7643	1.85	X	X		0.30
65	52.6025	0.16	23.	49.	1.7384	4.17	X	X		0.17
66	53.9525	0.32	41.	53.	1.6981	7.42	X	X		0.23
67	54.8875	0.12	81.	53.	1.6713	14.67	X	X		0.29
68	55.3200	0.08	55.	53.	1.6593	9.92	X	X		0.13
69	55.7650	0.12	31.	53.	1.6471	5.68	X	X		0.15
70	57.0050	0.12	20.	53.	1.6142	3.67	X	X		0.19
71	58.2525	0.12	34.	53.	1.5825	6.09	X	X		0.41
72	59.9275	0.16	55.	53.	1.5423	9.92	X	X		0.54
73	61.8675	0.12	193.	53.	1.4985	34.99	X			0.37
74	61.9725	0.12	196.	53.	1.4962	35.49	X	X		0.25
75	62.6600	0.24	46.	53.	1.4814	8.37	X	X		0.46

Table B32. Bentonite-Lime Cured at 50°C for 1 Day.

Peak no	Angle (deg)	Tip width (deg)	Peak (cts)	Backg (cts)	D spac (Ang)	I/Imax (%)	Type A1	A2	Qt	Sign
1	3.3975	0.12	10.	72.	25.9840	2.14	x	x		0.17
2	4.0675	0.12	10.	72.	21.7053	2.14	x	x		0.32
3	4.9500	0.16	25.	67.	17.8374	5.21	x	x		0.18
4	6.3525	0.12	81.	67.	13.9021	16.89	x	x		0.13
5	7.1675	0.12	128.	66.	12.3230	26.62	x	x		0.24
6	7.4000	0.08	119.	66.	11.9364	24.77	x	x		0.11
7	8.9100	0.12	53.	62.	9.9166	11.11	x	x		0.59
8	9.8775	0.16	10.	61.	8.9473	2.14	x	x		0.19
9	11.5550	0.24	10.	55.	7.6519	2.14	x	x		0.30
10	13.4200	0.12	10.	48.	6.5924	2.14	x	x		0.20
11	14.2725	0.12	13.	48.	6.2005	2.70	x	x		0.18
12	17.1575	0.12	10.	49.	5.1638	2.14	x	x		0.12
13	17.9675	0.12	21.	50.	4.9328	4.41	x	x		0.23
14	18.3700	0.16	18.	50.	4.8256	3.86	x	x		0.52
15	18.9325	0.12	12.	52.	4.6835	2.55	x	x		0.32
16	19.2125	0.12	12.	52.	4.6159	2.41	x	x		0.24
17	19.8425	0.20	303.	52.	4.4707	63.13	x	x		3.24
18	20.9100	0.12	119.	55.	4.2448	24.77	x	x		0.23
19	21.6000	0.08	53.	56.	4.1108	11.11	x	x		0.15
20	22.6800	0.08	55.	58.	3.9174	11.42	x			0.14
21	22.7600	0.08	52.	58.	3.9038	10.81	x	x		0.13
22	23.7075	0.16	49.	59.	3.7499	10.22	x	x		0.32
23	25.1600	0.08	32.	62.	3.5366	6.77	x	x		0.14
24	25.8100	0.12	83.	64.	3.4490	17.27	x	x		0.60
25	26.6600	0.20	480.	64.	3.3409	100.00	x	x		8.13
26	27.7200	0.08	119.	67.	3.2155	24.77	x	x		0.14
27	28.0700	0.12	119.	67.	3.1762	24.77	x	x		0.46
28	28.6150	0.24	92.	67.	3.1170	19.22	x	x		0.21
29	29.5350	0.20	161.	69.	3.0219	33.63	x	x		2.04
30	31.9500	0.16	56.	74.	2.7988	11.73	x	x		0.74
31	33.7250	0.12	10.	72.	2.6554	2.14	x	x		0.13
32	34.8325	0.16	135.	61.	2.5735	28.06	x	x		0.36
33	35.1875	0.24	139.	62.	2.5484	29.03	x	x		0.16
34	35.9800	0.24	132.	69.	2.4940	27.57	x	x		0.62
35	36.5250	0.20	121.	69.	2.4580	25.23	x	x		0.89
36	37.4475	0.12	53.	69.	2.3996	11.11	x	x		0.28
37	37.8400	0.08	45.	67.	2.3756	9.36	x	x		0.15
38	38.4200	0.12	45.	67.	2.3411	9.36	x	x		0.39
39	39.5200	0.24	66.	66.	2.2784	13.68	x	x		2.09
40	41.0775	0.12	25.	66.	2.1955	5.21	x	x		0.11
41	42.1250	0.12	32.	64.	2.1433	6.77	x	x		0.21
42	42.4475	0.32	42.	64.	2.1278	8.81	x	x		0.60
43	43.0500	0.12	31.	62.	2.0994	6.54	x	x		0.18
44	43.8225	0.12	22.	62.	2.0642	4.61	x	x		0.34
45	44.6000	0.08	29.	61.	2.0300	6.08	x	x		0.20
46	45.6975	0.16	34.	61.	1.9837	7.01	x	x		0.33
47	47.8400	0.08	23.	58.	1.8998	4.80	x	x		0.13
48	48.6550	0.32	14.	58.	1.8698	3.01	x	x		0.52
49	50.1000	0.12	64.	56.	1.8192	13.34	x	x		0.51
50	50.4800	0.08	40.	55.	1.8064	8.28	x	x		0.10
51	52.6500	0.12	79.	50.	1.7370	16.52	x	x		0.65
52	54.0225	0.24	66.	50.	1.6960	13.68	x	x		0.25
53	54.3650	0.16	96.	52.	1.6720	20.02	x	x		0.85
54	56.5825	0.24	25.	53.	1.6252	5.21	x	x		0.22
55	57.1625	0.24	27.	55.	1.6101	5.64	x	x		0.40
56	57.8225	0.24	14.	55.	1.5933	3.01	x	x		0.13
57	59.8575	0.12	37.	58.	1.5439	7.76	x			0.12
58	60.0350	0.12	38.	58.	1.5397	8.01	x	x		0.13
59	61.8900	0.56	180.	58.	1.4990	37.44	x	x		6.31
60	63.8450	0.12	18.	58.	1.4567	3.86	x	x		0.20
61	64.9850	0.12	50.	58.	1.4339	10.51	x			0.59
62	65.2000	0.08	32.	58.	1.4332	6.77		x		0.13
63	65.7350	0.32	14.	58.	1.4194	3.01	x	x		0.17
64	67.2100	0.12	18.	58.	1.3917	3.86	x			0.25
65	67.5100	0.12	25.	58.	1.3863	5.21	x	x		0.16
66	68.1475	0.12	56.	58.	1.3749	11.73	x	x		0.30
67	68.7525	0.12	12.	58.	1.3642	2.41	x	x		0.24

Table B33. Bentonite-Lime Cured at 50°C for 28 Days.

Peak no	Angle (deg)	Tip width (deg)	Peak (cts)	Backg (cts)	D spac (Ang)	I/Imax (%)	Type H1	H2	Ot	Sign
1	2.4400	0.08	45.	59.	36.1780	9.99	X	X		0.13
2	4.9800	0.08	23.	59.	18.0931	5.13	X	X		0.13
3	5.7550	0.12	37.	59.	15.3440	8.28	X	X		0.16
4	6.1600	0.16	55.	59.	14.3361	12.18	X	X		0.55
5	7.5600	0.08	106.	56.	11.6841	23.60	X	X		0.11
6	8.2000	0.24	76.	55.	10.7735	16.84	X	X		0.11
7	9.2925	0.12	24.	53.	9.5092	5.34	X	X		0.18
8	10.7025	0.12	10.	52.	8.2594	2.28	X	X		0.17
9	11.2800	0.08	10.	50.	7.8378	2.28	X	X		0.18
10	13.8275	0.12	19.	46.	6.3990	4.31	X	X		0.55
11	14.1500	0.16	10.	46.	6.2539	2.28	X	X		0.39
12	14.9850	0.32	12.	46.	5.9072	2.57	X	X		0.20
13	17.1350	0.12	11.	50.	5.1706	2.42	X	X		0.33
14	18.3075	0.12	24.	50.	4.8420	5.34	X	X		0.22
15	18.5200	0.08	20.	50.	4.7869	4.51	X	X		0.10
16	19.3325	0.12	15.	50.	4.5875	3.38	X	X		0.24
17	19.8750	0.24	292.	50.	4.4635	65.06	X	X		4.27
18	20.3450	0.12	149.	50.	4.3614	33.12	X	X		0.18
19	20.9425	0.12	130.	50.	4.2383	28.92	X	X		0.44
20	22.0275	0.12	83.	50.	4.0319	18.43	X	X		0.50
21	22.5925	0.12	45.	50.	3.9324	9.99	X	X		0.21
22	23.6500	0.12	71.	52.	3.7589	15.70	X	X		0.46
23	25.2125	0.16	49.	52.	3.5294	10.90	X	X		0.41
24	25.6700	0.12	74.	52.	3.4675	16.46	X	X		0.29
25	26.7175	0.16	449.	52.	3.3339	100.00	X	X		4.37
26	27.1600	0.08	86.	52.	3.2805	19.24	X	X		0.21
27	27.4100	0.12	104.	52.	3.2512	23.15	X	X		0.48
28	27.7900	0.12	159.	52.	3.2076	35.32	X	X		0.60
29	28.1600	0.16	108.	52.	3.1663	24.07	X	X		0.35
30	29.5650	0.16	174.	53.	3.0189	38.77	X	X		1.62
31	30.4050	0.12	37.	53.	2.9374	8.28	X	X		0.19
32	30.8625	0.12	44.	53.	2.8949	9.69	X	X		0.36
33	32.0750	0.12	56.	53.	2.7882	12.52	X	X		0.22
34	33.1575	0.24	22.	53.	2.6996	4.92	X	X		0.74
35	33.7850	0.12	27.	53.	2.6509	6.02	X	X		0.23
36	35.0475	0.12	151.	53.	2.5582	33.66	X	X		0.10
37	35.2725	0.12	156.	53.	2.5424	34.77	X	X		0.25
38	36.0875	0.12	139.	55.	2.4868	30.98	X	X		0.26
39	36.6275	0.16	161.	55.	2.4514	35.89	X	X		0.98
40	37.6000	0.08	64.	55.	2.3902	14.24	X	X		0.11
41	38.5150	0.12	79.	55.	2.3355	17.62	X	X		0.36
42	39.5225	0.16	59.	55.	2.2783	13.19	X	X		0.60
43	40.2000	0.16	45.	55.	2.2414	9.99	X	X		0.35
44	40.4000	0.32	35.	55.	2.2308	7.75	X	X		0.10
45	41.6725	0.32	37.	56.	2.1655	8.28	X	X		0.51
46	42.3875	0.32	46.	56.	2.1307	10.29	X	X		0.44
47	43.3325	0.12	50.	56.	2.0864	11.22	X	X		0.35
48	43.6750	0.12	32.	56.	2.0708	7.23	X	X		0.12
49	44.7300	0.12	69.	56.	2.0244	15.33	X	X		0.58
50	45.9125	0.16	36.	56.	1.9749	8.01	X	X		0.42
51	46.3200	0.16	14.	56.	1.9585	3.05	X	X		0.10
52	46.7200	0.08	11.	56.	1.9427	2.42	X	X		0.16
53	47.0400	0.16	15.	56.	1.9302	3.39	X	X		0.12
54	47.9925	0.12	10.	56.	1.8941	2.28	X	X		0.23
55	48.7175	0.12	17.	58.	1.8676	3.74	X	X		0.11
56	50.1050	0.12	58.	58.	1.8191	12.85	X			0.34
57	50.2650	0.16	36.	58.	1.8181	8.01		X		0.42
58	50.8225	0.32	18.	58.	1.7951	3.92	X	X		0.85
59	51.2800	0.12	10.	58.	1.7801	2.28	X	X		0.15
60	52.0425	0.24	10.	53.	1.7558	2.28	X	X		0.40
61	52.6300	0.16	21.	49.	1.7376	4.71	X	X		0.34
62	54.1125	0.16	67.	58.	1.6934	14.96	X	X		0.25
63	54.8800	0.08	77.	59.	1.6715	17.23	X	X		0.18
64	55.4300	0.12	41.	59.	1.6563	9.11	X	X		0.32
65	55.9325	0.12	29.	59.	1.6426	6.49	X	X		0.40
66	56.7500	0.12	15.	59.	1.6208	3.38	X	X		0.24
67	57.5050	0.20	17.	59.	1.6013	3.74	X	X		0.54
68	58.2400	0.16	10.	59.	1.5829	2.28	X	X		0.11
69	58.8800	0.16	16.	59.	1.5672	3.56	X	X		0.47
70	59.9950	0.12	42.	58.	1.5407	9.40	X	X		0.12
71	60.6675	0.32	21.	58.	1.5252	4.71	X	X		0.30
72	61.9525	0.20	207.	61.	1.4966	46.14	X	X		1.35
73	64.0075	0.12	22.	61.	1.4534	4.92	X	X		0.16
74	65.0200	0.12	117.	61.	1.4332	25.95	X	X		1.02
75	66.7475	0.12	12.	61.	1.4003	2.57	X	X		0.35
76	67.2650	0.12	29.	61.	1.3907	6.49	X	X		0.36
77	67.7125	0.12	41.	61.	1.3826	9.11	X	X		0.40
78	68.1200	0.08	48.	61.	1.3754	10.59	X	X		0.17
79	69.4000	0.08	13.	61.	1.3531	2.88	X	X		0.11

Table B34. Bentonite-Lime Cured at 50°C for 90 Days.

Peak no	Angle (deg)	Tip width (deg)	Peak (cts)	Backg (cts)	D spac (Ang)	I/Imax (%)	Type H1	Type H2	Type Ot	Sign
1	2.0800	0.08	90.	46.	42.4387	21.06	X	X		0.13
2	3.4600	0.16	29.	46.	25.5148	6.81	X	X		0.36
3	4.5675	0.24	40.	46.	19.3303	9.26	X	X		0.15
4	6.0050	0.16	130.	46.	14.7058	30.33	X	X		0.41
5	6.4250	0.24	154.	46.	13.7454	35.88	X	X		0.21
6	6.8225	0.12	156.	46.	12.9454	36.47	X	X		0.12
7	7.2475	0.12	132.	46.	12.1872	30.86	X	X		0.12
8	7.7625	0.16	66.	46.	11.3797	15.31	X	X		0.19
9	8.2800	0.08	40.	46.	10.6696	9.26	X	X		0.15
10	8.9850	0.16	24.	46.	9.8340	5.60	X	X		0.23
11	10.4425	0.24	10.	46.	8.4644	2.39	X	X		0.11
12	11.5600	0.08	10.	46.	7.6486	2.39	X	X		0.12
13	12.8800	0.32	10.	44.	6.8675	2.39	X	X		0.11
14	13.6725	0.24	10.	41.	6.4712	2.39	X	X		0.16
15	14.1475	0.16	14.	41.	6.2550	3.19	X	X		0.19
16	14.4200	0.16	17.	40.	6.1374	3.92	X	X		0.32
17	14.9025	0.24	10.	42.	5.9397	2.39	X	X		0.12
18	17.0800	0.08	14.	46.	5.1871	3.37	X	X		0.12
19	17.3150	0.12	12.	46.	5.1172	2.70	X	X		0.14
20	17.6375	0.12	16.	46.	5.0244	3.73	X	X		0.11
21	17.8400	0.32	12.	46.	4.9678	2.86	X	X		0.12
22	18.7200	0.16	12.	48.	4.7362	2.70	X	X		0.10
23	19.9325	0.20	259.	48.	4.4507	60.49	X	X		2.75
24	21.0150	0.12	128.	50.	4.2239	29.80	X	X		0.59
25	21.4400	0.08	74.	50.	4.1411	17.26	X	X		0.16
26	22.2175	0.12	45.	50.	3.9979	10.48	X	X		0.20
27	23.8800	0.08	64.	52.	3.7232	14.94	X	X		0.11
28	24.8125	0.20	49.	53.	3.5853	11.44	X	X		0.59
29	25.3600	0.08	44.	53.	3.5092	10.17	X	X		0.13
30	25.8950	0.16	52.	55.	3.4379	12.10	X	X		0.42
31	26.7950	0.16	428.	55.	3.3244	100.00	X	X		4.68
32	27.4550	0.12	146.	56.	3.2460	34.17	X	X		0.48
33	27.8375	0.12	85.	56.	3.2022	19.75	X	X		0.36
34	28.1450	0.16	92.	56.	3.1679	21.51	X	X		0.52
35	28.5125	0.12	100.	56.	3.1279	23.34	X	X		0.26
36	28.9150	0.12	128.	58.	3.0853	29.80	X	X		0.23
37	29.3600	0.08	146.	58.	3.0395	34.17	X	X		0.12
38	29.6300	0.16	182.	58.	3.0125	42.53	X	X		1.23
39	30.9700	0.32	35.	59.	2.8851	8.12	X	X		0.62
40	32.0700	0.20	94.	61.	2.7886	21.96	X	X		1.70
41	34.9250	0.16	164.	62.	2.5669	38.24	X	X		0.79
42	35.5675	0.16	135.	62.	2.5220	31.40	X	X		0.19
43	36.7175	0.12	117.	62.	2.4456	27.22	X	X		0.17
44	38.5025	0.12	213.	62.	2.3362	49.75	X	X		1.02
45	39.0000	0.08	34.	62.	2.3076	7.85	X	X		0.13
46	39.6250	0.12	81.	62.	2.2726	18.90	X	X		0.79
47	40.1700	0.12	48.	62.	2.2430	11.11	X	X		0.26
48	40.9475	0.12	31.	62.	2.2022	7.32	X	X		0.23
49	41.3475	0.16	31.	62.	2.1818	7.32	X	X		0.13
50	41.9200	0.16	37.	62.	2.1533	8.68	X	X		0.11
51	42.5775	0.40	55.	62.	2.1216	12.78	X	X		1.15
52	43.2150	0.12	40.	62.	2.0918	9.26	X	X		0.15
53	43.4675	0.32	40.	62.	2.0802	9.26	X	X		0.36
54	44.2600	0.12	94.	62.	2.0448	21.96	X	X		0.74
55	44.7300	0.24	50.	62.	2.0244	11.76	X	X		0.91
56	45.6400	0.08	22.	62.	1.9861	5.16	X			0.10
57	45.7675	0.24	18.	62.	1.9809	4.32	X	X		0.14
58	47.0500	0.12	10.	62.	1.9298	2.39	X			0.17
59	47.2000	0.16	10.	62.	1.9240	2.39	X	X		0.10
60	47.8825	0.32	17.	62.	1.8982	3.92	X	X		0.48
61	48.7650	0.12	22.	62.	1.8659	5.16	X	X		0.28
62	50.2075	0.32	59.	62.	1.8156	13.84	X	X		3.39
63	51.1600	0.08	13.	61.	1.7840	3.02	X	X		0.11
64	51.4825	0.12	22.	62.	1.7736	5.16	X	X		0.10
65	52.8950	0.12	27.	59.	1.7295	6.31	X	X		0.52
66	54.1200	0.08	71.	62.	1.6932	16.47	X	X		0.10
67	54.9475	0.12	104.	62.	1.6697	24.28	X	X		0.44
68	56.0325	0.12	26.	62.	1.6399	6.07	X	X		0.22
69	56.6800	0.08	22.	62.	1.6227	5.16	X	X		0.10
70	57.1850	0.16	17.	62.	1.6095	3.92	X	X		0.27
71	57.8675	0.80	13.	62.	1.5922	3.02	X	X		0.34
72	59.1000	0.24	10.	62.	1.5619	2.39	X	X		0.12
73	60.1850	0.12	37.	62.	1.5363	8.68	X	X		0.28
74	62.1275	0.12	250.	62.	1.4928	58.26	X	X		0.63
75	64.1250	0.24	18.	62.	1.4510	4.32	X	X		0.27

Table B35. Bentonite-Lime Cured at 50°C for 180 Days.

Peak no	Angle (deg)	Tip width (deg)	Peak (cts)	Backg (cts)	D spac (Ang)	I/Imax (%)	Type K1	Type K2	Type Qt	Sign
1	2.6075	0.16	15.	53.	33.3544	2.30	X	X		0.23
2	4.6450	0.12	14.	53.	19.0079	2.61	X	X		0.15
3	5.1975	0.12	19.	53.	16.9885	3.69	X	X		0.15
4	6.0400	0.08	45.	53.	14.6206	8.56	X	X		0.21
5	6.3200	0.08	44.	52.	13.9735	8.31	X	X		0.12
6	6.7200	0.08	61.	52.	13.1426	11.60	X	X		0.11
7	8.0250	0.12	64.	50.	11.0081	12.20	X	X		0.21
8	8.7800	0.40	40.	50.	10.0631	7.57	X	X		0.34
9	9.3500	0.12	24.	50.	9.4509	4.58	X	X		0.14
10	9.6650	0.12	14.	49.	9.1436	2.75	X	X		0.13
11	10.2875	0.12	12.	49.	8.5916	2.34	X	X		0.11
12	11.2800	0.08	13.	48.	7.8378	2.47	X	X		0.12
13	12.2375	0.12	10.	48.	7.2266	1.95	X	X		0.23
14	12.7575	0.12	10.	46.	6.9332	1.95	X	X		0.13
15	13.0850	0.16	10.	46.	6.7604	1.95	X	X		0.26
16	15.3125	0.12	11.	44.	5.7816	2.08	X	X		0.13
17	15.6350	0.12	17.	44.	5.6631	3.21	X	X		0.34
18	16.5900	0.12	16.	44.	5.3392	3.05	X	X		0.10
19	17.4225	0.24	16.	44.	5.0859	3.05	X	X		0.13
20	17.8075	0.12	18.	44.	4.9768	3.53	X	X		0.23
21	18.8125	0.12	25.	44.	4.7131	4.77	X	X		0.21
22	19.8900	0.20	228.	44.	4.4602	43.48	X	X		2.75
23	20.3350	0.12	119.	44.	4.3635	22.66	X	X		0.25
24	20.9325	0.12	156.	44.	4.2403	29.80	X	X		0.74
25	22.2325	0.12	55.	44.	3.9952	10.44	X	X		0.15
26	22.5275	0.12	52.	44.	3.9436	9.89	X	X		0.24
27	23.0400	0.08	52.	44.	3.8570	9.89	X	X		0.26
28	23.2875	0.12	41.	44.	3.8166	7.81	X	X		0.17
29	23.6650	0.12	58.	44.	3.7565	11.01	X	X		0.22
30	25.3275	0.16	61.	44.	3.5136	11.60	X	X		0.74
31	26.6975	0.12	524.	44.	3.3363	100.00	X	X		2.34
32	28.1200	0.08	121.	44.	3.1707	23.07	X	X		0.14
33	28.4500	0.16	114.	44.	3.1347	21.83	X	X		0.48
34	29.5550	0.16	151.	44.	3.0199	28.85	X	X		1.41
35	30.6125	0.16	71.	44.	2.9180	13.46	X	X		0.85
36	30.9550	0.12	55.	44.	2.8865	10.44	X	X		0.19
37	31.9975	0.16	69.	44.	2.7948	13.14	X	X		0.69
38	32.4400	0.08	79.	44.	2.7576	15.10	X	X		0.14
39	32.8400	0.08	36.	44.	2.7250	6.86	X	X		0.11
40	33.0800	0.08	37.	44.	2.7057	7.10	X	X		0.17
41	33.4550	0.12	56.	44.	2.6763	10.73	X	X		0.36
42	33.8975	0.12	40.	44.	2.6423	7.57	X	X		0.30
43	34.8025	0.12	110.	44.	2.5757	21.02	X	X		0.14
44	35.4400	0.08	139.	44.	2.5308	26.55	X			0.11
45	35.5200	0.16	137.	44.	2.5253	26.10	X	X		0.14
46	36.0550	0.12	114.	44.	2.4890	21.83	X	X		0.21
47	36.6450	0.20	110.	44.	2.4503	21.02	X	X		0.56
48	38.5250	0.16	81.	44.	2.3349	15.45	X	X		1.29
49	39.5075	0.12	88.	44.	2.2791	16.85	X	X		0.51
50	40.3125	0.12	62.	44.	2.2354	11.90	X	X		0.29
51	41.5350	0.24	40.	44.	2.1724	7.57	X	X		0.17
52	42.3725	0.32	46.	44.	2.1314	8.82	X	X		0.31
53	42.9775	0.12	62.	44.	2.1028	11.90	X	X		0.39
54	43.2800	0.08	50.	44.	2.0898	9.61	X	X		0.10
55	44.2900	0.12	32.	44.	2.0434	6.20	X	X		0.15
56	44.7250	0.20	62.	44.	2.0246	11.90	X	X		1.32
57	45.9150	0.16	34.	44.	1.9748	6.41	X	X		0.29
58	46.2000	0.08	29.	44.	1.9633	5.56	X	X		0.13
59	46.4425	0.20	29.	44.	1.9536	5.56	X	X		0.52
60	46.9600	0.32	29.	44.	1.9333	5.56	X	X		0.25
61	47.7950	0.16	40.	44.	1.9015	7.57	X	X		0.36
62	48.5375	0.12	30.	44.	1.8741	5.77	X	X		0.25
63	49.7600	0.16	27.	44.	1.8309	5.16	X	X		0.15
64	50.1575	0.24	110.	44.	1.8173	21.02	X	X		3.39
65	50.9375	0.24	27.	44.	1.7913	5.16	X	X		0.35
66	51.6500	0.24	14.	44.	1.7682	2.75	X	X		0.14
67	52.2400	0.08	24.	44.	1.7496	4.58	X	X		0.11
68	53.8000	0.08	55.	44.	1.7025	10.44	X	X		0.15
69	54.1325	0.48	62.	44.	1.6928	11.90	X	X		0.51
70	55.2700	0.12	50.	44.	1.6607	9.61	X	X		0.12
71	56.7675	0.24	25.	44.	1.6204	4.77	X	X		0.14
72	57.2000	0.20	24.	44.	1.6091	4.58	X			0.30
73	57.4900	0.16	32.	44.	1.6017	6.20	X	X		0.25
74	58.3000	0.12	25.	44.	1.5814	4.77	X	X		0.11
75	59.1325	0.24	29.	44.	1.5599	5.56	X	X		0.30

Table B36. Bentonite-Fly Ash-Lime Cured at 23°C for 1 Day.

Peak no	Angle (deg)	Tip width (deg)	Peak (cts)	Backg (cts)	D spac (Ang)	I Imax (%)	Type A1	Type A2	Type Ot	Sign
1	2.1550	0.12	49.	55.	40.9619	9.68	X	X		0.20
2	3.0300	0.12	19.	55.	29.1347	3.48	X	X		0.25
3	3.2800	0.08	19.	55.	26.9146	3.82	X	X		0.16
4	3.7000	0.12	10.	55.	23.8603	2.02	X	X		0.21
5	4.2700	0.12	14.	55.	20.6764	2.85	X	X		0.34
6	4.7575	0.16	19.	55.	18.5587	3.82	X	X		0.17
7	6.3850	0.12	79.	55.	13.8314	15.65	X	X		0.25
8	7.8000	0.08	76.	55.	11.3251	14.95	X	X		0.11
9	8.9200	0.08	31.	55.	9.9055	6.19	X	X		0.18
10	9.3600	0.16	21.	55.	9.4408	4.18	X	X		0.47
11	11.2700	0.12	10.	55.	7.8447	2.02	X	X		0.13
12	12.6225	0.16	10.	52.	7.0070	2.02	X	X		0.26
13	12.8900	0.08	10.	50.	6.8675	2.02	X	X		0.13
14	13.4875	0.12	14.	50.	6.5595	2.70	X	X		0.23
15	14.4975	0.64	10.	50.	6.1047	2.02	X	X		0.35
16	16.0800	0.16	10.	53.	5.5073	2.02	X	X		0.10
17	17.3200	0.08	12.	52.	5.1157	2.42	X	X		0.10
18	17.7675	0.12	15.	50.	4.9879	3.00	X	X		0.22
19	19.9025	0.20	216.	55.	4.4574	42.68	X	X		2.40
20	20.9475	0.12	142.	55.	4.2373	27.97	X	X		0.98
21	22.1525	0.12	34.	55.	4.0095	6.64	X	X		0.17
22	22.5125	0.12	45.	55.	3.9462	8.87	X	X		0.20
23	22.8650	0.16	31.	55.	3.8861	6.19	X	X		0.17
24	23.2725	0.12	37.	55.	3.8190	7.35	X	X		0.14
25	23.7200	0.16	71.	55.	3.7479	13.94	X	X		0.85
26	24.7325	0.12	49.	55.	3.5968	9.68	X	X		0.40
27	26.7200	0.16	506.	55.	3.3336	100.00	X	X		4.90
28	27.3875	0.12	166.	55.	3.2538	32.87	X	X		1.51
29	27.8125	0.12	76.	55.	3.2050	14.95	X	X		0.26
30	28.1100	0.12	94.	55.	3.1718	18.59	X	X		0.31
31	28.5625	0.12	106.	55.	3.1226	20.96	X	X		0.30
32	29.0150	0.12	104.	55.	3.0749	20.55	X	X		0.30
33	29.5725	0.12	202.	55.	3.0182	39.83	X	X		0.91
34	30.1125	0.12	69.	55.	2.9653	13.61	X	X		0.19
35	30.6000	0.08	45.	55.	2.9191	8.87	X	X		0.12
36	30.9700	0.12	48.	55.	2.8851	9.40	X	X		0.18
37	31.9850	0.12	59.	55.	2.7958	11.71	X	X		0.13
38	33.3450	0.40	34.	55.	2.6848	6.64	X	X		0.49
39	33.9600	0.08	31.	55.	2.6376	6.19	X	X		0.11
40	35.0400	0.16	142.	55.	2.5587	27.97	X	X		0.50
41	35.5500	0.20	123.	55.	2.5232	24.34	X	X		0.43
42	35.8800	0.08	112.	55.	2.5007	22.19	X			0.19
43	36.0000	0.16	102.	55.	2.4927	20.15	X	X		0.10
44	36.5725	0.28	117.	55.	2.4550	23.04	X	X		1.70
45	37.7800	0.12	49.	55.	2.3792	9.68	X	X		0.20
46	38.5175	0.16	79.	55.	2.3354	15.65	X	X		1.26
47	39.4850	0.16	55.	55.	2.2803	10.82	X	X		0.56
48	40.2600	0.24	41.	55.	2.2382	8.09	X	X		0.18
49	40.9275	0.12	40.	55.	2.2032	7.84	X	X		0.26
50	42.2000	0.08	41.	55.	2.1397	8.09	X	X		0.11
51	42.5150	0.12	66.	55.	2.1246	12.96	X	X		0.11
52	43.5300	0.48	36.	55.	2.0773	7.11	X	X		0.16
53	44.7175	0.16	53.	55.	2.0249	10.53	X	X		0.65
54	45.8450	0.48	26.	55.	1.9777	5.14	X	X		0.76
55	46.7450	0.12	10.	55.	1.9417	2.02	X	X		0.18
56	47.1600	0.08	14.	55.	1.9256	2.85	X	X		0.11
57	47.7825	0.24	19.	55.	1.9019	3.82	X	X		0.20
58	48.3100	0.12	14.	55.	1.8824	2.85	X	X		0.21
59	48.7475	0.24	23.	55.	1.8665	4.55	X	X		0.37
60	49.3600	0.16	24.	55.	1.8448	4.74	X	X		0.13
61	50.1875	0.20	92.	55.	1.8163	18.20	X	X		1.70
62	51.5375	0.24	11.	55.	1.7718	2.15	X	X		0.19
63	52.4300	0.24	14.	55.	1.7437	2.85	X	X		0.19
64	52.8850	0.12	23.	55.	1.7298	4.55	X	X		0.12
65	54.0150	0.40	53.	55.	1.6963	10.53	X	X		0.85
66	54.8925	0.32	58.	55.	1.6712	11.41	X	X		0.36
67	56.4450	0.12	28.	55.	1.6289	5.55	X	X		0.30
68	57.6875	0.16	24.	55.	1.5967	4.74	X	X		0.52
69	58.3450	0.12	14.	55.	1.5803	2.85	X	X		0.14
70	58.7050	0.12	16.	55.	1.5714	3.16	X	X		0.17
71	59.9150	0.36	53.	55.	1.5425	10.53	X	X		2.45
72	60.7200	0.08	24.	55.	1.5240	4.74	X	X		0.13
73	61.8275	0.12	142.	55.	1.4993	27.97	X	X		0.30
74	62.9200	0.08	28.	55.	1.4759	5.55	X			0.14
75	63.2175	0.12	19.	55.	1.4733	3.82		X		0.25

Table B37. Bentonite-Fly Ash-Lime Cured at 23°C for 28 Days.

Peak no	Angle (deg)	Tip width (deg)	Peak (cts)	Backg (cts)	D spac (Ang)	I Imax (%)	Type H1	H2	Qt	Sign
1	2.8800	0.12	34.	53.	30.6517	4.90	X	X		0.10
2	3.4900	0.24	15.	53.	25.2955	2.22	X	X		0.25
3	4.4025	0.16	18.	53.	20.0544	2.57	X	X		0.29
4	5.4900	0.08	29.	53.	16.1134	4.25	X	X		0.10
5	5.9200	0.08	34.	53.	14.9167	4.90	X	X		0.15
6	6.9975	0.24	49.	53.	12.8048	7.14	X	X		0.20
7	7.9500	0.16	59.	53.	11.1113	8.34	X	X		0.17
8	8.4300	0.32	41.	53.	10.3916	5.97	X	X		0.14
9	10.4800	0.08	18.	53.	8.4865	2.57	X	X		0.14
10	10.9850	0.24	10.	53.	8.0476	1.49	X	X		0.11
11	12.2150	0.32	10.	53.	7.2399	1.49	X	X		0.29
12	12.7800	0.32	10.	53.	6.9210	1.49	X	X		0.49
13	14.6700	0.12	10.	49.	6.0334	1.49	X	X		0.16
14	15.2750	0.12	10.	49.	5.7957	1.49	X	X		0.16
15	16.9150	0.12	10.	49.	5.2373	1.49	X	X		0.23
16	18.5500	0.12	29.	52.	4.7792	4.25	X	X		0.19
17	19.8900	0.20	216.	53.	4.4602	31.48	X	X		2.09
18	20.9200	0.16	112.	53.	4.2428	16.37	X	X		1.05
19	21.5775	0.12	49.	53.	4.1150	7.14	X	X		0.22
20	22.0650	0.12	132.	53.	4.0252	19.27	X	X		1.29
21	23.1725	0.16	45.	53.	3.8352	6.54	X	X		0.45
22	23.7200	0.08	46.	53.	3.7479	6.74	X	X		0.14
23	24.3675	0.12	37.	53.	3.6498	5.42	X	X		0.16
24	24.7600	0.08	35.	53.	3.5928	5.07	X	X		0.10
25	25.4450	0.20	50.	53.	3.4976	7.34	X	X		1.00
26	26.7225	0.16	686.	53.	3.3333	100.00	X	X		6.92
27	27.7850	0.12	159.	53.	3.2082	23.13	X	X		0.87
28	29.5625	0.16	146.	53.	3.0192	21.33	X	X		1.23
29	30.4800	0.08	46.	53.	2.9304	6.74	X	X		0.13
30	30.9100	0.24	38.	53.	2.8906	5.60	X	X		0.28
31	31.4225	0.12	37.	53.	2.8446	5.42	X	X		0.22
32	31.9925	0.16	61.	53.	2.7952	8.86	X	X		0.41
33	33.2150	0.12	45.	53.	2.6950	6.54	X	X		0.41
34	33.4675	0.12	34.	53.	2.6753	4.90	X	X		0.17
35	34.7200	0.08	71.	53.	2.5816	10.28	X	X		0.13
36	34.9550	0.32	100.	53.	2.5648	14.57	X	X		0.65
37	35.4500	0.32	117.	53.	2.5301	16.99	X	X		0.34
38	36.6375	0.12	100.	53.	2.4508	14.57	X	X		0.11
39	37.8150	0.12	45.	53.	2.3771	6.54	X	X		0.22
40	38.5175	0.16	92.	53.	2.3354	13.43	X	X		1.45
41	39.5150	0.20	61.	53.	2.2787	8.86	X	X		0.76
42	40.2800	0.16	53.	53.	2.2371	7.76	X	X		0.35
43	42.1275	0.12	41.	53.	2.1432	5.97	X	X		0.26
44	42.4275	0.12	46.	53.	2.1287	6.74	X	X		0.22
45	42.9875	0.24	41.	53.	2.1023	5.97	X	X		0.17
46	43.3400	0.16	38.	53.	2.0860	5.60	X	X		0.23
47	43.6850	0.12	31.	53.	2.0703	4.57	X	X		0.17
48	43.9200	0.08	26.	53.	2.0598	3.79	X	X		0.10
49	44.7875	0.12	61.	53.	2.0219	8.86	X	X		0.30
50	45.8225	0.12	45.	53.	1.9786	6.54	X	X		0.30
51	47.7750	0.12	53.	53.	1.9022	7.76	X	X		0.47
52	48.9100	0.12	20.	53.	1.8607	2.95	X	X		0.25
53	49.2650	0.12	15.	53.	1.8481	2.22	X	X		0.14
54	50.1100	0.12	79.	53.	1.8189	11.54	X	X		0.32
55	52.2325	0.12	11.	53.	1.7499	1.59	X	X		0.17
56	52.6300	0.16	15.	53.	1.7376	2.22	X	X		0.18
57	53.1075	0.12	14.	53.	1.7231	1.99	X	X		0.19
58	53.9450	0.40	46.	53.	1.6993	6.74	X	X		1.10
59	54.8400	0.12	61.	53.	1.6727	8.86	X	X		0.11
60	55.4075	0.32	38.	53.	1.6569	5.60	X	X		0.41
61	56.2400	0.12	24.	53.	1.6343	3.50	X	X		0.10
62	56.6275	0.12	26.	53.	1.6240	3.79	X	X		0.15
63	57.6450	0.16	20.	53.	1.5978	2.95	X	X		0.17
64	58.9350	0.12	20.	53.	1.5658	2.95	X	X		0.31
65	59.2400	0.08	20.	53.	1.5585	2.95	X	X		0.12
66	59.3675	0.16	55.	53.	1.5437	7.98	X	X		0.36
67	61.7750	0.12	123.	53.	1.5005	17.95	X			0.31
68	62.0350	0.12	139.	53.	1.4948	20.28	X	X		0.18
69	63.6275	0.12	11.	53.	1.4612	1.59	X	X		0.22
70	64.1875	0.12	18.	53.	1.4498	2.57	X	X		0.29
71	65.0525	0.12	100.	53.	1.4326	14.57	X	X		0.65
72	65.5825	0.12	29.	52.	1.4223	4.25	X	X		0.23
73	66.2850	0.12	15.	53.	1.4089	2.22	X	X		0.23
74	66.9125	0.12	18.	53.	1.3972	2.57	X	X		0.26
75	67.6525	0.12	42.	53.	1.3837	6.15	X	X		0.31
76	68.0525	0.12	50.	53.	1.3766	7.34	X			0.24
77	68.2900	0.12	49.	53.	1.3723	7.14	X	X		0.14
78	69.4475	0.16	26.	53.	1.3523	3.79	X	X		0.49

Table B38. Bentonite-Fly Ash-Lime Cured at 23°C for 90 Days.

Peak no	Angle (deg)	Tip width (deg)	Peak (cts)	Backg (cts)	D spac (Ang)	I Inst (%)	Type #1	Type #2	Sign
1	2.6075	0.12	38.	83.	33.8544	7.80	X	X	0.32
2	3.5625	0.12	10.	83.	24.7809	2.08	X	X	0.22
3	4.6800	0.08	10.	79.	18.8659	2.08	X	X	0.16
4	6.8950	0.16	92.	83.	12.8094	18.70	X	X	0.34
5	8.7600	0.08	10.	71.	10.0860	2.08	X	X	0.10
6	11.8400	0.08	10.	48.	7.4683	2.08	X	X	0.15
7	12.4200	0.16	10.	48.	7.1208	2.08	X	X	0.45
8	15.2900	0.12	10.	45.	5.7901	2.08	X	X	0.13
9	16.5775	0.24	12.	45.	5.3432	2.35	X	X	0.11
10	17.7150	0.12	22.	45.	5.0026	4.48	X	X	0.26
11	17.9600	0.08	14.	45.	4.9349	2.93	X	X	0.11
12	18.2050	0.12	27.	45.	4.8690	5.49	X	X	0.34
13	19.8625	0.20	237.	45.	4.4663	48.12	X	X	2.82
14	20.9350	0.12	132.	45.	4.2398	26.83	X	X	0.62
15	22.0525	0.12	56.	46.	4.0274	11.41	X	X	0.15
16	22.6725	0.12	41.	46.	3.9187	8.31	X	X	0.20
17	22.9200	0.08	48.	46.	3.8769	9.66	X	X	0.17
18	23.0875	0.32	41.	46.	3.8492	8.31	X	X	0.13
19	23.7925	0.12	55.	46.	3.7367	11.11	X	X	0.21
20	24.1175	0.12	45.	46.	3.6871	9.11	X	X	0.25
21	24.3675	0.12	42.	46.	3.6498	8.57	X	X	0.22
22	24.6075	0.12	42.	46.	3.6147	8.57	X	X	0.14
23	24.9150	0.12	48.	46.	3.5708	9.66	X	X	0.14
24	25.1200	0.08	53.	46.	3.5421	10.81	X	X	0.17
25	26.6825	0.16	493.	46.	3.3382	100.00	X	X	5.01
26	27.1950	0.12	77.	46.	3.2764	15.71	X	X	0.22
27	27.7450	0.12	151.	46.	3.2127	30.70	X	X	1.23
28	28.9600	0.08	109.	46.	3.0806	21.95	X	X	0.13
29	29.6025	0.16	128.	46.	3.0152	25.91	X	X	0.87
30	30.2325	0.12	55.	46.	2.9538	11.11	X	X	0.22
31	30.5850	0.12	48.	46.	2.9205	9.66	X	X	0.16
32	30.8725	0.12	44.	46.	2.8940	8.84	X	X	0.20
33	31.5775	0.12	48.	46.	2.8310	9.66	X	X	0.21
34	31.9800	0.16	72.	46.	2.7962	14.66	X	X	0.72
35	32.5600	0.16	30.	48.	2.7477	6.14	X	X	0.10
36	33.4550	0.12	44.	48.	2.6763	8.84	X	X	0.14
37	34.1275	0.12	32.	48.	2.6250	6.59	X	X	0.22
38	34.9725	0.12	130.	48.	2.5635	26.37	X	X	0.30
39	35.5150	0.32	121.	48.	2.5256	24.55	X	X	0.42
40	36.0100	0.12	117.	48.	2.4920	23.67	X	X	0.33
41	36.5750	0.24	128.	48.	2.4548	25.91	X	X	1.45
42	37.8000	0.08	52.	48.	2.3780	10.52	X	X	0.10
43	38.1500	0.16	49.	48.	2.3570	9.94	X	X	0.28
44	38.5050	0.16	83.	48.	2.3361	16.80	X	X	0.58
45	39.2075	0.12	42.	48.	2.2958	8.57	X	X	0.16
46	39.5200	0.08	83.	48.	2.2784	16.80	X	X	0.14
47	40.1600	0.32	50.	48.	2.2435	10.23	X	X	0.58
48	40.9600	0.16	40.	48.	2.2016	9.05	X	X	0.14
49	41.5600	0.08	40.	48.	2.1711	8.05	X	X	0.11
50	42.5200	0.12	64.	48.	2.1243	12.99	X	X	0.14
51	43.3275	0.16	58.	49.	2.0866	11.72	X	X	0.69
52	44.7200	0.08	64.	49.	2.0248	12.99	X	X	0.11
53	45.6000	0.08	34.	49.	1.9877	6.83	X		0.10
54	45.8325	0.12	38.	49.	1.9782	7.80	X	X	0.23
55	47.0175	0.24	18.	49.	1.9311	3.75	X	X	0.21
56	47.8800	0.16	22.	49.	1.8983	4.48	X	X	0.11
57	48.6300	0.16	20.	49.	1.8707	4.11	X	X	0.14
58	49.0325	0.12	17.	49.	1.8563	3.41	X	X	0.18
59	50.1075	0.12	76.	49.	1.8190	15.36	X	X	0.46
60	51.6000	0.16	12.	49.	1.7698	2.35	X	X	0.13
61	51.9450	0.12	10.	49.	1.7589	2.08	X	X	0.23
62	52.2250	0.12	12.	49.	1.7501	2.35	X	X	0.22
63	52.5475	0.12	26.	49.	1.7401	5.28	X	X	0.18
64	53.3200	0.08	21.	49.	1.7167	4.29	X	X	0.11
65	54.0150	0.48	55.	49.	1.6963	11.11	X	X	1.32
66	54.5125	0.12	56.	49.	1.6819	11.41	X		0.11
67	54.7775	0.12	61.	50.	1.6744	12.34	X	X	0.23
68	55.0650	0.12	56.	50.	1.6664	11.41	X	X	0.20
69	55.5225	0.12	35.	50.	1.6537	7.06	X	X	0.11
70	56.8400	0.08	26.	50.	1.6185	5.28	X		0.14
71	57.0550	0.12	24.	50.	1.6129	4.87	X	X	0.18
72	57.5700	0.12	26.	50.	1.5997	5.28	X	X	0.19
73	58.2500	0.16	18.	50.	1.5826	3.75	X	X	0.28
74	59.8675	0.16	52.	50.	1.5437	10.52	X	X	0.33
75	60.7200	0.16	27.	50.	1.5240	5.49	X	X	0.11

Table B39. Bentonite-Fly Ash-Lime Cured at 23°C for 180 Days.

Peak no	Angle (deg)	Tip width (deg)	Peak (cts)	Backg (cts)	D spac (Ang)	I/Imax (%)	Type A1	A2	Ot	Sign
1	2.6400	0.08	11.	58.	33.4377	1.71	X	X		0.16
2	4.9800	0.12	25.	58.	17.7300	3.94	X	X		0.32
3	6.0400	0.24	46.	58.	14.6206	7.28	X	X		0.10
4	6.5900	0.24	83.	56.	13.4016	13.04	X	X		0.25
5	7.3975	0.12	96.	56.	11.9404	15.12	X	X		0.13
6	7.6900	0.12	79.	56.	11.4869	12.47	X	X		0.30
7	8.1000	0.12	42.	55.	10.9063	6.65	X	X		0.13
8	8.9200	0.08	40.	55.	9.9055	6.25	X	X		0.15
9	9.5375	0.12	17.	53.	9.2655	2.65	X	X		0.15
10	11.6750	0.48	10.	52.	7.5735	1.61	X	X		0.12
11	13.1525	0.24	10.	52.	6.7259	1.61	X	X		0.12
12	14.0300	0.24	10.	48.	6.3071	1.61	X	X		0.17
13	14.6650	0.24	10.	49.	6.0354	1.61	X	X		0.11
14	15.2550	0.24	10.	49.	5.8033	1.61	X	X		0.15
15	15.8150	0.24	10.	53.	5.5990	1.61	X	X		0.20
16	16.5575	0.12	15.	53.	5.3496	2.40	X	X		0.27
17	17.7350	0.32	15.	49.	4.9970	2.40	X	X		0.20
18	18.1350	0.12	14.	49.	4.8876	2.16	X	X		0.11
19	18.7200	0.12	16.	56.	4.7362	2.52	X	X		0.14
20	19.8875	0.20	213.	56.	4.4607	33.57	X	X		2.88
21	20.9425	0.12	123.	56.	4.2383	19.40	X	X		0.69
22	23.3275	0.12	11.	81.	3.8101	1.71	X	X		0.19
23	23.6575	0.12	29.	81.	3.7577	4.59	X	X		0.36
24	24.5400	0.12	13.	81.	3.6245	2.04	X	X		0.26
25	24.7150	0.32	13.	81.	3.5993	2.04	X	X		0.50
26	25.4975	0.16	27.	77.	3.4905	4.26	X	X		0.30
27	25.7875	0.12	44.	77.	3.4519	6.86	X	X		0.34
28	26.7175	0.16	635.	77.	3.3339	100.00	X	X		6.17
29	27.8250	0.12	142.	79.	3.2036	22.30	X	X		1.12
30	28.4000	0.08	76.	79.	3.1401	11.92	X	X		0.16
31	28.6600	0.12	69.	79.	3.1122	10.85	X	X		0.10
32	29.6000	0.16	182.	79.	3.0154	28.70	X	X		1.86
33	31.0400	0.08	15.	79.	2.8788	2.40	X	X		0.11
34	31.4700	0.12	19.	79.	2.8404	3.05	X	X		0.11
35	31.7600	0.08	23.	79.	2.8151	3.63	X	X		0.14
36	32.6800	0.08	10.	77.	2.7379	1.61	X	X		0.13
37	33.4150	0.16	14.	77.	2.6794	2.27	X	X		0.27
38	34.7825	0.12	67.	74.	2.5771	10.59	X	X		0.19
39	35.0050	0.12	98.	74.	2.5612	15.43	X	X		0.15
40	35.4400	0.08	106.	74.	2.5308	16.71	X	X		0.14
41	36.5925	0.32	79.	77.	2.4537	12.47	X	X		0.29
42	37.8000	0.08	26.	76.	2.3780	4.10	X	X		0.11
43	38.1100	0.12	18.	76.	2.3594	2.78	X	X		0.28
44	38.5175	0.16	58.	76.	2.3354	9.10	X	X		0.87
45	39.4075	0.16	30.	76.	2.2846	4.76	X	X		0.43
46	39.6250	0.20	32.	76.	2.2726	5.12	X	X		0.55
47	40.1300	0.12	14.	76.	2.2452	2.27	X	X		0.19
48	40.4750	0.12	23.	76.	2.2268	3.63	X	X		0.26
49	41.0750	0.12	17.	76.	2.1957	2.65	X	X		0.19
50	42.4550	0.12	40.	74.	2.1274	6.25	X	X		0.35
51	42.9525	0.12	38.	74.	2.1039	6.05	X	X		0.22
52	43.3600	0.08	28.	74.	2.0851	4.42	X	X		0.15
53	43.8300	0.12	10.	74.	2.0638	1.61	X	X		0.17
54	44.0875	0.16	11.	74.	2.0524	1.71	X	X		0.46
55	44.8200	0.20	28.	74.	2.0205	4.42	X	X		1.07
56	45.7600	0.16	12.	72.	1.9812	1.93	X	X		0.10
57	46.9650	0.16	10.	69.	1.9331	1.61	X	X		0.20
58	47.7075	0.24	10.	69.	1.9047	1.61	X	X		0.13
59	48.8500	0.12	10.	66.	1.8628	1.61	X	X		0.22
60	49.1200	0.08	10.	66.	1.8532	1.61	X			0.14
61	49.2800	0.16	10.	67.	1.8476	1.61	X	X		0.11
62	50.1375	0.16	81.	62.	1.8180	12.76	X	X		0.79
63	50.8800	0.08	10.	71.	1.7932	1.61	X	X		0.10
64	51.8100	0.48	10.	64.	1.7631	1.61	X	X		0.58
65	52.7200	0.32	11.	58.	1.7348	1.71	X	X		0.15
66	54.0625	0.12	45.	61.	1.6949	7.07	X	X		0.21
67	54.3550	0.12	49.	61.	1.6864	7.72	X	X		0.19
68	55.2250	0.12	32.	69.	1.6619	5.12	X	X		0.20
69	56.0650	0.12	12.	69.	1.6390	1.82	X	X		0.23
70	56.7875	0.12	10.	69.	1.6198	1.61	X	X		0.20
71	57.5825	0.24	10.	69.	1.5994	1.61	X	X		0.28
72	58.2000	0.08	10.	66.	1.5838	1.61	X			0.11
73	58.4400	0.08	14.	66.	1.5779	2.16	X	X		0.17
74	59.8750	0.12	50.	62.	1.5435	7.94	X	X		0.22
75	61.9050	0.24	139.	67.	1.4976	21.93	X	X		1.78

Table B40. Bentonite-Fly Ash-Lime Cured at 50°C for 1 Day.

Peak no	Angle (deg)	Tip width (deg)	Peak (cts)	Backg (cts)	D spac (Ang)	I/Imax (%)	Type A1	A2	Qt	Sign
1	6.0900	0.12	50.	58.	14.5007	10.61	X	X		0.14
2	6.6025	0.24	98.	58.	13.3762	20.62	X	X		0.14
3	7.1175	0.12	146.	59.	12.4095	30.81	X	X		0.14
4	8.6000	0.08	25.	61.	10.2733	5.26	X	X		0.10
5	8.9200	0.16	29.	61.	9.9055	6.14	X	X		0.63
6	9.8150	0.24	10.	62.	9.0041	2.15	X	X		0.18
7	10.2900	0.24	10.	64.	8.5895	2.15	X	X		0.11
8	11.2000	0.08	10.	64.	7.8936	2.15	X	X		0.10
9	11.5250	0.20	10.	58.	7.6717	2.15	X	X		0.35
10	12.4800	0.08	10.	52.	7.0867	2.15	X	X		0.12
11	12.7275	0.12	10.	52.	6.9495	2.15	X	X		0.19
12	13.5600	0.08	11.	52.	6.5246	2.29	X	X		0.15
13	14.4750	0.12	10.	52.	6.1142	2.15	X	X		0.16
14	15.3175	0.32	10.	52.	5.7797	2.15	X	X		0.39
15	15.8800	0.08	14.	52.	5.5763	2.88	X	X		0.12
16	16.9525	0.24	10.	53.	5.2258	2.15	X	X		0.11
17	17.4000	0.08	10.	53.	5.0924	2.15	X	X		0.11
18	17.7500	0.16	12.	53.	4.9928	2.58	X	X		0.35
19	17.8400	0.16	10.	53.	4.9678	2.15	X	X		0.11
20	18.3550	0.12	10.	53.	4.8295	2.15	X	X		0.14
21	19.8700	0.20	237.	53.	4.4646	49.90	X	X		2.69
22	20.9450	0.12	125.	59.	4.2378	26.40	X	X		0.68
23	23.0650	0.12	16.	83.	3.8529	3.37	X	X		0.31
24	23.6800	0.08	16.	83.	3.7542	3.37	X	X		0.11
25	24.8400	0.08	17.	81.	3.5814	3.54	X	X		0.15
26	26.6875	0.16	475.	79.	3.3375	100.00	X	X		4.90
27	27.2725	0.12	74.	79.	3.2673	15.56	X	X		0.42
28	28.4000	0.32	67.	79.	3.1401	14.15	X	X		0.37
29	29.5675	0.16	188.	77.	3.0187	39.49	X	X		2.09
30	29.9925	0.12	88.	77.	2.9769	18.59	X	X		0.45
31	30.5600	0.16	27.	77.	2.9229	5.69	X	X		0.13
32	31.5050	0.12	27.	76.	2.8373	5.69	X	X		0.34
33	32.0125	0.16	64.	76.	2.7935	13.47	X	X		0.72
34	33.2650	0.40	15.	76.	2.6911	3.20	X	X		0.76
35	34.3625	0.12	18.	74.	2.6076	3.71	X	X		0.17
36	35.2800	0.08	106.	74.	2.5419	22.32	X	X		0.15
37	36.6050	0.12	96.	72.	2.4529	20.21	X	X		0.18
38	37.7600	0.16	30.	72.	2.3804	6.37	X	X		0.12
39	38.5075	0.12	64.	71.	2.3359	13.47	X	X		0.60
40	39.5075	0.16	55.	71.	2.2791	11.52	X	X		0.79
41	40.3425	0.12	30.	71.	2.2338	6.37	X	X		0.31
42	41.7650	0.12	16.	69.	2.1610	3.37	X	X		0.11
43	42.5575	0.32	29.	69.	2.1225	6.14	X	X		0.18
44	43.2675	0.16	49.	67.	2.0893	10.31	X	X		0.46
45	43.9800	0.24	19.	67.	2.0571	4.07	X	X		0.22
46	44.7525	0.20	48.	67.	2.0234	10.02	X	X		0.87
47	45.7075	0.24	17.	66.	1.9833	3.54	X	X		0.20
48	48.6625	0.16	12.	64.	1.8696	2.43	X	X		0.46
49	49.3125	0.24	19.	64.	1.8464	4.07	X	X		0.41
50	50.1250	0.16	85.	64.	1.8184	17.81	X	X		1.02
51	50.6000	0.08	10.	64.	1.8024	2.15	X	X		0.11
52	50.9600	0.16	23.	62.	1.7905	4.85	X	X		0.22
53	52.4100	0.12	10.	61.	1.7444	2.15	X	X		0.17
54	52.7075	0.24	16.	59.	1.7352	3.37	X	X		0.16
55	53.8000	0.08	40.	61.	1.7025	8.35	X	X		0.15
56	54.6575	0.12	50.	62.	1.6778	10.61	X			0.33
57	54.8850	0.12	50.	62.	1.6714	10.61	X	X		0.13
58	55.2800	0.08	41.	61.	1.6604	8.62	X	X		0.12
59	55.6000	0.08	29.	61.	1.6516	6.14	X	X		0.13
60	55.9900	0.16	25.	61.	1.6410	5.26	X	X		0.48
61	56.7475	0.12	18.	61.	1.6209	3.89	X			0.11
62	56.8900	0.24	20.	61.	1.6172	4.26	X	X		0.19
63	57.6800	0.08	28.	61.	1.5969	5.91	X	X		0.19
64	59.1200	0.08	19.	59.	1.5614	4.07	X	X		0.13
65	59.9075	0.12	50.	59.	1.5427	10.61	X	X		0.35
66	60.6325	0.12	20.	59.	1.5260	4.26	X	X		0.15
67	61.9850	0.32	149.	59.	1.4959	31.32	X	X		2.69
68	62.3200	0.16	85.	58.	1.4887	17.81	X	X		0.39
69	64.0425	0.24	18.	58.	1.4527	3.71	X	X		0.33
70	65.0200	0.12	117.	58.	1.4332	24.54	X	X		0.76
71	66.0975	0.12	53.	56.	1.4124	11.21	X	X		0.95
72	66.9450	0.12	14.	56.	1.3966	2.98	X			0.24
73	67.2400	0.08	11.	56.	1.3912	2.29	X	X		0.11
74	67.6450	0.12	40.	56.	1.3838	8.35	X	X		0.13
75	68.0425	0.24	52.	56.	1.3767	10.91	X	X		0.43
76	68.9175	0.28	16.	56.	1.3614	3.37	X	X		1.20

Table B41. Bentonite-Fly Ash-Lime Cured at 50°C for 28 Days.

Peak no	Angle (deg)	Tip width (deg)	Peak (cts)	Backg (cts)	D spac (Ang)	I/Imax (%)	Type A1	A2	Ot	Sign
1	2.2250	0.32	62.	56.	39.6734	9.45	X	X		0.11
2	3.4600	0.12	19.	56.	25.5143	2.93	X	X		0.23
3	3.8275	0.12	18.	56.	22.7684	2.67	X	X		0.10
4	4.5950	0.12	15.	56.	19.3909	2.45	X	X		0.18
5	6.5325	0.12	48.	56.	13.5194	7.00	X	X		0.24
6	7.4050	0.24	72.	56.	11.9283	10.94	X	X		0.10
7	8.3050	0.12	48.	56.	10.6376	7.21	X	X		0.14
8	8.5275	0.12	46.	56.	10.3605	7.00	X	X		0.13
9	8.9375	0.12	62.	56.	9.9979	9.45	X	X		0.29
10	11.2525	0.24	10.	56.	7.8569	1.55	X	X		0.17
11	12.4400	0.16	10.	55.	7.1094	1.55	X	X		0.11
12	13.8725	0.12	12.	52.	6.3784	1.85	X	X		0.18
13	14.1675	0.12	12.	52.	6.2462	1.85	X	X		0.27
14	14.9775	0.16	10.	50.	5.9102	1.55	X	X		0.33
15	15.5800	0.12	10.	52.	5.6829	1.55	X	X		0.16
16	17.2325	0.12	18.	53.	5.1415	2.67	X	X		0.32
17	17.7200	0.08	14.	53.	5.0012	2.07	X	X		0.11
18	18.4425	0.24	18.	55.	4.8068	2.67	X	X		0.15
19	18.9200	0.08	14.	55.	4.6866	2.19	X	X		0.13
20	19.8425	0.24	199.	58.	4.4707	30.10	X	X		3.31
21	20.9200	0.08	114.	58.	4.2428	17.33	X	X		0.19
22	21.2575	0.12	61.	58.	4.1762	9.21	X	X		0.27
23	22.2325	0.12	37.	58.	3.9952	5.63	X	X		0.15
24	23.6500	0.24	36.	58.	3.7589	5.45	X	X		0.23
25	24.3675	0.12	32.	58.	3.6498	4.92	X	X		0.17
26	24.8000	0.16	32.	58.	3.5871	4.92	X	X		0.11
27	25.1450	0.12	25.	58.	3.5387	3.79	X	X		0.16
28	26.7050	0.12	660.	58.	3.3354	100.00	X	X		2.82
29	27.4800	0.08	114.	58.	3.2431	17.33	X	X		0.21
30	27.7425	0.12	428.	58.	3.2130	64.87	X	X		2.57
31	28.0475	0.12	104.	58.	3.1787	15.75	X	X		0.50
32	28.4800	0.08	66.	58.	3.1314	9.93	X	X		0.12
33	29.1150	0.12	98.	58.	3.0646	14.84	X	X		0.33
34	29.5350	0.20	132.	58.	3.0219	20.02	X	X		0.95
35	30.6800	0.08	46.	58.	2.9117	7.00	X	X		0.13
36	30.9700	0.12	31.	58.	2.8851	4.75	X	X		0.25
37	32.0300	0.16	83.	58.	2.7920	12.54	X	X		0.76
38	32.4400	0.08	40.	58.	2.7576	6.01	X	X		0.11
39	33.4000	0.08	34.	59.	2.6805	5.09	X	X		0.17
40	35.3200	0.08	121.	59.	2.5391	18.32	X	X		0.11
41	36.5450	0.16	100.	59.	2.4567	15.14	X	X		0.39
42	36.7875	0.12	83.	59.	2.4411	12.54	X	X		0.22
43	37.0975	0.16	76.	59.	2.4214	11.46	X	X		0.44
44	37.7675	0.12	42.	59.	2.3800	6.40	X	X		0.21
45	38.5200	0.16	69.	59.	2.3352	10.43	X	X		0.93
46	38.9325	0.12	22.	59.	2.3114	3.34	X	X		0.14
47	39.4800	0.08	59.	59.	2.2806	8.98	X			0.16
48	39.5600	0.08	58.	59.	2.2762	8.75	X	X		0.10
49	40.3600	0.12	35.	59.	2.2329	5.27	X	X		0.11
50	40.9000	0.40	23.	59.	2.2046	3.49	X	X		0.32
51	41.6375	0.24	19.	59.	2.1673	2.93	X	X		0.19
52	42.6725	0.12	35.	59.	2.1171	5.27	X	X		0.21
53	43.1750	0.16	42.	59.	2.0936	6.40	X	X		0.45
54	44.1600	0.08	16.	59.	2.0492	2.42	X	X		0.14
55	44.4050	0.12	21.	59.	2.0384	3.20	X	X		0.33
56	44.7450	0.24	46.	59.	2.0237	7.00	X	X		2.14
57	45.8325	0.24	26.	59.	1.9782	3.94	X	X		0.43
58	46.3250	0.16	10.	59.	1.9583	1.55	X	X		0.20
59	47.5200	0.32	12.	61.	1.9118	1.85	X	X		0.11
60	48.7800	0.20	31.	61.	1.8653	4.75	X	X		0.76
61	49.6800	0.16	22.	61.	1.8336	3.34	X	X		0.11
62	50.1250	0.12	64.	59.	1.8184	9.69	X	X		0.21
63	50.8850	0.16	18.	61.	1.7930	2.80	X	X		0.52
64	51.3175	0.12	10.	61.	1.7789	1.55	X	X		0.17
65	52.7200	0.08	23.	56.	1.7348	3.49	X	X		0.12
66	53.9300	0.40	35.	61.	1.6987	5.27	X	X		0.91
67	54.7500	0.12	53.	61.	1.6752	8.07	X			0.25
68	54.8725	0.12	61.	61.	1.6718	9.21	X	X		0.19
69	55.3600	0.16	37.	61.	1.6582	5.63	X	X		0.13
70	56.2000	0.08	18.	61.	1.6354	2.80	X			0.12
71	56.3200	0.16	14.	61.	1.6322	2.19	X	X		0.11
72	57.4850	0.12	14.	61.	1.6018	2.19	X	X		0.15
73	58.8400	0.08	10.	61.	1.5681	1.55	X	X		0.12
74	59.2375	0.12	10.	61.	1.5586	1.55	X	X		0.19
75	59.9025	0.12	50.	61.	1.5428	7.63	X	X		0.29
76	60.4525	0.12	18.	59.	1.5301	2.80	X	X		0.24

Table B42. Bentonite-Fly Ash-Lime Cured at 50°C for 90 Days.

Peak no	Angle (deg)	Tip width (deg)	Peak (cts)	Backg (cts)	D spac (Ang)	I/Imax (%)	Type H1	Type H2	Type Ot	Sign
1	5.7775	0.32	32.	66.	15.2943	7.16	X	X		0.17
2	6.3600	0.08	62.	66.	13.8857	13.76	X	X		0.11
3	7.2775	0.12	117.	67.	12.1370	25.71	X	X		0.27
4	8.6675	0.12	15.	67.	10.1935	3.35	X	X		0.36
5	9.4800	0.08	10.	67.	9.3216	2.26	X	X		0.10
6	9.8250	0.16	10.	67.	8.9950	2.26	X	X		0.34
7	10.4000	0.16	10.	56.	8.4989	2.26	X	X		0.13
8	11.2200	0.12	10.	48.	7.8796	2.26	X	X		0.28
9	11.4400	0.32	10.	48.	7.7285	2.26	X	X		0.14
10	13.3475	0.12	12.	45.	6.6280	2.55	X	X		0.18
11	14.8400	0.08	10.	49.	5.9646	2.26	X	X		0.12
12	15.1350	0.12	10.	49.	5.8490	2.26	X	X		0.12
13	15.5375	0.24	10.	49.	5.6984	2.26	X	X		0.26
14	16.4925	0.12	12.	49.	5.3705	2.55	X	X		0.23
15	16.9600	0.16	14.	46.	5.2235	3.18	X	X		0.12
16	17.4325	0.16	12.	46.	5.0830	2.55	X	X		0.22
17	18.8400	0.08	10.	52.	4.7063	2.26	X	X		0.11
18	19.8550	0.20	202.	55.	4.4679	44.44	X	X		2.69
19	20.9350	0.12	108.	53.	4.2398	23.84	X	X		0.68
20	21.5525	0.12	12.	76.	4.1197	2.70	X	X		0.10
21	21.9275	0.12	22.	76.	4.0501	4.87	X	X		0.33
22	22.4425	0.24	12.	77.	3.9583	2.55	X	X		0.28
23	23.6200	0.12	18.	77.	3.7636	4.08	X	X		0.22
24	25.8400	0.08	56.	79.	3.4451	12.40	X	X		0.13
25	26.7075	0.12	454.	79.	3.3351	100.00	X	X		2.29
26	27.4000	0.08	31.	79.	3.2524	6.91	X	X		0.10
27	27.6875	0.12	49.	79.	3.2192	10.80	X	X		0.17
28	27.9875	0.12	71.	79.	3.1854	15.55	X	X		0.19
29	29.1675	0.16	85.	79.	3.0592	18.66	X	X		0.45
30	29.5550	0.20	128.	79.	3.0199	28.14	X	X		1.91
31	30.5175	0.12	37.	79.	2.9268	8.20	X	X		0.11
32	31.7250	0.16	17.	79.	2.8181	3.71	X	X		0.26
33	32.0775	0.16	56.	79.	2.7880	12.40	X	X		0.69
34	32.4250	0.12	15.	79.	2.7589	3.35	X	X		0.32
35	33.3250	0.12	19.	79.	2.6864	4.27	X	X		0.13
36	33.9200	0.08	10.	79.	2.6406	2.26	X	X		0.13
37	35.3125	0.12	96.	77.	2.5396	21.17	X	X		0.19
38	36.3075	0.12	90.	79.	2.4723	19.89	X	X		0.38
39	36.6400	0.20	92.	79.	2.4506	20.31	X	X		0.91
40	37.0000	0.08	53.	79.	2.4276	11.75	X	X		0.17
41	37.4450	0.16	42.	79.	2.3997	9.31	X	X		0.38
42	38.0000	0.08	50.	79.	2.3660	11.11	X	X		0.10
43	38.4375	0.16	276.	79.	2.3400	60.74	X	X		3.02
44	39.7050	0.12	85.	79.	2.2682	18.66	X	X		0.46
45	40.2400	0.08	27.	79.	2.2393	5.96	X	X		0.11
46	42.3875	0.32	29.	79.	2.1307	6.43	X	X		0.65
47	43.3375	0.24	31.	79.	2.0861	6.91	X	X		0.79
48	44.6600	0.12	28.	77.	2.0274	6.19	X	X		0.19
49	45.9100	0.12	19.	77.	1.9750	4.27	X	X		0.25
50	47.6550	0.32	10.	67.	1.9067	2.26	X	X		0.33
51	48.2800	0.16	10.	67.	1.8835	2.26	X	X		0.42
52	48.6200	0.16	18.	67.	1.8711	3.89	X	X		0.60
53	49.4575	0.12	15.	66.	1.8414	3.35	X			0.12
54	49.6000	0.16	17.	66.	1.8364	3.71	X	X		0.10
55	50.0950	0.12	67.	61.	1.8194	14.82	X	X		0.45
56	50.8350	0.24	10.	69.	1.7946	2.26	X	X		0.81
57	51.2475	0.12	10.	69.	1.7812	2.26	X			0.22
58	51.4700	0.12	10.	69.	1.7740	2.26	X	X		0.19
59	51.8775	0.24	10.	62.	1.7610	2.26	X	X		0.19
60	52.3525	0.12	18.	56.	1.7461	3.89	X	X		0.22
61	53.8925	0.12	34.	64.	1.6998	7.41	X	X		0.13
62	54.7750	0.16	56.	64.	1.6745	12.40	X	X		0.54
63	56.3525	0.12	14.	69.	1.6313	3.02	X	X		0.17
64	56.6525	0.12	14.	69.	1.6234	3.02	X	X		0.17
65	57.2800	0.08	10.	69.	1.6071	2.26	X	X		0.12
66	58.7600	0.08	10.	64.	1.5701	2.26	X			0.21
67	59.0000	0.08	10.	64.	1.5681	2.26		X		0.19
68	59.3125	0.16	14.	64.	1.5568	3.02	X	X		0.23
69	60.0000	0.32	64.	58.	1.5406	14.11	X	X		1.51
70	61.7725	0.12	121.	66.	1.5005	26.67	X			0.21
71	62.0100	0.12	149.	66.	1.4954	32.81	X	X		0.30
72	62.6750	0.16	28.	64.	1.4811	6.19	X	X		0.21
73	63.3600	0.08	14.	64.	1.4667	3.02	X	X		0.16
74	64.0400	0.24	10.	64.	1.4528	2.26	X	X		0.13
75	64.3725	0.12	231.	62.	1.4342	50.92	X	X		1.02

Table B43. Bentonite-Fly Ash-Lime Cured at 50°C for 180 Days.

VITA

GOKHAN I. BAYKAL

Candidate for the Degree of

Doctor of Philosophy

Dissertation: THE EFFECT OF MICROMORPHOLOGICAL DEVELOPMENT ON THE ELASTIC MODULI OF FLY ASH-LIME STABILIZED BENTONITE

Major Field: Civil Engineering Minor: Geology

Biographical:

Personal Data: Born in Amasya, Turkey, June 14, 1958, the son of Mrs. Neriman and Mr. Orhan H. Baykal .

Education: Received Bachelor of Science Degree in Civil Engineering from Istanbul Technical University in July 1980. Received Master of Science Degree in Civil Engineering from Bogazici University in March 1982.

Experience: Teaching assistant in Bogazici University in 1981. Research and teaching assistant at LSU since 1984. Worked for Woodward Clyde Consulting Company in summer 1984.

Professional Memberships: Student member of ASCE, member of Chamber of Civil Engineers in Istanbul.

DOCTORAL EXAMINATION AND DISSERTATION REPORT

Candidate: Gökhan I. Baykal

Major Field: Civil Engineering

Title of Dissertation: The Effect of Micromorphological Development on the Elastic Moduli of Fly Ash - Lime Stabilized Bentonite

Approved:

Major Professor and Chairman

Dean of the Graduate School

EXAMINING COMMITTEE:

Ray E. Ferrell Jr.

Roger R. Seals

Robert D. Hussey

Date of Examination:

Nov. 12, 1987